Order Number 9402448

Mechanisms of high-durability performance of plain and blended cements

Hussain, Syed Ehtesham, Ph.D.

King Fahd University of Petroleum and Minerals (Saudi Arabia), 1991

U·M·I
300 N. Zeeb Rd.
Ann Arbor, MI 48106

MECHANISMS OF HIGH DURABILITY PERFORMANCE OF PLAIN AND BLENDED CEMENTS

BY

SYED EHTESHAM HUSSAIN

A Thesis Presented to the

FACULTY OF THE COLLEGE OF GRADUATE STUDIES

KING FAHD UNIVERSITY OF PETROLEUM & MINERALS

DHAHRAN, SAUDI ARABIA

In Partial Fulfillment of the
Requirements for the Degree of

DOCTOR OF PHILOSOPHY

In

CIVIL ENGINEERING

AUGUST, 1991

KING FAHD UNIVERSITY OF PETROLEUM & MINERALS

DHAHRAN, SAUDI ARABIA

This Dissertation, written by **Syed Ehtesham Hussain** *under the direction of his Dissertation Advisor and approved by his Dissertation Committee, has been presented to and accepted by the Dean of the College of Graduate Studies, in partial fulfillment of the requirements for the degree of* **DOCTOR OF PHILOSOPHY IN CIVIL ENGINEERING**

Dissertation Committee

Chairman (Prof. Rasheeduzzafar)

Co-Chairman (Dr. Saadoun S. Al-Saadoun)

Member (Prof. Fahad H. Al-Dakhil)

Member (Dr. Ahmed S. Al-Gahtani)

Member (Dr. Islem A. Basunbul)

Member (Prof. Mazhar ul-Haque)

Dr. Ghazi J. Al-Sulaimani
Department Chairman

Dr. Ala H. Al-Rabeh
Dean College of Graduate Studies

Date : August, 1991.

كلية الدراسات العليا
COLLEGE OF GRADUATE STUDIES

dedicated to:

my parents and wife

ACKNOWLEDGEMENTS

Acknowledgement is due to King Fahd University of Petroleum and Minerals for support of this research.

I wish to express my sincere appreciation to my major advisor Prof. Rasheeduzzafar for his invaluable guidance and support throughout the course of this work and to co-advisor Dr. S.S. Al-Saadoun and other members of my dissertation committee Prof. Fahd H. Dakhil, Dr. A.S. Al-Gahtani, Dr. I.A. Basunbul and Prof. Mazhar ul-Haque for their useful suggestions.

I am thankful to the Research Institute, King Fahd University of Petroleum and Minerals for allowing the use of their facilities. The assistance provided by Mr. Ahmed Ali, Mr. Abdul Bari, Mr. Shamim Khan and Mr. Abdullah Aitani in carrying out some of the experiments at the Research Institute is gratefully acknowledged.

I wish to express my sincere thanks to Mr. Mukarram Khan, Mr. Mohammed Maslehuddin and Mr. Mohammed Saleem for their help and suggestions in conducting the experimental work, and to Mr. Najeeb Shaikh and Mohammed Muqtar for helping in preparation of this manuscript.

I thank my parents and my wife for their moral support during this work, which made this work easier and enjoyable.

TABLE OF CONTENTS

Chapter *Page*

ACKNOWLEDGEMENT ..... **iv**

LIST OF TABLES ..... **x**

LIST OF FIGURES ..... **xiii**

ABSTRACT ..... **xxi**

1. INTRODUCTION 1

1.1 Concrete durability problem in Arabian Gulf region 1

1.1.1 Concrete deterioration in the Gulf environment 1

1.1.2 Environment-durability material selection interaction 2

1.1.3 Gulf environment relevant to concrete durability 3

1.1.3.1 General geomorphic and climatic factors affecting concrete durability 3

1.1.3.2 Specific factors affecting concrete durability 4

1.2 Mechanisms of predominant concrete deteriorations in the Gulf region. 6

1.2.1 Corrosion of reinforcement 6

1.2.2 Sulfate attack 10

1.2.3 Alkali-silica reactivity 12

1.3 Blended cements 12

1.3.1 Mechanism of hydration of blended cements 13

1.3.2 Sulfate resistance of blended cements 13

1.3.3 Corrosion of reinforcement in blended cements 15

1.3.4 Control of alkali-silica reactivity blended cements 16

1.3.5 Physical factors 17

1.3.5.1 Permeability to water and chloride ions 17

1.3.5.2 Pore size distribution 18

1.3.5.3 Electrical resistivity 18

1.4 Cement factors affecting concrete durability 18

1.4.1 Cement compositional parameters and concrete durability 19

1.4.1.1 Chloride combining capacity 20

1.4.1.2 Formation of products causing expansion and degradation of concrete 27

1.4.1.3 Deteriorations due to alkali-silica reactions 28

1.4.2 Cement properties affecting the alkalinity of cement 29

1.4.3 Cement characteristics affecting the physical structure of cement 30

2. OBJECTIVES AND RESEARCH PROGRAM 33

2.1 Specific Objectives and Research Program 36

2.1.1 Chloride Binding Mechanism in Plain Cements 36

2.1.2 Determination of Threshold Cl^-/OH^- Ratio in Plain Cements 36

2.1.3 Chloride Binding Mechanism in Blended Cements 36

2.1.4 Mechanism of Reduction of OH^- Ions from Pore Solution in Blended Cements 37

2.1.5 Effect of Physical Characteristics on Durability Mechanisms 37

3. METHODOLOGY OF RESEARCH 44

3.1 Materials and Mixes Used 45

3.1.1 Mixed Used 45

3.1.1.1 Cement Pastes 45

3.1.1.2 Cement Mortar 46

3.1.1.3 Concrete Mixes 46

3.1.2 Cements Used 47

3.1.3 Blending Material Used 47

3.2 Experimental Methods 48
3.2.1 Corrosion Monitoring Tests 48
3.2.1.1 Corrosion Initiation Time 48
3.2.1.2 Corrosion Rates 48
3.2.2 Pore Solution Extraction and Analysis 50
3.2.2.1 Specimen Preparation for Pore Solution Extraction 51
3.2.2.2 Pore Solution Expression Device 51
3.2.3 Determination of OH^- and Cl^- Concentration in Pore Solution 53
3.2.4 Permeability Test 54
3.2.4.1 Description of the Apparatus 54
3.2.4.2 Operation 55
3.2.5 Chloride Ion Diffusion 56
3.2.6 Measurement of Electrical Resistivity 57
3.2.7 Measurement of Oxygen Diffusion 58
3.2.8 Alkali-Silica Reactivity Test 59
3.2.8.1 Test Specimen 59
3.2.8.2 Storage of Test Specimens 59
3.2.8.3 Expansion Measurements 60
4. RESULTS AND DISCUSSIONS 75
4.1 Durability Performance of Plain and Blended Cements 75
4.1.1 Corrosion Resistance Performance of Steel in Plain and Blended Cement Concrete 75
4.1.1.1 Corrosion Initiation Time 77
4.1.1.2 Corrosion Rates 77
4.1.2 Alkali-Silica Reactivity in Plain and Blended Cements 95
4.2 Chemical Environment of Plain and Blended Cements 100

4.2.1 Chloride Binding Mechanism in Plain Cements 100

4.2.1.1 Effect of C_3A Content of Cement 100

4.2.1.2 Effect of Alkali Content of Cement 118

4.2.1.3 Effect of Sulfates 126

4.2.1.4 Effect of Temperature 147

4.2.1.5 External Chlorides 160

4.2.2 Chloride Binding Mechanism in Blended Cements 167

4.2.2.1 Microsilica Blended Cement 167

4.2.2.2 Blast Furnace Slag Cement 188

4.2.2.3 Fly Ash Blended Cement Concrete 197

4.2.3 Influence of Microsilica, Blast Furnace Slag and Fly Ash Alkaline Environment of Hardened Cements 207

4.2.4 Determination of Threshold Cl^-/OH^- Ratio 221

4.3 Physical Characteristics of Plain and Blended Cements 225

4.3.1 Pore Size Distribution of Hardened Cement Pastes 225

4.3.2 Permeability 238

4.3.2.1 Permeability of Plain Cement Concrete 238

4.3.2.2 Permeability of Blended Cement Concrete 252

4.3.3 Chloride Ion Diffusion 269

4.3.4 Electrical Resistivity 276

4.3.5 Oxygen Diffusion 279

4.4 Mechanism of Control of Alkali-Silica Reactions in Blended Cement Concrete 283

5. DURABILITY MECHANISMS 289

5.1 Corrosion of Reinforcing Steel 289

5.1.1 Passivation of Steel in Concrete 289

5.1.2 Loss of Passivation 290

5.1.3 Significance of Chloride Induced Corrosion 290

5.2 Mechanism of Chloride Induced Corrosion of Steel in Concrete 292

5.3 Mechanism of Corrosion Resistance Performance in Plain Cements ... 294

5.3.1 C_3A effect 294

5.3.2 Chloride Sulfate Interaction 296

5.3.3 Temperature Effect 297

5.3.4 Effect of Alkali Content of Cement 299

5.3.5 Mode of Occurrence of Chlorides 300

5.4 Mechanism of Corrosion Resistance Performance of Blended Cements 303

5.4.1 Chemical Environment and Corrosion Resistance of Blended Cement 304

5.4.2 Physical Characteristics and Corrosion Resistance Performance of Blended Cements 309

5.5 Mechanism of Control of Alkali-Silica Reaction in Plain and Blended Cements 312

REFERENCES **332**

LIST OF TABLES

Table		*Page*
2.1	Broad Overview of the Research Program for Studying Durability Mechanisms in Plain and Blended Cements.	38
2.2	Research Program for Studying Chloride Binding Mechanism in Plain Cements.	39
2.3	Research Program for Determination of Threshold Cl^-/OH^- Ratio in Plain Cements.	40
2.4	Research Program for Studying Chloride Binding Mechanism in Blended Cements.	41
2.5	Research Program for Mechanism of Reduction of OH^- Ions from Pore Solution and $Ca(OH)_2$ Depletion in Blended Cements.	42
2.6	Research Program for Studying Physical Characteristics on Durability Mechanism.	43
3.1	Composition of Cements Used (% by weight)	61
3.2	Physical and Chemical Characteristics Fly Ash, Blast Furnace Slag and Microsilica Used (% by weight)	62
4.1.1.1	Corrosion Rates of Steel in Plain Cement Concrete	79
4.1.1.2	Corrosion Rates of Steel in Blended Cement Concrete	80
4.1.2.1	Hydroxyl Ion Concentration and pH of Pore Solutions Extruded from Plain and Blended Cements	97
4.2.1.1	Analysis of Pore Solution from Chloride-Bearing Specimens of Different Cements	106
4.2.1.2	Percentage of Unbound Chlorides for Different C_3A Cements	107
4.2.1.3	Ratio of Bound to Unbound Chlorides for Different C_3A Cements	108
4.2.1.4	Critical Cl^-/OH^- Ratios for Onset of Depassivation	109

4.2.1.5	Threshhold Chloride Values for Different C_3A Cements	110
4.2.1.6	Pore Solution Composition of Medium and High Alkali Content Cements Treated With Different Levels of Chloride	121
4.2.1.7	Pore Solution Composition of Hydrated Cement Pastes With Different Levels of Chloride and Sulfate	134
4.2.1.8	Unbound Chlorides in Pore Solution of Hydrated Cement Pastes Treated with Different Levels of Chloride and Sulfates	135
4.2.1.9	Rates of Increase of Cl^- and OH^- Ion Concentrations due to Sulfate Addition	136
4.2.1.10	Effect of Curing Temperature of Pore Solution Composition of 14% C_3A Cement Treated with Different Levels of Chloride	151
4.2.1.11	Unbound Chlorides in Pore Solution of Cements Containing External Chlorides	164
4.2.1.12	Unbound and Bound Chlorides in Cements Containing Internal and External Chlorides	165
4.2.2.1	Pore Solution Composition of Plain and Microsilica Blended Cements Treated with Different Levels of Chloride	176
4.2.2.2	Effect of Alkali Content of Cement on Pore Solution Composition of Microsilica Blended Cements Treated with Different Chloride Levels (Parent Cement C_3A : 14%)	177
4.2.2.3	Pore Solution Composition of Plain and Blast Furnace Slag Blended Cement Treated with Different Levels of Chloride	192
4.2.2.4	Pore Solution Composition of Plain and Fly Ash Blended Cement Treated with Different Levels of Chloride	201
4.2.2.5	Unbound Chlorides in Pore Solution of Plain and Fly Ash Blended Cement Treated with Different Levels of Chloride	202
4.2.3.1	Pore Solution Alkalinity and Calcium Hydroxide Content in Hydrated Plain and Blended Cement Pastes	209
4.2.4.1	Pore Solution Composition of Specimens Used For Threshold Cl^-/OH^- Ratio Determination	223
4.3.1.1	Pore Size Distribution of Plain Cement	226

4.3.1.2	Pore Size Distribution of Fly Ash Blended Cement	227
4.3.1.3	Pore Size Distribution of Blast Furnace Slag Cement	228
4.3.1.4	Pore Size Distribution of 10% Microsilica Blended Cement	229
4.3.1.5	Pore Size Distribution of 20% Microsilica Blended Cement	230
4.3.1.6	Average Pore Radius of Plain and Blended Cements	231
4.3.2.1	Effect of Water Cement Ratio and Age on Coefficient of Permeability of Plain Cement Concrete	249
4.3.2.2	Coefficient of Permeability of Plain and Blended Cement Concrete	267
4.3.3.1	Chloride Diffusivity of Plain and Blended Cement Concrete	275
4.3.4.1	Electrical Resistivity of Plain and Blended Cement Concrete	277
4.3.5.1	Oxygen Flux of Plain and Blended Cement	281

LIST OF FIGURES

Figure		*Page*
3.1	Cross-Sectional View of the Specimen Used for Threshold Cl^-/OH^- Ratio Determination.	63
3.2	Specimen Used for Corrosion Rate Measurements	65
3.3	Instrumentation for Corrosion Rate Measurement Tests	67
3.4	Cross-Sectional View of Pore Solution Expression Device	68
3.5	Schematic View of High Pressure Permeability Apparatus	70
3.6	Cross-section View of Chloride Diffusion Cell	72
3.7	Experimental Set-up for Measuring Oxygen Diffusion	74
4.1.1.1	Potential Measurement Record Showing the Effect of C_3A Content on Corrosion of Reinforcing Steel in Concrete	81
4.1.1.2	Effect of C_3A Content of Cement on Time to Initiation of Corrosion of Reinforcing Steel in Concrete	82
4.1.1.3	Potential Measurement Record of Steel in Plain and Blended Cement Concrete	83
4.1.1.4	Corrosion Initiation Time of Steel and Blended Cements Concrete	84
4.1.1.5	Anodic and Cathodic Polarization Curves for Steel in Type V (C_3A :2%) Cement Concrete	85
4.1.1.6	Anodic and Cathodic Polarization Curves for Steel in Type I (C_3A : 9 %) Cement Concrete	86
4.1.1.7	Anodic and Cathodic Polarization Curves for Steel in Type I (C_3A : 11 %) Cement Concrete	87
4.1.1.8	Anodic and Cathodic Polarization Curves for Steel in Type I (C_3A : 14 %) Cement Concrete	88

4.1.1.9 Anodic and Cathodic Polarization Curves for Steel in 30% Fly Ash Blended Cement Concrete 89

4.1.1.10 Anodic and Cathodic Polarization Curves for Steel in 70% Blast Furnace Slag Cement Concrete 91

4.1.1.11 Anodic and Cathodic Polarization Curves for Steel in 10% Microsilica Blended Cement Concrete 91

4.1.1.12 Anodic and Cathodic Polarization Curves for Steel in 20% Microsilica Blended Cement Concrete 92

4.1.1.13 Effect of C_3A Content on Corrosion Rate of Steel in Plain Cement Concrete 93

4.1.1.14 Corrosion Rate of Steel in Plain and Blended Cement Concrete

4.1.2.1 Expansion in Plain and Blended Cements due to AlkaliSilica Reaction 98

4.1.2.2 Alkali - Silica Reactions of Plain and Blended Cements after 7 months of test with a Highly Reactive Aggregate 99

4.2.1.1 Chloride Concentrations in Pore Solutions of Different Cements Treated with Various Levels of Chloride Addition 111

4.2.1.2 Unbound Chlorides in Pore Solutions of Various C_3A Cements Treated with Different Levels of Chloride 112

4.2.1.3 Effect of C_3A Content of Cement on Chloride Remaining Unbound in Pore Solution 113

4.2.1.4 DTA Curves of 2.43% and 14% C_3A Cements Pastes Treated with 1.2% Chlorides 114

4.2.1.5 Chlorides Remaining Unbound in Pore Solutions of Different Cements Treated with Various Levels of Chloride Addition 115

4.2.1.6 Average Corrosion Resistance Performance of Type I (C_3A : 9.5 %) to Type V (C_3A : 2.8 %) Cement 116

4.2.1.7 Cl^-/OH^- Ratios in Pore Solutions of Different Cements for Various Levels of Chloride Addition 117

4.2.1.8 Effect of Alkali Content of Cement of OH^- Concentrations in the

Pore Solution of Type I Cement (C_3A : 14%) 122

4.2.1.9 Effect of Alkali Content of Cement on Unbound Chlorides in the Pore Solution of Type I Cement (C_3A : 14%) 123

4.2.1.10 DTA Curves of Hydrated Cement Pastes of Medium and High Alkali Cements 124

4.2.1.11 Effect of Alkali Content of Cement on Cl^-/OH^- Ratio in the Pore Solution of Type I Cement (C_3A : 14%) 125

4.2.1.12 Effect of Sulfate Addition on OH^- Concentration in the Pore Solution of Cements Treated with 0.6% Chloride Level 137

4.2.1.13 Effect of Sulfate Addition on OH^- Concentration in the Pore Solution of Cements Treated with 1.2% Chloride Level 138

4.2.1.14 DTA Curves of 2.43% C_3A Cement with Chloride and (Chloride + Sulfate) Additions 139

4.2.1.15 Effect of Sulfate Addition on Unbound Chlorides in Pore Solutions of Cement Treated with 0.6% Chloride Level 140

4.2.1.16 Effect of Sulfate Addition on Unbound Chlorides in Pore Solutions of Cements Treated with 1.2% Chloride Level 141

4.2.1.17 Effect of C_3A Content on Unbound Chlorides in Pore Solutions of Cements Treated with 0.6% Chloride Level 142

4.2.1.18 Effect of C_3A Content on Unbound Chlorides in Pore Solutions of Cements Treated with 1.2% Chloride Level 143

4.2.1.19 Performance Ratio of Type I to Type V Cement 144

4.2.1.20 Effect of Sulfate Addition on $Cl^- OH^-$ Ratios in the Pore Solutions of Cements Treated with 0.6% Chloride Level 145

4.2.1.21 Effect of Sulfate Addition on Cl^-/OH^- Ratios in the Pore Solutions of Cements Treated with 1.2% Chloride Level 146

4.2.1.22 Effect of Temperature on Unbound Chlorides in Pore Solutions of 2.43% C_3A Cement Treated with Different Levels of Chloride 152

4.2.1.23 Effect of Temperature on Unbound Chlorides in Pore Solutions of 7.59% C_3A Cement Treated with Different Levels of Chloride 153

4.2.1.24 Effect of Temperature on Unbound Chlorides in Pore Solutions of 14% C_3A Cement Treated with Different Levels of Chloride 154

4.2.1.25 Effect of Temperature on Unbound Chlorides in Pore Solutions of Different C_3A Cements 155

4.2.1.26 Effect of Temperature on OH^- Concentration in Pore Solutions of 2.43% C_3A Cement Treated with Different Levels of Chloride 156

4.2.1.27 Effect of Temperature on OH^- Concentration in Pore Solutions of 7.59% C_3A Cement Treated with Different Levels of Chloride 157

4.2.1.28 Effect of Temperature on OH^- Concentration in Pore Solutions of 14% C_3A Cement Treated with Different Levels of Chloride 158

4.2.1.29 Effect of Temperature on Cl^-/OH^- Ratio in Pore Solutions of Different C_3A Cement Treated with Different Levels of Chloride 159

4.2.1.30 Bounded Chlorides in Different C_3A Cements for Internal and External Chlorides 166

4.2.2.1 OH^- Concentration in Pore Solutions of Plain and Microsilica Blended Cements Treated with Different Levels of Chloride 178

4.2.2.2 OH^- Concentration in Pore Solutions of Chloride-Free and Chloride-Bearing Plain and Microsilica Blended Cements 174

4.2.2.3 DTA Curves for 1.2% Chloride Bearing Plain and Microsilica Blended Cement Pastes 180

4.2.2.4 Unbound Chlorides in Pore Solutions of of Plain and Blended Cements Treated with 0.3% Chloride Level 181

4.2.2.5 Unbound Chlorides in Pore Solutions of of Plain and Blended Cements Treated with 0.6% Chloride Level 182

4.2.2.6 Unbound Chlorides in Pore Solutions of Plain and Microsilica Blended Cements Treated with 1.2% Chloride Level 183

4.2.2.7 Effect of Alkali Content of Cement on OH^- Concentration in Pore Solution of Plain and Microsilica Blended Cements 184

4.2.2.8 Effect of Alkali Content of Cement on Unbound Chlorides in Pore Solution of Plain and Blended Cements treated with 0.6% Chloride . 185

4.2.2.9 Effect of Alkali Content of Cement on Unbound Chlorides in Pore Solution of Plain and Blended Cements treated with 1.2% Chloride . 186

4.2.2.10 Cl^-/OH^- Ratio in Pore Solution of Plain and Microsilica Blended Cements Treated with Different Chloride Levels 187

4.2.2.11 OH^- Concentration in Pore Solutions of Plain and Blast Furnace Slag Cements Treated with Different Chloride Levels 193

4.2.2.12 DTA Curves of Hydrated Plain and Slag Cement Treated with 1.2% Cl^- 194

4.2.2.13 Unbound Chlorides in Pore Solution of Plain and Blast Furnace Slag Cements Treated with Different Chloride Levels 195

4.2.2.14 Cl^-/OH^- Ratio in Pore Solutions of Plain and Blast Furnace Slag Cements Treated with Different Chloride Levels 196

4.2.2.15 OH^- Concentration in Pore Solutions of Plain and Fly Ash Blended Cements Treated with Different Chloride Levels 203

4.2.2.16 DTA Curves of Plain and Fly Ash Blended Cement with 14% C_3A Parent Cement (1.2% Cl^- Addition) 204

4.2.2.17 Unbound Chlorides in Pore Solution of Plain and Fly Blended Cements Treated with Different Chloride Levels 205

4.2.2.18 Cl^-/OH^- Ratio in Pore Solutions of Plain and Fly Ash Blended Cements Treated with Different Chloride Levels 206

4.2.3.1 DTA and TGA Curves for Hydrated Plain Cement Paste 210

4.2.3.2 DTA and TGA Curves for Hydrated Paste of 30% Fly Ash Blended Cement 211

4.2.3.3 DTA and TGA Curves for Hydrated Paste of 70% Blast Furnace Slag Blended Cement 212

4.2.3.4 DTA and TGA Curves for Hydrated Paste of 5% Microsilica Blended Cement 213

4.2.3.5 DTA and TGA Curves for Hydrated Paste of 10% Microsilica Blended Cement 214

4.2.3.6 DTA and TGA Curves for Hydrated Paste of 20% Microsilica Blended Cement 215

4.2.3.7	DTA and TGA Curves for Hydrated Paste of 25% Microsilica Blended Cement	216
4.2.3.8	Effect of Microsilica Addition on OH^- Concentration in Pore Solution	217
4.2.3.9	Effect of Microsilica Addition on Calcium Hydroxide Content in Hydrated Cement	218
4.2.3.10	Effect of Fly Ash and Blast Furnace Slag on OH^- Concentration in Pore Solution	219
4.2.3.11	Effect of Fly Ash and Blast Furnace Slag on Calcium Hydroxide Content in Hydrated Cement	220
4.2.4.1	Potential Measurement Record of Steel in Cement Motors	224
4.3.1.1	Pore Size Distribution of Plain Cement Paste	232
4.3.1.2	Pore Size Distribution of 30% Fly Ash Blended Cement	233
4.3.1.3	Pore Size Distribution of 70% Blast Furnace Slag Cement	234
4.3.1.4	Pore Size Distribution of 10% Microsilica Blended Cement	235
4.3.1.5	Pore Size Distribution of 20% Microsilica Blended Cement	236
4.3.1.6	Average Pore Radius of Plain and Blended Cements	237
4.3.2.1	'q' vs 't' Curve for Plain Cement Concrete (W/C: 0.35; Age: 7 days)	240
4.3.2.2	'q' vs 't' Curve for Plain Cement Concrete (W/C: 0.35; Age: 14 days)	241
4.3.2.3	'q' vs 't' Curve for Plain Cement Concrete (W/C: 0.35; Age: 28 days)	242
4.3.2.4	'q' vs 't' Curve for Plain Cement Concrete (W/C: 0.45; Age: 7 days)	243
4.3.2.5	'q' vs 't' Curve for Plain Cement Concrete (W/C: 0.45; Age: 14 days)	244
4.3.2.6	'q' vs 't' Curve for Plain Cement Concrete (W/C: 0.45; Age: 28 days)	245
4.3.2.7	'q' vs 't' Curve for Plain Cement Concrete (W/C: 0.55; Age: 7	

days) 246

4.3.2.8 'q' vs 't' Curve for Plain Cement Concrete (W/C: 0.55; Age: 14 days) 247

4.3.2.9 'q' vs 't' Curve for Plain Cement Concrete (W/C: 0.55; Age: 28 days) 248

4.3.2.10 Effect of Water Cement Ratio on Coefficient of Permeability of Plain Cement Concrete 250

4.3.2.11 Effect of Age on Coefficient of Permeability of Plain Cement Concrete 251

4.3.2.12 'q' vs 't' Curve for Plain Cement Concrete (Age: 90 days) 253

4.3.2.13 'q' vs 't' Curve for Plain Cement Concrete (Age: 180 days) 254

4.3.2.14 'q' vs 't' Curve for Fly Ash Blended Cement Concrete (Age: 28 days) 255

4.3.2.15 'q' vs 't' Curve for Fly Ash Blended Cement Concrete (Age: 90 days) 256

4.3.2.16 'q' vs 't' Curve for Fly Ash Blended Cement Concrete (Age: 180 days) 257

4.3.2.17 'q' vs 't' Curve for Blast Furnace Slag Cement Concrete (Age: 28 days) 258

4.3.2.18 'q' vs 't' Curve for Blast Furnace Slag Cement Concrete (Age: 90 days) 259

4.3.2.19 'q' vs 't' Curve for Blast Furnace Slag Cement Concrete (Age: 180 days) 260

4.3.2.20 'q' vs 't' Curve for 10% Microsilica Blended Cement Concrete (Age: 28 days) 261

4.3.2.21 'q' vs 't' Curve for 10% Microsilica Blended Cement Concrete (Age: 90 days) 262

4.3.2.22 'q' vs 't' Curve for 10% Microsilica Blended Cement Concrete (Age: 180 days) 263

4.3.2.23 'q' vs 't' Curve for 20% Microsilica Blended Cement Concrete (Age: 28 days) 264

4.3.2.24 'q' vs 't' Curve for 20% Microsilica Blended Cement Concrete

(Age: 90 days) 265

4.3.2.25 'q' vs 't' Curve for 20% Microsilica Blended Cement Concrete (Age: 180 days) 266

4.3.2.26 Coefficient of Permeability of Plain and Blended Cement Concrete .. 268

4.3.3.1 Rate of Increase in Chloride Concentration in Chamber B for Plain Cements 273

4.3.3.2 Rate of Increase in Chloride Concentration in Chamber B for Blended Cements 274

4.3.4.1 Electrical Resistivity of Plain and Blended Cement Concrete 278

4.3.5.1 Oxygen Flux for Plain and Blended Cement Concrete 282

5.1 Model for Corrosion Process of Steel in Conctere (ref.62) 317

5.2 Relationship Between Total Tolerable Chloride Content and Corrosion Initiation Time of Steel in Different C_3A Cement Concretes 318

5.3 Model for Corrosion Process of Steel in Plain and Blended Cement Concrete 319

DISSERTATION ABSTRACT

FULL NAME: SYED EHTESHAM HUSSAIN

TITLE OF STUDY: MECHANISMS OF HIGH DURABILITY PERFORMANCE OF PLAIN AND BLENDED CEMENTS

MAJOR FIELD: CIVIL ENGINEERING

DATE OF DEGREE: AUGUST 1991

Durability of concrete has been recently become a problem of major concern for construction industry in the Middle East and throughout the world. Concrete structures in the Middle East have shown premature deterioration within a short span of 10-15 years, the main causes for which are corrosion of reinforcement sulfate attack. Results of comprehensive study on concrete durability at King Fahd University of Petroleum and Minerals indicate that higher C_3A cements show better corrosion resistance than low C_3A cements and that certain blended cements perform manifold better than plain cements in terms of resistance to corrosion and alkali-silica reactivity (ASR).

In this research, an attempt has been made to study the mechanisms controlling the performance of plain and blended cements against corrosion of reinforcement and ASR. The effect of various compositional and environmental factors, such as C_3A and alkali contents, concomitant presence of sulfates, temperature and mode of occurrence of chlorides, on chloride binding and pore solution alkalinity has been studied in plain cements, in an effort to evaluate their influence on mechanism of corrosion resistance. Mechanisms controlling resistance to corrosion and ASR of blended cements, formulated using fly ash, blast furnace slag and microsilica have been studied through their effect on chemical environment and physical characteristics of hardened concrete.

Results show that high C_3A cements have more chloride binding capacity than low C_3A cements, explaining their higher corrosion resistance. Increase in curing temperature and alkali content of cement and concomitant presence of sulfates decrease chloride binding capacity in plain cements. Plain cement bind more primary chlorides than secondary external chlorides. Fly ash and slag have little effect on chemical environment of concrete compared to microsilica, which drastically increases aggressivity of the chemical environment. The blending materials bring about significant improvement in the physical structure of concrete through pore refinement, decrease in permeability, chloride and oxygen diffusion and increase in electrical resistivity. These significant improvements in the physical characteristics due to blending materials are responsible for the improved corrosion resistance of the blended cements. Also, the blending materials significantly reduce OH^- concentration in pore solution. The reduction in the OH^- concentration and possibly the improved physical structure of blended cements are responsible for their increased resistance against ASR.

ملخص

لقد أصبحت متانة الخرسانة مشكلة رئيسية تشغل العاملين في مجال الخرسانة في العالم وخاصة في منطقة الشرق الأوسط . فقد تعرضت المباني الخرسانية في منطقة الشرق الأوسط إلى تدهور سريع في وقت قصير من عمرها الزمني . ويعتبر صدأ حديد التسليح وتأثير الأملاح الكبريتية من العوامل الرئيسية لهذا التدهور . إن الأبحاث التي أجريت في جامعة الملك فهد للبترول والمعادن تبين أن الاسمنت الذي يحتوي على نسبة عالية من الالمنيوم ثلاثي الكالسيوم أفضل من الاسمنت الذي يحتوي على نسبة أقل من الالمونيوم ثلاثي الكالسيوم في مقاومته لصدأ حديد التسليح . كذلك فان الاسمنت الممزوج بمواد اضافية مثل الرماد المتطاير أو خبث الفرن العالي أو دخان السيليكا أثبت فعاليته في مقاومة صدأ حديد التسليح وتفاعل السيليكا بالقلويات .

في هذا البحث يتم دراسة تأثير العوامل التي تؤثر على أداء الاسمنت العادي والاسمنت الممزوج بالمواد الاضافية في مقاومة صدأ حديد التسليح وتفاعل السيليكا بالقلويات . كذلك يتم دراسة تأثير العوامل التركيبية والمناخية مثل مركب الالمونيوم ثلاثي الكالسيوم وكمية المواد القلوية والاملاح الكبريتية والكلوريدات على ميكانيكية مقاومة الصدأ وتأثيرها على الخواص الكيميائية والفيزيائية للخرسانة .

إن نتائج هذه الدراسة تبين بأن مقدرة الاسمنت الذي يحتوي على نسبة عالية من الالمونيوم ثلاثي الكالسيوم على امتصاص الكلوريدات أفضل من الاسمنت الذي يحتوي على نسبة أقل من الالمونيوم ثلاثي الكالسيوم وهذا يوضح مقاومته الأعلى لصدأ حديد التسليح . كذلك فان زيادة الحرارة وقت ترطيب الخرسانة وكمية القلويات في الاسمنت ووجود الاملاح الكبريتية والكلوريدات يقلل من قدرة امتصاص الكلوريدات وقد أثبتت التجارب بان الاسمنت العادي له مقدرة على امتصاص الكلوريدات الاساسية والتي داخل الخرسانة أكثر من الكلوريدات الثانوية من خارج الخرسانة .

إن تأثير اضافة الرماد المتطاير وخبث الفرن العالي على الخواص الكيميائية قليل مقارنة بتأثير دخان السيليكا الذي يزيد من قساوة الخاصية الكيميائية . كذلك فان المواد المضافة تعمل على تحسين التركيبه الفيزيائية للخرسانة بواسطة تضييق المسامات مما يقلل من نفاذ الكلوريدات والاكسجين ويزيد المقاومة الكهربائية وهذا يزيد من مقاومة الاسمنت الممزوج لصدأ حديد التسليح . ولذلك تعمل المواد المضافة على التقليل من تركيز ايون الهيدروكسيل وهذا يزيد من مقاومة الخرسانة لتفاعل السيليكا بالقلويات .

Chapter 1

INTRODUCTION

1.1 CONCRETE DURABILITY PROBLEM IN THE ARABIAN GULF REGION

1.1.1 CONCRETE DETERIORATION IN THE GULF ENVIRONMENT

Concrete construction in countries on the sea board of Arabian Gulf is showing an alarming degree of deterioration within a short span of 10 to 15 years. The low durability performance of concrete is due to several interactive factors. These are characterized mainly by adverse climatic and geomorphic conditions in conjunction with inadequate specifications related to materials and construction practices. The data developed through field studies at King Fahd University of Petroleum and Minerals (1-3) indicate that corrosion of reinforcing steel with concrete cracking and spalling, and sulfate attack with expansion, cracking and reduction in concrete strength are the two main forms of concrete deterioration in this region (1-3).

There is a feeling amongst concrete technologists that there is a suitable concrete even for the most aggressive service conditions **provided** the right concrete materials have been specified and appropriate construction practices have been adopted to commensurate with the nature and aggressivity of the exposure conditions. Whenever concrete deteriorates prematurely, there is a strong possibility that there exists an

inadequacy in either of three phases which taken together ensure a durable concrete material (4):

(a) realistic evaluation of the severity of in-service exposure conditions

(b) formulating material specifications to match the severity of in service exposure conditions evaluated in (a)

(c) adopting correct practices to obtain exactly what has been specified in (b).

These are the highly interactive phases which constitute the framework for durable concrete. A deficiency at any of the three stages constitutes a serious source of error in concrete practice and concrete performance is bound to suffer significantly; this is specially true of the Gulf conditions which undoubtedly constitute an aggressive service environment for concrete construction unmatched anywhere else in the world.

1.1.2 ENVIRONMENT-DURABILITY-MATERIAL SELECTION INTERACTION

The basic question, therefore, is: what is the right choice of concrete materials for the production of a durable concrete for the uniquely aggressive Gulf environment It is this environment-concrete durability-material selection interaction which should become the focus of attention in order to be able to deal with the concrete durability problem in this region in an effective and practical manner. What is needed is rationalized and refined specifications for concrete materials to match the nature and aggressivity of exposure conditions.

1.1.3 GULF ENVIRONMENT RELEVANT TO CONCRETE DURABILITY

1.1.3.1 General Geomorphic and Climatic Factors Affecting Concrete Durability

The most prevalent modes of concrete deterioration in the Gulf region are concrete cracking and spalling due to **reinforcing bar corrosion,** expansive cracking and loss of strength due to **sulfate attack.** These deteriorations are the visible manifestations of excessive salt presence in the concrete. Cracking due to alkali-silica reactivity has also been reported in the Gulf (5,6), which is due to the presence of reactive and potentially reactive aggregates.

Concrete construction on the coastal flats of the Arabian Gulf is continually exposed to ground and atmosphere charged with sulfate and chloride salts. Chlorides and sulfates are inducted into the concrete through mix constituents, salt contaminated reinforcement, brackish service water used for curing, and the frequent layers of salt laden moisture precipitated in the form of dew on exposed concrete surfaces. Salt on concrete surfaces is dissolved in surface moisture and enters the pores of concrete by capillary action. Salt deposits are retained in the pores of concrete after evaporation. Usually more salt penetrates than is leached out, thereby causing significant concentration to develop within the concrete over a period of years. Pockets of hygroscopic salts within concrete tend to retain moisture even when the external humidity is temporarily low, thus creating microclimates within the concrete pores which promote corrosive action.

The high incidence of corrosion against the backdrop of a highly salt polluted environment puts the chloride ion as the most important cause of reinforcement corrosion in the Gulf states. Chloride ion is a specific destroyer of the corrosion passivating

gamma ferric oxide film (7) formed on the steel surface by the alkaline environment in concrete (pH = 13), thereby initiating reinforcement corrosion.

Sulfate attack is characterized by the combination of sulfate salt with certain products of cement hydration resulting in expansion, cracking and loss of strength (8).

Several investigators have focussed on the deterioration caused by alkali-silica reactions as a result of use of aggregates in making concrete which are potentially reactive. The alkali-silica reactivity deterioration results in profuse map cracking, pop outs, exudation of gel and discoloration of concrete surfaces.

The extreme hot and hot-humid climatic conditions of the coastal hot-arid regions are almost ideal for accelerated chemical and electrochemical actions resulting in enhanced rebar corrosion, sulfate attack and alkali-silica reactivity. Temperatures as high as 70° C may be achieved on concrete surfaces due to solar radiation effects. As a rule of thumb, the rate of chemical reaction increases by 70% for each 10° C rise (9) in temperature. In addition to enhanced rate of reaction, the penetration of aggressive substances such as chloride ions, carbon dioxide, magnesium ions and sulfate ions proceed more rapidly. Time to corrosion initiation at 30° C is approximately one-third of that at 10° C due to the enhanced chloride penetration into concrete at higher temperature (10).

1.1.3.2 Specific Factors Affecting Concrete Durability

The specific factors which affect concrete durability in the Gulf region are:

(i) the **initial induction of sufficient chlorides** through coarse/fine aggregates and mix/curing water which are beyond the threshold

level. Such chloride salts are inducted right at the time of mixing and the detrimental chloride action commences at a very early stage when concrete is still very weak and porous and a corrosion passivating film is in the process of being formed on the surface of the reinforcement.

(ii) subsequent **additional ingress of chlorides from the external environment** to the steel-concrete interface through cracks, micro-cracks and pores in concrete.

(iii) the **concomitant presence of high chloride and sulfate concentrations** in soils and groundwater on construction sites along the Gulf seaboard. This is a unique situation in which chlorides and sulfates simultaneously permeate into concrete substructures such as foundations and subject them concurrently to sulfate attack and chloride induced rebar corrosion.

There are **four clear concrete environment conditions** which are significantly relevant to concrete durability in this region:

(i) predominant action of chlorides

(ii) conjoint action of chlorides and sulfates

(iii) predominant action of sulfates.

(iv) reaction of cement alkalies with reactive siliceous aggregates.

Further, chloride presence can be attributed to two mechanisms:

(i) **primary inclusion** of uniformly distributed chlorides called **primary chlorides**

(ii) **secondary permeation** of possibly non-uniformly distributed chlorides from external environment called **secondary chlorides.**

1.2 MECHANISMS OF PREDOMINANT CONCRETE DETERIORATIONS IN THE GULF REGION

1.2.1 CORROSION OF REINFORCEMENT

The corrosion of reinforcement in concrete is an electrochemical process involving a galvanic cell wherein chemical energy is converted to electrical energy. In the Gulf region electrochemical reactions result from chloride-laden pore moisture in contact with the reinforcement . For such reactions to occur on embedded steel in concrete, there must exist on or around the rebar in the steel-concrete system areas of differential electro-chemical potential which are electrically connected in concrete by an electrolyte. This electrolyte exists in the form of salt laden pore fluid in the Gulf concrete. When these conditions are met, corrosion occurs through the dissolution of metal ions to the moisture, leaving electrons behind (Reaction 1). By definition, this is an anodic reaction and the areas that corrode are called anodes. The remaining electrons move through the conductor metal from the anodic areas to non-corroding locations where they react with either water or oxygen to form hydroxyl ions(Reaction 2). By definition, this is a cathodic reaction and the locations at which this occurs are called cathodes. The electrons neutralize cations in the electrolyte, thus completing the electrical circuit.

$$Fe \longrightarrow Fe^{2+} + 2\,e^{-} \text{ -------- (1)}$$

$$O_2 + 2\,H_2O + 4\,e^{-} \longrightarrow 4\,(OH)^{-} \text{ -------- (2)}$$

Differences in metal potential may be obtainable either due to differences in metal itself (metal defects or differential impurities), or much more readily due to differences in the physical and/or chemical environment of highly heterogeneous concrete. The latter may result due to differences in alkalinity, chloride concentrations, oxygen availability, segregation, compaction, bleeding, permeability and the exposure conditions.

The usual chloride free environment of uncarbonated concrete is highly protective against corrosion of embedded steel for three reasons. **Firstly,** the aqueous environment within concrete matrix is characterized by significant presence of highly alkaline uncombined water in the well-distributed pores or voids of concrete; this environment passivates steel against corrosion. **Secondly,** concrete cover over reinforcement forms a defensive shield/barrier against the ingress of chlorides (from external source) and oxygen required for cathodic depolarization. **Thirdly,** concrete offers high resistivity to the flow of corrosion current.

In accordance with the Pourbaix diagram the redox potential for iron (-0.44 E_{H}) with respect to the hydrogen electrode lies above the region of immunity in both acid and alkaline solutions implying that iron will dissolve with the evolution of hydrogen in solutions of all pH values. However, passivation for iron/steel is indicated in an alkaline environment characterized by a pH range 9.5 to 12.5. The aqueous phase o concrete provides exactly such an environment. Calcium hydroxide constitutes, on an average 20 percent of the hydrated products and passes into solution till the pore water is saturated and acquires a high degree of alkalinity corresponding to a pH of 12.5. Soluble alkalies present in cement raise the pH to values in excess of 13.0 within a few weeks of hydration.

The passivation of steel in concrete system is attributed to the formation of a pro-

tective sub-microscopically thin oxide film in accordance with Reaction 3. The stability, integrity and protective quality of this film is characterized by the high alkalinity (OH^- ions) and oxygen availability.

$$2\,Fe + 3\,(OH)^- \longrightarrow Fe_2O_3 + 6e^- \text{ -------- (3)}$$

The loss of corrosion protection of steel is characterized by a decomposition of the protective oxide film by two specific circumstances. First by the ingress of atmospheric carbon dioxide to steel-concrete interface (Reaction 4) resulting in carbonation and second by the presence of chloride ions in concrete in the vicinity of steel. Chloride ion has been described as "a specific and unique destroyer" of the passivating film (Reaction 5 and 6).

$$Ca(OH)_2 + CO_2 \longrightarrow CaCO_3 + H_2O \text{ -------- (4)}$$

$$Fe^+ + 2\,Cl^- + 2\,H_2O \longrightarrow Fe_2(OH)_2 + 2\,H^+ + 2\,Cl^- \text{ -------- (5)}$$

$$Fe + 2\,Cl^- \longrightarrow FeCl_2 + 2\,e^- \text{ -------- (6)}$$

The unusually high incidence of corrosion against the backdrop of a highly chloride polluted environment puts the chloride ion as the most important cause of steel corrosion in the Gulf region.

In an attempt to elucidate the role of chlorides in the corrosion process, Hausmann (11) has proposed the "Chloride threshold" concept. According to Hausmann, the ratio of Cl^- to OH^- concentration should not exceed threshold of 0.60. Part of the local chloride may combine with the compositional phases of cement, specially with C_3A phase, to form insoluble compounds such as calcium chloroaluminates.

The precise mechanism by which chlorides actually disrupt the passivating film is not resolved as yet. The chloride corrosion reactions at anodes and cathodes in the absence and presence of oxygen are shown in Reactions 7 through 12.

In the absence of oxygen,

$$Fe + 2\,Cl^- \longrightarrow Fe^{2+} + 2\,Cl^- + 2\,e^- \text{ -------- (7)}$$

$$Fe^{2+} + 2\,Cl^- + 2\,e^- + 2\,H_2O \longrightarrow Fe(OH)_2 + 2\,H^+ + c\,Cl^- \text{ -------- (8)}$$

$$2\,H^+ + 2\,e^- \longrightarrow H_2 \text{ -------- (9)}$$

In the absence of oxygen,

$$Fe \longrightarrow Fe^{2+} + 2\,e^- \text{ -------- (10)}$$

$$O_2 + 2\,H_2O + 4\,e^- \longrightarrow 4\,(OH)^- \text{ -------- (11)}$$

$$Fe^{2+} + 2\,(OH)^- \longrightarrow Fe(OH)_2 \text{ -------- (12)}$$

It may be noted that :

(i) chloride corrosion causes a rapid reduction in the alkalinity at anodic sites to a pH level of about 5, due to iron chloride complexing followed by the hydrolysis and the release of hydrogen (Reaction 9) and,

(ii) chloride is regenerated which would perpetuate the corrosion even without further chloride addition.

Chloride corrosion in concrete may take place by both of the two common mechanisms: **micro-cell** as well as **macro-cell** . The first type is the general form of

uniform corrosion while the second type is characterized by a form of localized pitting corrosion that often occurs in concrete structures.

Corrosion products formed at anodic sites depend on the interactive effect of oxygen supply, alkalinity and type of corrosion cell developed at anodic sites. These are seldom of a single compositional variety and vary from white ferrous hydroxide, to yellowish green/greenish blue ferrous chloride/hydrated ferrous chloride to black granular corrosion products Fe_2O_3 (Reaction 13).

1.2.2 SULFATE ATTACK

Sulfate attack in concrete is primarily characterized by a reaction of sulfates with monosulfoaluminate hydrate or calciumaluminate hydrates which exist as a hydration product in high C_3A cements in accordance with the following reactions:

$$C_3A + 26H + 3C\overline{S} \,.\, 2H \longrightarrow C_3A \,.\, 3C\overline{S} \,.\, H_{32}$$

$$2C_3A + C_3A\ 3C\overline{S}\ H_{32} \longrightarrow 3C_3A \,.\, C\overline{S}H_{18}$$

The reaction of monosulfoaluminate hydrate and/or calcium aluminate hydrate with sulfates results in the formation of ettringite in accordance with the following reactions:

$$C_3A.C\overline{S}\,H_{18} + 2CH + 2\overline{S} + 12H \longrightarrow C_3A.3C\overline{S}.H_{32}$$

$$C_3A.CH \,.\, H_{18} + 2CH + 3\overline{S} + 11H \longrightarrow C_3A.3C\overline{S}.H_{32}$$

Formation of ettringite is associated with an overall expansion and cracking of concrete.

The sulfates may be derived from $CaSO_4$, Na_2SO_4 and $MgSO_4$. $MgSO_4$ causes the severest type of sulfate deterioration as it is capable of attacking the binder C-S-H gel. The reaction products are gypsum, brucite, silica gel and a magnesium silicate of possible composition $4MgO . SiO_2 . 8.5 H_2O$.

The expansive type of sulfate attack is associated with cements of high C_3A content, more porous and permeable concretes, and relatively high concentrations of calcium hydroxide in the cement matrix. It appears that the low sulfate form of calcium sulfo-aluminate present in such concretes reacts with sulfate ions in the presence of calcium hydroxide to produce initially a colloidal form of ettringite which is responsible for the swelling pressure and damage to concrete. When the expansion has created sufficient space, acicular radiating clusters of ettringite crystals form in the resultant voids and cavities.

Another type of sulfate attack which is commonly prevalent in the Middle East occurs when sulfates react with excessive calcium hydroxide produced in high C_3S cements. The product of reaction is gypsum which heavily inducts SO_4 ions into the C-S-H gel causing loss of strength and cohesion. This type of attack is manifested by an eating away or softening of the cement matrix, which leaves the aggregate standing out from the eroded concrete. The gypsum oriented sulfate attack may occur in the so called low C_3A sulfate resistant cements if the C_3S content of such cements is unusually high, as is the position in the locally manufactured cements in the Gulf States.

1.2.3 ALKALI-SILICA REACTIVITY

Damage due to alkali-silica reaction has received considerable attention in the Middle East (5,6) and over the years the problem has assumed global concern. The deteriorations caused by the alkali-silica reactions as a result of reactions between cement alkalies and reactive aggregates results in profuse map cracking, pop outs, gel exudations and discoloration of concrete surfaces. It is now generally recognised that the development of high concentrations of alkali hydroxides in the pore solution of concrete is the first and the most vital step in the sequence of responses which precede and eventually lead to the visible manifestations of alkali-silica reaction deteriorations.

1.3 BLENDED CEMENTS

In recent years, pozzolanic and cementitious by-products such as fly ashes , blast furnace slag and silica fume are being strongly suggested as admixtures to improve the properties of concrete in general and durability in particular. When used as partial replacement of or addition to cement, they modify both the physical structure and the chemical environment of the hydrated cement. On one hand they improve the impermeability but on the other they weaken the favourable alkaline environment of the hydrated cement. It is hoped by many researchers that there is a potential for making these materials environment-friendly materials.

It is generally accepted now that the cementitious and pozzolanic properties of cementitious and pozzolanic by-products used as cement additives depend on their particle shape / size distribution and mineralogical composition and not on their chemical composition and source of origin alone. A classification of cementitious and pozzolanic materials based on their cementitious or pozzolanic activity when used in combi-

nation with portland cement given by Mehta (12). They are classified as cementitious (e.g. blast furnace slag), cementitious and pozzolanic (e.g. high calcium fly ashes), normal pozzolans (e.g. low calcium fly ashes) and highly pozzolanic (e.g. silica fume and rice husk ash).

1.3.1 MECHANISM OF HYDRATION OF BLENDED CEMENTS

Hydration of fly ash, blast furnace and silica fume blended cements is a three stage reaction. Immediately after mixing with water, particles of these admixtures are surrounded by rims of cement hydration products. When alkali and calcium hydroxides and sulfates are available due to further reaction of cement, the hydroxide ions activate the hydration of glasses present in the mineral admixtures. Finally, the pozzolanic reaction takes place in which calcium hydroxide is consumed to form secondary calcium silicate hydrates. The resulting structure is likely to be dense with a refined and discontinuous pore structure (12).

1.3.2 SULFATE RESISTANCE OF BLENDED CEMENTS

Sulfate resistance of fly ash blended cements is studied by Dunstan (13), Mehta (14) and others. Due to a wide variation in physical properties and chemical composition, the behavior of different fly ashes to attack by sulfate ions is also different. From his study conducted on 13 concrete mixes made from lignite or subbituminous coal sources, Dunstan (13) established an empirical sulfate resistance factor R, which is given by the ratio of percentage of calcium hydroxide in excess of 5% to iron oxide of the fly ash. Dunstan found that when R is less than 1.5, the sulfate resistance of the fly ash blended cement was improved. However, when R is more than 3, the sulfate resis-

tance was reduced. Mehta (14), based on his experimental data showed that even the fly ashes having an R factor of less than 1.5 reduced the sulfate resistance. He suggested that rather than the chemical composition or R factor of a fly ash, it is the mineralogical composition of the cement+fly ash interaction product that controls the sulfate resistance. When the hydrated cement-fly ash mixtures contained the monosulfate hydrate or calcium aluminate hydrates, on sulfate immersion, they showed expansion and strength loss associated with ettringite formation. However, when the cement pastes containing fly ashes contained ettringite prior to immersion in sulfate, they performed satisfactorily in the sulfate test. Whether a hydrated cement-fly ash contain monosulfate hydrate and calcium aluminate hydrates or ettringite depends on the alumina-sulfate ratio of the hydrating system (14).

Partial replacement of cement with blast furnace slag is found to improve the sulfate resistance when the slag proportion exceeds 50% of the total cementitious material (15). When a high proportion of slag is used, the C_3 A content of the mixture is proportionally reduced, thereby increasing the sulfate resistance of the slag cement. However, according to Lea (16) the increased sulfate resistance not only depends on the C_3 A content of the cement alone, but also on the alumina content of the slag. Lea reports that sulfate resistance of the slag cement was increased when the alumina content of the slag was less than 11%, regardless of the C_3 A content of the cement, when cement was replaced in the range of 20-50% with granulated slag. The increased sulfate resistance of the slag cements is also attributed to the reduction of calcium hydroxide due to formation of secondary calcium silicate hydrate which reduces the environment required for the formation of expansive ettringite and the reduced permeability of the slag cements to the ionic diffusion (17-19).

Results of tests conducted by Rasheeduzzafar et al (20) and Cohen and Bentur (21) show that silica fume addition to portland cement improves the resistance to sodium sulfate attack, however, it can impair resistance to magnesium sulfate attack . Rasheeduzzafar et al (20) found that the pozzolanic reaction between calcium hydroxide and silica fume removed most of the calcium hydroxide from the hydrated cement paste, as confirmed by X-Ray diffraction analysis. Apart from decreasing the vulnerability to formation of gypsum, the reduction in calcium hydroxide concentration due to reaction with silica fume increases the solubility of the hydrated calcium aluminates thereby causing the sulfate reaction to occur through solution and therefore without expansion (20). Mehta (22) has hypothesized that in the absence of calcium hydroxide, the ettringite produced is in the form of large lath-like crystals which are not expansive. It is only under conditions of high hydroxyl ion concentration, due to the presence of calcium hydroxide, that a microcrystalline ettringite is formed which is capable of adsorbing large amounts of water on the surface causing considerable expansion (22).

1.3.3 CORROSION OF REINFORCEMENT

Time to corrosion initiation tests carried out by Rasheeduzzafar et al (23) on plain blended cement concrete using microsilica, blast furnace slag and fly ash on partial replacement basis showed that the incorporation of the blended materials significantly improved corrosion initiation times of reinforcing steel.

Once the corrosion initiation takes place, corrosion propagation depends upon resistivity of concrete, rates of oxygen and moisture flow to the steel level and aggressivity of pore solution. Electrical resistivity and oxygen diffusion are significantly improved due to the incorporation of blending materials. However, on the other hand, these materials increase pore solution aggressivity. In view of these facts, it would be of

considerable interest to study the effect of these blending materials on corrosion rate of steel in concrete in the active corrosion state.

1.3.4 CONTROL OF ALKALI-SILICA REACTIVITY

In terms of suppression of alkali-silica reaction (ASR), it is now widely recognised that microsilica possesses a remarkable ability to actively remove alkali hydroxides from the pore solution, thereby virtually eliminating the physico-chemical responses resulting in the expansion and cracking of concrete. Though slag also suppresses ASR, its role as an alkali remover is unclear, and the mechanism by which it acts remains unresolved and controversial.

It is of considerable significance to optimize cement replacement by microsilica as an efficient preventive method against ASR. Apart from the practical consideration that the cost of microsilica is about twelve to fourteen times the cost of ordinary portland cement in the Middle East market, an overdose of microsilica may bring about other concomitant adverse effects which may mitigate its now widely recognised beneficial role in improving the general performance of concrete. It has been found that the replacement of portland cement by increasing proportions of microsilica leads to a lowering of the pH and to an increase in the proportion of the free chlorides in the pore solution, thereby significantly increasing the Cl^-/OH^- ratio and the risk of chloride-induced corrosion.

In terms of potential use of slag and fly ash in the prevention of ASR in concrete, sufficient data is not available to evaluate their effectiveness as alkali removers and to elucidate the mechanism by which they act to suppress ASR.

1.3.5 PHYSICAL FACTORS

1.3.5.1 Permeability to Water and Chloride Ions

Microcracks in concrete are a principal source of permeability which is the single most important criterion of concrete durability. Mineral admixtures such as fly ash, blast furnace slag and silica fume can be used to reduce the microcracks and thereby improve general durability of concrete.

Studies conducted at King Fahd University of Petroleum and Minerals (24) show that 20% replacement of cement by a Class F fly ash in concrete cured for 90 days reduced permeability. Berry and Malhotra (25)cited studies of Davis to show that concrete pipes containing 30 or 50% fly ash as cement replacement and cured for 6 months were approximately five times impermeable than corresponding plain concrete. Holden et. al (26) reported that the chloride ion diffusion was decreased when 30% fly ash was used as cement replacement.

According to a recent review by Douglas (27), detailed data on permeability of concrete with slags are not available. Douglas cited Kondo et al and Baker's work on cement mortars to show that, with curing age, the diffusion coefficient in slag cement mortars diminished faster than the diffusion coefficient in a portland cement mortar and that slag cement mortars were 10 to 100 times less permeable to water than portland cement mortar.

Water permeability of a lean concrete mix (100 kg./cu.m cement content) with silica fume of 10% by weight of total cementitious material was found to be less by four order than that of control concrete (28). However at high cement contents the degree of effectiveness of silica fume in reducing permeability was found to be diminished.

Sellevold and Nilsen (28) report that the available data indicate that the silica fume in concrete reduces the permeability more than it improves the compressive strength i.e., the efficiency factor is greater with respect to permeability than with respect to compressive strength.

1.3.5.2 Pore Size Distribution

Very few studies have been conducted on pore size distribution of blended cements. Studies conducted by Manmohan and Mehta (29) and Marsh et al (30) show refinement of pores in fly ash and slag blended cements. The pore refinement in blended cements is responsible for the reduced permeability to water and aggressive ions.

1.3.5.3 Electrical Resistivity

There is no systematic data available on electrical resistivity of blended cements. Recent literature review on supplementary cementing materials by P.K.Mehta (12) reports only one study conducted on electrical resistivity of silica fume blended cement by Gjorv. Gjorv (31) found that the electrical resistivity of a concrete incorporating 20% silica fume by weight of total cementitious material, was about 15 times that of the plain concrete.

1.4 CEMENT FACTORS AFFECTING CONCRETE DURABILITY

Concrete is a diphasic material comprising hardened cement paste and aggregates. Although the aggregates constitute about 70% of concrete, it is regarded as neutral,

innocuous, passive, cheap filler material. It is the hardened cement paste which is the active component and is responsible for all the good and bad qualities of concrete. Cement paste has a pre-eminent position in determining the most important property of plastic concrete i.e workability and the most important properties of hardened concrete, strength, durability and dimensional stability. This focuses on the decisive and critical role of cement in determining the durability performance of concrete structures.

Three cement factors can be identified which very strongly affect the concrete durability in the Gulf region:

(i) **cement compositional** variables

(ii) **cement properties** affecting the **alkalinity of concrete**

(iii) **cement characteristics** affecting the **physical structure of concrete.**

1.4.1 CEMENT COMPOSITIONAL PARAMETERS AND CONCRETE DURABILITY

It is of considerable significance that cement is not a unified chemical entity. It comprises of four distinctly separate phases C_3S, C_2S, C_3A and C_4AF, which hydrate, generate products of hydration and contribute to concrete properties in accordance with their individual characteristics and properties.

Cement compositional variables affect concrete durability in two ways:

(i) through the **chloride combining capacity** of its phases and hydration products.

(ii) through the formation of products which **cause expansions/ cracking** as well as degradation of cohesion/strength of hardened cement paste.

1.4.1.1 Chloride Combining Capacity

(a) C_3A Factor :

Corrosion of reinforcement is promoted by free dissolved or unbound chloride ions present in the pore fluid of concrete. Chlorides which are chemically bound or strongly adsorbed by cement phases and hydration products are innocuous or passive in terms of corrosion action on concrete reinforcement. In view of the fact that the corrosion of reinforcing steel in the Gulf region is entirely chloride oriented, the complexing of free chlorides with cement is a reaction of great significance in concrete. The combining of chlorides with cement phase/hydration products is akin to chloride removal from its hazardous role of steel corrosion promotion.

The predominant phase of cement which complexes with chlorides is tricalcium aluminate (C_3A) forming either insoluble calcium monochloroaluminate ($3CaO.Al_2O_3.CaCl_2.10H_2O$) or calcium trichloroaluminate ($3CaO.Al_2.O_3.3CaCl_2.32H_2O$) also called Friedel's salt. This implies that high C_3A cements would tolerate more chlorides without corrosion initiation and should offer higher chloride corrosion resistance than low C_3A cements. This beneficial effect of the C_3A content on corrosion resistance has been established by Rasheeduzzafar et al (32) and is confirmed by other studies (33-36).

In the pore solution study carried out by Page and Vennesland (37) on a medium Type II 7.2% C_3A cement, two levels of chloride additions (0.6 and 1.6% calcium chloride) were made. In a second study carried out by Diamond (38) a 9.1% type I OPC was used and chloride levels of 0.05, 0.2, 0.5, 1.0, 1.5 and 2.0% by wight of

cement derived from calcium chloride and were inducted. Sodium chloride was also used to study cation effect for chloride concentration corresponding to 1.0, 0.5, 0.2% calcium chloride.

The comparison of these two data show about a 100% differential in the values of equilibrium chloride concentrations remaining free in the pore solution. This differential obviously cannot be explained by their relatively small differential of C_3 A content (7.2% and 9.1%) in the two cements used.

In addition to the inconsistency, these data are also limited to only medium C_3 A contents giving no information on the free chlorides which would be available in low or high C_3 A cements.

However, in this significant chloride combining mechanism there are several unresolved issues which need further investigation. Firstly, the relationship between C_3 A content and chloride removal is affected by several parameters and is not understood quantitatively. Some of these interactive parameters are discussed below:

(i) Chloride Combining Capacity of C_3A in the presence of sulfates :

C_3A has great reaction affinity for sulfate ions and is known to combine preferentially with sulfates in the presence of chlorides (39). Schwiete et al (40) investigated the order of combination of aluminates in cement pastes containing calcium hydroxide, gypsum and calcium chloride. The combination of sulfate and chloride occurred in the following order : formation of the trisulfoaluminate hydrate until the sulfate was consumed, formation of the chloroaluminate hydrate until the chloride was consumed and formation of the monosulfoaluminate hydrate from the trisulfoaluminate and excess aluminate or aluminoferrites present. C_3 A combination with sulfates results in the

initial formation of trisulfoaluminate hydrate ($C_3A.3CaSO_4.32H_2O$) which converts over a period of days to weeks into a monosulfoaluminate hydrate ($C_3A.3CaSO_4.32H_2O$) (41). Since 3-4 percent gypsum ($CaSO_4.2H_2O$) is added to cement to regulate its time of set, stoichiometric calculations show that about 2.5 percent C_3A will be needed for combination with 4 percent gypsum to form trisulfoaluminate, if it is the stable product of hydration. However, about 6 percent C_3A will be preferentially consumed in the complete combination of 3-4 percent gypsum into monosulfoaluminate hydrate, if trisulfoaluminate hydrate is unstable due to the presence of unconsumed C_3A. This implies that in low C_3A cements having C_3A less than 6 percent, no C_3A will be available for chloride removal. In high C_3A cements, only the balance C_3A which has not been used in sulfate reactions would be available for chloride removal.

The interactive effect of sulfate ions on chloride removal is also of great practical significance for the **corrosion durability of concrete substructures such as foundations in the Gulf States.** On the Gulf seaboard the unique situation on construction sites is usually characterized by concomitant presence of high chloride and sulfate concentrations in soils and groundwater. Foundations are concurrently subjected to sulfate attack and chloride induced rebar corrosion. In such a situation the reduction in the chloride removal capacity of C_3A by sulfates is of considerable practical significance.

(ii) Type of chlorides :

Chlorides derived from calcium chloride have been shown as having higher complexing ability with C_3 A than chlorides derived from sodium chloride (42). Further,

calcium chloride based chlorides cause higher pore solution concentration of OH^- ions than sodium chloride based chloride (42,43). Calcium chloride is the most commonly used accelerator and deicing salt, whereas the sodium derived chlorides are commonly induced into concrete through sea-dredged sand and seawater.

(iii) Chloride Binding Capacity Limits of C_3 A :

Another fact of considerable significance is the limiting chloride binding capacity of C_3A. Studies carried out at King Fahd University of Petroleum and Minerals (44) showed that the differential in the corrosion resistance performance in terms of time-to-cracking of a high C_3A (9.5%) and low C_3A (2.8%) cement was reduced as the chloride content of the concrete is measured. This indicates a definite chloride binding limit of a specified C_3 A content in cement. However, a view has been expressed without evidence (45) that the chloride present, up to several percents by weight of cement, is distributed in a specific ratio (depending on various parameters) between the solid cement phases of hydration products and the pore solution of the hardened cement paste. This implies that when the chloride included is greater, the volume of combined bound chloride would also be higher. No data exist on the chloride binding limits of various C_3A contents, and research in this area is needed to elucidate this relationship.

(iv) Stability of Calcium Chloroaluminate Compounds :

In the Gulf region concrete surfaces may be heated up to 70^oC in summer months due to dried solar radiation effect. No organised research has been carried out on the stability of calcium monochloroaluminate and trichloroaluminate compounds at temperatures higher than room temperatures and under the influence of carbonation.

(v) Manner of Occurrence of Chlorides :

There are two mechanisms by which chlorides enter concrete. In the Gulf condition, significant chlorides may be induced by the constituent materials at the time of mixing and subsequently at very early ages through the brackish curing water. This **primary chloride** is, therefore, present in concrete when cement hydration reactions are vigorously proceeding and, it seems, would have a significantly better chance of complexing with hydration products of C_3A or other phases of cement such as C_3S. On the other hand chlorides could also permeate into hardened mature concrete from external environment when the hydration process is advanced or completed and the structure is in service. Such **secondary chlorides** are inducted into concrete through de-icer salts or through chloride bearing soils and groundwater and marine environments. In such a situation it may be presumed that with advanced or virtually completed hydration, the extent of chloride combination would be less. Also, probably the combination compounds formed would be less stable. One investigation (46) confirms the presence of calcium chloroaluminate and hence the chloride combination in concrete wherein chlorides diffused at a later age. However there are also indications that in such cases chloride combination occurs to a significantly lesser extent.

There is no organised research data available to elucidate the differential in the chloride binding capacity of primary and secondary chlorides in cements of different types, which vary with respect to the C_3A content.

(b) Chloride Binding Capacity of Alite Phase of Cement

While the effect of C_3A is the dominant mechanism for the removal of free chloride ions from pore water, other processes also contribute, because even cements that do not contain C_3 A have been found to exhibit significant chloride binding capacity

(36,47). There is, however, little quantitative information available in the literature concerning the relative influence of cement minerals other than C_3 A. In the case of ferrite phase, C_4AF, reactions leading to the formation of calcium chloroaluminate and chloroferrite hydrates have been shown to occur (35) though their practical importance in binding free chloride ions is reported to be small(39).

As regards to calcium silicates, specially the alite (C_3 S) phase of cement, there is significant controversy about its effectiveness in chloride removal. Ramachandran (48,49) has suggested that a high proportion of the chloride ions contributed by the admixture are rapidly removed from the solution phase, forming an interlayer chemisorbed complex within C-S-H gel. More recent investigation by Ramachandran et al (50) also confirms that in mature pastes of C_3S , hydrated at a water/solid ratio of 1.0 in the presence of calcium chloride, a significant proportion of chloride ions becomes bound to hydration products. However, this later work indicates that the extent of binding by C_3S is considerably lesser than suggested by Ramachandran in his earlier studies (48,49). Sidney Diamond and Lopez-Flores (51) in a 1981 study, however, appear to negate Ramachandran's conclusions. Using high pressure sampling technique (52), it was found that in cement pastes, made with calcium chloride addition and w/c ratio of 0.4 to 0.5, high concentration of dissolved chloride ions in pore liquid were retained throughout fairly long periods of hydration. In another study Sidney Diamond (38) has , however, confirmed that he has observed many times the presence of chloride within local regions of calcium-silicate-hydrate (C-S-H) gel hydration product in examining concrete exposed to salts by energy-dispersive X-ray analysis in a scanning electron microscope. He is of an opinion that it is extremely likely that a portion of the chloride removed from solution is resident within (or perhaps in part adsorbed on) C-S-H gel hydration product within the paste. However, in a 1985 study carried out

on chloride binding capacities of alite (C_3S) phase using the technique of pore fluid chemistry, Lambert et al (53) have concluded that "the quantity of chloride ion that became incorporated into hydration products of alite was insignificant".

(c) Influence of Blending Admixtures on Chloride Binding Capacity

Silica fume, blast furnace slag and fly ash are the three blending admixtures which have a high potential of usage in the Gulf region for the production of durable concrete. It would therefore be of considerable interest to investigate the effect of these additions on chloride removal mechanisms. Formulation of high performance blended cement is a relatively recent development and scant organised research data are available on this aspect. In a 1983 study by Page and Vennesland (37) using the technique of pore fluid chemistry, it was found that with increasing percentage of cement by silica fume replacement (10 to 30 percent), the capacity of the cement to bind chloride ions, introduced during mixing, declined. They have hypothesized that this may be due to the increased solubility of Friedel's salt at reduced pH levels caused by silica fume addition. A recent study carried out by Kawamura and Kayyali (43), has developed data pertaining to the effect of fly ash on chloride ion concentrations in pore fluid. They found that fly ash has little effect on chloride ion concentration in pore solution of mortars below the dosage of 2% Cl^- as $Ca\ Cl_2$. However, the addition of fly ash considerably reduced Cl^- concentration in mortars treated with NaCl at 1 and 2 % chloride levels.

Both the aforesaid studies have developed only limited data, specially with respect to the effect of these admixtures on different cement types in terms of C_3A factor. The study by Page was carried out on a 7.18% C_3A cement whereas the Japanese study on

fly ash was carried out on a 3.73% C_3 A cement. The C_3A content of the first study is relatively low where as that of the second investigation is too low for any significant chloride binding role of C_3A in the presence of these admixtures. In view of their high usage potential it would be of great interest to see the chloride binding effect of varying C_3A cement contents in conjunction with these three blending materials.

1.4.1.2 Formation of Products Causing Expansion and Degradation of Concrete

Deterioration of concrete in sulfate bearing soil and groundwater can take place in either or both of the following manners:

(i) Overall expansion and cracking due to formation of ettringite ($3CaO.Al_2O_3.3CaSO_4.32H_2O$) as a result of reaction between sulfate ions and the hydration products of C_3 A, mainly calcium monosulfoaluminate ($3CaO.Al_2O_3.CaSO_4.10H_2O$).

(ii) Eating away or softening of concrete due to the conversion of hydration product $Ca(OH)_2$ to gypsum as a result of reaction of calcium hydroxide with sulfate ions.

In terms of cement composition, there has been a definite perception of a general correlation between C_3 A content and sulfate resistance for quite sometime now. An increase of C_3 A beyond 8 percent results in a sharp increase in the sulfate attack.

Another factor which controls sulfate resistance of plain cements is the ratio of two silicates (C_3S/C_2S) which constitute about 75% of cement by weight. When the content of the two aluminates (C_3A and C_4AF) is relatively constant, the ratio of the

silicates (C_3S/C_2S) controls the quantum of calcium hydroxide in hydrated cement paste as well as the rate of early age hydration and strength development. High C_3S/C_2S cements result in higher proportions of calcium hydroxide and higher amounts of gypsum on exposure to sulfates. The formation of gypsum results in softening of concrete. In order to evaluate the influence of C_3S/C_2S factor on the sulfate resistance of cements, Rasheeduzzafar et al (20) carried out tests on cements designated as cements 6 and 7. Cement 6 had C_3 A of 9.3% and C_3 S/C_2 S ratio of 2.57 while cement 7 had C_3 A of 11.9% and C_3 S/C_2 S ratio of 7.88. The results showed that at an immersion age of 150 days, the strength loss due to sulfate attack for cement 7 (C_3 S/C_2 S : 7.88) was 1.8 times that for cement 6 (C_3S/C_2S : 2.57). It is obvious that such a big difference in sulfate deterioration can not be attributed to the relatively small difference in the C_3 A contents of the two cements alone. It is most likely due to the higher proportion of C_3 S and a lower C_2 S content of cement 7 in comparison to these values in cement 6.

1.4.1.3 Deteriorations Due to Alkali-Silica Reactions

Damage due to alkali-silica reaction has received considerable attention in the Middle East (5,6) and over the years the problem has assumed global concern. The deteriorations caused by the alkali-silica reactions as a result of reactions between cement alkalies and reactive aggregates results in profuse map cracking, pop outs, gel exudations and discoloration of concrete surfaces.

It is now generally recognised that the development of high concentrations of alkali hydroxides in the pore solution of concrete is the first and the most vital step in

the sequence of responses which precede and eventually lead to the visible manifestations of alkali-silica reaction deteriorations.

In terms of suppression of alkali-silica reaction (ASR), it is now widely recognised that microsilica possesses a remarkable ability to actively remove alkali hydroxides from the pore solution, thereby virtually eliminating the physico-chemical responses resulting in the expansion and cracking of concrete. Although slag and fly ash also suppress ASR, their role as alkali removers is unclear, and the mechanism by which they act remains unresolved and controversial.

1.4.2 CEMENT PROPERTIES AFFECTING ALKALINITY OF CEMENT

The chloride concentration that can be tolerated by steel before corrosion is initiated is dependent on the electrochemical potential of the steel and more significantly on the pH of the surrounding cement paste. While it is certainly of interest to establish the equilibrium chloride ion concentration that would remain indefinitely in the pore solution of a given cement, it is reasonably well established that the depassivation of steel, where it occurs, is a function not only of chloride ion concentration but also of OH^- concentration as well. Hausmann (11) has suggested a threshold Cl^-/OH^- value of 0.60, Hausmann's tests were carried out on simulated pore solution of pH less than that obtainable in cement. Gouda (54) has also carried out tests on artificial solution of varying pH values and has suggested different threshold Cl/OH ratios for different pH values. Both their studies were carried out on simulated solutions and there is no concrete derived data as yet which establishes the threshold chloride values for steel corrosion in concrete. There are difficulties in establishing a critical chloride level in the absence of an authentic concrete based Cl / OH threshold value.

Two studies (38,53) carried out on Cl^-/OH^- ratio in pore solution of plain cements are related to medium C_3A cements (9.1% and 7.2%) and give widely divergent results with 100% differential.

It is a matter of considerable practical significance that both chloride binding capacity (and hence free chloride content in pore solution) and the pH (and hence the OH^- concentration of the pore electrolyte) are strong function of the cement composition. The pH and consequently the OH^- concentration of the pore solution would be significantly affected by the addition of blending materials such as silica fume, fly ashes and blast furnace slag because of the calcium hydroxide consumption (37,55) in secondary reaction between the reactive silica of the pozzolanic material and the calcium hydroxide of hydrated cement. This significant modification of the OH^- concentration in conjunction with the effect of blending materials on chloride binding capacity will completely alter Cl^-/OH^- ratio in the pore solutions of the blended cements. No study has been carried out to evaluate the Cl / OH ratios in low and high C_3A cements which are of considerable importance for this region because o their high sulfate and chloride resistances respectively.

1.4.3 CEMENT CHARACTERISTICS AFFECTING PHYSICAL STRUCTURE OF CEMENT

Physical structure of cement paste and concrete, signifying its impermeability to aggressive ions, moisture and gases, is a cornerstone of several mechanisms which explain the high durability performance of certain special modified cements. Impermeability and dense structure as a **physical factor** has received scant attention compared to **chemical factors** which are being extensively investigated currently in durability

studies. Two examples illustrate this contention.

The first example is from the data developed in preliminary tests of this research program on a plain and microsilica blended cements. The parent cement used for both the cements was a 14% C_3A cement. The data show that in spite of a 36 time higher Cl^-/OH^- ratio for the pore fluid of microsilica blended cement compared to plain cement, its corrosion resistance performance is 3 times better. This corrosion performance position is a total reversal of the pore solution chemistry indication, which show the microsilica blended cement to be 36 times more vulnerable to corrosion initiation.

The second example is from research carried out by Bakker(56) on alkali-silica expansion performance of plain and blast furnace slag cements. The alkali concentrations (as equivalent Na_2O) in the pore fluid of plain and 75% blast furnace slag cements were 0.72% and 0.95% respectively. The alkali-silica reaction expansions of these two cements in 40x40x160 mm, 0.5 W/C ratio mortar prisms made with reactive pyrex glass were 4.0 mm/m and 0.6 mm/m respectively. The data show that although the alkali concentrations in the pore solution of blast furnace slag cement was 1.4 times higher, the expansions in the blast furnace slag cement specimens were 7 times lower than for the plain cement specimens.

Both the behaviors can be explained on the basis of the **physical structure** of the microsilica and the blast furnace slag cements. Microsilica blended cement concrete was observed to be more than ten times more impermeable than ordinary portland cement concrete. Bakker has also explained (56) the higher alkali-silica expansion resistance performance of blast furnace slag on the basis of its dense impermeable structure. The transport of alkali ions in two-week old blast furnace slag cement mortar was found to be 15 times slower than in ordinary portland cement mortar and the blast fur-

nace slag cement mortar was found to be ten to one hundred fold more impermeable to water than ordinary portland cement (56).

This durability performance pattern of blended cements emphasises the physical factor as pre-eminent criterion of concrete durability. The **two most important characteristic signifying the physical factor** are the **impermeability** and the **electrical resistivity of concrete.**

The mechanisms of both the dominant and most widely prevalent causal factors, rebar corrosion and sulfate attack, generating concrete deterioration in the Gulf environment are extremely permeability oriented. Sulfate attack occurs when sulfate solutions permeate into the concrete matrix, and rebar corrosion cells are developed and activated by the diffusion of chlorides and oxygen to the steel-concrete interface. Chlorides depassivate the steel and oxygen depolarizes the cathode, thereby creating conditions for the onset of corrosion.

Rebar corrosion being an electrochemical process, the flow of corrosion current is a strong function of the electrical resistivity of concrete. Electrical resistivity of concrete predominantly depends on the moisture conditions and the **denseness of concrete structure** (57,58).

In terms of permeability, the most important factor is the pore size distribution and not the total porosity (29). A larger number of smaller pores resulting from segmentation of larger linked pores significantly reduces permeability to water and moisture and ionic transportation into concrete. Relatively little work has been done on pore size distribution evaluation of blended cements.

Electrical resistivity data for plain concrete is also scant, and virtually no data exist on the electrical conductance characteristics of blended cements.

Chapter 2

2. OBJECTIVES AND RESEARCH PROGRAM

Research carried out at King Fahd University of Petroleum and Minerals (23) on concrete durability indicates that the corrosion resistance performance of plain cement is a strong function of its C_3A content. Higher C_3A content improves corrosion resistance performance. Concrete made with 14% C_3A plain cement performed 2.5 times better than a 2% C_3A cement in terms of corrosion initiation time. Also, certain blended cements performed manifold better than even the 14% C_3A plain cement in terms of corrosion resistance. A 20 and 10% microsilica blended cement concrete performed 3 times better than plain 14% C_3A Type I cement concrete, whereas a 70% blast furnace slag cement and 30% fly ash blended cement performed 2.11 and 1.75 times better than the corresponding plain 14% C_3A cement concrete respectively.

Likewise, in terms of expansions and resulting disruption due to alkali-silica reactivity , incorporation of 10 and 20% microsilica and 60 and 70% slag reduced expansions from nine times the permissible expansion to safe values ranging from one-tenth to one-half the allowable expansion.

There is a general lack of information about the mechanisms which determine the durability performance of certain plain and blended cements. Amongst the important broad factors which influence durability mechanisms related with corrosion of rein-

forcement and deterioration due to alkali-silica reactivity of plain and blended cements are:

(a) the chemical environment of concrete

(b) the physical structure of concrete

The chemical environment of concrete determines the aggressivity of the pore solution affecting corrosion risk and the severity of the alkali-silica reactions culminating in the cracking of concrete. The physical structure determines the mobility of aggressive substances toward steel-concrete interface for corrosion and mobility of hydroxyl ions toward the reaction sites for alkali-silica reactivity.

From the standpoint of reinforcing steel corrosion and alkali- silica reactivity deteriorations, the **chemical environment** of concrete is characterized by the concentration of chloride and hydroxyl ions in the pore solution of concrete. The predominant factors which affect the concentration of the aforesaid ions in the pore solution are those which influence the **chloride binding capacity** of cement and its **alkalinity.** The following factors may be identified as affecting **chloride binding capacity** of cement and its **alkalinity:**

(i) compositional characteristics of cement in terms of C_3A and **alkali contents.**

(ii) concomitant presence of **sulfate ions**

(iii) **temperature**

(iv) **mode of occurrence** of chlorides

(v) **level** of chloride contamination

(vi) **Presence of mineral admixtures** such as microsilica, blast furnace slag and fly ash.

The **physical structure** of concrete is mainly governed by the pore size distribution of the hardened cement paste. A refinement of the pore size distribution retards the mobility of aggressive substances such as chlorides and oxygen as well as increases the electrical resistivity of concrete, thereby reducing the flow of corrosion current. The single most important factor which brings about desirable changes in the physical structure of cement paste is the inclusion of mineral admixtures such as microsilica, blast furnace slag and fly ash.

The objective of this research is to study the effect of the following factors on the **chemical environment** and **physical characteristics** of concrete in an effort to evaluate their influence on the mechanism of corrosion resistance and alkali-silica reactivity:

(i) C_3A **content** of cement

(ii) **alkali content** of cement

(iii) **level** of chlorides

(iv) **sulfate-chloride** interaction

(v) **temperature** of concrete

(vi) **mode of occurrence** of chlorides (internal and external)

(vii) **presence of mineral admixtures** such as microsilica, blast furnace slag and fly ash.

The presence of mineral admixtures such as microsilica, blast furnace slag and fly ash significantly modifies the basic compositional characteristics of cement. Cements formulated by the blending of these materials are called blended cements. The study therefore includes a study of durability mechanisms of plain as well as blended cements.

The details of the program are given in Table 2.1.

2.1 SPECIFIC OBJECTIVES AND RESEARCH PROGRAM

2.1.1 Chloride Binding Mechanism in Plain Cements

Tests have been conducted to study the effect of C_3A **content, alkali content, level** of chlorides, **concomitant presence** of sulfates, **temperature** and the **mode of occurrence** of chlorides on chloride binding mechanism and alkalinity of plain cements. The detailed program is given in Table 2.2

2.1.2 Determination of Threshold Cl^-/OH^- Ratio in Plain Cements

Cl^-/OH^- ratio is a rough measure of corrosion risk of reinforcing steel in concrete. Data on threshold Cl^-/OH^- ratio for depassivation of steel in concrete is not available on actual concrete. Hence, this study attempts to quantify the threshold Cl^-/OH^- ratio of steel in cement mortar using three different C_3A plain cements. The details of the program are shown in Table 2.3.

2.1.3 Chloride Binding Mechanism in Blended Cements

Tests have been conducted to study the mechanism of chloride binding in Type I and Type V cements blended with microsilica, blast furnace slag, and fly ash on a partial replacement basis. The details of the test program are shown in Table 2.4.

2.1.4 Mechanism of Reduction of OH^- Ions from Pore Solution in Blended Cements

OH^- ion concentration decreases the aggressivity of pore solution for corrosion of reinforcement whereas it increases the risk of alkali-silica reactivity and its consequent deterioration. Pore solution extruded from chloride-free pastes of Type I 14% C_3A cement blended with several levels of microsilica, blast furnace slag and fly ash has been analysed for OH^- ion concentrations. The details of the test program for corrosion and alkali-silica reactivity study are given in Table 2.5.

2.1.5 Effect of Physical Characteristics on Durability Mechanisms

Physical structure characterized by the pore size distribution affects the mobility of aggressive substances into concrete as well as the electrical resistivity which control corrosion current flow. This study evaluates the pore size distribution of plain and microsilica, blast furnace slag and fly ash blended cements and their effect on permeability, chloride ion diffusion, electrical resistivity and oxygen diffusion. These data explain the significantly improved durability performance mechanism of blended cements in spite of enhanced aggressivity of the pore solution. The detailed program is shown in Table 2.6.

TABLE 2.1: **Broad Overview of the Research Program for Studying Durability Mechanisms in Plain and Blended Cements.**

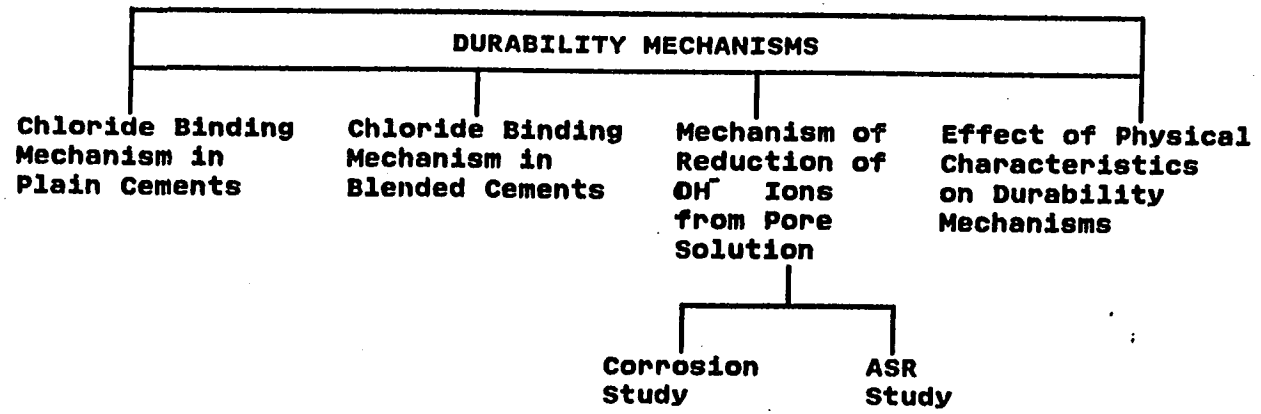

TABLE 2.2: Research Program for Studying Chloride Binding Mechanism in Plain Cements.

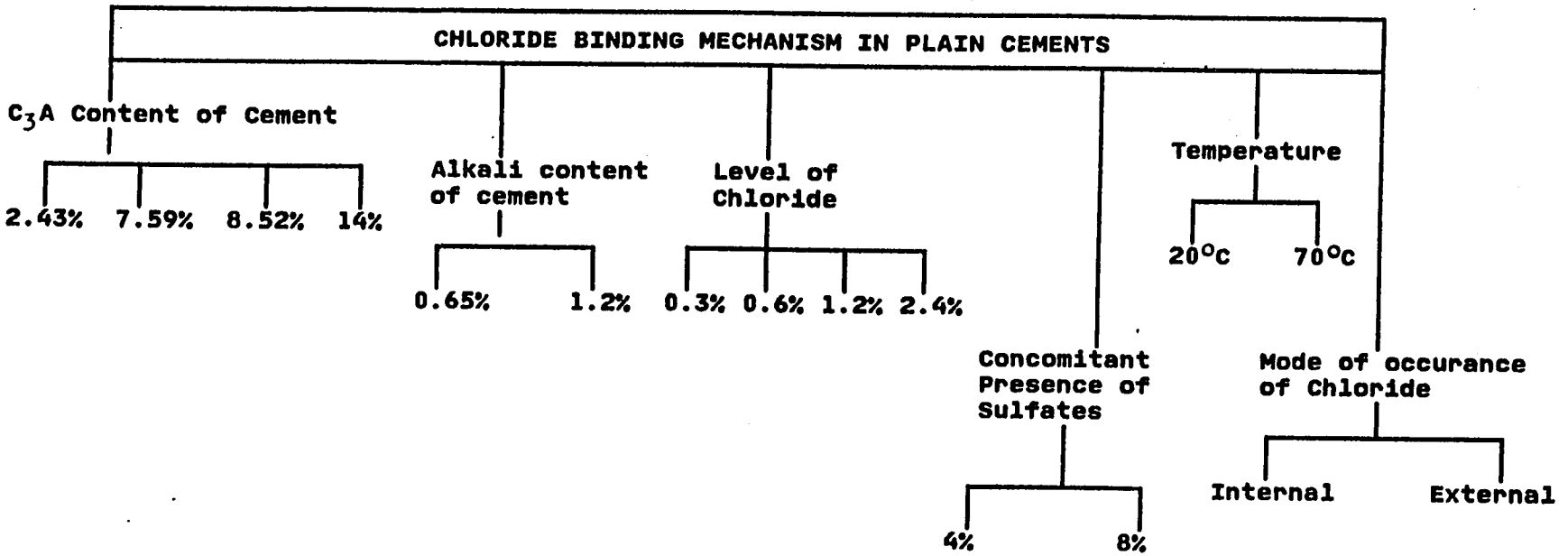

TABLE 2.3 Research Program for Determination Threshold Cl^-/OH^- Ratio in Plain Cements

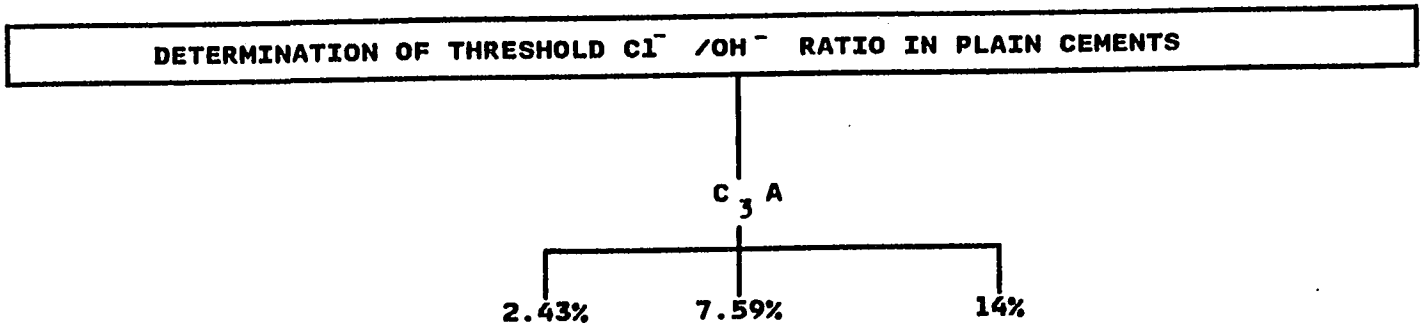

TABLE 2.4 **Research Program for Studying Chloride Binding Mechanism in Blended Cements.**

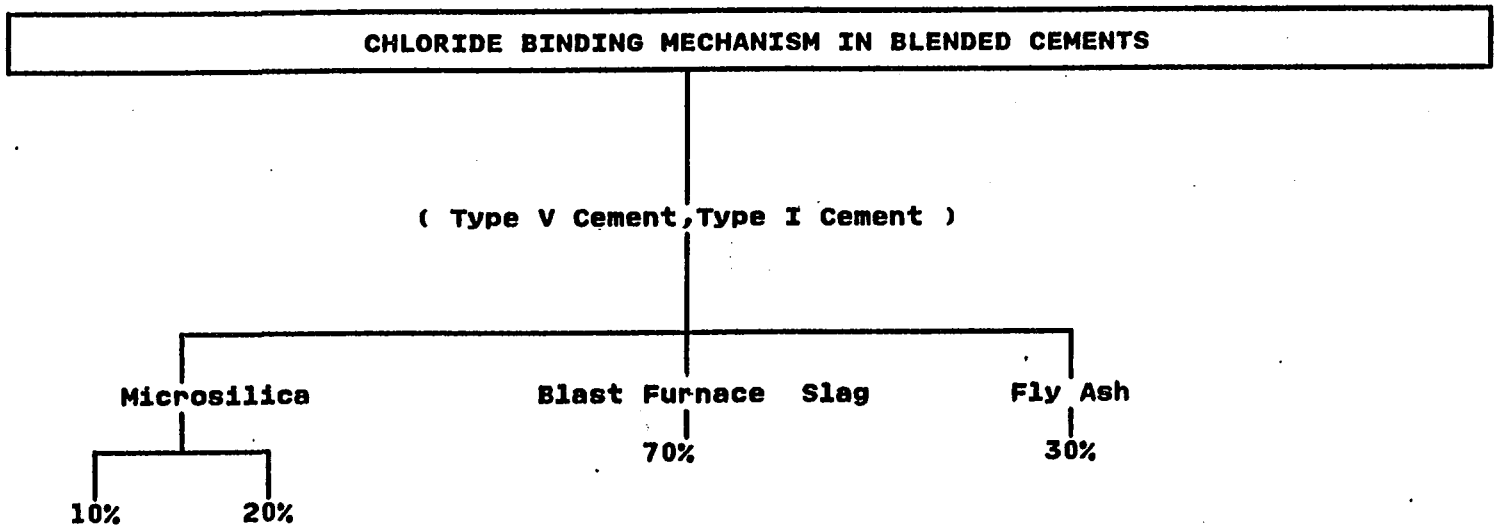

TABLE 2.5 **Research Program for Mechanism of Reduction of OH^- Ions from Pore Solution and $Ca(OH)_2$ Deplation in Blended Cements.**

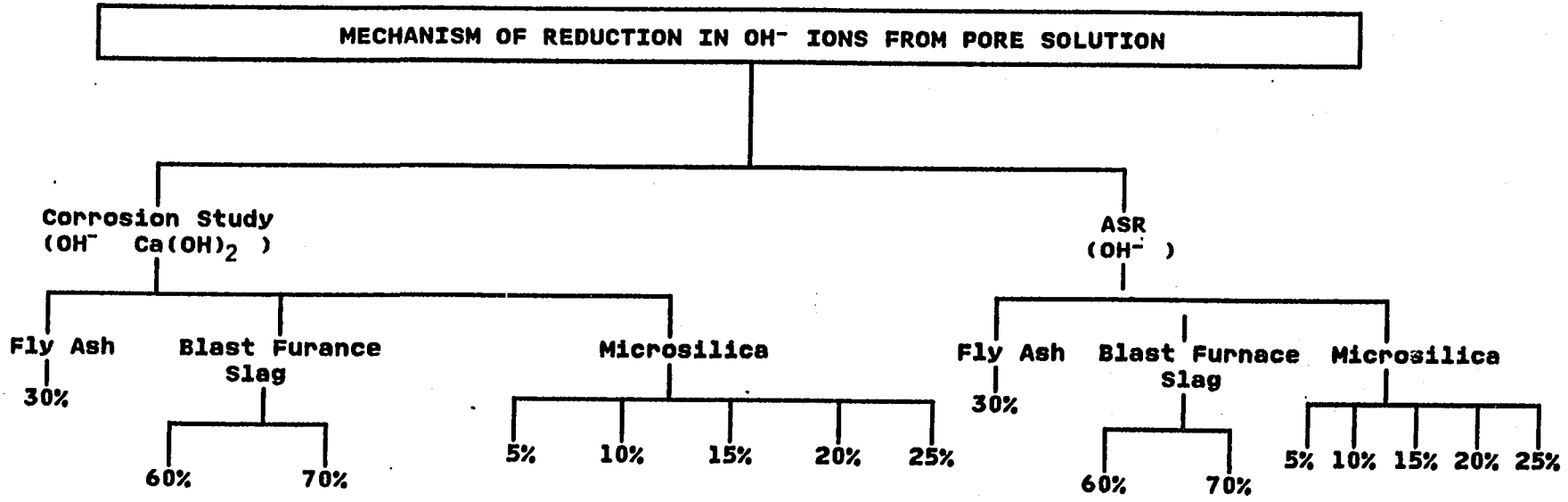

TABLE 2.6 Research Program for Studying Physical Characteristics on Durability Mechanism.

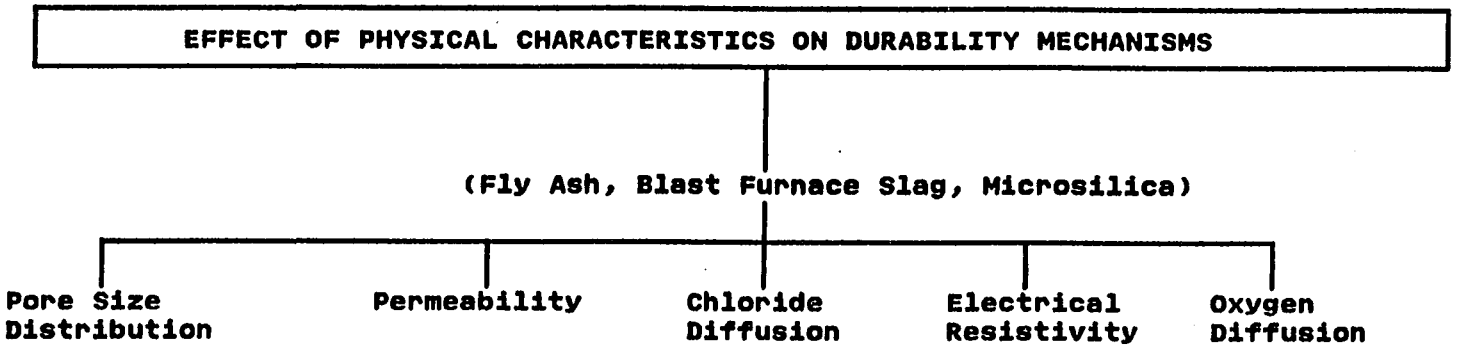

Chapter 3

3. METHODOLOGY OF RESEARCH

In the course of this research following tests have been conducted:

(i) corrosion monitoring tests to evaluate corrosion behavior of steel reinforcement in plain and blended cement concretes in terms of corrosion rates in active corrosion state,

(ii) mortar bar expansion tests to quantify deteriorations due to alkali-silica reactions,

(iii) pore fluid extraction and analysis to characterize chemistry of pore electrolyte in terms of free chloride ion and hydroxyl ion concentrations in the pore solution,

(iv) tests on permeability to evaluate coefficient of permeability of concrete to water using a rapid high pressure permeability apparatus,

(v) chloride diffusion tests to evaluate diffusion coefficient of chloride ions through mature hydrated cement paste,

(vi) resistivity tests to evaluate electrical resistivity of concrete,

(vii) oxygen diffusion tests to evaluate diffusion of oxygen in concrete, necessary for corrosion process to proceed, and

(viii) pore size distribution analysis to characterize pore size and volume distribution system in hardened plain and blended cement pastes.

3.1 MATERIALS AND MIXES USED

3.1.1 MIXES USED

The above mentioned tests were conducted either on cement paste or concrete depending on the test requirements. Two types of cement pastes and two types of concrete mixes were used.

3.1.1.1 Cement Pastes

Cement pastes used for pore fluid extraction and analysis tests were made with a water to cementitious ratio of 0.60 by weight. The cement was thoroughly mixed with water in a container till uniform before the molds being filled in two layers , each layer being compacted by vibration. In case of blended cements, required quantities of the cement and the blending material were mixed thoroughly in dry state till a uniform color is appeared and then mixed with water thoroughly. The mold were filled with the paste in two layers, each layer being compacted by vibration.

For chloride diffusion and pore size distribution analysis tests, cement paste was used with a water to cementitious ratio of 0.50. For chloride diffusion tests, same mixing and casting procedure was adopted as for the pore fluid extraction and analysis tests. However, for pore size distribution analysis tests, a different method of mixing was adopted to ensure a more uniform mixing of the cement and the blending material. Required quantities of the cement and the blending material were mixed in dry state in a kitchen blender at a low speed. Water is then added and the blender run for one minute intervals thrice, each time ensuring visually the proper mixing of the paste. Cylindrical PVC molds of 25x50 mm size were filled with the mixed paste in two layers,

compacting each layer by vibration.

3.1.1.2 Cement Mortar

Cement mortar was used for determining expansions caused due to alkali-silica reactions. The aggregate used was obtained by crushing and grading lump cullet Pyrex No. 7740 in accordance with the ASTM C441 specification. The graded pyrex in the ASTM C441 comprises equal amounts of five fractions: #4-8, #8-16, #16-30, #30-50 and #50-100 mesh.

3.1.1.3 Concrete Mixes

Same type of concrete mix was used for corrosion monitoring, resistivity and oxygen diffusion tests. However, a different type of concrete mix was used for permeability test specimens. An effective water to cementitious material ratio of 0.50, a cement factor of 600 lbs/cu.yd. and coarse to fine aggregate ratio of 2.0 were used for the concrete mix used for corrosion monitoring, resistivity and oxygen diffusion tests. The coarse aggregate, crushed limestone, was used after washing to remove salt contamination. The fine aggregate used was beach sand. The absorption capacities of the coarse and the fine aggregates were 2.65% and 0.50% respectively.

The concrete mix used for permeability tests had an effective water to cementitious materials ratio of 0.55, a cement factor of 550 lbs/cu.yd. and coarse aggregate to fine aggregate ratio of 2.0. A smaller sized coarse aggregate was used because of the limitation on the size of the specimen (the wall thickness of the hollow cylindrical specimen was 3/4 inch). The coarse aggregate washed crushed limestone comprising of 60% 3/8-3/16 inch size and 40% 3/16-3/32 inch size aggregate. The fine aggregate was beach

sand. The absorption coefficients of the coarse and the fine aggregate are 2.65% and 0.50% respectively.

The mixing of the concrete for all the tests was carried out in accordance with ASTM C305. The samples were cast in two layers, each layer being compacted by vibration.

3.1.2 CEMENTS USED

A total number of four ordinary portland cements were used in this study namely, Saudi Kuwaiti OPC Type V (cement 1), Saudi Kuwaiti OPC Type I (cement 2), Saudi Cement OPC Type I (cement 3) and Blue Circle Cement (U.K.) OPC Type I (cement 4). The oxide and potential Bogue compound compositions of the cements are given in Table 3.1.

3.1.3 BLENDING MATERIALS USED

Three types of blending materials were used, namely, fly ash, blast furnace slag, and microsilica (silica fume). The fly ash used was an ASTM Class F of bituminous origin and was obtained from U.K. The blast furnace slag used was supplied by Atlantic Cement Company, U.K. and microsilica was obtained from Elkem Chemicals, Norway. The compositions of fly ash, blast furnace slag, and microsilica used are given in Table 3.2. In all the tests, only one cement replacement level was used for fly ash and blast furnace slag, which were 30% and 70% by weight for the fly ash and the blast furnace slag respectively. However, two cement replacement levels of 10% and 20% by weight were used for microsilica.

3.2 EXPERIMENTAL METHODS

3.2.1 CORROSION MONITORING TESTS

3.2.1.1 Corrosion Initiation Time

Corrosion initiation tests were conducted on triplicate specimens to determine threshold Cl^-/OH^- ratio in plain cement mortars made with different C_3A cements. Primastic cement mortar specimens 2x2x12 inch (50x50x300 mm) with a 1/2 inch (12 mm) diameter steel bar embedded centrally, as shown in Fig.3.1 and Plate 3.1, were cast and cured for the 14 days prior to partial immersion in 5% NaCl solution. A water to cement ratio of 0.55 and sand to cement ratio of 2 were used. Corrosion was monitored by obtaining half cell potential. The threshold potential for corrosion inititaion was taken at -270 mV (SCE). Immediately after initiation of corrosion, the specimens were taken from the chloride solution and pore solution extracted from the mortar surrounding the steel bar. For this, the specimens were cut to a cross-section of 1x1 inch (25x25 mm) by a cutting blade, as shown by the hatched area in Fig. 3.1. Dry cutting was employed and care was taken not loose moisture from the specimens during cutting. The specimens were transferred to plastic bags immediately after cutting, sealed and crushed to small pieces. The crushed material was then immediately transferred to the pore solution expression device and pore solution extracted.

3.2.1.2 Corrosion Rates

Corrosion rates were measured for the plain cement concretes and blended cement

concretes using fly ash blended cement, blast furnace slag cement, and 10% and 20% microsilica blended cement concretes. Corrosion rates were measured on triplicate 4x2.5x12 inch (100x62.5x300 mm) concrete prismatic specimens containing a 1/2 inch (12 mm) diameter steel bar embedded centrally. The specimen is shown in Fig. 3.2 and Plate 3.2. The specimens were cast in aluminium molds and were covered with a wet burlap after one hour. The specimens were demolded after 24 hours and cured in potable water for 28 days before they were partially immersed in 5% sodium chloride solution. The specimens were recovered from the sodium chloride solution after 1200 days of exposure for corrosion rate measurement. At the time of corrosion rate measurement, the half cell potential measurement record showed the reinforcing steel in all the plain and the blended cement concretes to be in a state of active corrosion.

The corrosion rates were determined using Tafel plot technique. At the open circuit potential (corresponding to half cell potential E_{corr}), the measurement of corrosion current I_{corr} is rendered impossible by the equilibrium of charges between anodic cathodic regions, resulting in a zero net measurable current. This necessitates the application of finite incremental potential scans between the specimen and reference electrode, in a range of say ± 250 mV from E_{corr}, in both the anodic and cathodic directions. Each of these potential scans provides a net measurable current differential between anodic and cathodic regions, corresponding to the applied potential scan. A plot, called Tafel plot, can then be drawn between incremental potential scans and the corresponding currents. The typical Tafel plot comprises of two curves of identical shape, and the identical linear portions of the anodic and cathodic plots are extrapolated backwards to intersect at co-ordinates (E_{corr},I_{corr}). This enables evaluation of I_{corr}, which when substituted in the following equation gives the corrosion rate:

$$\text{Corrosion Rate (\ m/year)} = \frac{3.27 \times I_{corr} \times E.W}{d}$$

where,

I_{corr} = Corrosion current density (A/cm^2),

E.W = Equivalent weight of steel (gm),

d = Density of steel (gm/cm^3).

The instrumentation comprised EG & G Model 273 Potentiostat/Galvanostat with IR compensation option, a computer and a printer. A stainless steel frame was used as counter electrode. Fig. 3.3 is a schematic representation of the test set-up. The potential scan was applied at an incremental rate of 0.2 mV/sec in the range (E_{corr}-250 mV) to (E_{corr} + 250mV). IR drops between the reference and the working electrode (steel embedded in concrete), are automatically compensated by the system using current interrupt technique. Softcorr Model 332 was used for data acquisition and analysis. This program uses a chi-squared minimization technique for data interpretation.

3.2.2 PORE SOLUTION EXTRACTION AND ANALYSIS

Pore solution study was carried to study the effects of various parameters on free chloride ion and hydroxyl ion concentrations in the pore solution of hydrated cement pastes. The various parameters studied are C_3A content of cement, level of chlorides, concomitant presence of sulfates, temperature effect, presence of blending materials and effect of alkali content of cement. Also, OH^- concentrations were measured in the plain and blended chloride-free cements to study alkali-silica reactivity.

3.2.2.1 Specimen Preperation for Pore Solution Extraction

Cement paste specimens with a water to cementitious material ratio of 0.60 was used for all the pore solution tests. Deionized water was used for the preparation of cement pastes. AR grade sodium chloride, sodium sulfate, calcium chloride and sodium hydroxide were used. The required quantities of the salts were pre-dissolved in the mix water. Cement paste specimens were prepared by using a standard Hobart mixer and a mixing procedure in accordance with ASTM C305. After mixing, the specimens were cast in 49mmx75mm impermeable cylindrical PVC molds. The molds were sealed and stored at $20 \pm 2°C$. Pore solution was extracted after six months of curing in sealed containers.

3.2.2.2 Pore Solution Expression Device

(i) Description of the Device

The pore solution expression device used is similar in design to that described by Longuet (52) and Barneyback and Diamond (59). A cross-section of the device is shown in Fig. 3.4. Plate 3.3 shows a view of the pore solution expression device. It consists of a support cylinder, a platen and a plunger. All the components of the device are made of high strength alloy steel and are heat treated. The die body is designed as a jacketed cylinder. A teflon disc is used to seal the top of the specimen placed in the bore of the die. The top of the platen is scribed with a drain ring intersected by the fluid drain. A heavy plastic tubing is inserted in the fluid drain which is projected out of the die body. Pore solution is collected by inserting a syringe into the end of the plastic tubing.

(ii) Procedure for Pore Solution Expression

Before each pore solution expression cycle, all the parts of the device were cleaned by distilled water and acetone. A thin layer of PTFE spray (commercially available as ROCOL MRS non-silicone spray) was applied on the mating surfaces of the platen and the die body and on the shaft of the piston. The platen was placed centrally on the base of compression testing machine of 200 kN capacity. The die body is slided gently across the mating surface until located against the two fixed pins. The final locking pin was then inserted in position. The specimen was loaded into the bore of the die body with the as-cast bottom in contact with the platen. The teflon sealing disc was inserted into the bore with gentle taps with a soft faced rubber hammer onto the top of the specimen. The piston was inserted into the bore. Before applying load to the piston, a disposable sterilized 10 ml syringe was attached to the plastic tubing of the fluid drain. Load was applied to the piston at a slow rate of 0.4 kN/sec up to a load of 50 kN so as to prevent the die body lifting. Afterwards, a loading rate of 1 kN/sec was used. As the loading proceeded, the plunger of the syringe was drawn back to create a slight vacuum which could draw the expressed pore fluid into the syringe. Although a maximum pressure of 375 MPa was used, in most of the cases a pressure of 225 MPa was sufficient to draw 3 to 6 ml. of the pore fluid. The maximum pressure was sustained for about 5 to 10 minutes. In some cases, the maximum pressure had to be sustained for longer periods of about one hour to draw the required quantity of the fluid. If sufficient quantity of the fluid was not collected on the first loading cycle, one or two more loading cycles were applied between half and full pressure. The pore fluid was transferred to sealed plastic vials for analysis.

After the desired quantity of the pore fluid was collected, the load was removed and the piston and the die body assembly was slided off. The specimen was removed

from the die body bore by applying pressure in the testing machine. The hollow base cylinder was placed on the platen of the testing machine and the die body and the piston assembly was placed centrally above the base cylinder. Load was applied to the piston slowly. A loading rate of 3 kN/sec was found to be convenient. With the application of the load, the specimen was slowly moved downwards till it was ejected out of the bore. The load application was stopped and the piston, the die body and the base cylinder removed from the machine. The piston was removed by rotating and gently pulling out of the die body bore. If the piston could not come out manually, it was removed by applying pressure in the testing machine. To do so, the hollow base cylinder was placed in position on the platen of the testing machine. The collar of the piston was removed. The die body was placed centrally on the base cylinder. The plunger was placed centrally on the top of the piston shaft and load applied till the piston shaft came out and dropped into the base cylinder. To avoid any damage to the piston shaft, a piece of soft cloth was inserted in the hollow cylinder bore. When the piston is removed from the die body bore, all the parts of the device were removed from the machine and cleaned with distilled water and acetone. All the mating parts were sprayed with the PTFE spray before reuse. The parts of the device had to be coated with a thick layer of the spray coating during its storage.

3.2.3 DETERMINATION OF OH^- AND Cl^- CONCENTRATIONS IN PORE SOLUTION

0.2 to 0.5 ml of the pore solution was diluted with deionized water to 10 ml. OH ion concentration was measured by titration with 0.01 M nitric acid using phenolphthalein as indicator. The pH of the pore solution was calculated from the measured OH^- concentration as:

$$pH = 14 + \log_{10}[OH^-]$$

where $[OH^-]$ = Hydroxyl ion concentration in M/L.

Chloride concentrations in the pore solution were determined by a microprocessor ion-analyzer in conjunction with a solid-state chloride ion activity double junction reference electrode. The values obtained were regularly checked by titration using the Gran plot method (60).

3.2.4 PERMEABILITY TEST

3.2.4.1 Description of the Apparatus

Permeability of concrete to water was measured using a high pressure permeability apparatus developed in this study. The permeability measurement is based on the principle of Darcy's law of flow through porous media. Water was forced to flow through concrete under a constant pressure and the coefficient of permeability was measured when a steady state of flow was reached.

The permeability apparatus is shown in Fig. 3.5 and Plate 3.4. It consists of a pressure vessel where the specimen is placed, a pressure gage to measure the water pressure in the pressure vessel. The pressure is applied with the help of a nitrogen cylinder connected to the air cylinder. A ram forces the water into the pressure vessel. The apparatus is fitted with several valves, the functions of which are described below. The specimen used was a hollow concrete cylinder (Fig. 3.5), 2.75 inch external diameter, 1.25 inch internal diameter and 3 inch height. The specimen was sealed at top and bottom with 1/2 inch thick plexiglass disc using an epoxy.

3.2.4.2 Operation

The specimen was placed in the pressure vessel and the pressure vessel was filled with distilled water. Air bubbles, if any, were removed from the vessel. The pressure vessel was fixed in place by bolting loosely. Water was pumped into the system with values A and B open and C shut. This pumped water into the pressure vessel.

When it was ensured that the vessel was full with water, the bolts were tightened firmly. The valve C was opened and water pumped in. This would pump water into the vessel and water could come out from the valve C. When the water coming out from valve C was in the form of a continous stream, the pumping was stopped. Valve A was shut and water pumped in to move the ram to right. When the ram moved to the extreme right position, pumping was stopped. Valve B was shut and valve A was opened. Pressure was applied from the nitrogen cylinder to move the ram to the extreme left position, This flushes out the water out from the system through valve C and hence, any air trapped in along with the water. The pumping in and flushing out of the water was repeated for three to four times. Finally, air release valve D, and valves B and C were shut and desired pressure was applied from the nitrogen cylinder. The pressure could be read from the pressure gage attached to th pressure vessel. Immediately after the application of the pressure, the reading on the scale and time were recorded. The readings of time and the ram movement were noted with different intervals of time. For a normal permeability concrete, it took about 24 hours for the completion of the test. A pressure of 300 psi was used for all the specimens tested except for the specimens of 6-month age for which a pressure of 600 psi was used.

Volume of water injected into the specimen through its walls was computed from the ram movement, which calibrated to the volume of water being forced in. The data was plotted to obtain a q vs t curve (q being water injected into the specimen through

its walls and t being the interval of time). The slope of the straight line portion, (dq/dt) of the curve was taken as the steady state slope. K, the coefficient of permeability was calculated using Darcy's law.

3.2.5 CHLORIDE ION DIFFUSION

Chloride ion diffusion was measured using a chloride diffusion cell on hydrated cement paste discs as shown in Fig. 3.6 and Plate 3.5. The discs were cut from the central portion of 4 inch (100 mm) dia. cylindrical specimens cured in water for the required period. The discs were 8 mm thick. An impermeable ring of epoxy was cast around the disc so that its diameter was 5 inch (125 mm). The specimen was fixed in the diffusion cell and chloride ion diffusion through the disc was measured.

The diffusion cell was similar in design to that used by Page et al (61). The diffusion cell consists of two chambers, A and B, made up of impermeable plexiglass. The specimen disc was fitted between the two chambers with the help of rubber 'O' rings and closely spaced bolts. Before starting the test, it was ensured that the assembly was free from leakage from one chamber to the other as well as from the chambers to outside. 5M sodium chloride solution was filled in chamber A and saturated calcium hydroxide solution was filled in chamber B. Concentration of chloride ions was measured in the chamber B at suitable time intervals. Variation of chloride ion concentration in chamber B was plotted against time from which diffusion coefficient of chloride ions D into the hardened cement was computed as follows:

$$dC_2/dt = \frac{DA}{VL}(C_1 - C_2)$$

C_1 = chloride ion concentration in chamber A (M/L)

C_2 = chloride ion concentration in chamber B (M/L)

A = area of cross section of the disc (cm^2)

V = volume of solution in B (cm^3)

L = thickness of the disc (cm)

D = diffusion Coefficient (cm^2/sec.)

dC_2/dt = slope of the concentration vs time curve

3.2.6 MEASUREMENT OF ELECTRICAL RESISTIVITY

Electrical resistivity was measured on 3x6 inch (75x150 mm) concrete cylinders after curing periods of 28, 60 and 120 days. A 4 terminal null balancing ohm meter (commercially available as Nilson 400) was used to measure the electrical resistance directly. It measures the resistance in the range of 0.01ohm to 1.1 mega ohms. The sample, cylinder was held between two terminals with the help of a frame. The resistivity meter unit generates a low voltage 97 Hz square wave current between the terminals. The detector senses the voltage drop between the terminals, compares it with the internal standard resistors and indicates a difference on the null detector. When the null detector was balanced, the resistance of the sample between the terminals was read directly. Resistivity of the sample R (kOhm-cm) was calculated as follows:

$$\frac{R = rA}{L}$$

where, r = measured resistance (kOhm)

L = length of the sample (cm)

A = area of cross-section of the sample (cm^2).

3.2.7 MEASUREMENT OF OXYGEN DIFFUSION

The principle used in the measurement of diffusion of oxygen through concrete was that when a potential in the range of -650 to -900 mV SCE is applied to a steel plate embedded in concrete by means of a potentiostat, the most likely reaction on the steel surface is the oxygen reduction according to the following equation:

$$\frac{1}{2}O_2 + H_2O + 2e^- \longrightarrow 2OH^-$$

The current caused by this reaction is therefore a direct measure of the amount of oxygen reacting at the embedded steel plate. The oxygen flux was calculated from the I-time curves, when a steady-steate current is reached using Faraday's law:

$$J(O_2) = \frac{I}{nF},$$

where I = steady state current density,

n = 4,

R = Faraday's constant (96494 Coulombs/mole)

Oxygen flux measurements were carried out on duplicate concrete specimens after a curing of three months in potable water. The test specimen and the experimental set-up are shown in Fig. 3.7. The test specimen was a concrete prism 4x2.5x12 inch(100x62.5x300 mm) with a steel plate 2.5x0.125x8 inch (62.5x3x200 mm) embedded inside. The edges of the steel plate were painted with an epoxy paint to leave an exposed surface area of 12 in^2 (75cm^2) on each side. A potential of -850 mV SCE was applied to the steel plate embedded in the concrete specimen. The values of current were recorded using a data logger till a constant current was achieved. The tests were carried out under complete submersion condition.

3.2.8 ALKALI-SILICA REACTIVITY TEST

3.2.8.1 Test Specimen

The test was conducted in accordance with ASTM 227. The specimens comprising 2.5x2.5x28.5 mm mortar bars have been used to test expansions resulting from the alkali-silica reactions. Standard reactive aggregate in accordance with ASTM C441 was used, comprising of graded pyrex glass obtained by crushing and grading lump cullet pyrex Glass No. 7740 procured from Corning, USA. The grading of the aggregate was adopted to meet ASTM C227 requirements.

One OPC and four blended cements were prepared. The OPC contained 14% C_3A. The blended cements used were 30% fly ash, 70% blast furnace slag and 10 and 20% microsilica blended cements. Appropriate amounts of NaOH were added to raise the Na_2O content of the parent cement to 1.2%. Thus, Na_2O content of each blended cement comprises the contributions made by the OPC and the blending material. The specimens were made by proportioning the dry materials for the test mortar using 1 part of cement to 2.25 parts of graded aggregate by weight. The amount of mixing water was such as to produce a flow of 105 to 120% (as determined in accordance with ASTM C109).

3.2.8.2 Storage of Test Specimens

The specimens were stored in specially designed and fabricated containers to fulfill the requirements of ASTM C227. The containers were made up of stainless steel. A tight seal between the container wall and cover is maintained to eliminate loss of mois-

ture. The inner sides of the container were lined with absorbent towel cloth to act as a wick and to ensure that the atmosphere in the container is quickly saturated with water vapor when it is sealed after the specimens are placed therein. The specimens were supported in a vertical position on a galvanized welded network such that the lower end of the bar is approximately 1 inch (25 mm) above the surface of water. The storage containers were kept in an oven at 38° C.

3.2.8.3 Expansion Measurements

Expansion measurements were made every week after cooling the specimens in accordance with ASTM C227. The measurements of length change were made using a length comparator fitted with a sensitive dial gage in accordance with ASTM C490. The procedure followed for measuring changes in length followed were in accordance with ASTM C1012.

Table 3.1: Composition of Cements Used (% by weight)

Cement No.	1	2	3	4
CaO	64.20	65.03	64.07	64.70
SiO_2	21.90	20.90	22.00	19.92
Al_2O_3	3.98	5.26	4.08	6.54
Fe_2O_3	4.80	3.75	4.24	2.09
SO_3	1.71	2.54	1.96	2.61
Na_2O	-	-	0.19	0.28
K_2O	-	-	0.36	0.56
Equivalent Na_2O	0.58	0.60	0.43	0.65
C_3S	54.30	55.83	54.57	54.50
C_2S	21.80	17.80	21.91	16.00
C_3A	2.43	7.59	8.52	14.00
C_4AF	14.61	11.41	12.90	6.50

Table 3.2: Physical and Chemical Characteristics of Fly Ash, Blast Furnace Slag and Microsilica Used (% by weight)

Admixture	Fly Ash	Slag	Microsilica
CaO	2.00	43.70	0.10
SiO_2	51.30	35.40	97.20
Al_2O_3	24.10	7.80	0.18
Fe_2O_3	12.60	0.52	0.08
SO_3	0.84	1.13	0.05
Na_2O	0.32	0.39	0.07
K_2O	3.06	0.11	0.35
Equivalent Na_2O	2.33	0.46	0.30

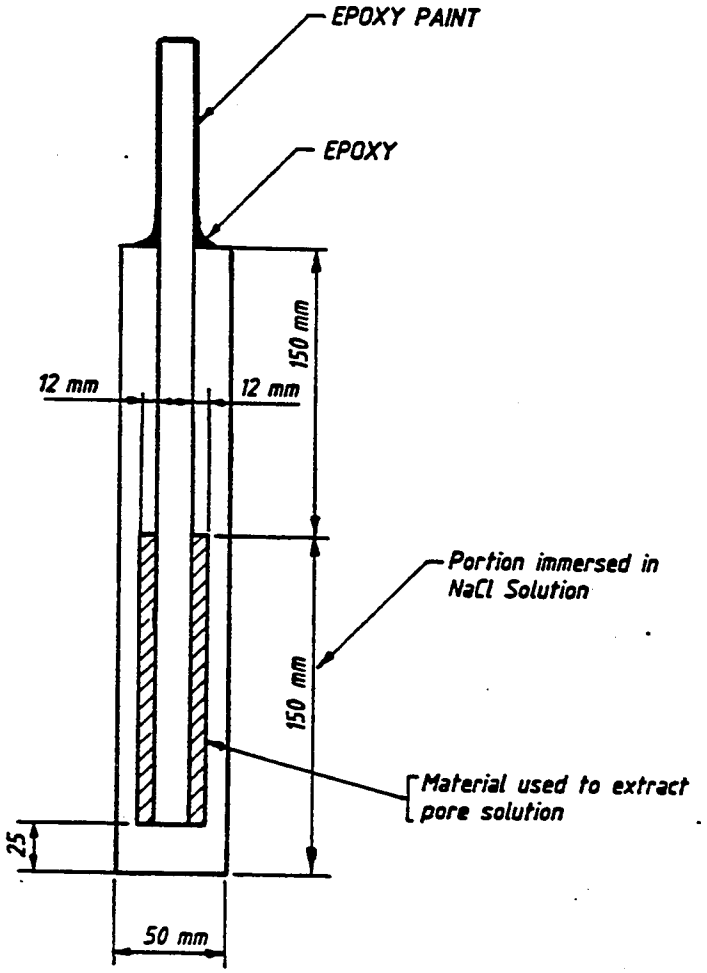

Fig. 3.1: Cross-sectional View of the Specimen Used for Threshold Cl^-/OH^- Ratio Determination.

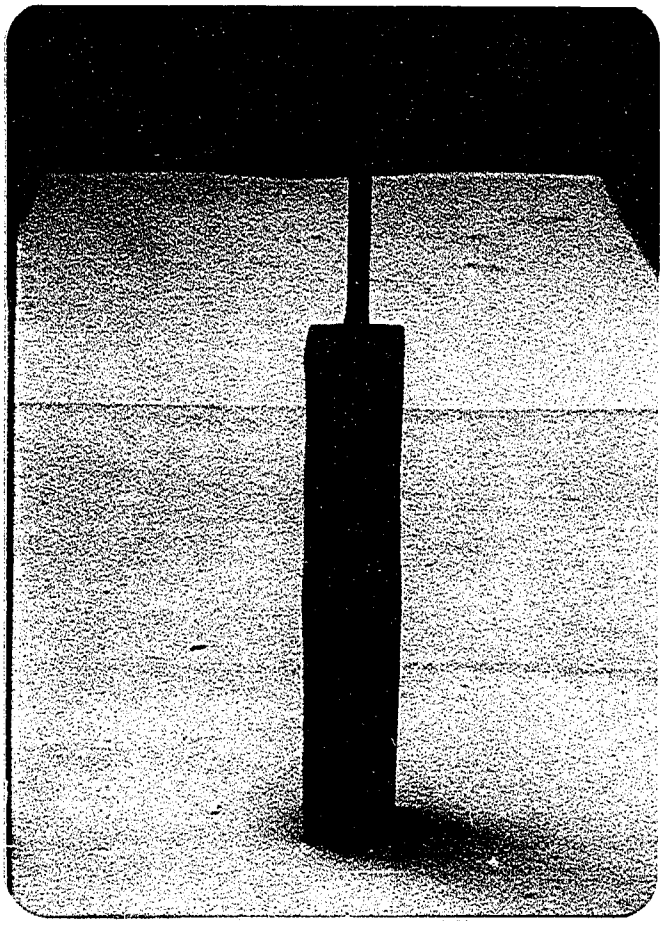

Plate 3.1 : Specimen Used for Threshold Cl^-/OH^- Ratio Determination

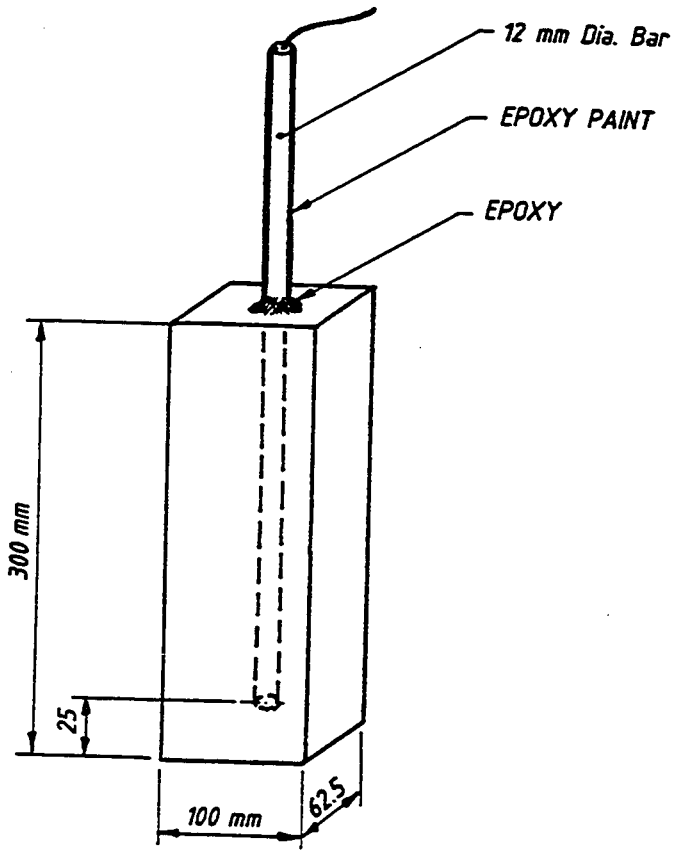

Fig. 3.2: Specimen Used for Corrosion Rate Measurements.

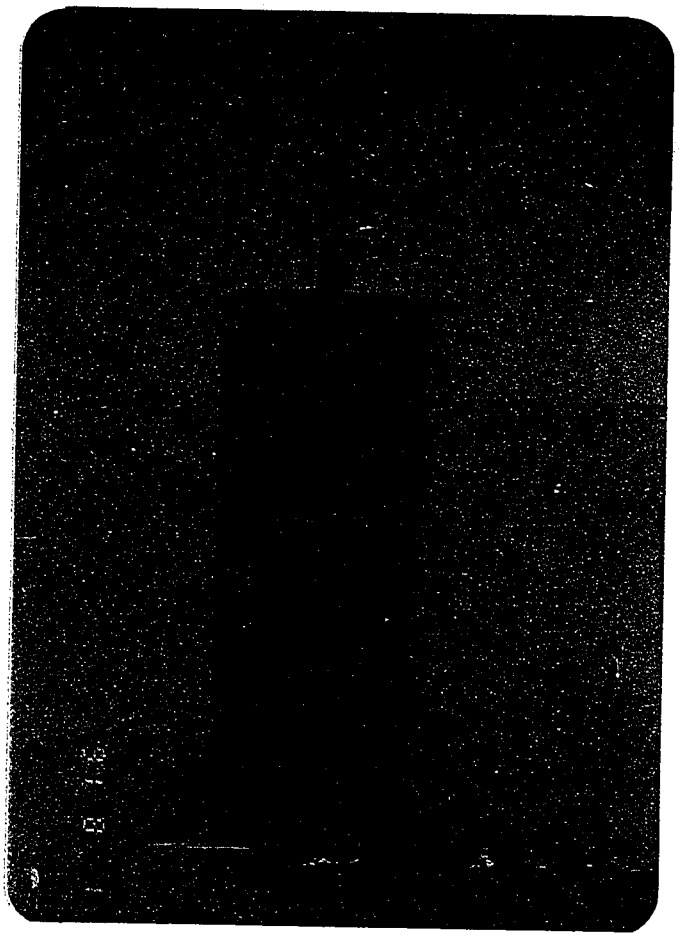

Plate 3.2 : Specimen Used for Corrosion Rate Measurements

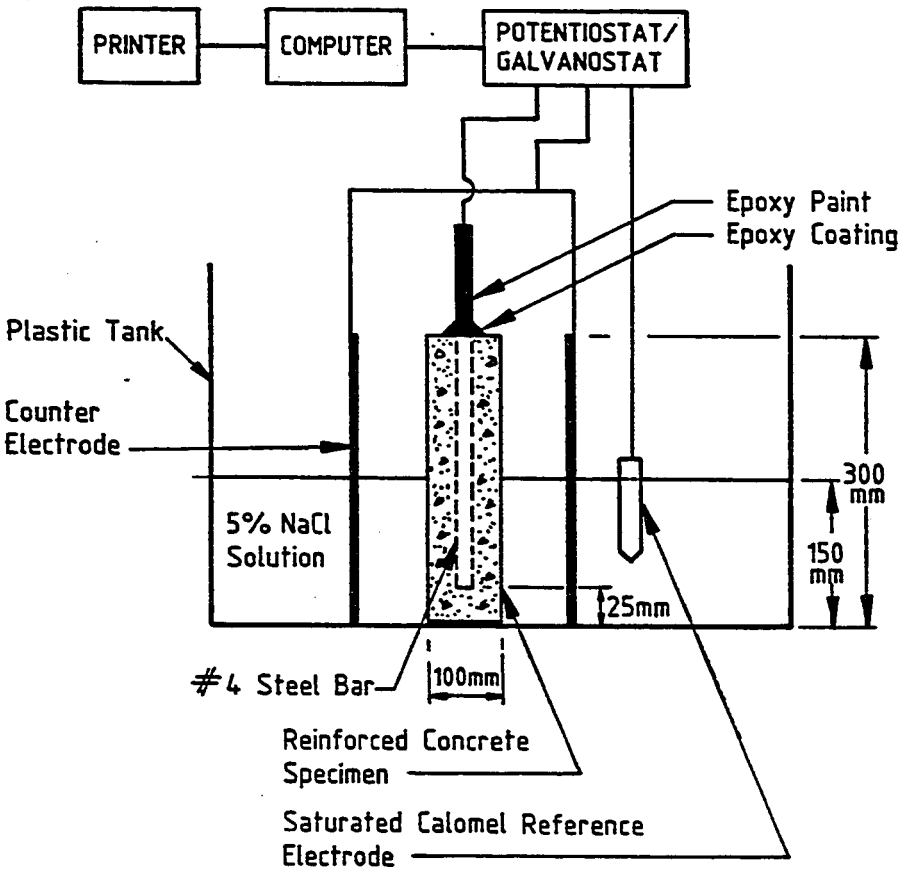

Fig. 3.3: Instrumentation for Corrosion Rate Measurement Tests

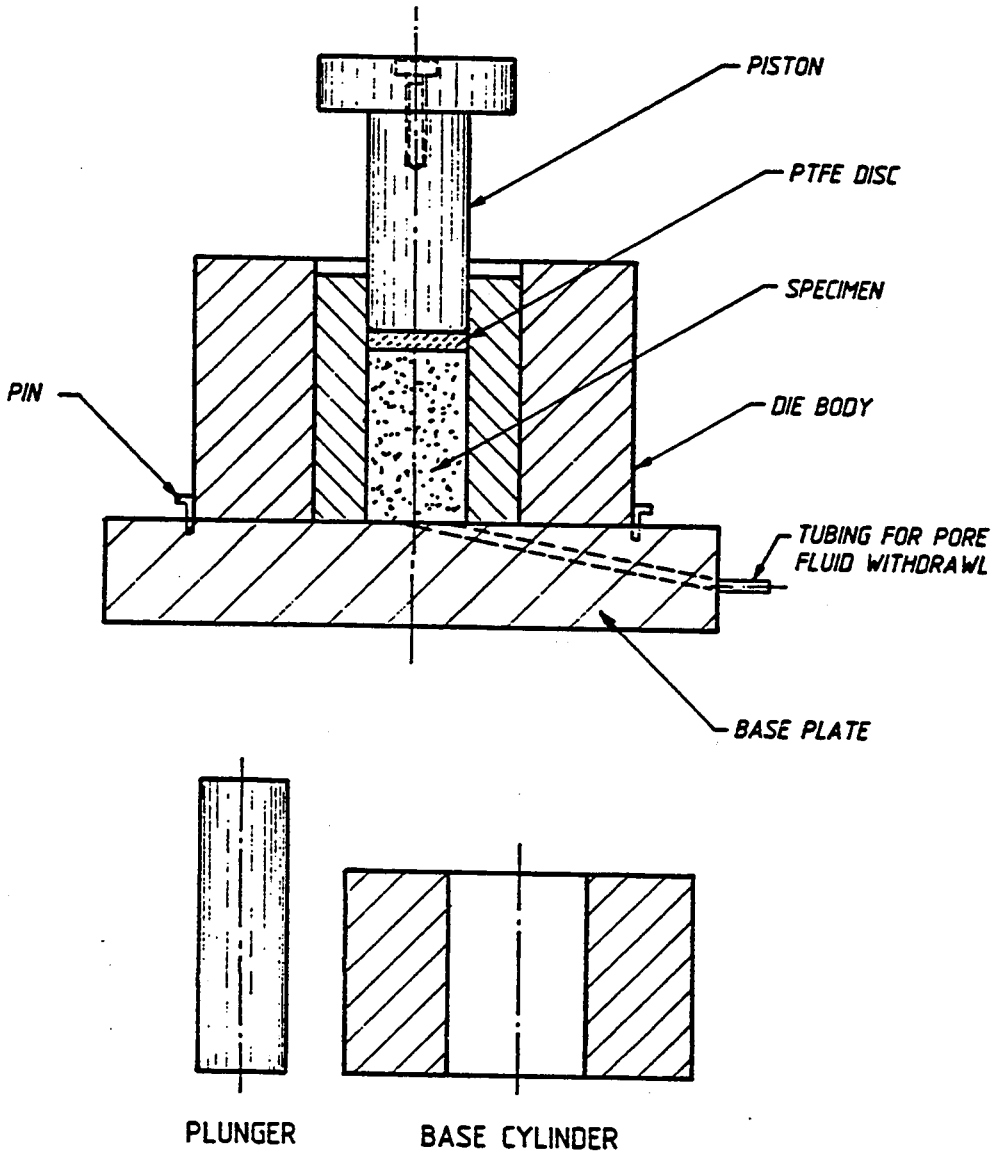

Fig. 3.4: Cross-sectional View of Pore Solution Expression Device

Plate 3.3(a) : Components of Pore Solution Expression Device

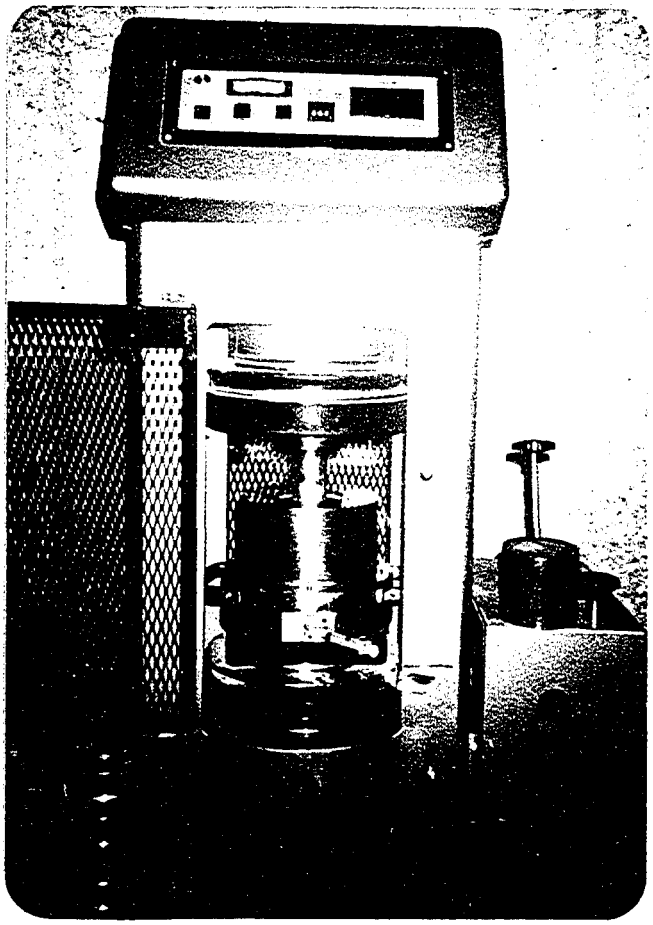

Plate 3.3(b) : Pore Solution Expression Device (assembled)

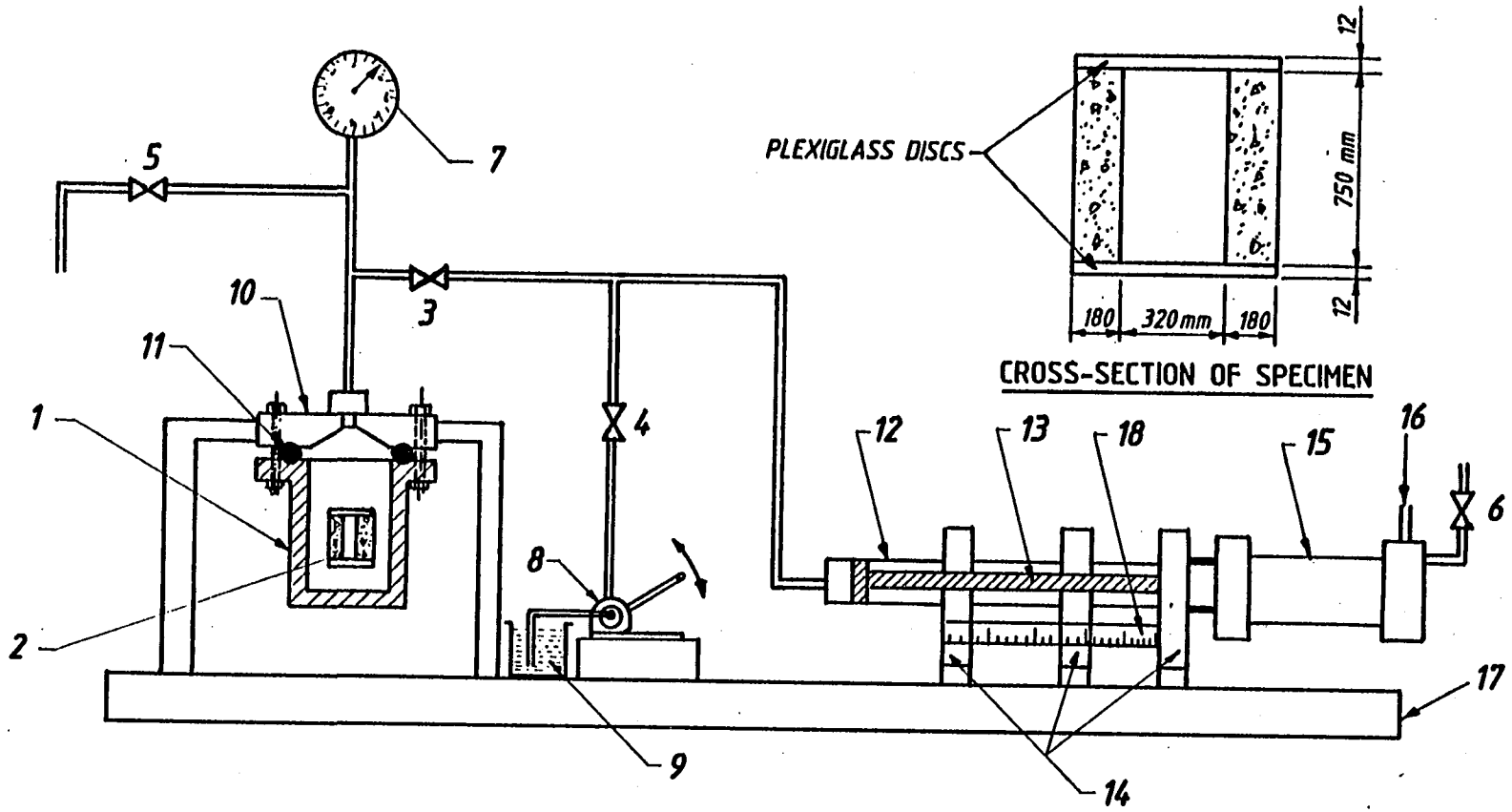

No.	Description	No.	Description	No.	Description
1	PRESSURE VESSEL	7	PRESSURE GAUGE	13	STAINLESS STEEL RAM
2	SPECIMEN	8	HAND PUMP	14	GUIDE RAILS
3	VALVE - A	9	BEAKER WITH WATER	15	AIR CYLINDER
4	VALVE - B	10	PRESSURE VESSEL TOP	16	TO NITROGEN SUPPLY
5	VALVE - C	11	RUBBER 'O' RING	17	STEEL BASE
6	AIR RELEASE VALVE	12	HYDRAULIC CYLINDER	18	GRADUATED SCALE

Fig..3.5: Schematic View of High Pressure Permeability Apparatus.

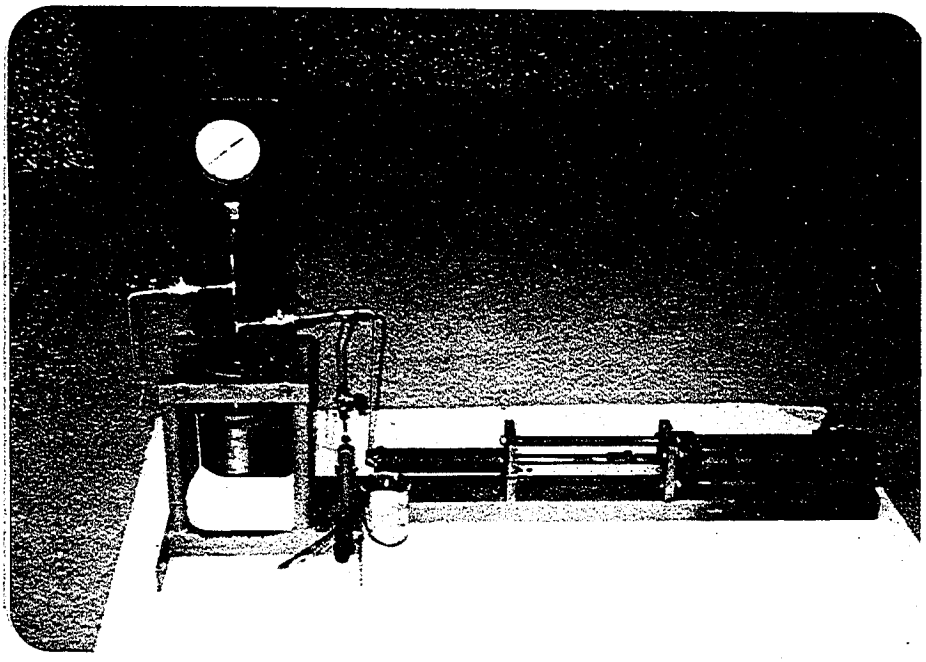

Plate 3.4 : High Pressure Permeability Apparatus

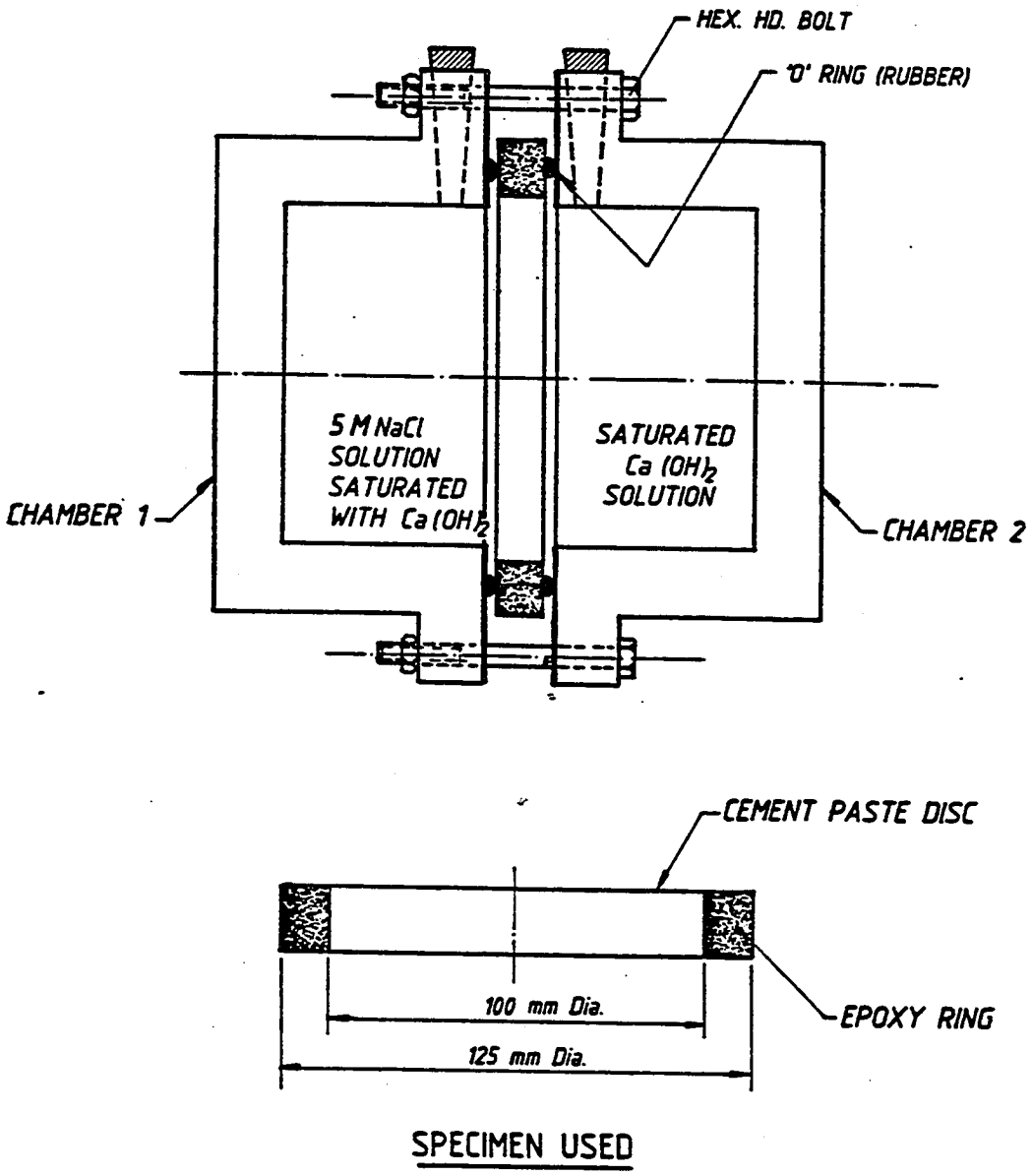

Fig. 3.6: Cross-section View of Chloride Diffusion Cell.

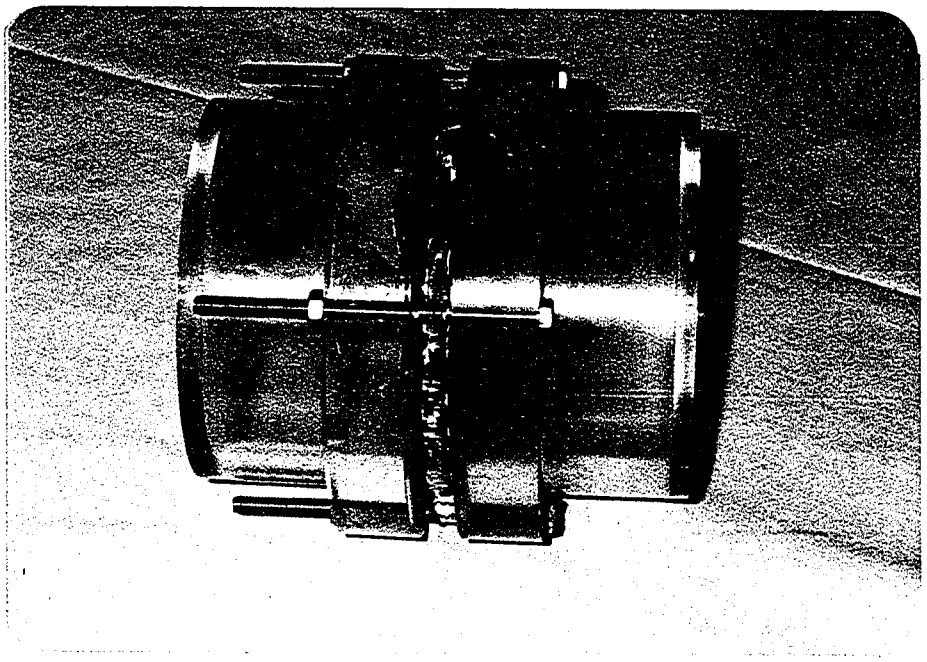

Plate 3.5 : Chloride Diffusion Cell

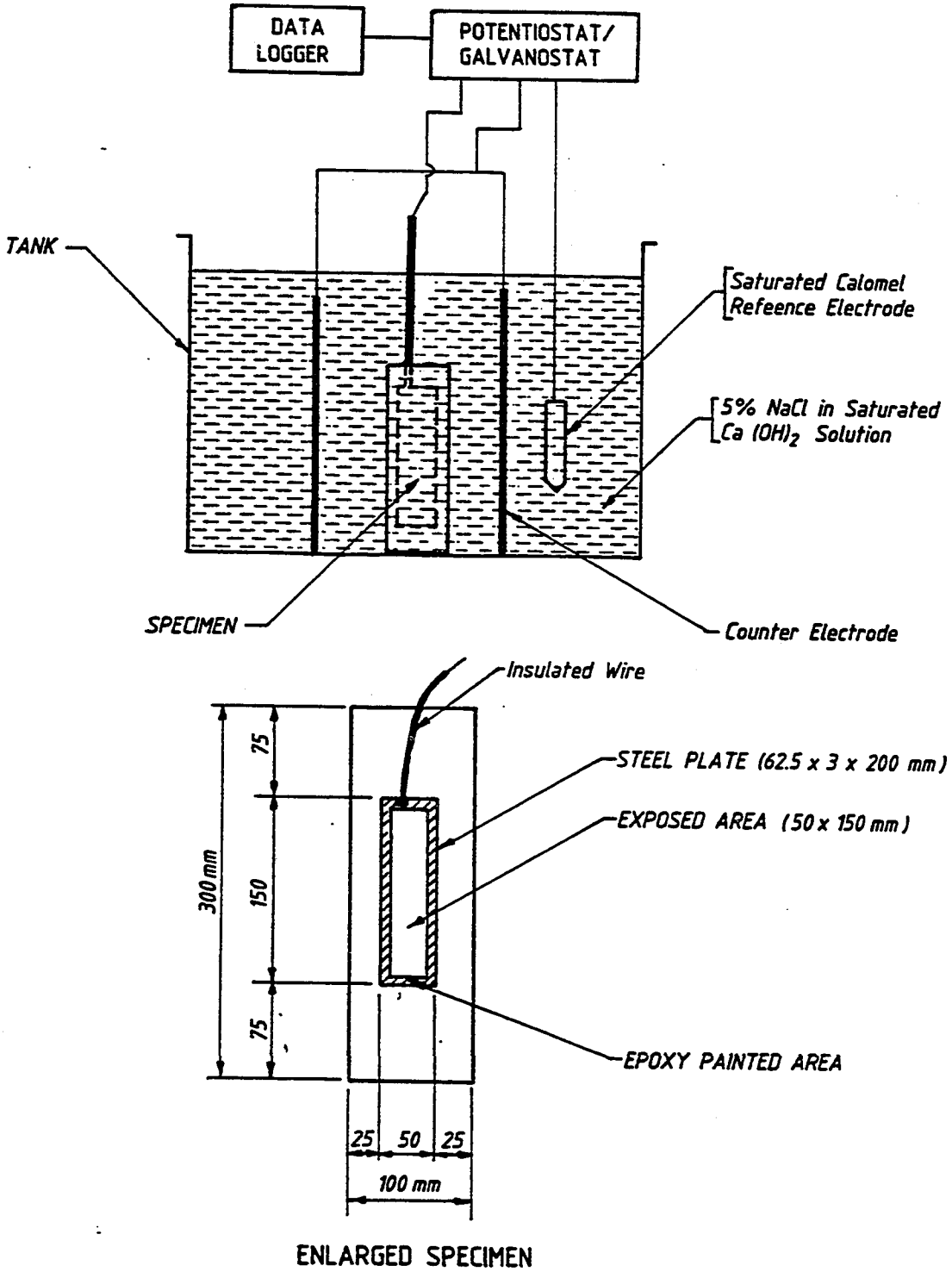

Fig. 3.7: Experimental Set-up for Measuring Oxygen Diffusion.

Chapter 4

RESULTS AND DISCUSSION

4.1 DURABILITY PERFORMANCE OF PLAIN AND BLENDED CEMENTS

4.1.1 CORROSION RESISTANCE PERFORMANCE OF STEEL IN PLAIN AND BLENDED CEMENT CONCRETE

The corrosion process of steel reinforcement in concrete comprises of two distinct phases (62,63) : the corrosion initiation period and corrosion propagation period. The corrosion initiation time and the subsequent corrosion rate of steel in concrete together determines the corrosion resisting characteristics of concrete.

Corrosion is initiated when chloride ions permeate through concrete cover and reach the steel surface in sufficient quantity required to cause depassivation of the steel. Hausmann (11) on the basis of corrosion tests carried out on steel exposed to artificial concrete-simulated environment of $Ca(OH)_2$, suggested a threshold Cl^-/OH^- value of 0.6 for the depassivation of steel. Diamond (38), using results of tests conducted by Gouda (54), has proposed a value of 0.3 for alkaline condition of a typical concrete pore solution. In a concrete free from chlorides inducted during its manufacture, corrosion initiation of steel reinforcement depends on the chemical environment

of its pore solution in terms of alkalinity and chloride-binding capacity as well as its physical structure.

Once the corrosion of steel is initiated, corrosion proceeds at a rate which depends on the pore solution composition (Cl^-/OH^- ratio), electrical resistivity of concrete, and diffusion of oxygen and moisture to the steel surface for a given service environment. The corrosion propagation leads to cracking and spalling of concrete causing serviceability failure.

Since corrosion initiation time and subsequent corrosion propagation of steel reinforcement together determines the corrosion resisting characteristics of a concrete, corrosion initiation data on plain and blended cements developed by Rasheeduzzafar et al (23) in the same laboratory are reproduced here. The four plain cements and the blending materials which were used in the present study for the corrosion rate measurement were used for the corrosion initiation time measurement by Rasheeduzzafar et al (23).

The corrosion rate measurement tests carried out in the present study used the same concrete specimens as used by Rasheeduzzafar et al (23) for corrosion initiation time measurement. To evaluate the corrosion initiation time, prismatic concrete specimens 4.2x2.5x12 inch(100x62.5x300 mm) containing a 1/2 inch (12 mm) diameter steel bar embedded centrally, were cured for 28 days in potable water. The specimen were then immersed partially in 5% NaCl solution in tanks located in the controlled laboratory environment at 23 to 25°C. Corrosion was monitored by obtaining half cell potentials on a Hewlett Packard 3054 DL data acquisition system, in conjunction with a saturated calomel electrode. The threshold potential for corrosion initiation was taken at -270 mV (SCE). Triplicate specimens were tested and the average values of the half cell potential were plotted against exposure time. Corrosion initiation time is

taken as the exposure time at which the half cell potential reaches the -270 mV (SCE) value.

4.1.1.1 Corrosion Initiation Time

Fig. 4.1.1.1 shows the potential measurement record of steel in plain cement concretes developed by Rasheeduzzafar et al (23). Fig. 4.1.1.2 shows the corrosion initiation times of the steel in 2,9, 11 and 14% C_3A cement concrete. It can be seen that the corrosion initiation times in the 9,11 and 14% C_3A cement concretes were 1.75, 1.93 and 2.45 times more than that in the 2% C_3A cement concrete.

Assuming that the physical structure of the four plain cement concretes were similar, the corrosion initiation times would depend on the chloride-binding capacity of these cements. Fig. 4.1.1.3 shows the potential measurement record and Fig. 4.1.1.4 shows the corrosion initiation times of steel in plain and blended cement concretes developed by Rasheeduzzafar et al (23). The fly ash, blast furnace slag, 10 and 20% microsilica blended cement concretes performed 1.75, 2.11 , 3.0 and 3.04 times better than the plain cement concrete in terms of corrosion initiation time.

4.1.1.2 Corrosion Rates

Corrosion rates of steel were measured in the post-initiation period using Tafel plot technique. Duplicate specimens were used for corrosion rate measurement in plain cement concretes whereas triplicate specimens were used for the blended cement concretes. Typical Tafel plots of steel in the plain and the blended cement concretes are shown in Fig. 4.1.1.5 through 4.1.1.12. Corrosion rates in plain and blended cement

concretes are given in Table 4.1.1.1 and 4.1.1.2 and Figs. 4.1.1.13 and 4.1.1.14. It can be seen that the corrosion rate of steel in plain cement concretes is more or less constant and does not show any definite relationship with the C_3A content of the cements. However, corrosion rate of steel in blended cement concretes is different than in the plain cement concrete. In the 30% fly ash and the 70% blast furnace slag blended cement, the corrosion rates drop from 0.97 to 0.60 and 0.62 mpy respectively.

In the 10% microsilica cement concrete, the corrosion rate falls by about 24% only to a value of 0.74 mpy. However, in 20% microsilica blended cement concrete, the corrosion rates increases to 1.13%.

Although the corrosion rates of steel in blended cement concretes is different than in the plain cement concrete , the difference is not significant compared to the variability normally encountered in corrosion rate measurements.

TABLE 4.1.1.1: Corrosion Rates of Steel in Plain Cement Concrete

Cement Type	Half Cell Potential E (mV) SCE			Tafel Constants				Corrosion Current Density ($\mu A/cm^2$)			Corrosion Rate (mpy)		
				Anodic		Cathodic							
	(1)	(2)	mean	(1)	(2)	(1)	(2)	(1)	(2)	mean	(1)	(2)	mean
OPC Type V (C_3A:2%)	-670	-738	-704	340	341	186	163	2.06	1.74	1.90	0.96	0.81	0.89
OPC Type I (C_3A:9%)	-582	-631	-607	454	-	347	-	2.19	-	2.19	1.02	-	1.02
OPC Type I (C_3A:11%)	-609	-801	-705	442	-	330	-	2.31	-	2.31	1.07	-	1.07
OPC Type I (C_3A:14%)	-614	-647	-631	472	447	279	300	1.53	2.62	2.08	0.71	1.22	0.97

TABLE 4.1.1.2: Corrosion Rates of Steel in Blended Cement Concrete

Cement Type	Half Cell Potentential E_{corr} (mV) SCE				Tafel Constants (mV/decade) Anodic			Cathodic			Corrosion Current Density (μ A/cm)				Corrosion Rate (mpy)			
	(1)	(2)	(3)	mean	(1)	(2)	(3)	(1)	(2)	(3)	(1)	(2)	(3)	mean	(1)	(2)	(3)	mean
Plain Cem- (C_3A:14%)	-614	-647	-	-631	472	447	-	279	300	-	1.53	2.62	-	2.08	0.71	1.21	-	0.97
30% Fly Ash Blended Cement	-819	-622	-	-720	356	413	-	179	298	-	1.04	1.03	-	1.04	0.48	0.48	0.85	0.60
70% Blast Furnace Slag Cement	-596	-646	-658	-633	342	461	343	235	310	235	1.18	1.68	1.16	1.34	0.55	0.78	0.54	0.62
10% Micro-silica Blended Cement	-611	-562	-605	-593	403	396	377	257	273	270	1.51	1.56	1.74	1.60	0.70	0.72	0.80	0.74
20% Micro-silica Blended Cement	-625	-603	-	-614	377	288	-	288	308	-	2.31	2.55	-	2.43	1.07	1.18	-	1.13

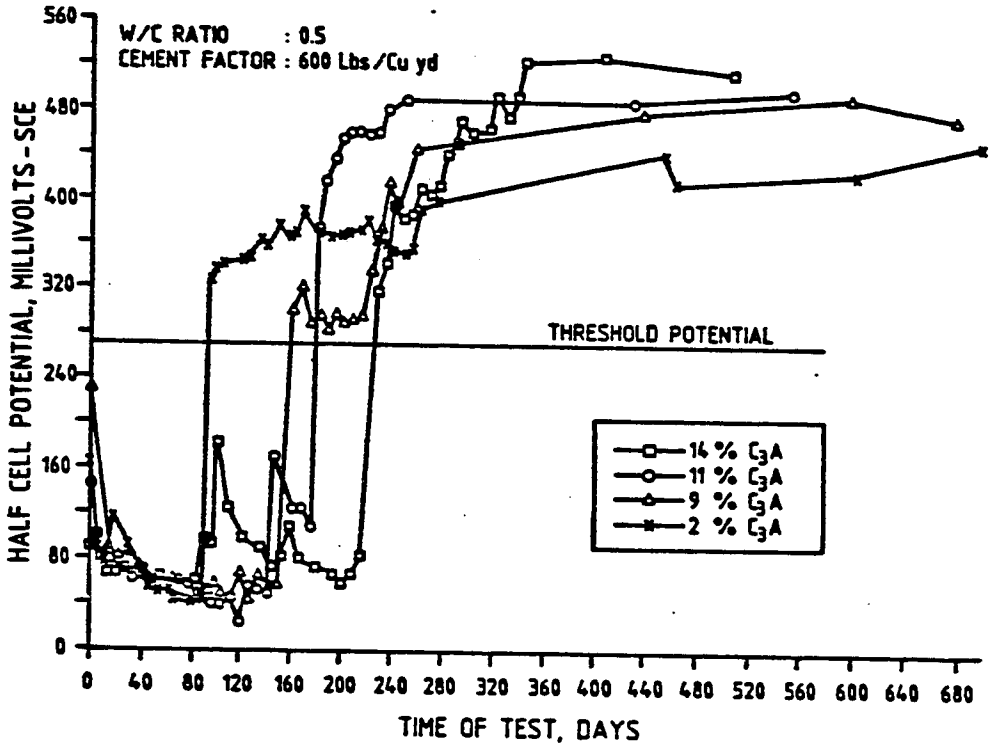

Fig. 4.1.1.1: Potential Measurement Record Showing the Effect of C_3A Content on Corrosion of Reinforcing Steel in Concrete

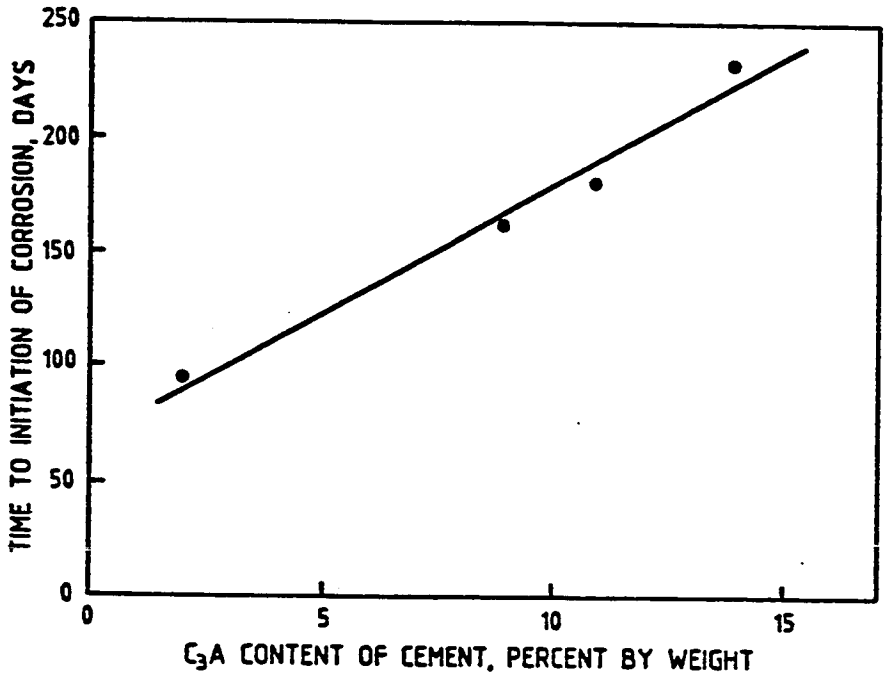

Fig. 4.1.1.2: Effect of C_3A Content of Cement on Time to Initiation of Corrosion of Reinforcing Steel in Concrete

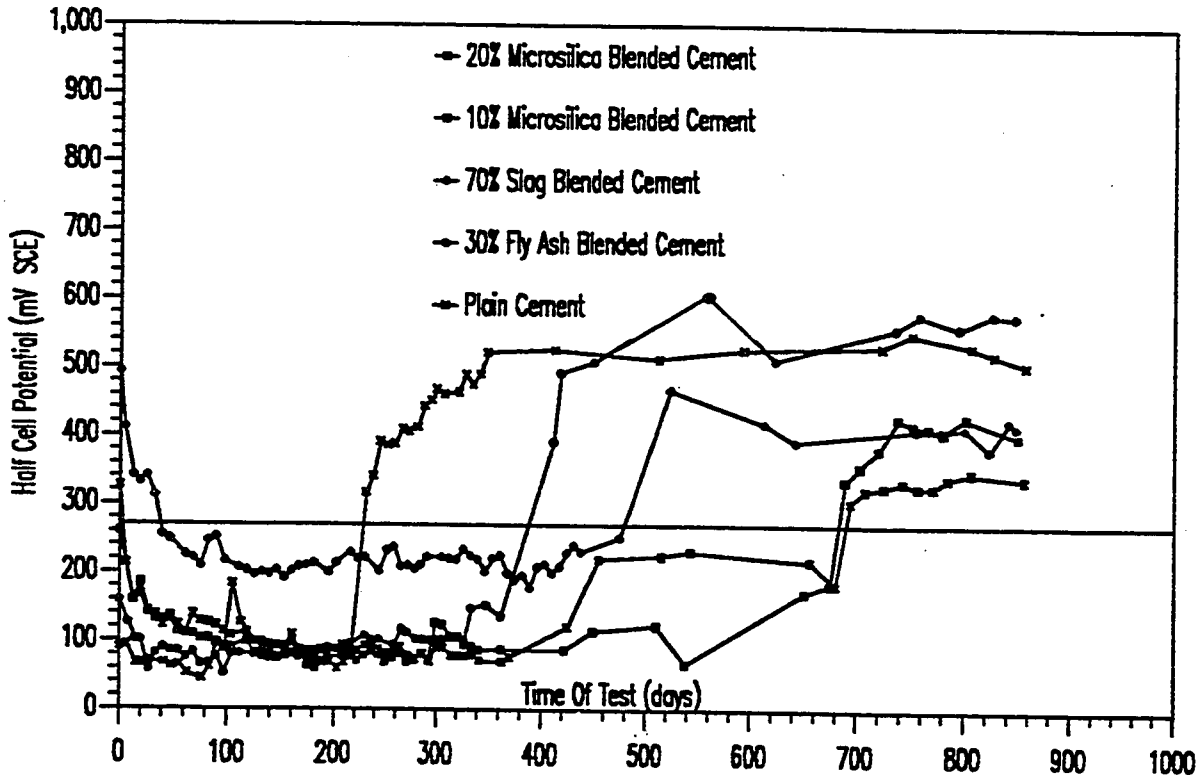

Fig. 4.1.1.3: Potential Measurement Record of Steel in Plain and Blended Cement Concrete

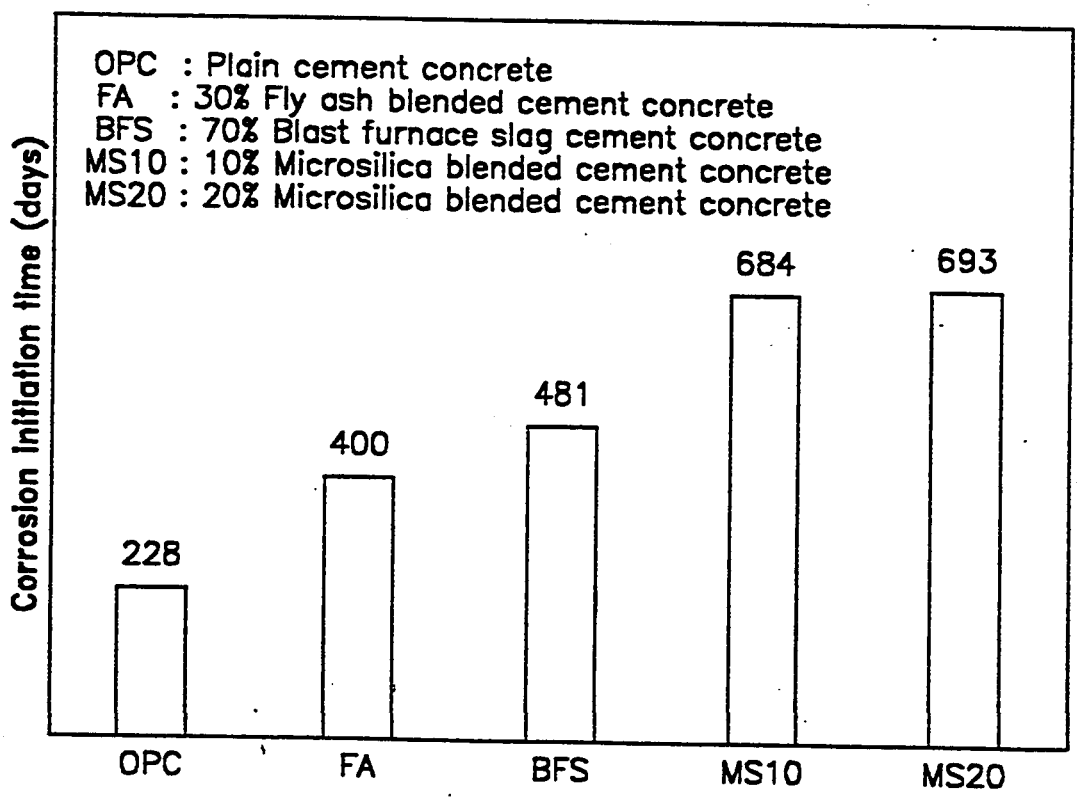

Fig. 4.1.1.4: Corrosion Initiation Time of Steel in plain and Blended Cements Concrete

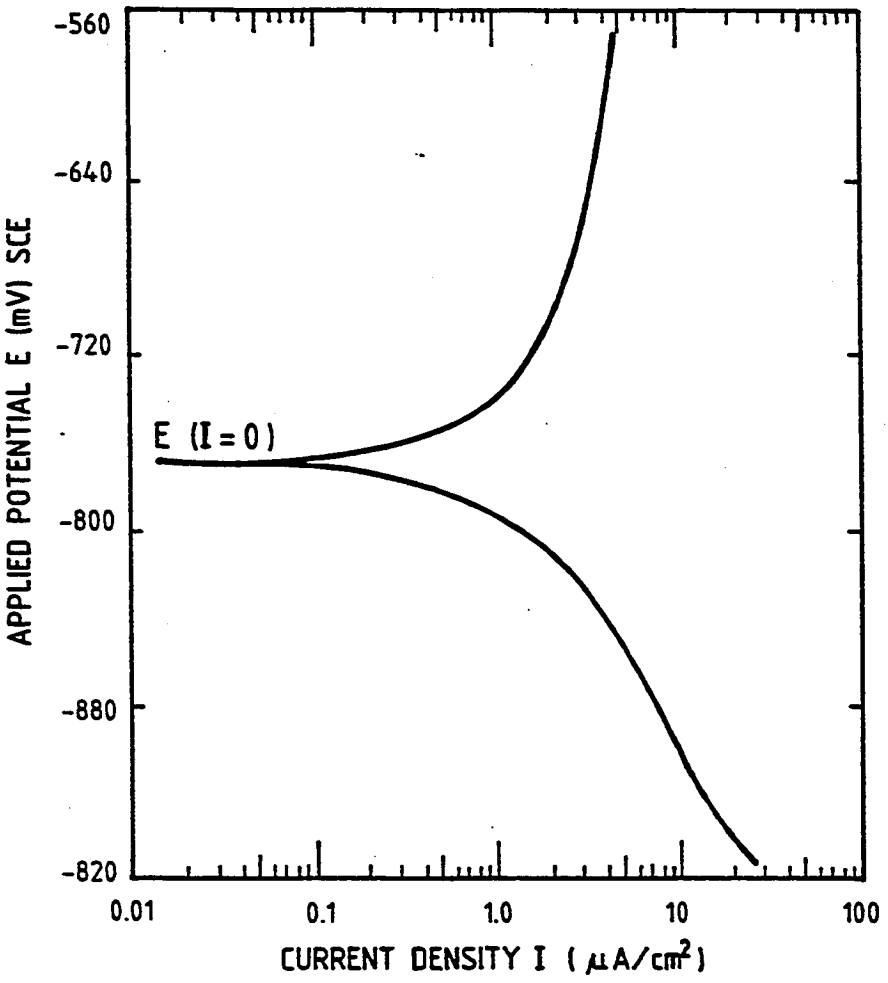

Fig. 4.1.1.5: Anodic and Cathodic Polarization Curves for Steel in Type V (C_3A : 2%) Cement Concrete.

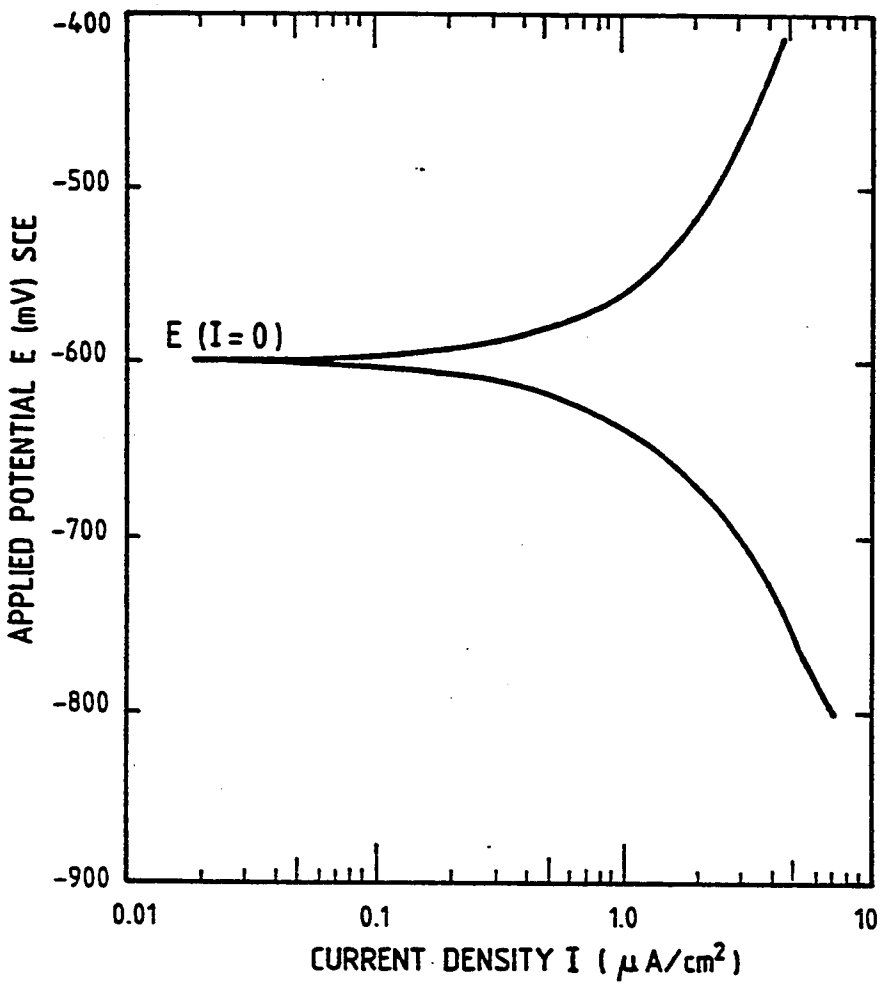

Fig. 4.1.1.6: Anodic and Cathodic Polarization Curves for Steel in Type I (C_3A : 9%) Cement Concrete.

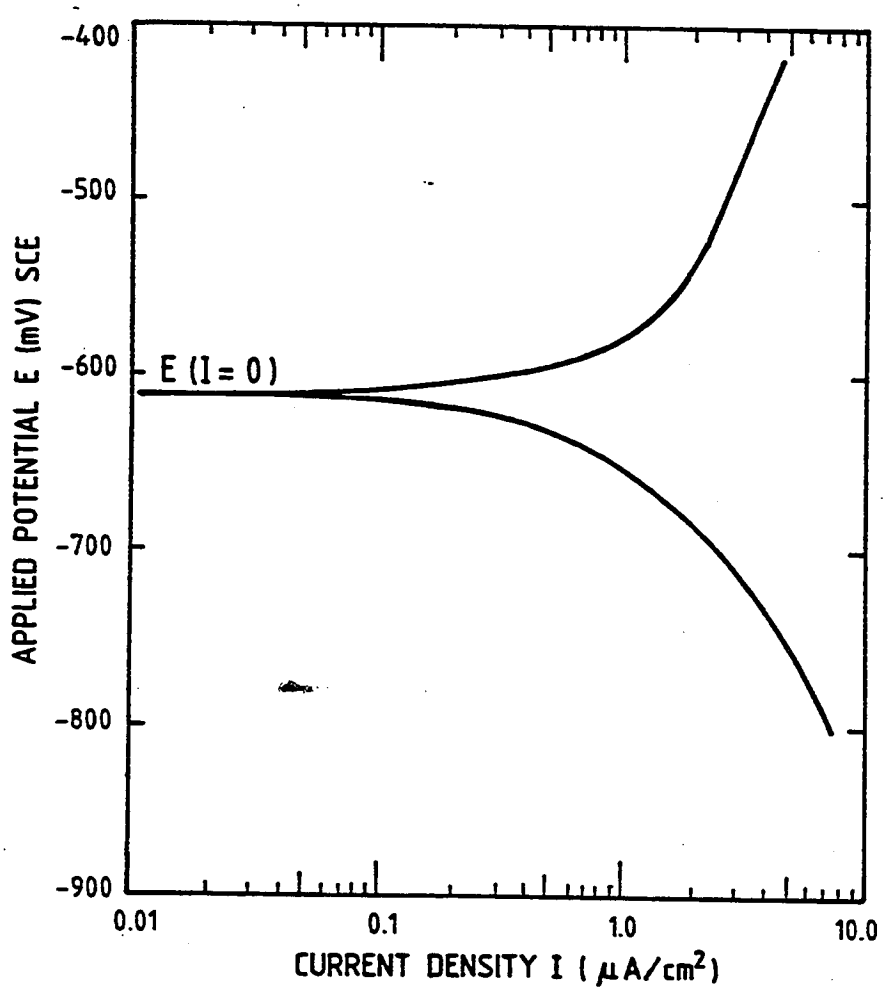

Fig. 4.1.1.7: Anodic and Cathodic Polarization Curves for Steel in Type I (C_3A : 11%) Cement Concrete.

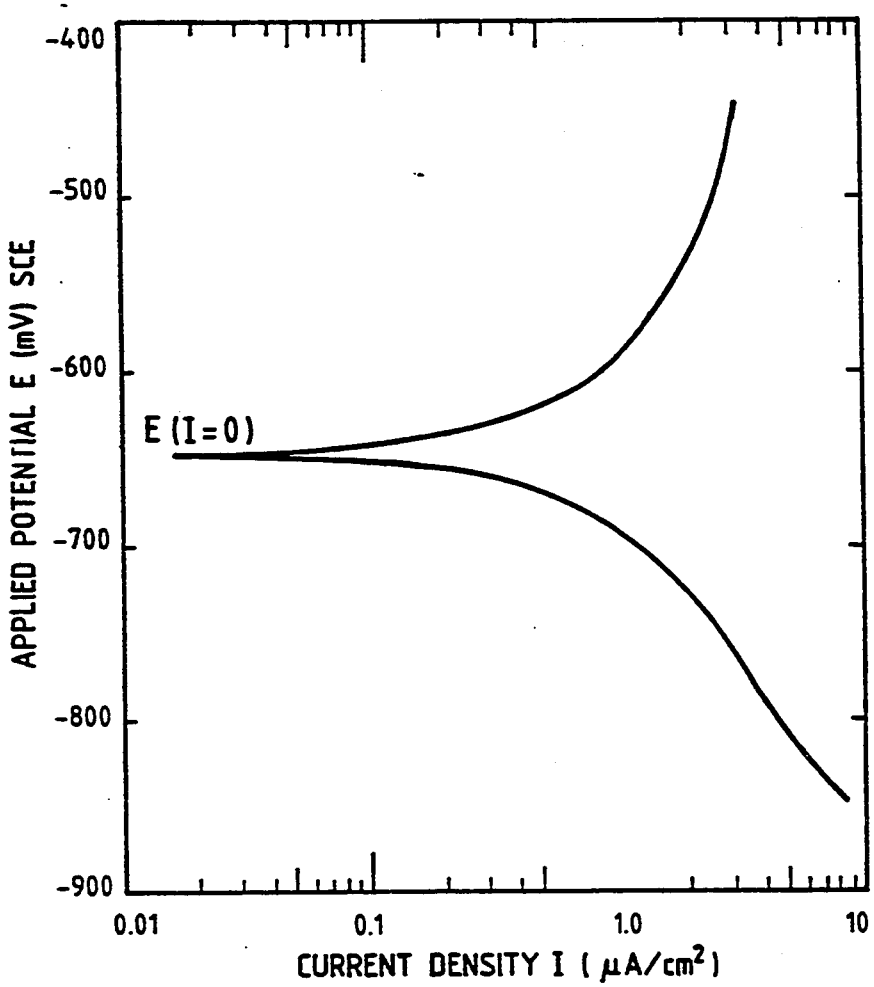

Fig. 4.1.1.8: Anodic and Cathodic Polarization Curves for Steel in Type I (C_3A : 14%) Cement Concrete.

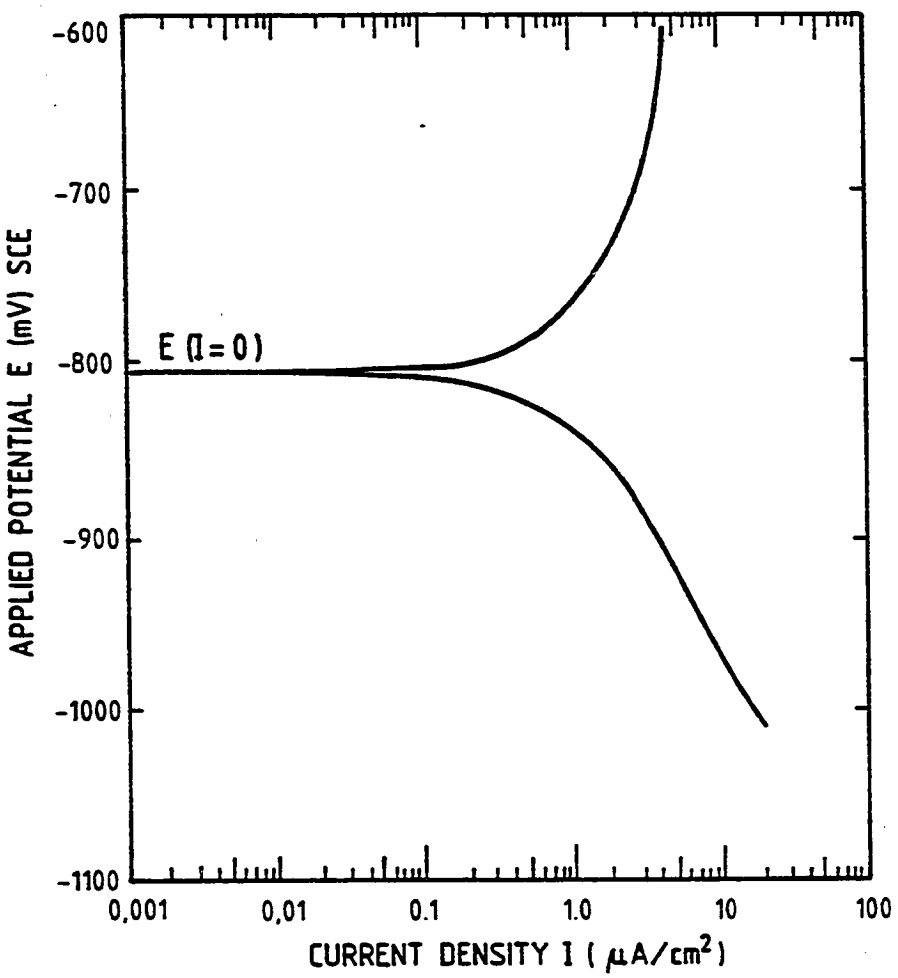

Fig. 4.1.1.9: Anodic and Cathodic Polarization Curves for Steel in 30% Fly Ash Blended Cement Concrete.

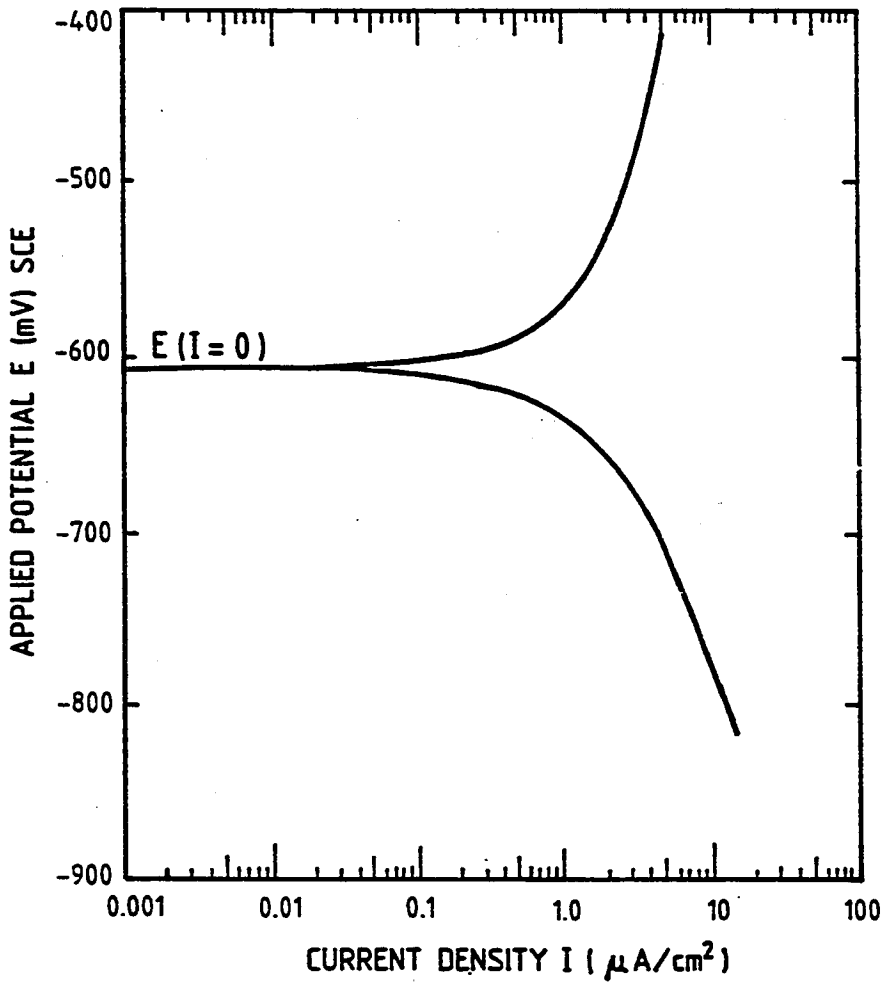

Fig. 4.1.1.10: Anodic and Cathodic Polarization Curves for Steel in 70% Blast Furnace Slag Cement Concrete.

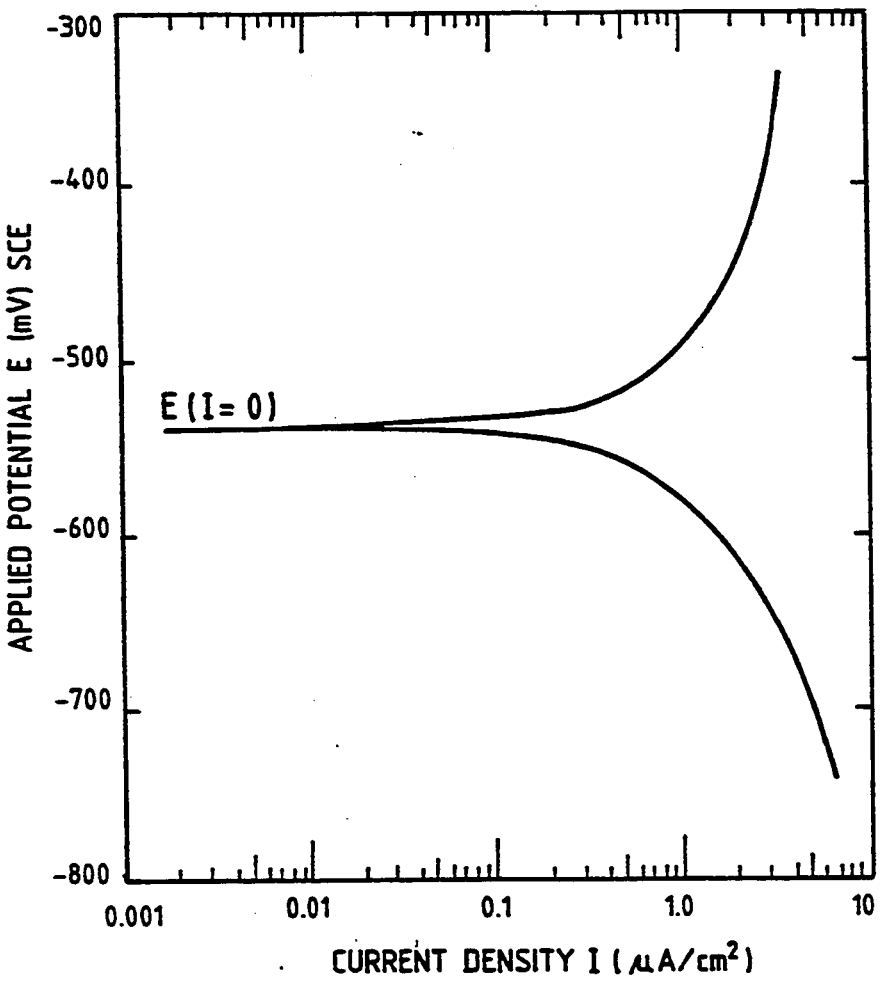

Fig. 4.1.1.11: Anodic and Cathodic Polarization Curves for Steel in 10% Microsilica Blended Cement Concrete.

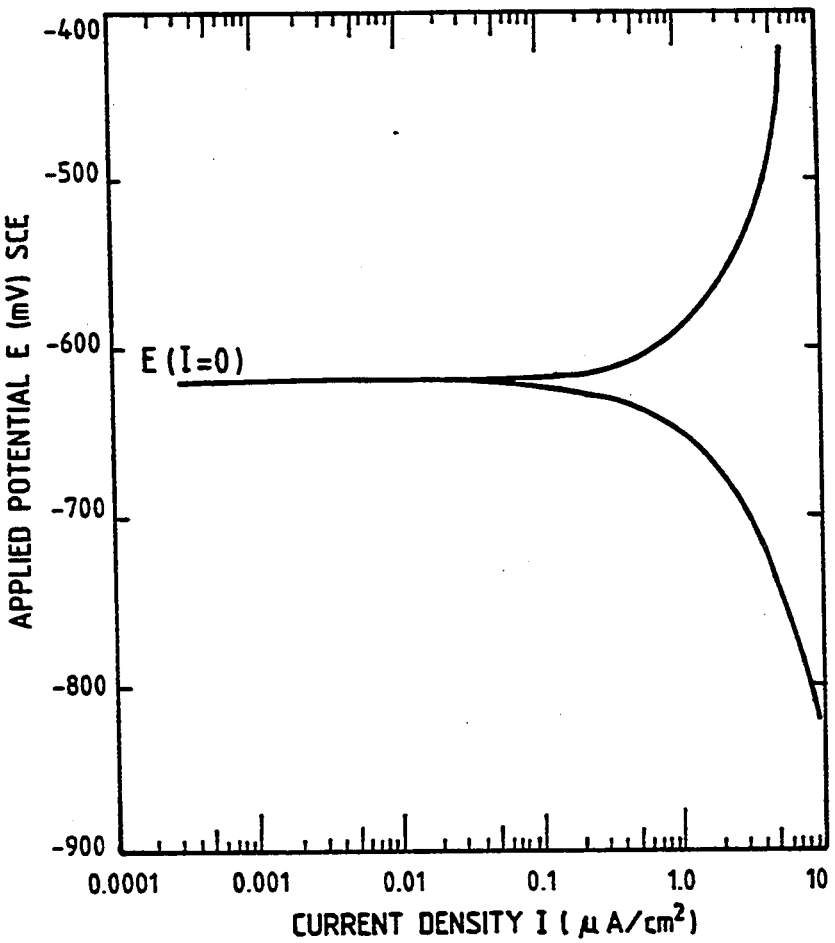

Fig. 4.1.1.12: Anodic and Cathodic Polarization Curves for Steel in 20% Microsilica Blended Cement Concrete.

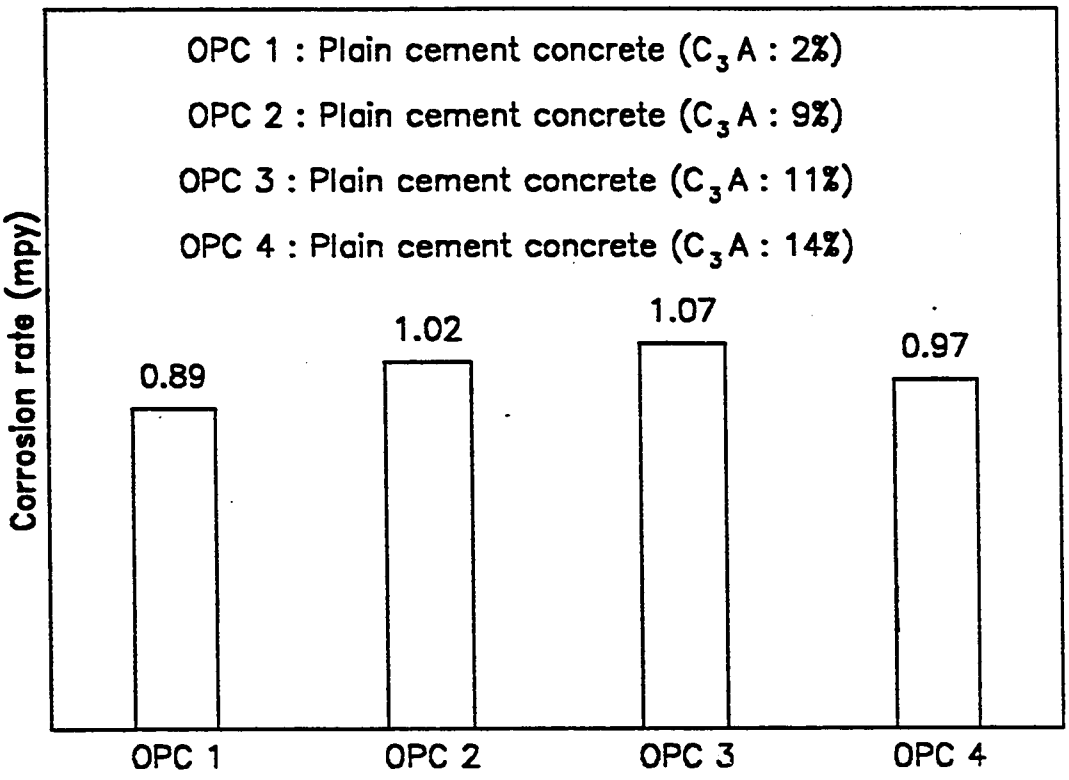

Fig. 4.1.1.13: Effect of C_3A Cement on Corrosion Rate of Steel in Plain Cement Concrete

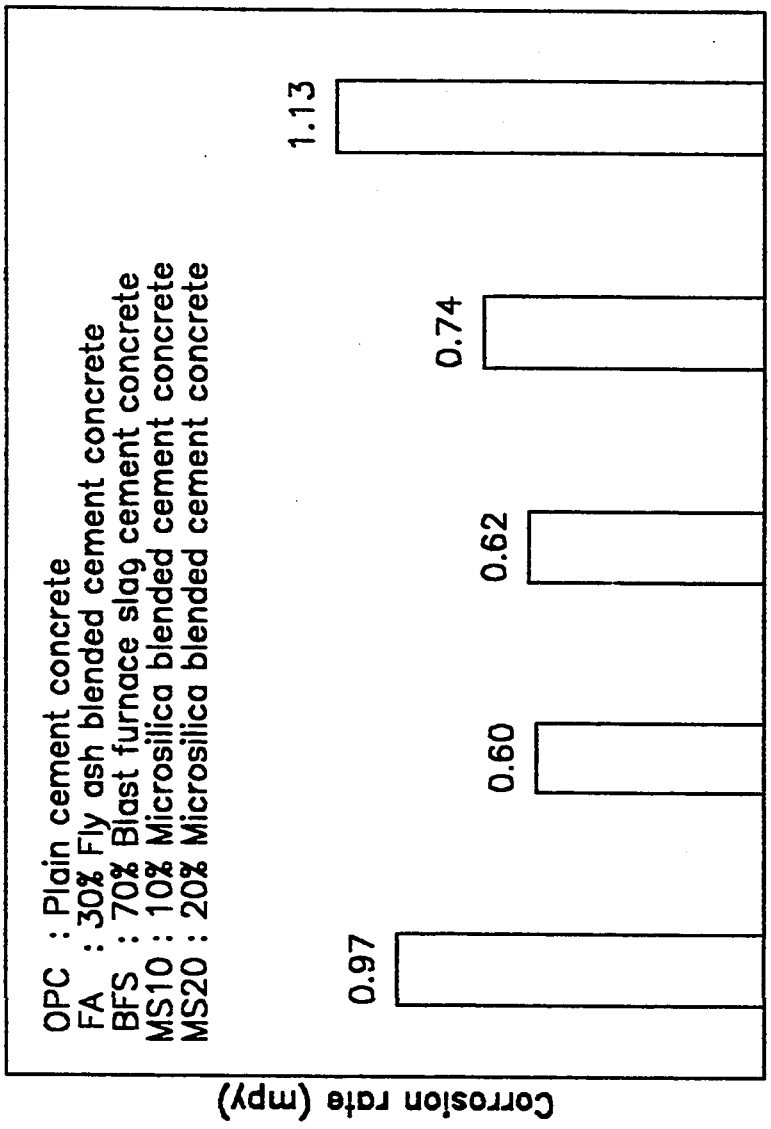

Fig. 4.1.1.14: Corrosion Rate of Steel in Plain and Blended Cement Concrete

4.1.2 ALKALI-SILICA REACTIVITY IN PLAIN AND BLENDED CEMENTS

Mortar-bar expansion data up to a period of six months for the plain parent cement (control) and the microsilica, slag and fly ash blended cements are plotted in Fig.4.1.2.1. The final six-month expansions are shown in Fig. 4.1.2.2 to facilitate quantitative comparison.

The hydroxyl ion concentrations and the pH values of the pore solutions extruded from various plain and blended cements containing different levels of alkalies are given in Table 4.1.2.1.

It must be noted that the measured values represent changes in the OH^- concentrations only, without taking into account the volume of pore solution due to its chemical consumption during the formation of chemical hydrates. The proportion of chemically bound water in mature hydrated cement pastes of constant water/solids ratio decreases in blended cements. Also, the "evaporable water", which is the residual capillary water after its progressive reduction by the ongoing process of cement hydration, increases as the replacement level by blend material increases.

The mortar-bar expansion results show that for the plain parent cement (equivalent Na_2O 1.2%), the expansions began immediately with no incubation period with the highest rate obtainable for the first 20 days, thereafter decreasing gradually to a low value. A highly unacceptable final value of 0.865%, 8.65 times the allowable 0.1% value, was measured at the end of the six-month period for the plain cement. Replacement by 10% and 20% microsilica (1.11 and 1.02% alkalies) decreased the six-month

expansion values to 0.023% and 0.009% respectively. For the 60% and 70% blast furnace slag cements (equivalent Na_2O values 0.76% and 0.69% respectively), the corresponding values were 0.04% and 0.028%. Expansion with 30% fly ash blended cement is at the 6 months permissible limit (0.1%) and in view of the fact that the reactivity of the aggregate is unusually high and the alkali content is also high, this performance should be acceptable.

The measured OH^- concentrations in the pore solution ranged from a maximum of 946 mM/L for the high 1.5% alkali content to a low of 13 mM/L for the 25% microsilica blended cement with 0.65% alkali content. The corresponding pH levels ranged from 13.98 to 12.82.

Microsilica, slag and fly ash inductions reduced hydroxide ion concentrations significantly. The reduction, however, was drastic (for example, from 946 mM/L to 16 mM/L for the 1.5% alkali cements) with 25% microsilica. Also, in medium 0.9% alkali cements, 60% blast furnace slag appears to be an alkali remover comparable to 10% microsilica. However, in the case of high 1.5% alkali cements, even 10% microsilica is appreciably more effective in removing hydroxide ions than 60% slag. It is seen that in the case of 1.5% alkali plain and blended cements, whereas 10% microsilica reduces OH^- concentration from 946 mM/L to 533 mM/L, 60% slag reduces it only to a level of 708 mM/L. 20% microsilica is manifold more effective as an alkali oxide remover than even 70% slag for the whole range of alkali contents included in this program. This is specially so for the high 1.5% alkali cement where 25% microsilica is 37 times as effective as 70% slag.

Table 4.1.2.1 : Hydroxyl Ion Concentration and pH of Pore Solutions Extruded from Plain and Blended Cements

Cement	Replacement Level	OH^- Ion Concentration								Pore Solution pH							
		Equivalent Na_2O Content								Equivalent Na_2O Content							
		1.2	0.90	1.11	1.02	1.50	0.76	0.69	0.65	1.2	0.90	1.11	1.02	1.50	0.76	0.69	0.65
OPC Type1 (C_3A:14%)	0	735#	510	679	622	946	425	376	348	13.87	13.71	13.83	13.79	13.98	13.63	13.58	13.54
Microsilica Blended Cement	5	724	490	650#	580	942	390	355	306	13.86	13.69	13.81	13.76	13.97	13.59	13.53	13.49
- do -	10	403	273	368#	-	533	-	-	165	13.61	13.44	13.57	-	13.73	-	-	13.22
- do -	15	234	160	215	200#	290	155	145	135	13.37	13.26	13.33	13.30	13.46	13.19	13.16	13.13
- do -	20	69	67	-	68#	70	-	-	66	12.84	12.83	-	12.83	12.85	-	-	12.82
- do -	25	15	14#	15	14	16	13	13	13	12.18	12.15	12.18	12.15	12.20	12.11	12.11	12.11
Blast Furnace Slag Cement	60	465	215	-	-	708	137#	-	-	13.67	13.33	-	-	13.85	13.14	-	-
- do -	70	350	113	-	-	600	-#	-	-	13.54	13.05	-	-	13.85	-	-	-
Fly Ash Blended Cement	30	265	95	215	160	440#	-	-	-	13.42	12.98	13.33	13.20	13.64	-	-	-

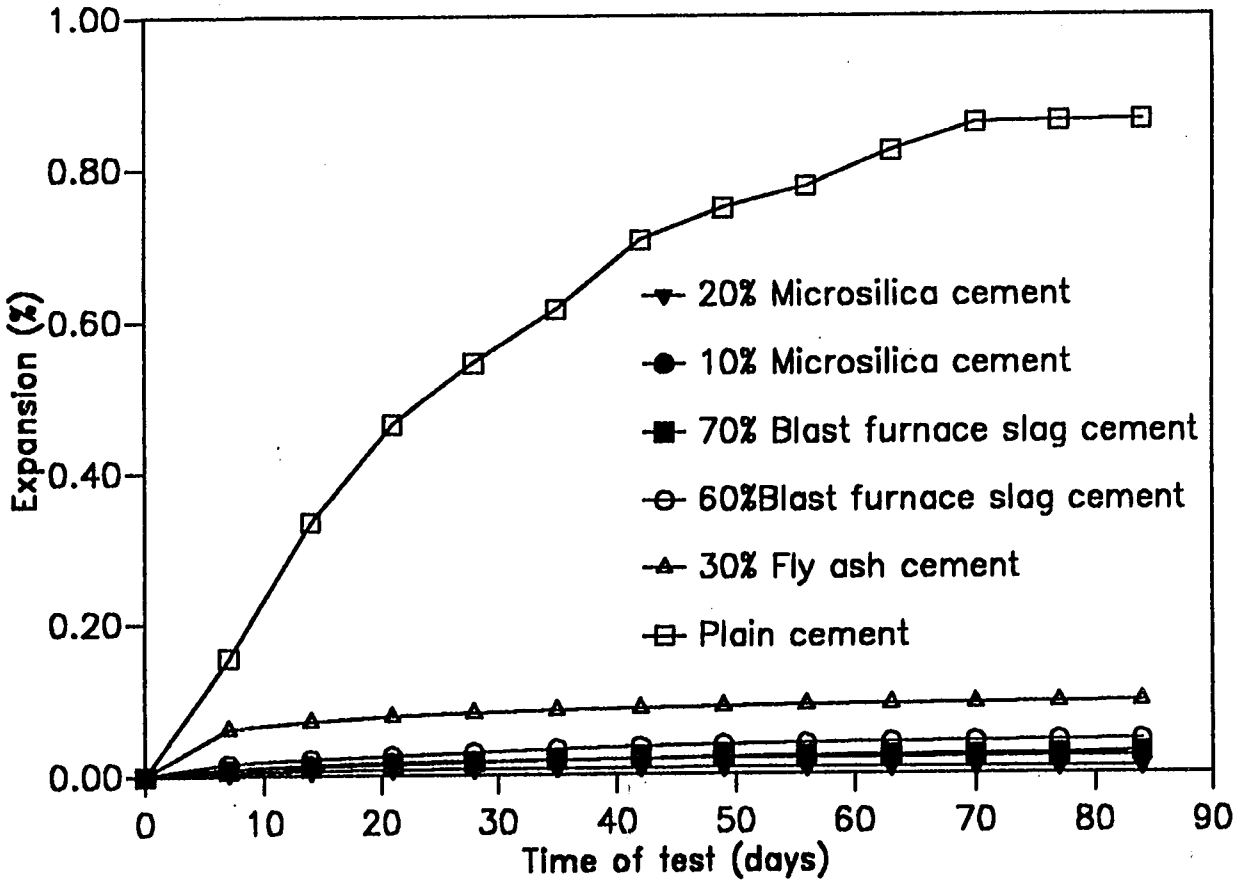

Fig. 4.1.2.1: Expansion in Plain and Blended Cements due to Alkali - Silica Reaction

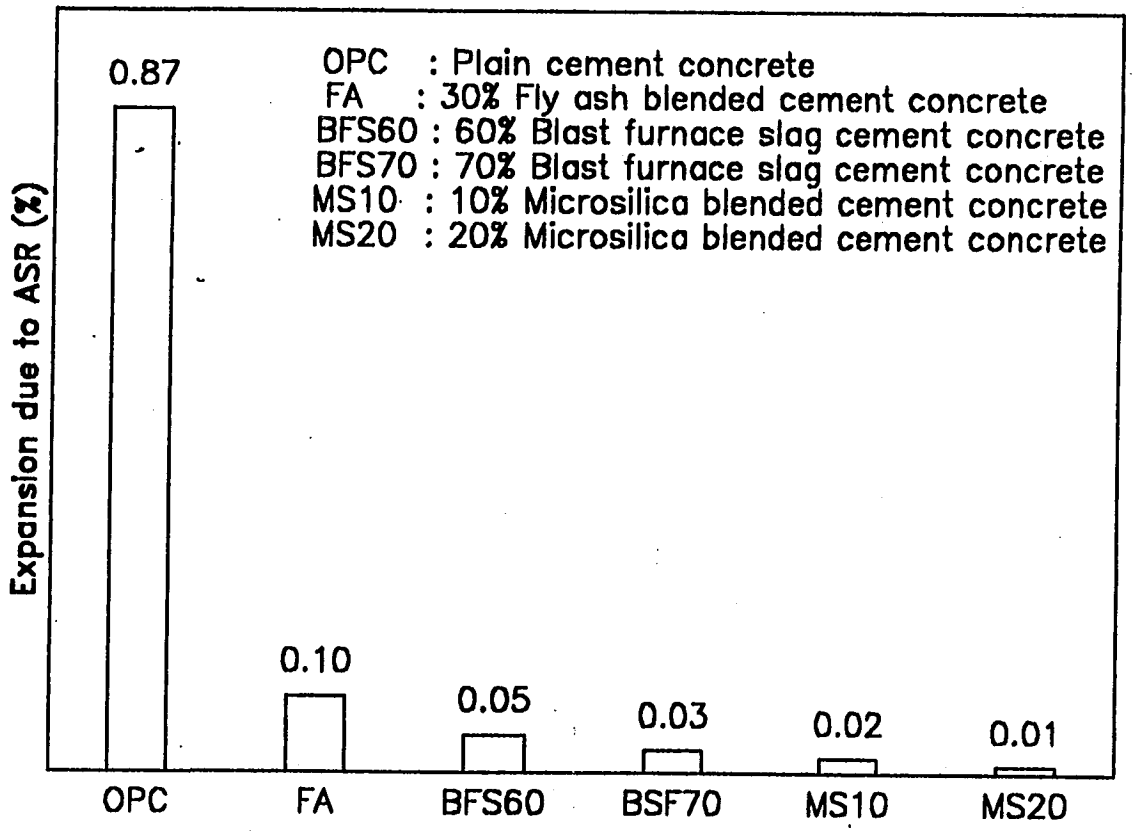

Fig. 4.1.2.2: Alkali - Silica Reaction Expansions of Plain and Blended Cements after 7 months of test with a Highly Reactive Aggregate

4.2 CHEMICAL ENVIRONMENT OF PLAIN AND BLENDED CEMENTS

4.2.1 CHLORIDE BINDING MECHANISM IN PLAIN CEMENTS

4.2.1.1 Effect of C_3A Content of Cement

(i) Equilibrium Chloride Ion Concentrations in Pore Solution

Table 4.2.1.1 gives the free chloride concentrations measured in the pore water for 2.43, 7.59, 8.52 and 14% C_3A cements. The unbound chloride concentrations were measured for four chloride levels of 0.3, 0.6, 1.2 and 2.4% by weight of cement. The free chloride concentrations in the pore water are plotted in Fig. 4.2.1.1 as a percentage of chloride concentration in mix water for the four cements and the four chloride treatment levels.

From the data of Table 4.2.1.2 and Fig. 4.2.1.1, it is seen that the free chloride concentrations in the pore water decrease significantly with increasing C_3A content of cement. Typically, for a 0.6% chloride treatment level, the unbound chloride concentrations were 74.4, 38.7, 32.0 and 18.1% of the total chloride in the mix water for the 2.43, 7.59, 8.52 and 14% C_3A cements respectively. It must be noted that these values represent changes in the chloride concentrations only, without taking into account the changes in the volume of the pore solution due to its chemical consumption during the formation of cement hydrates. Hence these concentrations per se do not represent the

actual amount of chlorides bound by the solid hydration products.

The unbound chlorides for the four cements as percentage of total chlorides are given in Column 5 of Table 4.2.1.2. Here the total mass of chloride unbound by the hydration products is calculated on the basis of "evaporable water" which is the residual capillary water after its progressive reduction by the ongoing process of cement hydration. The original mix water of 60 g./100 g. of cement is reduced to quantities shown in column 4 of Table 4.2.1.2 as "evaporable water", which forms the basis of calculating total unbound chloride. The data of Table 4.2.1.2 and Figs. 4.2.1.2 and 4.2.1.3 show that the unbound chloride fraction decreases significantly as the C_3A content of cement increases. Typically, for the 0.6% chloride treatment level, the unbound chlorides for 2.43, 7.59, 8.52 and 14% C_3A cements are 50.7, 24.6, 20.6 and 11.6% of the total chlorides respectively. The decrease in the unbound chloride is attributable to the increase in the formation of Friedel's salt with increasing C_3A content of cement as shown by DTA patterns in Fig. 4.2.1.4.

The unbound chloride-C_3A relationships in Figs. 4.2.1.2 and 4.2.1.3 show that for the four chloride additions of 0.3, 0.6, 1.2 and 2.4% there is 4.94, 4.37, 2.53 and 1.51 fold decrease in the free unbound chloride content of the pore solution with an increase in the C_3A content from 2.43 to 14%. It is noteworthy that the C_3A effect is specially beneficial for binding chlorides in the range of 0.3% to 0.6%, which is well within the range of chloride induction through inadequately prepared constituent concrete materials and brackish curing water.

(ii) Influence of the Level of Total Chloride Content in Concrete

The data pertaining to bound and unbound chlorides for the four cements with level of chloride addition increasing from 0.3% to 2.4% are shown in Table 4.2.1.3 and Fig. 4.2.1.5. Assuming that other cement hydrates do not combine with chlorides, these data show that the amount of chlorides which will complex with cement will depend on the C_3A content of cement and the amount of chloride inducted into the concrete. For each of the four cements, with increase in chloride addition, more chlorides are bound, but far more chlorides also remain free. As an example, for the 8.52% C_3A cement, when initial chloride addition is increased from 0.3% to 2.4%, the bound chlorides are quadrupled, but the free chlorides increase 31 fold, and the ratio of bound to unbound chloride decreases from 6.32 to 0.84. Thus, the data of Table 4.2.1.3 (column 7) and Fig. 4.2.1.5 show that for each of the four cements, although the absolute amount of the bound chloride increases, the ratio of bound to unbound chlorides decreases with increasing levels of chloride addition. The chloride binding increases almost linearly up to a chloride treatment level of 0.6% beyond which it tends to level out specially for cements 1, 2 and 3. 14% C_3A cement 4 shows a higher rate of chloride-binding up to 1.2% chloride addition as against a chloride level of 0.6% shown by other three cements 1, 2 and 3. Fig. 4.2.1.5 shows that the ratio of bound to unbound chlorides decreases significantly with increasing level of chloride addition. For 2.43, 7.59, 8.52 and 14% C_3A cements the ratios of bound to unbound chloride are respectively 6.77, 6.56, 7.5 and 14.4 times more for the lower level of 0.3% chloride addition compared to 2.4% chloride addition. These data also show that as the total chloride content increases, the chloride-binding performance ratio between higher and lower C_3A cements decreases sharply. In terms of bound to unbound chloride ratio, the 6.9

fold superiority of the 14% C_3A cement over the 2.43% C_3A cement at the 0.3% chloride addition level, drops to 3.2 for 2.4% chloride addition; also, a differential of higher than 2 in the ratio of bound to unbound chlorides between the 14% and 7.59/8.52% C_3A cements at 0.3% chloride addition, almost vanishes at 2.4% chloride treatment level.

This behavior in terms of chloride binding is explained by the fact that C_3A or any other cement hydrate can complex only with a limited amount of chlorides. As the quantity of chlorides progressively exceeds this complexing capacity, more and more chlorides would be left uncombined.

This conclusion is also supported by the exposure site test data developed at King Fahd University of Petroleum and Minerals by Rasheeduzzafar et al (44). Two cements, one Type I (C_3A: 9.5%) and the other Type V (C_3A: 2.8%) were included in the exposure site program with chlorides of 1, 2, 4, 8, 16 and 32 lbs/cu.yd. (0.6, 1.2, 2.4, 4.8, 9.6 and 19.2 kg/m^3) inducted into the concrete through mix water. The exposure site specimens were $4\frac{7}{8}$x$4\frac{7}{8}$x14 inch (120x120x350 mm) prisms each containing four completely embedded 1/2 inch (12.5 mm) diameter plain grade 60 steel bars, one at each corner, at a clear cover of 1 inch (25 mm), also maintained at the top and bottom. All the specimens in the test series designed to evaluate the effect of C_3A content on corrosion were made with a water cement ratio of 0.50 and cement contents of 550, 650 and 750 lbs/cu.yd. (330, 390 and 450 kg/m^3). Corrosion monitoring of the specimens was carried out using two techniques: (i) time required for the appearance of the first crack, and (ii) metal loss measured as loss in weight of the steel bar after the removal of corrosion products. Both time to cracking and metal loss data after 1200

days of exposure showed that C_3A complexes only with a limited quantum of chlorides. As the amount of chlorides becomes excessive, the benefits of the complexing characteristics of C_3A become less perceptible. This is shown in Fig. 4.2.1.6 by a progressively reduced differential in the performance ratio of Type I to Type V cement, using loss of metal as corrosion criterion. Similar results were obtained from time to cracking data.

(iii) Cl^-/OH^- Ratio in Pore Solution

In spite of their critical importance, chloride concentrations alone do not determine decisive corrosion risk. It is now well recognized that depassivation of steel is a function of the Cl^-/OH^- ratio in the pore solution rather than chloride concentrations alone, and this parameter can be regarded as a rough measure of relative corrosion risk in the alkaline chloride bearing pore solutions of concrete. Hausmann (11) on the basis of mild steel corrosion tests in concrete-simulated artificial $Ca(OH)_2$ solution of pH around 12.5, has proposed a threshold depassivation Cl^-/OH^- ratio of 0.60. However, this value cannot be considered to be adequately representing conditions in real concrete, primarily because the pH levels of real concrete pore solutions are significantly higher than 12.5. Table 4.2.1.1 shows that for a sodium chloride-bearing cement, the pore solution pH varies from 13.40 to 13.73. In a later work, Gouda (54) carried out tests similar to Hausmann's in solutions where maximum NaCl threshold concentrations have been evaluated for six pH values ranging from 11.8 to 13.95. Diamond (38) has carefully scaled these data and has converted the results into Cl^-/OH^- ratios for easier comparison. These values are given in Table 4.2.1.4. These data showing Cl^-/OH^- ratio of 0.57 for pH 11.75 and 0.78 for a pH of 12.1 indicate reasonably

good agreement with Hausmann's value of 0.6 for a pH of 12.5. However, the alkaline conditions of a typical concrete pore solution are much more closely represented by a pH of 13.3, which corresponds to a Cl^-/OH^- value of 0.30.

This indicates that the Hausmann's criterion of 0.60 is not adequately representative of the conditions in real concrete, and hence Diamond recommends a depassivation Cl^-/OH^- threshold value of 0.30 to be more appropriate for concrete.

(iv) Threshold Chloride Values

Cl^-/OH^- ratios corresponding to various levels of chloride addition for cements 1, 2, 3 and 4 have been plotted in Fig. 4.2.1.7. A Cl^-/OH^- ratio of 0.30 proposed by Diamond (38) has been adopted to signify onset of depassivation and corrosion. Table 4.2.1.5 shows the threshold chloride contents for the 2.43, 7.59, 8.52 and 14% C_3A cements in terms of unbound water-soluble and total acid-soluble chlorides.

All the four cements have chloride addition from the same sodium cation source. Cements 1, 2 and 4 have very similar alkali contents; cement 3 with 8.52% C_3A, which has a lower alkali content of 0.43%, is shown to have chloride-binding behavior very similar to cement 2 with a C_3A content of 7.59%, thereby discounting a significant effect of alkali difference in this range of values.

In view of this position, it is seen from the data of Table 4.2.1.4 that the C_3A content of cement has a very significant role in chloride binding and in determining threshold chloride content. For sodium chloride addition the level of total acid-soluble chloride tolerable in the Type I 14% C_3A cement 4 (1% by weight of cement) is about

Table 4.2.1.1: Analysis of Pore Solution from Chloride-Bearing Specimens of Different Cements

Cement No.	C_3A Content of Cement (% by weight)	NaCl Addition (% by weight of cement)	Cl^- Addition		Pore Solution Composition				Cl^- Concentration in Pore Solution (% of Cl^- Concentration in Mix Water)
			(% by weight of cement)	In Mix Water (mM/L)	Cl^- (mM/L)	OH^- (mM/L)	pH	Cl^-/OH^-	
1	2.43	0.5	0.3	141	69.7	258	13.41	0.2702	49.4
1	2.43	1.0	0.6	282	209.9	265	13.42	0.7921	74.4
1	2.43	2.0	1.2	563	529.9	254	13.40	2.0862	94.1
1	2.43	4.0	2.4	1126	1368.0	231	13.36	5.9221	121.5
2	7.59	0.5	0.3	141	35.0	385	13.59	0.091	24.8
2	7.59	1.0	0.6	282	109.0	391	13.59	0.279	38.7
2	7.59	2.0	1.2	563	342.0	413	13.62	0.828	60.7
2	7.59	4.0	2.4	1126	987.0	268	13.43	3.683	87.7
3	8.52	0.5	0.3	141	30.0	334	13.53	0.090	21.5
3	8.52	1.0	0.6	282	90.0	376	13.57	0.239	32.0
3	8.52	2.0	1.2	563	331.0	477	13.68	0.694	58.8
3	8.52	4.0	2.4	1126	965.0	350	13.54	2.757	85.7
4	14.00	0.5	0.3	141	14.8	524	13.72	0.028	10.5
4	14.00	1.0	0.6	282	51.0	503	13.70	0.101	18.1
4	14.00	2.0	1.2	563	216.0	534	13.73	0.405	38.4
4	14.00	4.0	2.4	1126	904.0	518	13.71	1.745	80.3

Table 4.2.1.2: Percentage of Unbound Chlorides for Different C_3A Cements

Cement No.	C_3A Content of Cement (% by weight)	Cl^- Addition (% by weight of cement)	Evaporable Water (% by weight of cement)	Unbound Cl^- (% by weight of Cl^- Addition)
1	2.43	0.3	40.1	33.1
1	2.43	0.6	40.8	50.7
1	2.43	1.2	39.4	61.8
1	2.43	2.4	38.0	76.9
2	7.59	0.3	38.7	15.9
2	7.59	0.6	38.2	24.6
2	7.59	1.2	39.8	40.3
2	7.59	2.4	38.0	55.5
3	8.52	0.3	38.2	13.7
3	8.52	0.6	38.6	20.6
3	8.52	1.2	38.4	37.6
3	8.52	2.4	38.0	54.2
4	14.00	0.3	38.4	6.7
4	14.00	0.6	38.4	11.6
4	14.00	1.2	38.2	24.4
4	14.00	2.4	38.0	50.8

Table 4.2.1.3: Ratio of Bound to Unbound Chlorides for Different C_3A Cements

Cement No.	C_3A Content of Cement (% by weight of cement)	Cl^- Addition (% by weight of cement)	Unbound Cl^- (% by weight of Cl^- Addition)	Unbound Cl^- (% by weight of cement)	Bound Cl^- (% by weight of cement)	$\frac{\text{Bound } Cl^-}{\text{Unbound } Cl^-}$
1	2.43	0.3	33.1	0.100	0.200	2.00
1	2.43	0.6	50.7	0.304	0.296	0.97
1	2.43	1.2	61.8	0.742	0.458	0.62
1	2.43	2.4	76.9	1.846	1.554	0.30
2	7.59	0.3	15.9	0.048	0.252	5.25
2	7.59	0.6	24.6	0.148	0.452	3.05
2	7.59	1.2	40.3	0.484	0.716	1.48
2	7.59	2.4	55.5	1.332	1.068	0.80
3	8.52	0.3	13.7	0.041	0.259	6.32
3	8.52	0.6	20.6	0.124	0.476	3.84
3	8.52	1.2	37.6	0.451	0.749	1.66
3	8.52	2.4	54.2	1.301	1.099	0.84
4	14.00	0.3	6.7	0.020	0.280	14.00
4	14.00	0.6	11.6	0.070	0.530	7.57
4	14.00	1.2	24.4	0.293	0.907	3.10
4	14.00	2.4	50.8	1.219	1.181	0.97

Table 4.2.1.4: Critical Cl^-/OH^- Ratios for Onset of Depassivation

Point	pH	Estimated Cl^-/OH^- Ratio
1	11.8	0.57
2	12.1	0.48
3	12.6	0.29
4	13.0	0.27
5	13.3	0.30
6*	(13.95)	(0.09)

* Validity of this point considered dubious.

Table 4.2.1.5: Threshold Chloride Values for Different C_3A Cements

Cement No.	C_3A Content of Cement (% by weight of cement)	Alkalies as Equivalent Na_2O Content of Cement (% by weight)	Threshold Chloride (% by weight of cement)	
			Free Cl^-	Total Cl^-
1	2.43	0.58	0.135	0.35
2	7.59	0.60	0.165	0.62
3	8.52	0.43	0.170	0.65
4	14.00	0.65	0.215	1.00

ACI 318- 83 : 0.15 % Water-soluble (free) chlorides

CP 110 : 0.35 % total acid soluble chlorides

RILEM : 0.40 % total acid-soluble chlorides

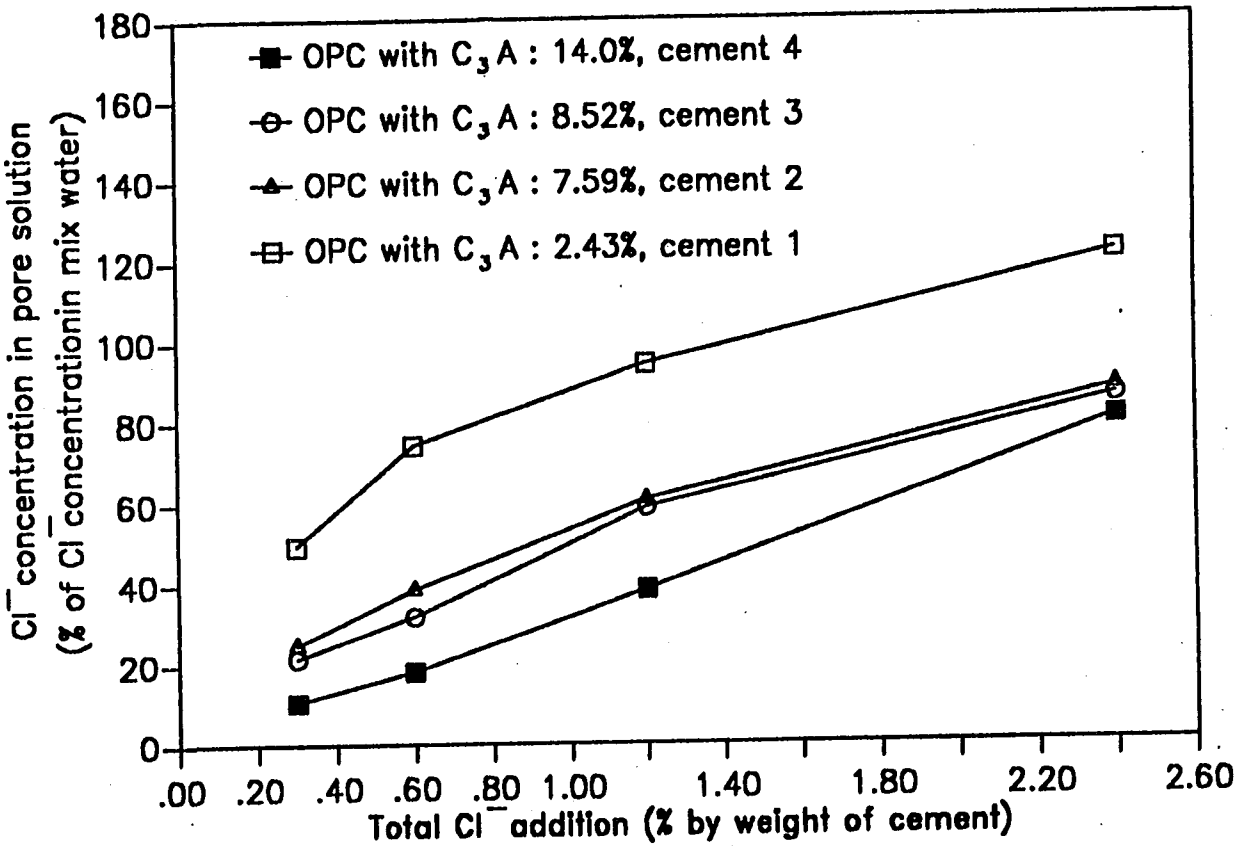

Fig. 4.2.1.1: Chloride Concentrations in Pore Solutions of Different Cements Treated with Various Levels of Chloride addition

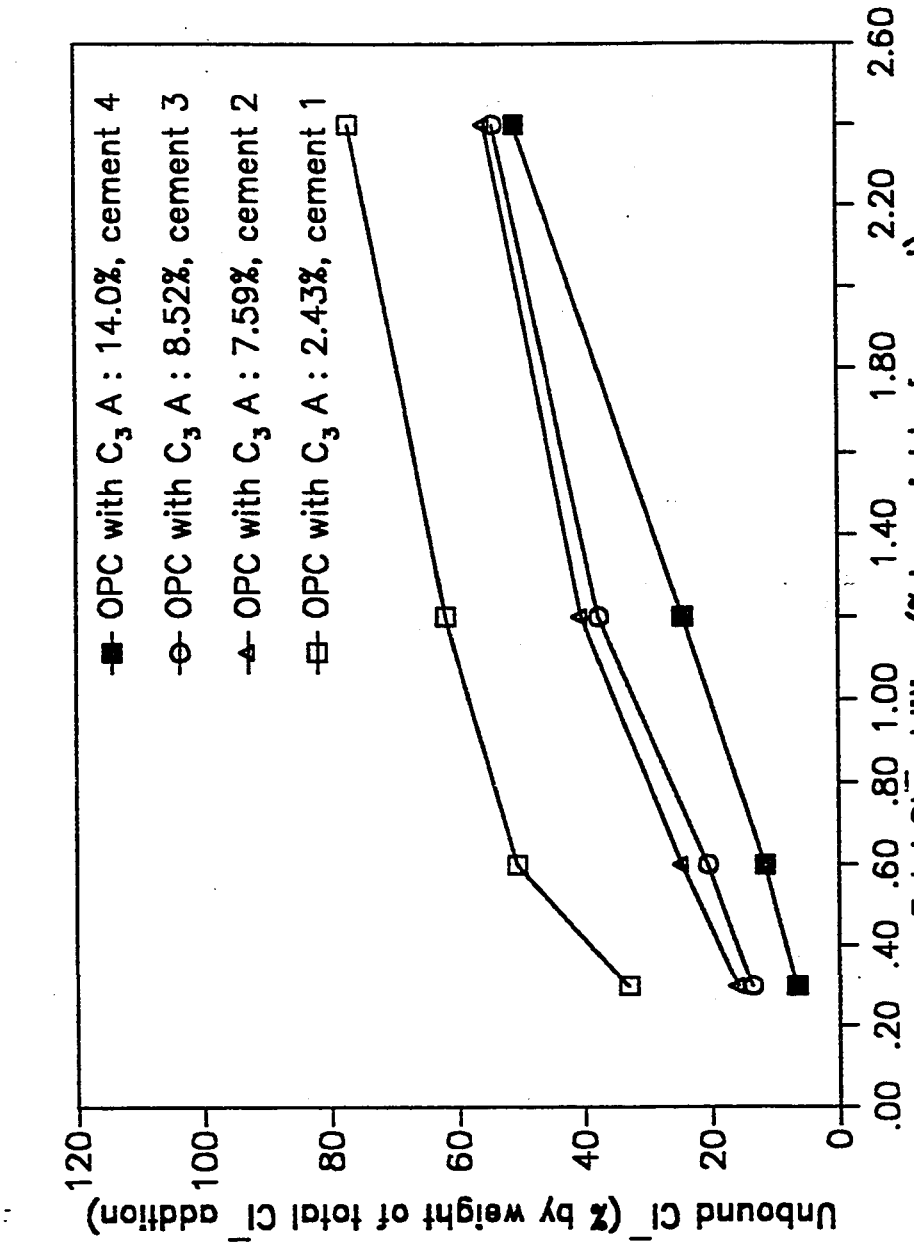

Fig. 4.2.1.2: Unbound Chlorides in Pore Solutions of Various C_3A Cements Treated with Different Levels of Chloride

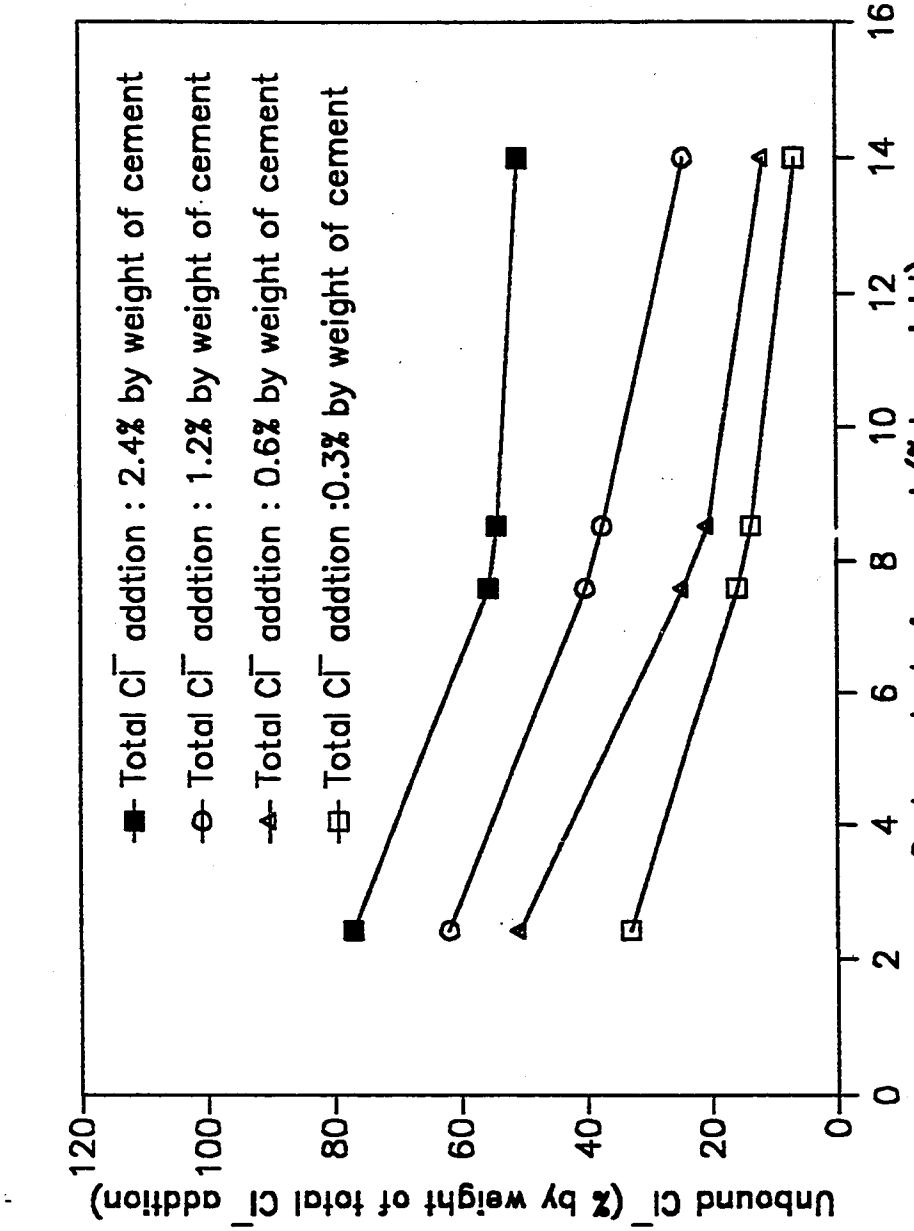

Fig. 4.2.1.3: Effect of C_3A Content of Cement on Chloride Remaining Unbound in Pore Solution

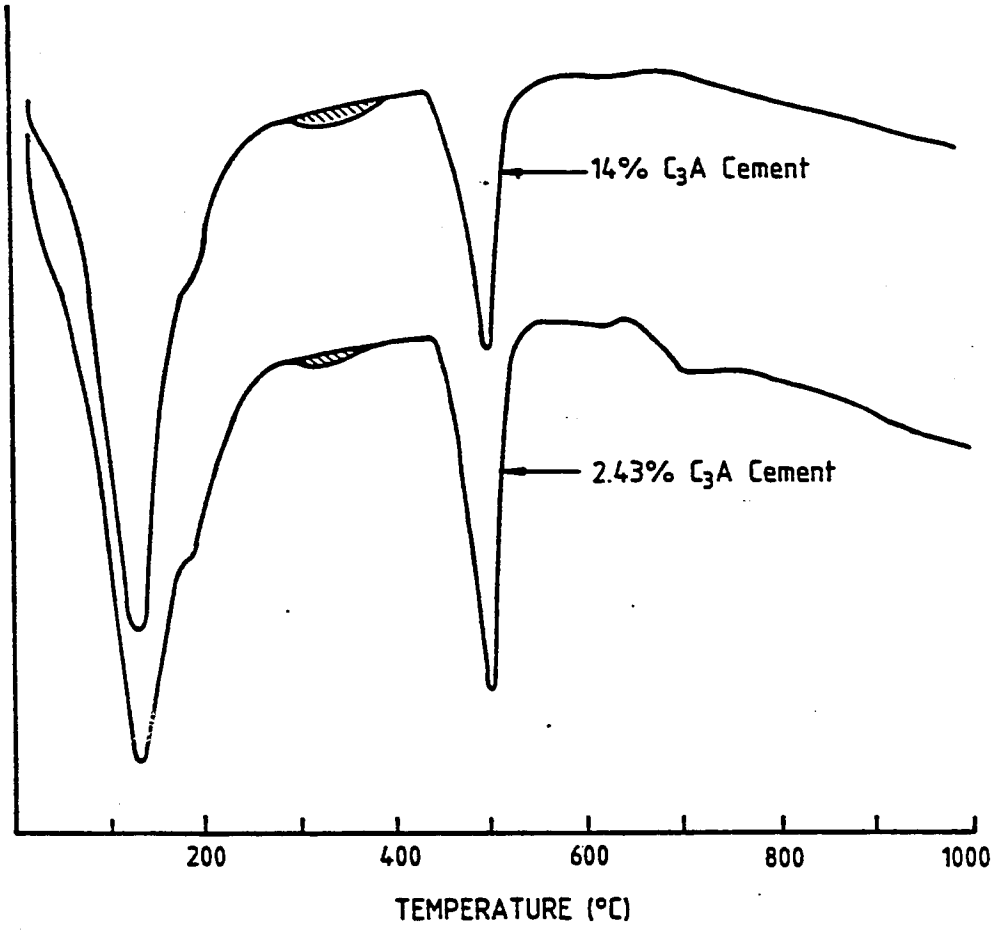

Fig. 4.2.1.4 : DTA Curves of 2.43% and 14% C_3A Cement Pastes Treated with 1.2% Chlorides.

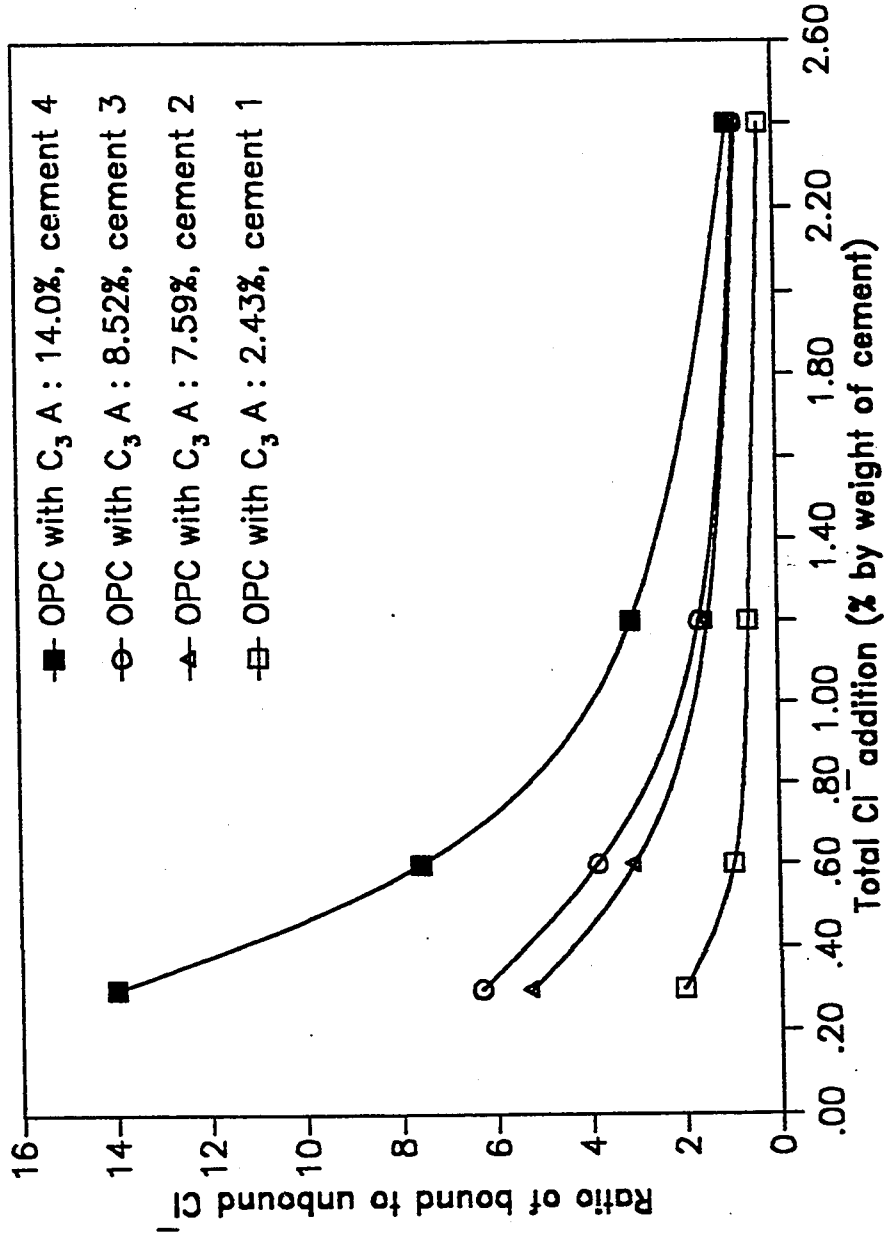

Fig. 4.2.1.5 Chlorides Remaining Unbound in Pore Solutions of of Different Cements Treated with Various Levels of Chloride Addition

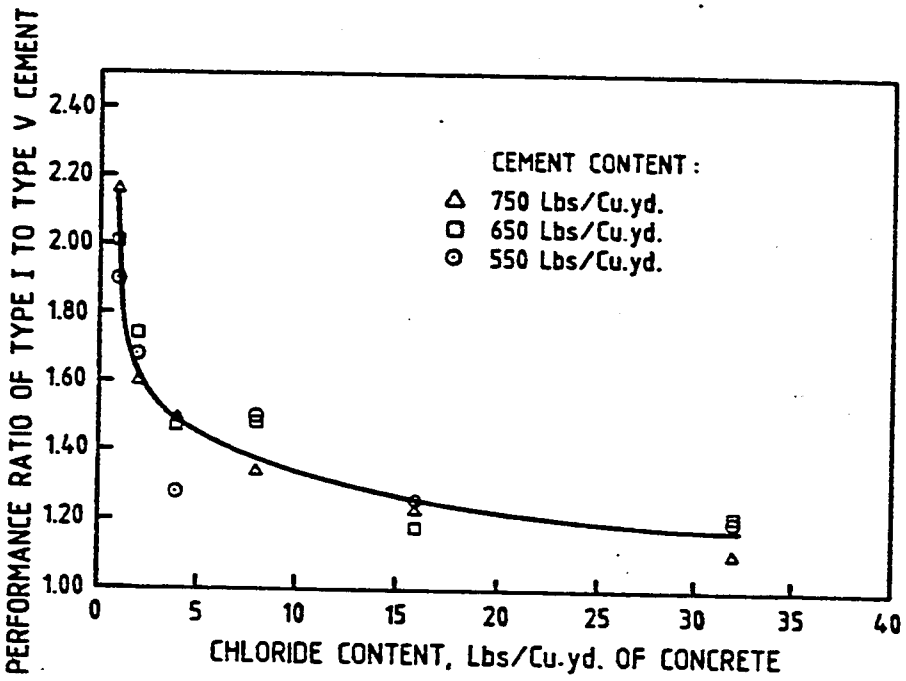

Fig. 4.2.1.6 Average Corrosion Resistance Performance of Type I (C_3A : 9.5%) to Type V (C_3A : 2.8%) Cement

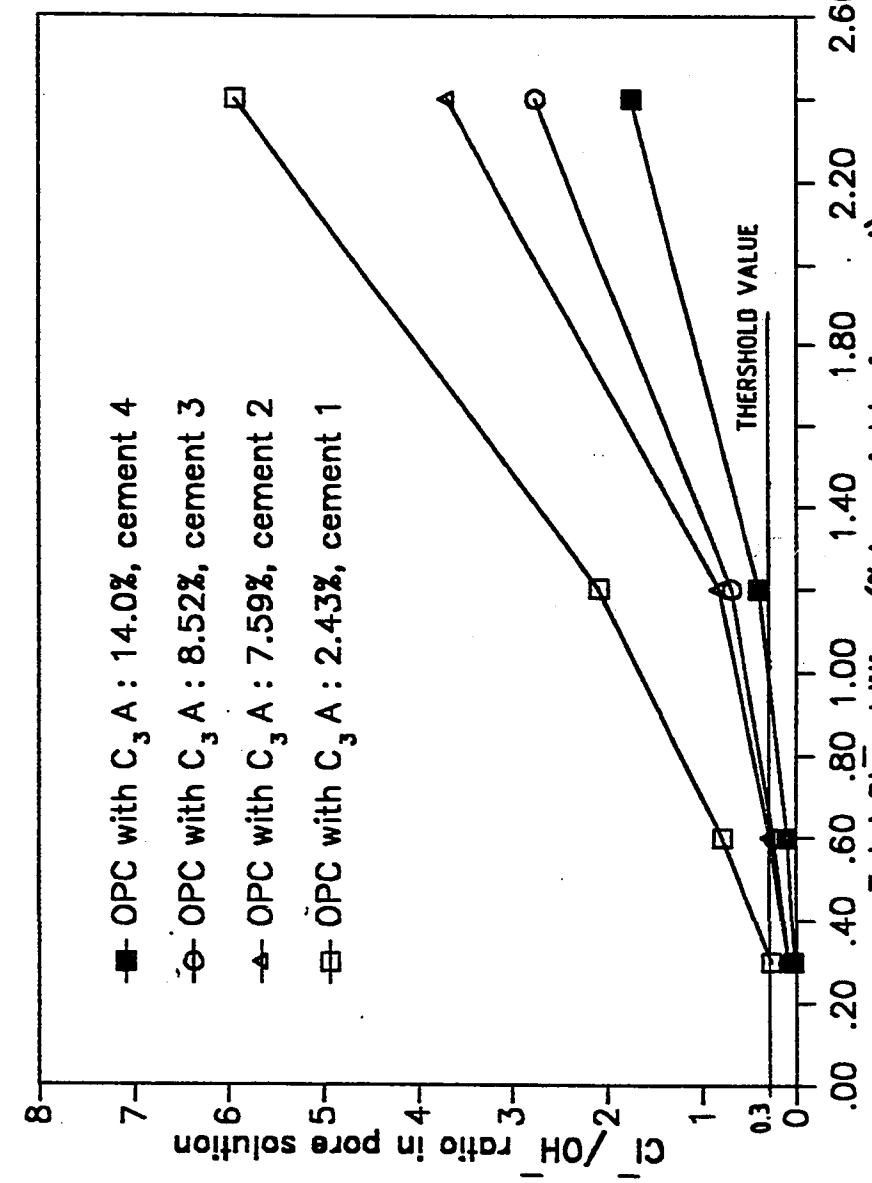

Fig. 4.2.1.7 Cl^-/OH^- Ratios in Pore Solutions of Different Cements for Various Levels of Chloride Addition

2.8 times the corresponding threshold chloride for the Type V 2.43% C_3A cement (0.35% by weight of cement). In terms of free water-soluble chlorides, this ratio is 1.60.

It is of interest to compare currently prevailing permissible chloride values with the chloride threshold levels developed in this study. Chloride limits in national codes vary widely. ACI 318-'83 allows a maximum water-soluble free chloride ion content of 0.15% for reinforced concrete exposed to chloride in service. The British Code, CP 110, allows an acid-soluble total chloride ion content of 0.35% for 95% of the test results with no result greater than 0.50%. The Norwegian Code, NS 3474, allows an acid-soluble chloride content of 0.6%, RILEM permits 0.4% and the revised Australian Standard for Concrete Structures, AS 3600-1988, allows an acid-soluble total chloride content of 0.80 kg/m^3 of concrete (0.22% by weight of cement for a typical concrete mix).

Threshold limits of Table 4.2.1.4 for cements up to 8% C_3A agree very well with the ACI limit of 0.15% water-soluble chlorides as well as with the CP 110 limit of 0.4% total acid-soluble chlorides. The ACI and CP 110 limits in terms of free and total chlorides respectively, appear to be quite reconcilable. However, these and the Australian Code limits appear to be conservative for concretes made with high C_3A cements.

4.2.1.2 Effect of Alkali Content of Cement

To study the effect of alkali content of cement on OH^-,Cl^- concentrations and hence Cl^-/OH^- ratio in the pore solution, a high alkali cement was formulated by adding NaOH to the 14% C_3A cement 4 to raise its equivalent Na_2O content from

0.65 to 1.2%. The high alkali cement so formulated and the 14% C_3A cement 4 were used for this study.

(i) OH^- Concentration in Pore Solution

OH^- ion concentrations of pore solution of medium and high alkali content are shown in Table 4.2.1.6 (column 6) and Fig. 4.2.1.8, which show that the OH^- concentration in the pore solution of the high alkali cement is around 1.4 times that in medium alkali cement for all chloride levels. However, for the chloride-free pastes, the OH^- ion concentration in the high alkali cement is twice that in the medium alkali cement. The pH values increase from an average value of 13.72 to 13.88 when the alkali content is increased from 0.65 to 1.2%.

(ii) Cl^- Concentration in Pore Solution

Chloride ions remaining free in the pore solutions of the medium and the high alkali cements are shown in Table 4.2.1.6 (column 5 and 10) and Fig. 4.2.1.9. An increase in the equivalent Na_2O content from 0.65 to 1.2% doubles the unbound chlorides in the pore solution for all the three chloride levels. Tritthart (64) tested chloride binding in an ordinary portland cement treated with different chloride salts. NaCl, $CaCl_2$, $MgCl_2$ and HCl acid were used to induct 1% chloride by weight of cement. The different chloride salts used, resulted in different pore solution alkalinity. The free chlorides in the pore solution were found to be proportional to the alkalinity of the pore solution. Thus, the results of the present study are in agreement with those of Tritthart (64).

Results of DTA tests (Fig. 4.2.1.10) conducted on hydrated pastes of the two cements tested containing 1.2% chloride show that the Friedel's salt (calcium chloro aluminate) peak at around 300° C is smaller in the high alkali cement than in the medium alkali cement. Increased chloride ion concentration and reduced Friedel's salt formation in the high alkali cement show that, the solubility of Friedel's salt is increased with increasing alkalinity of the pore solution. Roberts (33) tested the solubility of pure calcium chloro aluminate compound in different solutions at different temperatures. The solutions included 0.5% NaOH, 1.0% NaOH, 0.5% KOH and 1.0% KOH, all containing crystalline $Ca(OH)_2$. His results showed that the solubility of calcium chloro aluminate was increased and Cl^- ions were liberated to the solution when the concentration of the alkali hydroxides was increased from 0.5 to 1.0%. The increase in the Cl^- ion concentration with increasing alkali content, in the present study, can thus be explained by the phenomenon of increase in the solubility of calcium chloro aluminate with an increase in the pore solution alkalinity.

(iii) Cl^-/OH^- Ratio in Pore Solution

An increase in alkali content of cement concomitantly increases the OH^- and Cl^- ion concentrations of the pore solution, the net effect being a slight increase in the Cl^-/OH^- ratio. Fig. 4.2.1.11 shows the Cl^-/OH^- ratio for the medium and high alkali cements for different levels of chloride, which indicate an average marginal increase of about 25% when the alkali content increases from 0.65 to 1.2%.

The marginal increase in the Cl^-/OH^- ratio introduced by the increase in the alkali content of cement therefore is not expected to change the reinforcement corrosion behavior of concrete significantly.

Table 4.2.1.6: Pore Solution Composition of Medium and High Alkali Content Cements Treated With Different Levels of Chloride

C_3A Content of Cement (% by weight)	Equivalent Na_2O Content of Cement (% by weight)	Total Cl^- Addition (% by weight of cement)	Pore Solution Composition				Evaporable Water (% by weight of cement)	Unbound Cl^- (% by weight of Total Cl^-)
			Cl^- (mM/L)	OH^- (mM/L)	pH	Cl^-/OH^-		
14	0.65	0.0	-	348	13.54	-	-	-
14	1.20	0.0	-	735	13.87	-	-	-
14	0.65	0.3	14.8	524	13.72	0.0282	38.4	6.7
14	1.20	0.3	28.5	755	13.88	0.0377	40.0	13.5
14	0.65	0.6	50.9	503	13.70	0.1014	38.4	11.6
14	1.20	0.6	93.8	740	13.87	0.1268	40.5	22.5
14	0.65	1.2	216.0	534	13.73	0.4045	38.2	24.4
14	1.20	1.2	362.8	750	13.88	0.4837	41.2	44.2

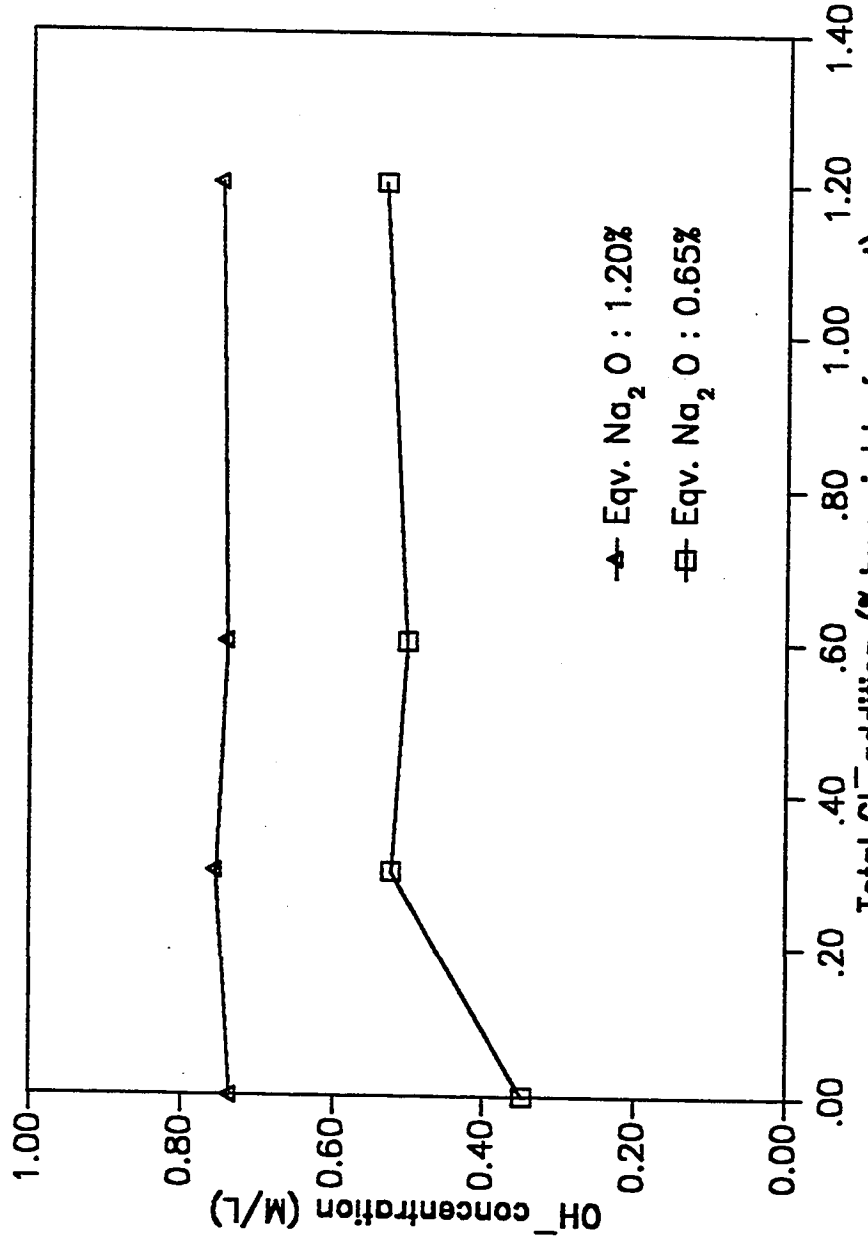

Fig. 4.2.1.8 Effect of Alkali Content of Cement on OH^- Concentrations in the Pore Solution of Type I Cement (C_3A : 14%)

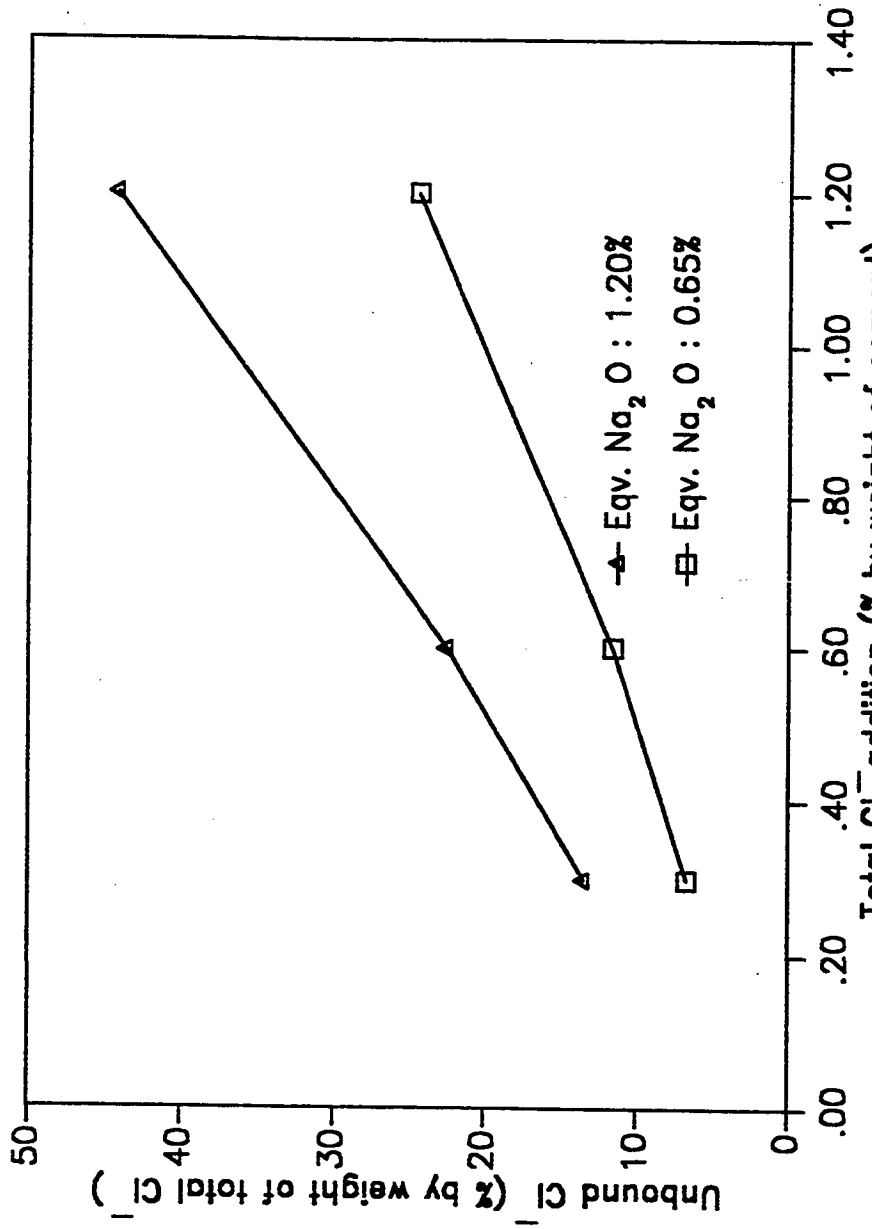

Fig. 4.2.1.9: Effect of Alkali Content of Cement on Unbound Chlorides in the Pore Solution of Type I Cement (C_3A : 14%)

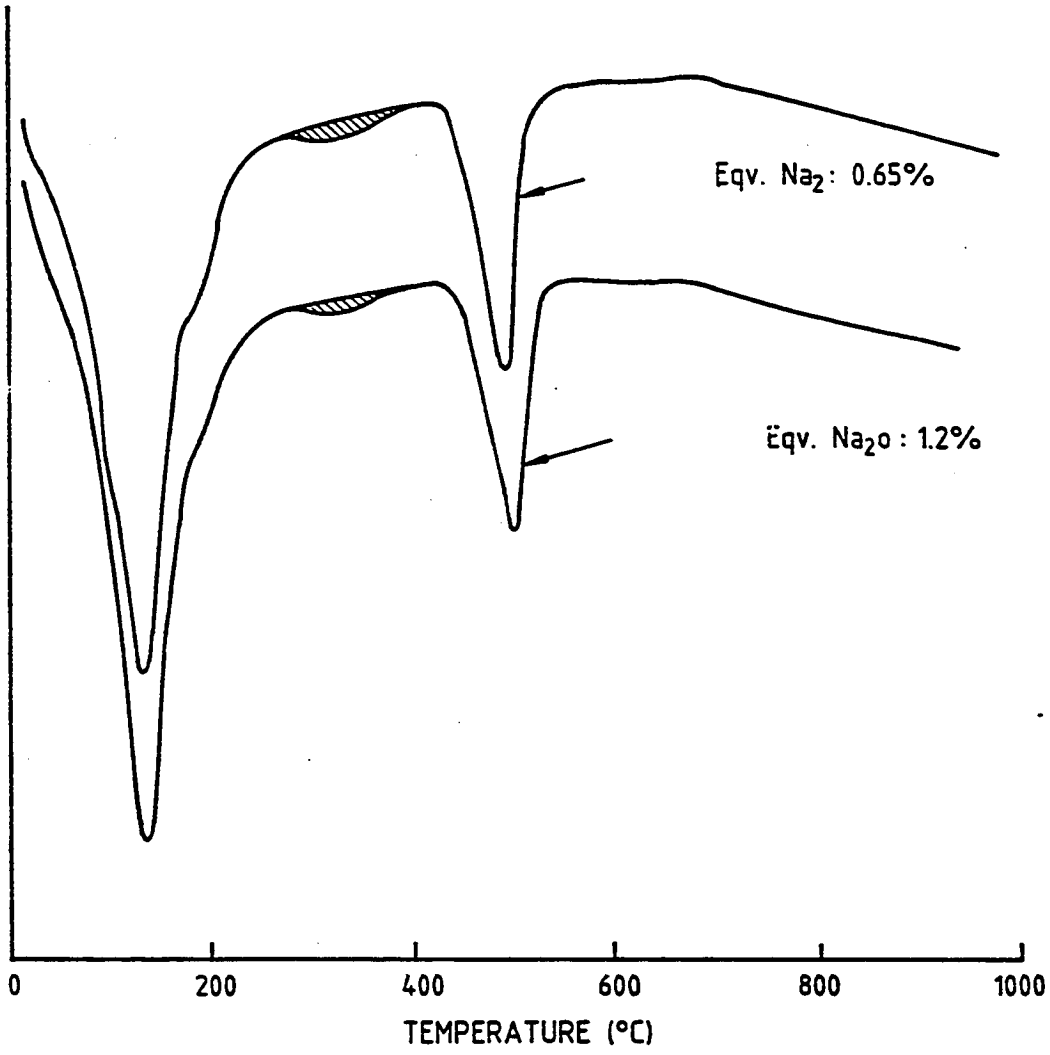

Fig. 4.2.1.10: DTA Curves of Hydrated Cement Pastes of Medium & High Alkali Cements.

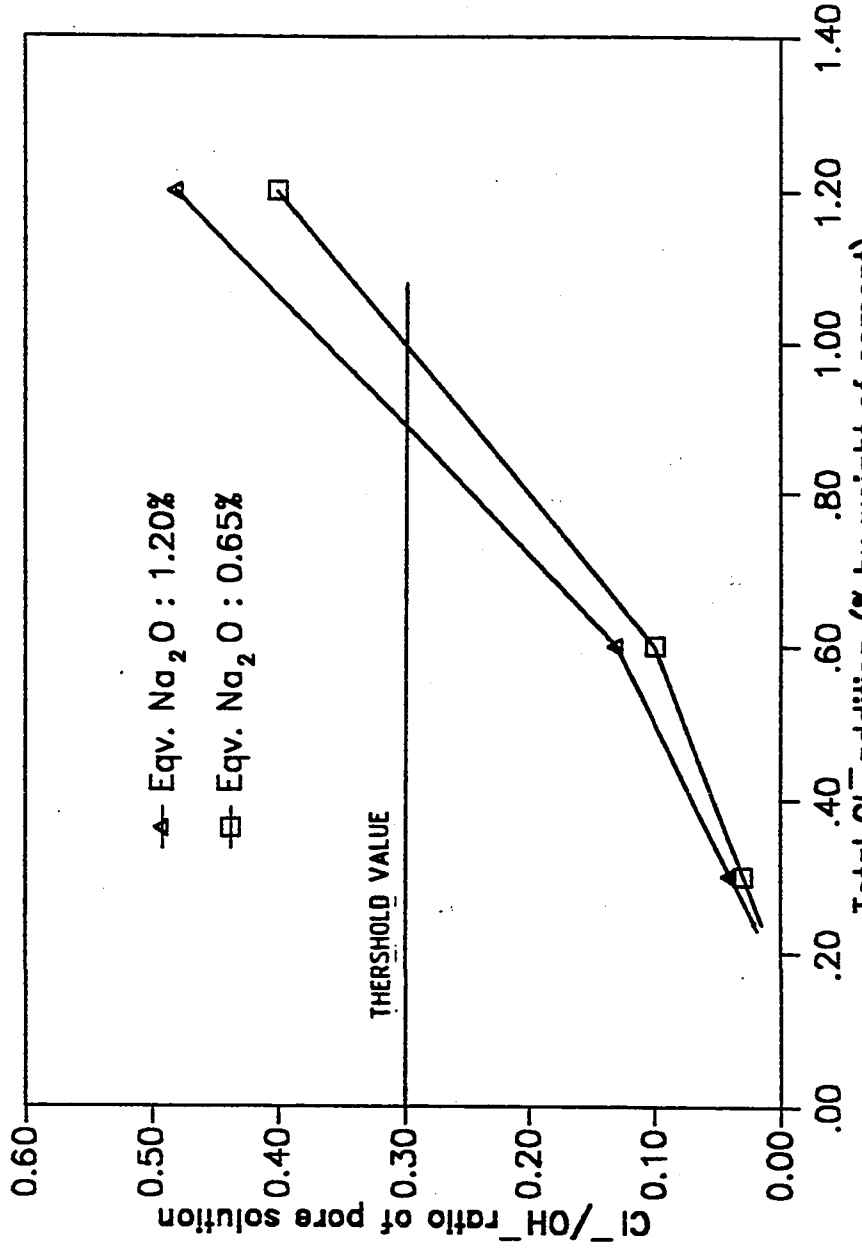

Fig. 4.2.1.11: Effect of Alkali Content of Cement on Cl^-/OH^- Ratio in the Pore Solution of Type I Cement (C_3A : 14%)

4.2.1.3 Effect of Sulfates

To study the effect of sulfates on pore solution composition of chloride-bearing plain cements, cements 1, 2 and 4 with C_3A contents of 2.43%, 7.59% and 14% were used. The levels of chloride addition used were 0.6% and 1.2% by weight of cement, derived from sodium chloride. In addition, two levels of SO_3 additions, derived from sodium sulfate, were made to each of the 0.6 and 1.2% chloride-bearing cement pastes in such a manner that the total SO_3 content of the cements were raised to 4% and 8% on a weight basis.

(i) Alkalinity of Pore Solution

Table 4.2.1.7 (columns 6 and 7) and Figs. 4.2.1.12 and 4.2.1.13 show the effect of sulfate addition on alkalinity of pore solutions of hydrated cement pastes. For the 0.6% chloride-bearing paste the addition of 4% SO_3 increases the OH^- concentration 2.9, 2.0 and 1.6 folds for the 2.43%, 7.59% and 14% C_3A cements respectively. The resulting increases in the pH values are from 13.42 to 13.89 for the 2.43% C_3A cement, from 13.59 to 13.90 for the 7.59% C_3A cement and from 13.70 to 13.91 for the 14% C_3A cement. Doubling the SO_3 content to 8% registers only marginal increases in the OH^- concentrations and the pH values of the pore solutions for the three cements. For example, with an increase in the SO_3 content from 4 to 8% in the

0.6% chloride-bearing paste, the OH^- concentrations increased from 770 mM/L to 786 mM/L for the 2.43% C_3A cement, from 786 mM/L to 960 mM/L for the 7.59% C_3A cement, and from 812 mM/L to 980 mM/L for the 14% C_3A cement. An increase in the pore solution alkalinity due to the addition of sulfates is also observed in cement pastes treated with 1.2% chloride level. However, for both levels of chloride addition, OH^- concentrations in the pore solution of the 1.2% chloride-treated cements were observed to be relatively lower compared to 0.6% chloride-treated cements.

The increase in the OH^- concentration in pore solution with sulfate addition is due to the formation of sodium hydroxide (NaOH) as a result of reaction between sodium sulfate (Na_2SO_4) with calcium hydroxide ($Ca(OH)_2$) liberated during cement hydration:

$$Ca(OH)_2 + Na_2SO_4 \text{ ------ } 2NaOH + CaSO_4$$

According to the above reaction, $Ca(OH)_2$ is consumed and NaOH is formed. The consumption of $Ca(OH)_2$ due to sulfate addition is confirmed by DTA and TGA test results. For example, in the case of 2.43% C_3A cement containing 1.2% chlorides, a comparison for the DTA patterns of the 1.7% SO_3 and 8% SO_3 pastes show that the $Ca(OH)_2$ content in 8% SO_3 paste is less compared to 1.7% SO_3 paste. TGA tests show that the $Ca(OH)_2$ is reduced from 31.2 to 27.6% (Fig. 4.2.1.14).

(ii) Chloride Ion Concentration in Pore Solutions

The free chloride ion concentrations in the pore solution of the hydrated cement

pastes are given in Table 4.2.1.7 (column 5). In Table 4.2.1.8 (column 4) chloride ion concentrations are given as percentages of initial chloride ion concentrations in the mix water. It is seen from the data of Table 4.2.1.8 that the chloride ion concentrations in the pore solutions of some pastes are more than the chloride ion concentrations in the mix water. This indicates that, in these cases, the amount of water consumed in the hydration of cement is more than the amount of chlorides bound by the hydration products. In order to make an allowance for the amount of water chemically combined during hydration, the chloride ion concentrations are converted into chlorides remaining unbound in the pore solution using only the evaporable water content of the hydrated cement pastes. In column 6 of Table 4.2.1.8 these unbound chlorides in the pore solution are expressed as the percentages of total chlorides added to the cement pastes. The data of Table 4.2.1.7 (columns 4 and 6) and Figs. 4.2.1.15 and 4.2.1.16 show that in all the three cements and for both chloride treatment levels of 0.6 and 1.2%, chloride ion concentration in pore solution increases with the addition of sulfates. In the 2.43% C_3A cement for both chloride levels, the unbound chlorides in the cement pastes containing 8% SO_3 are 1.5 times the unbound chlorides in the cement pastes in which no sulfate was added. For the 7.59% C_3A cement, 8% SO_3 addition results in 2.5 and 1.7 fold increases in the unbound chlorides for the 0.6% and 1.2% chloride bearing pastes respectively. Likewise, for the 14% C_3A cement, 8% SO_3 addition causes 4.1 and 2.4 fold increases in the unbound chlorides for the 0.6% and 1.2% chloride-treated pastes respectively. Holden et al (26) observed a similar effect of sulfate addition on chloride binding capacity of cements. Three plain cements with C_3A contents of 1.9%, 7.7% and 14.3% were used in their study. Chloride and sulfate additions of 0.4% and 1.5% respectively by weight of cement, derived from sodium chloride and sodium sulfate, respectively, were made. The cements contained an average base SO_3 content of

3%, making total sulfate content of the cements around 4.5% after 1.5% sulfate addition. In all the three cements, an increase in the free chloride ion concentration in the pore solutions was observed due to the sulfate addition.

Increase in free chlorides in the pore solution due to sodium sulfate addition may be attributable to either an increase in the pore solution alkalinity or to the preferential combination of C_3A with sulfate ions in comparison to chloride ions, thereby inhibiting the formation of Friedel's salt ($3CaO.Al_2O_3CaCl_2.10H_2O$). Addition of SO_3 as sodium sulfate significantly increases the alkalinity of the pore solution of the hydrated cement pastes. Tritthart (64) has carried out a pore solution study of hydrated cement pastes treated with 1.0% Cl^- derived from four different chloride sources, NaCl, $CaCl_2$, $MgCl_2$ and HCl. Results of his study showed the chloride ion concentration in the pore solution to be a function of the alkalinity of the pore solution; chloride ion concentration increases with higher alkalinity. The inhibiting effect of alkali content of a cement on its chloride binding capacity has also been shown by Rasheeduzzafar et al (65). It has been shown that the unbound chlorides in the pore solution of a Type V cement (C_3A: 2.43% and equilibrium Na_2O content: 0.58%) and a Type I cement (C_3A: 7.37% and equilibrium Na_2O content: 1.19%) are fairly close due to the difference in the equivalent alkali contents of the cements. The increase in the chloride ion concentration due to the addition of sulfates in the present study, may therefore be partly attributed to an increase in the pore solution alkalinity caused by sulfate addition.

The other relevant factor which may cause a lowering of the chloride binding in cement pastes containing sulfate is the possibility of preferential complexing of C_3A of the cement with sulfates compared to chlorides. This would result in a decrease in the

C_3A available for the removal of chlorides by the formation of Friedel's salt.

To confirm the reasons for the mitigation of chloride binding in sulfate-bearing cement pastes, DTA and TGA tests were carried out on the 2.43% C_3A cement containing 1.2% Cl^- without added sulfates, as well as on pastes containing 1.2% Cl^- with 8% SO_3. The DTA curves of these two cement pastes are shown in Fig. 4.2.1.14. In Fig. 4.2.1.14, a well defined peak of Friedel's salt clearly exists around 300° C for the paste specimen containing 1.2% Cl^-, with no added sulfates; however, no such peak is observed in the specimen containing 1.2% Cl^- with 8% SO_3. These results show that SO_3 addition significantly reduced the formation of Friedel's salt which has possibly resulted in an increase in the Cl^- concentration in the pore solution (Table 4.2.1.7 and 4.2.1.8). Whether the mitigation in the formation of Friedel's salt is due to the preferential binding of C_3A with SO_3 or due to an increase in the pore solution alkalinity, is not clear; or it may be due to both causes since they are not mutually exclusive. Kawamura et al (43) has carried out a pore solution study on cement pastes with and without fly ash, treated with different levels of Cl^- derived from NaCl and $CaCl_2$. The results show that in both plain and fly ash cement pastes, more Friedel's salt was detected by DTA in samples containing $CaCl_2$ than NaCl. The pore solution analysis showed that the pore solution alkalinity of $CaCl_2$ treated paste was lower compared to the alkalinity of the paste treated with NaCl. Results of Kawamura et al (43), therefore, indicate that the mitigation of Friedel's salt formation may at least partly be attributed to an increase in pore solution alkalinity. The exact mechanism of formation of Friedel's salt and the factors affecting chloride binding in cements are matters which have yet to be resolved fully.

(iii) C_3A -Chloride-Sulfate Interaction

The above data show that free chloride ion concentrations in the pore solution of a hydrated plain cement depends not only on the C_3A content of the cement, but also on other factors such as pore solution alkalinity (64,65) and the concomitant presence of sulfates. The unbound chloride concentrations in the pore solutions of the three cement pastes with various additions of chlorides and sulfates used in this study, are shown in Figs. 4.2.1.17 and 4.2.1.18 as a function of the C_3A content of cement. The data of Figs. 4.2.1.17 and 4.2.1.18 show that the unbound chlorides decrease as the C_3A content of the cement is increased, for chloride-treated cements as well as for cements which contain both chlorides and sulfates concomitantly. Also, the unbound chlorides increase as the sulfate addition is increased. The performance ratio of Type I 14% C_3A cement against Type V 2.43% C_3A cement, defined as the ratio of the unbound chlorides in the pore solutions of the two cements is shown Fig. 4.2.1.19. It can be seen from Fig. 4.2.1.19 that at a chloride level of 0.6%, the performance of the Type I 14% C_3A cement in terms of chloride binding is 4.4, 2.4 and 1.7 times better than the performance of the Type V 2.43% C_3A cement, for the sulfate additions of 0, 4 and 8% respectively. However, for the chloride treatment level of 1.2%, the performance ratios drop to 2.5, 1.8 and 1.6 for the sulfate additions of 0, 4 and 8% respectively. These data indicate that the beneficial effect of C_3A content in reducing the pore solution free chlorides decrease as the level of chloride and sulfate addition is increased.

(iv) Cl^-/OH^- Ratio in Pore Solution

The effect of sulfate addition to a chloride-treated cement paste is to increase the pore solution alkalinity as well as to decrease the chloride-binding capacity of the cement paste. However, the interactive combined effect is not a consistent increase or decrease in the Cl^-/OH^- ratio. Figs. 4.2.1.20 and 4.2.1.21 show the effect of SO_3 addition on Cl^-/OH^- ratio of 0.6% and 1.2% chloride-treated cement pastes. It can be seen from Figs. 4.2.1.20 and 4.2.1.21 that the effect of increase in sulfate addition from 4 to 8% is a consistent marginal increase in the Cl^-/OH^- ratio for all the cements. However, for sulfate addition up to 4%, the Cl^-/OH^- ratios of the pore solutions are either less or more than the values obtainable in corresponding cements treated with chlorides only. For 2.43% and 7.59% C_3A cements, 4% SO_3 addition lowers the Cl^-/OH^- ratio of the pore solution for both chloride levels of 0.6% and 1.2%. However, for the 14% C_3A cement, the addition of 4% SO_3 increases the Cl^-/OH^- ratio of the pore solution, for both the levels of chloride. Holden et al (26), in a pore solution study on three cements C_3A :1.9, 7.7 and 14.3%) used a chloride addition of 0.4% in conjunction with a sulfate addition of 1.5%. They observed an increase in the Cl^-/OH^- ratio in the pore solutions of all the three cements in the presence of sulfates. The SO_3 content of the cements used by them was around 3.0%, so that the total SO_3 content of the cements after 1.5% addition was around 4.5%. The analysis of the results on Cl^-/OH^- ratio of the pore solution of the present study shows that the effect of sulfate addition can either result in an increase or a decrease in the Cl^-/OH^- ratio of the pore solution. The change in the Cl^-/OH^- ratio is governed by the relative ratios of increase of Cl^- and OH^- ions in the pore solution due to sul-

fate addition. If due to sulfate addition the Cl^- concentration of the pore solution increases at a faster rate than the OH^- concentration, the net effect would result in an increase in the Cl^-/OH^- ratio. Table 4.2.1.9 shows the rate of increase in the OH^- and Cl^- concentrations of the pore solution due to 4% sulfate addition to the 0.6% chloride-bearing paste. Results of Holden et al (26) are also presented in Table 4.2.1.9 for comparison. It can be seen that in cements 5, 6 and 7 used by Holden et al, with the addition of sulfate the rate of increase in the Cl^- concentration exceeds the rate of increase in the OH^- concentration in the pore solution. This causes a resultant increase in the Cl^-/OH^- ratio of the pore solutions. However, in cements 1, 2 and 4 used in the present study, with the addition of sulfate, the increase in the Cl^- concentration is more than in the OH^- concentration only in cement 4. In cements 1 and 2, the increase in the Cl^- concentration is less than that in the OH^- concentration, with sulfate addition. Therefore, unlike an increase in the Cl^-/OH^- ratio of the cement 4, sulfate addition causes a reduction in the Cl^-/OH^- ratio for cements 1 and 2.

A closer look at the rate of increase of OH^- ion concentrations in the pore solutions of cements 1, 2 and 4 show that, the increase in the OH^- concentration is inversely proportional to the equivalent alkali content of cement. The lower the equivalent alkali content of cement, the higher the increase in the OH^- concentration, as a result of sulfate addition. Similar behavior can also be noticeable for cements 5, 6 and 7, where levels of chlorides and sulfates are different from the present study. Data of Table 4.2.1.9 also show that the increase in the Cl^- concentration, due to sulfate addition, is proportional to the C_3A content of cement, for a given level of chloride and sulfate in the cement paste. This would imply that the increase in the free Cl^- concentration of the pore solution due to sulfate addition is different in different C_3A

Table 4.2.1.7: **Pore Solution Composition of Hydrated Cement Pastes Treated with Different Levels of Chlorides and Sulfates**

Cement No.	C_3A Content of Cement (% by weight)	Total Cl^- Addition (% by weight of cement)	Total SO_3 Content (% by weight of cement)	Pore Solution Composition			
				Cl^- (mM/L)	OH^- (mM/L)	pH	Cl^-/OH^-
1	2.43	0.6	1.71	210	265	13.42	0.79
1	2.43	0.6	4.00	267	770	13.89	0.35
1	2.43	0.6	8.00	300	786	13.90	0.38
1	2.43	1.2	1.71	530	254	13.40	2.09
1	2.43	1.2	4.00	590	646	13.81	0.91
1	2.43	1.2	8.00	705	694	13.84	1.02
2	7.59	0.6	2.50	109	391	13.59	0.28
2	7.59	0.6	4.00	161	786	13.90	0.20
2	7.59	0.6	8.00	263	960	13.98	0.27
2	7.59	1.2	2.50	342	413	13.62	0.83
2	7.59	1.2	4.00	415	786	13.90	0.53
2	7.59	1.2	8.00	580	816	13.91	0.71
4	14.00	0.6	2.60	51	503	13.70	0.10
4	14.00	0.6	4.00	121	812	13.91	0.15
4	14.00	0.6	8.00	201	980	13.99	0.21
4	14.00	1.2	2.60	216	534	13.73	0.40
4	14.00	1.2	4.00	341	784	13.89	0.43
4	14.00	1.2	8.00	503	920	13.96	0.55

Table 4.2.1.8: Unbound Chlorides in Pore Solution of Hydrated Cement Pastes Treated with Different Levels of Chlorides and Sulfates

Cement No.	C_3A Content of Cement (% by weight)	Total Cl^- Addition (% by weight of cement)	Total SO_3 Content (% by weight of cement)	Cl^- Concentration in Pore Solution (% by Cl^- concentration in mix water)	Evaporable Water (% by weight of cement)	Unbound Cl^- (% by weight of Total Cl^-
1	2.43	0.6	1.71	74.5	40.8	50.7
1	2.43	0.6	4.00	94.7	43.2	68.2
1	2.43	0.6	8.00	106.4	44.6	79.1
1	2.43	1.2	1.71	94.1	39.4	61.8
1	2.43	1.2	4.00	104.8	43.0	75.0
1	2.43	1.2	8.00	125.2	44.4	92.5
2	7.59	0.6	2.50	38.7	38.2	24.6
2	7.59	0.6	4.00	57.1	38.6	36.8
2	7.59	0.6	8.00	93.3	39.3	61.2
2	7.59	1.2	2.50	60.7	39.8	40.3
2	7.59	1.2	4.00	73.7	40.4	49.6
2	7.59	1.2	8.00	103.0	40.2	69.0
4	14.00	0.6	2.60	18.1	38.4	11.6
4	14.00	0.6	4.00	42.9	40.0	28.6
4	14.00	0.6	8.00	71.3	40.0	47.6
4	14.00	1.2	2.60	38.4	38.2	24.4
4	14.00	1.2	4.00	60.6	42.3	42.7
4	14.00	1.2	8.00	89.3	39.9	59.4

Table 4.2.1.9: **Rates of Increase of Cl^- and OH^- Ion Concentrations due to Sulfate Addition**

Cement No.	C_3A Content of Cement (% by weight)	Eq.Na_2O Content of Cement (% by weight)	OH^- in (C+S)# / OH^- in (C)#	Cl^- in (C+S)# / Cl^- in (C)#
1	2.43	0.58	2.9	1.3
2	7.59	0.60	2.0	1.5
4	14.00	0.65	1.6	2.4
5*	1.91	0.54	2.0	2.3
6*	7.70	0.63	1.8	2.6
7*	14.30	0.86	1.6	3.7

* Results of Holden et al(26)

(C+S): (0.6% Cl^-+4% SO_3 addition) for cements 1,2,4 and (0.4% Cl^-+4.5% SO_3 addition) for cements 5,6,7

(C): (0.6% Cl^- addition) for cements 1,2,4 and (0.4% Cl^- addition) for cements 5,6,7

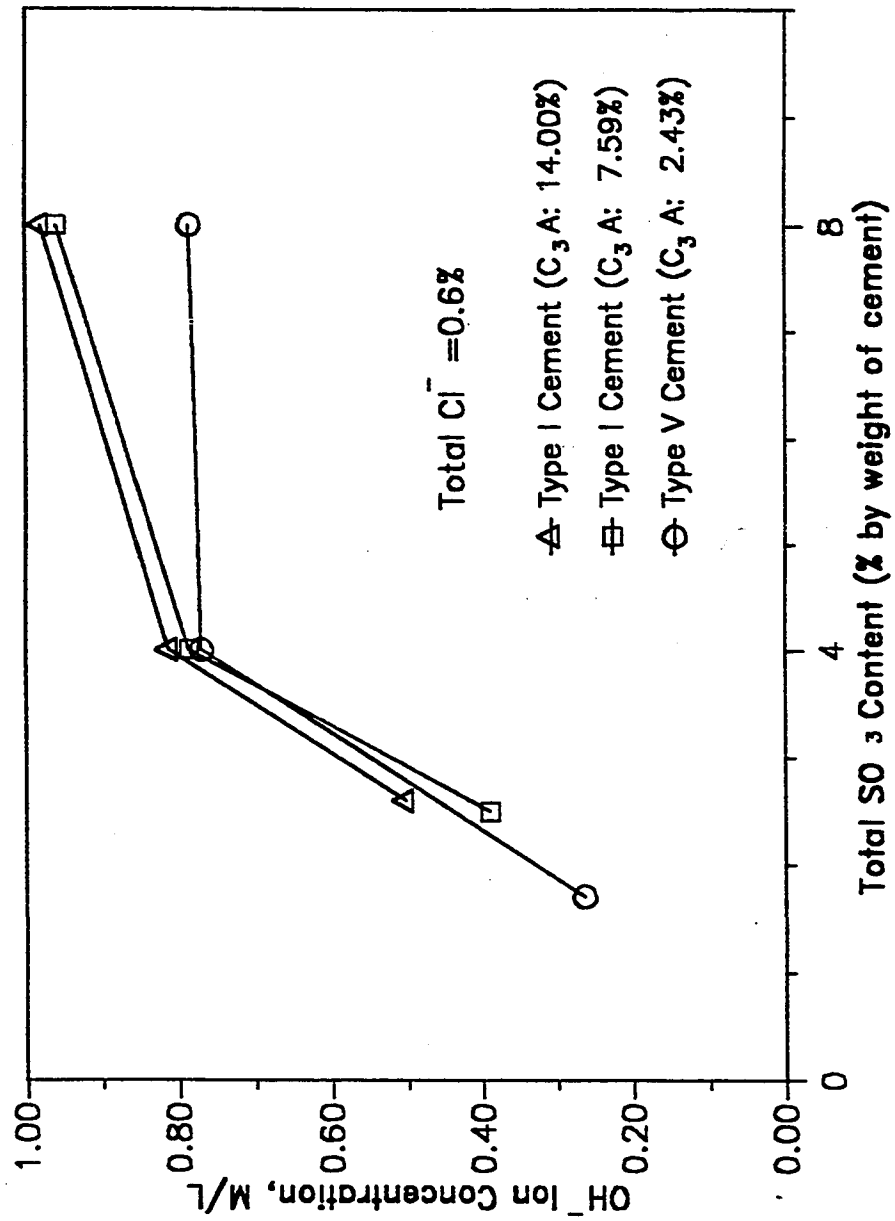

Fig. 4.2.1.12 Effect of Sulfate Addition on OH^- Concentration in the Pore Solutions of Cements Treated with 0.6% Chloride Level

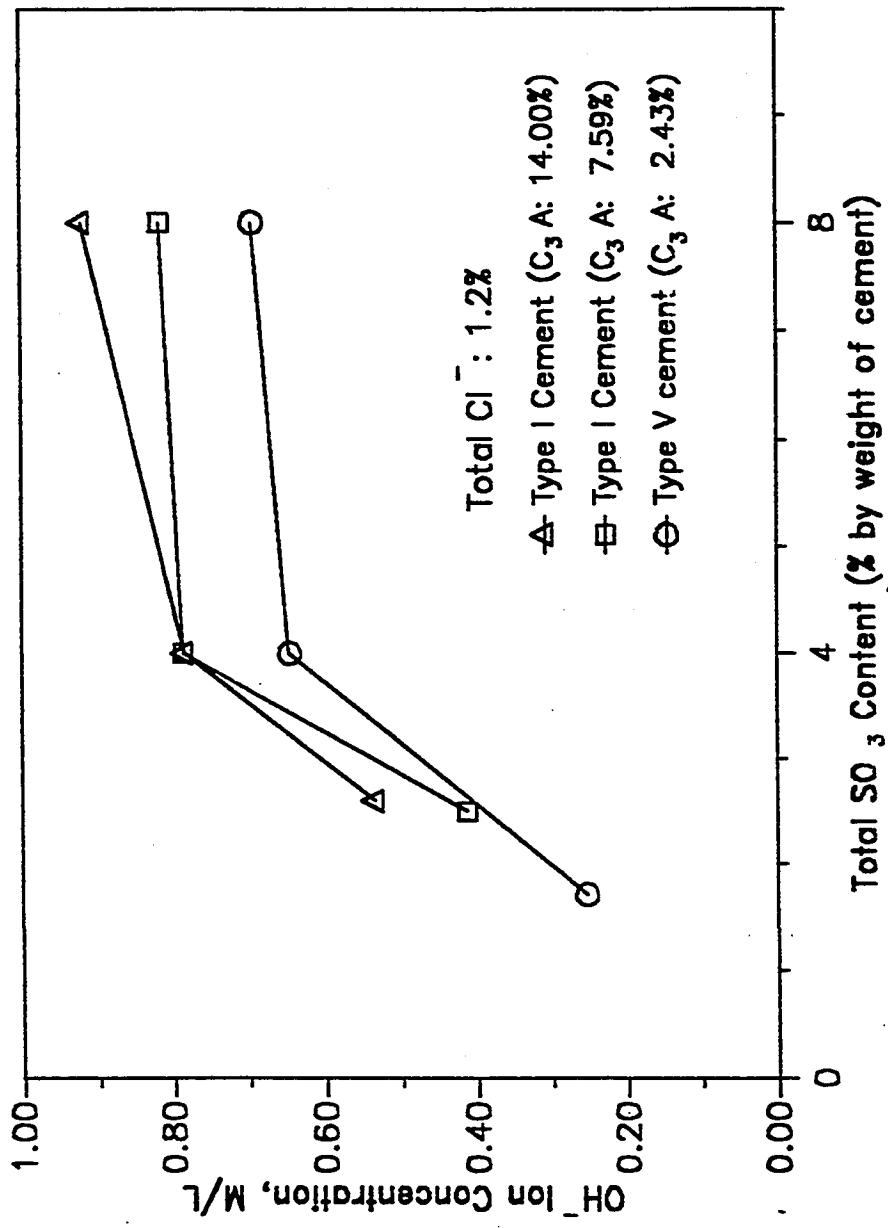

Fig. 4.2.1.13 Effect of Sulfate Addition on OH^- Concentration in the Pore Solutions of Cements Treated with 1.2% Chloride Level

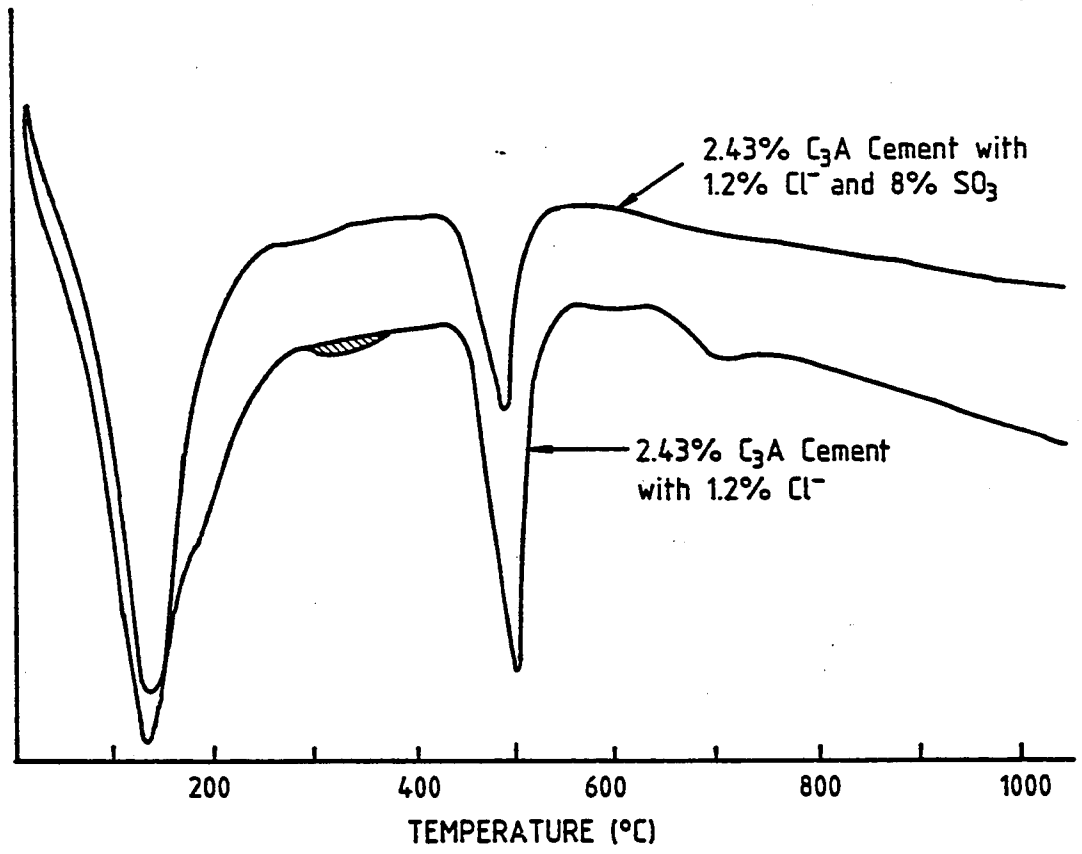

Fig. 4.2.1.14 DTA Curves of 2.43% C_3A Cement with Chloride and (Chloride + Sulfate) Additions.

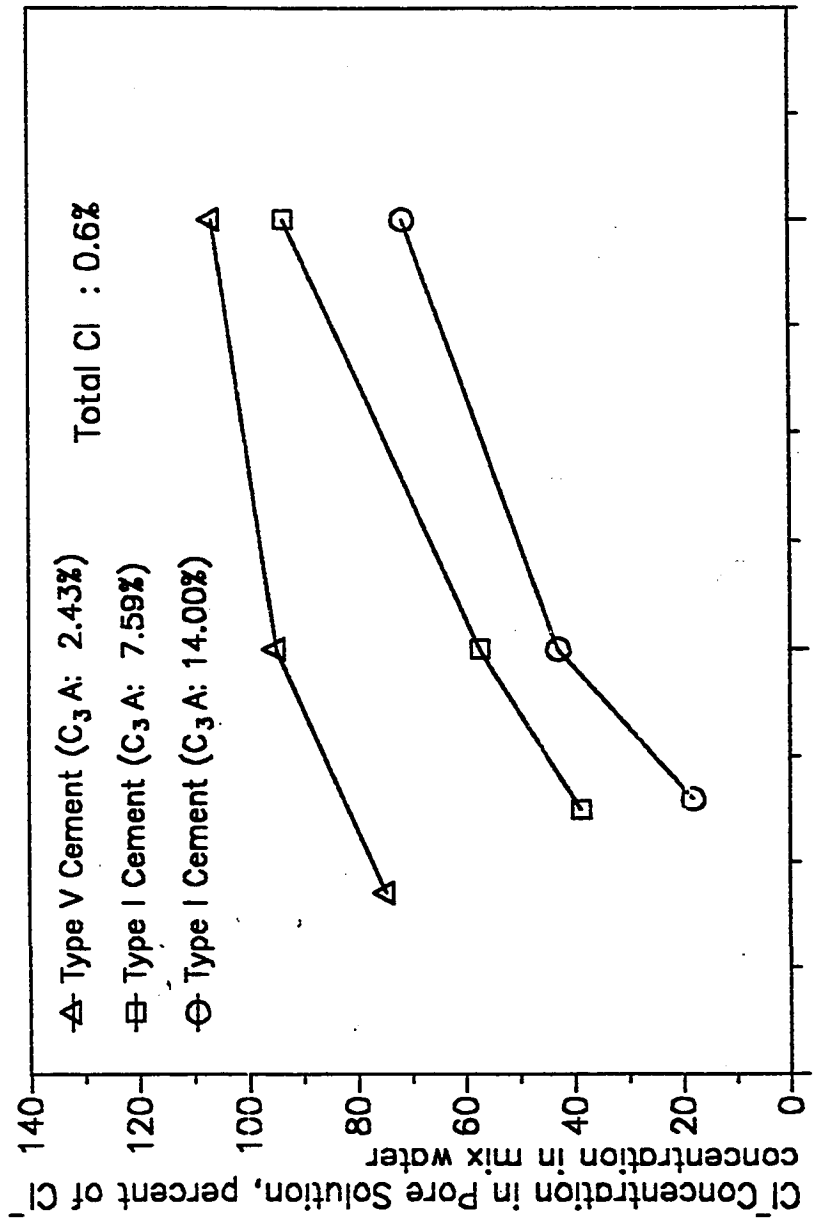

Fig. 4.2.1.15 Effect of Sulfate Addition on Unbound Chlorides in Pore Solutions of Cement Treated with 0.6% Chloride Level

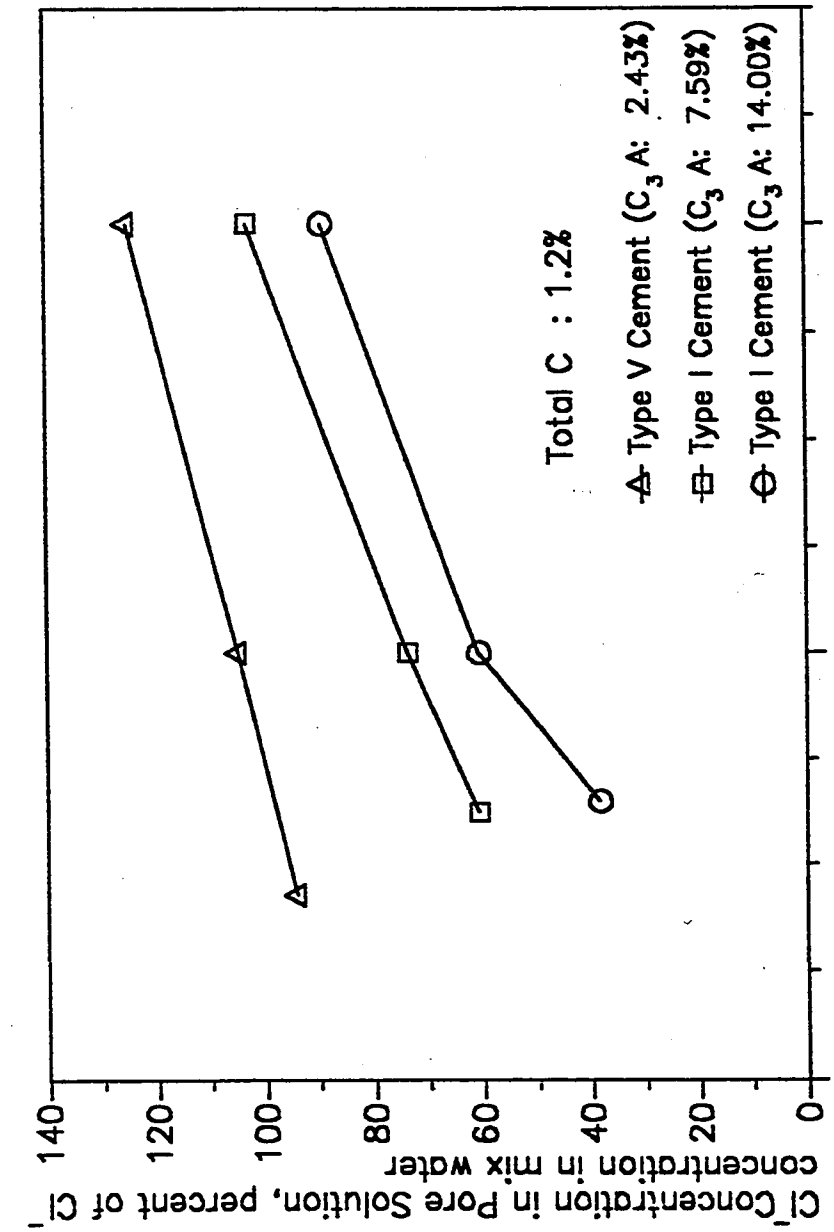

Fig. 4.2.1.16 Effect of Sulfate Addition on Unbound Chlorides in Pore Solutions of Cement Treated with 1.2% Chloride Level

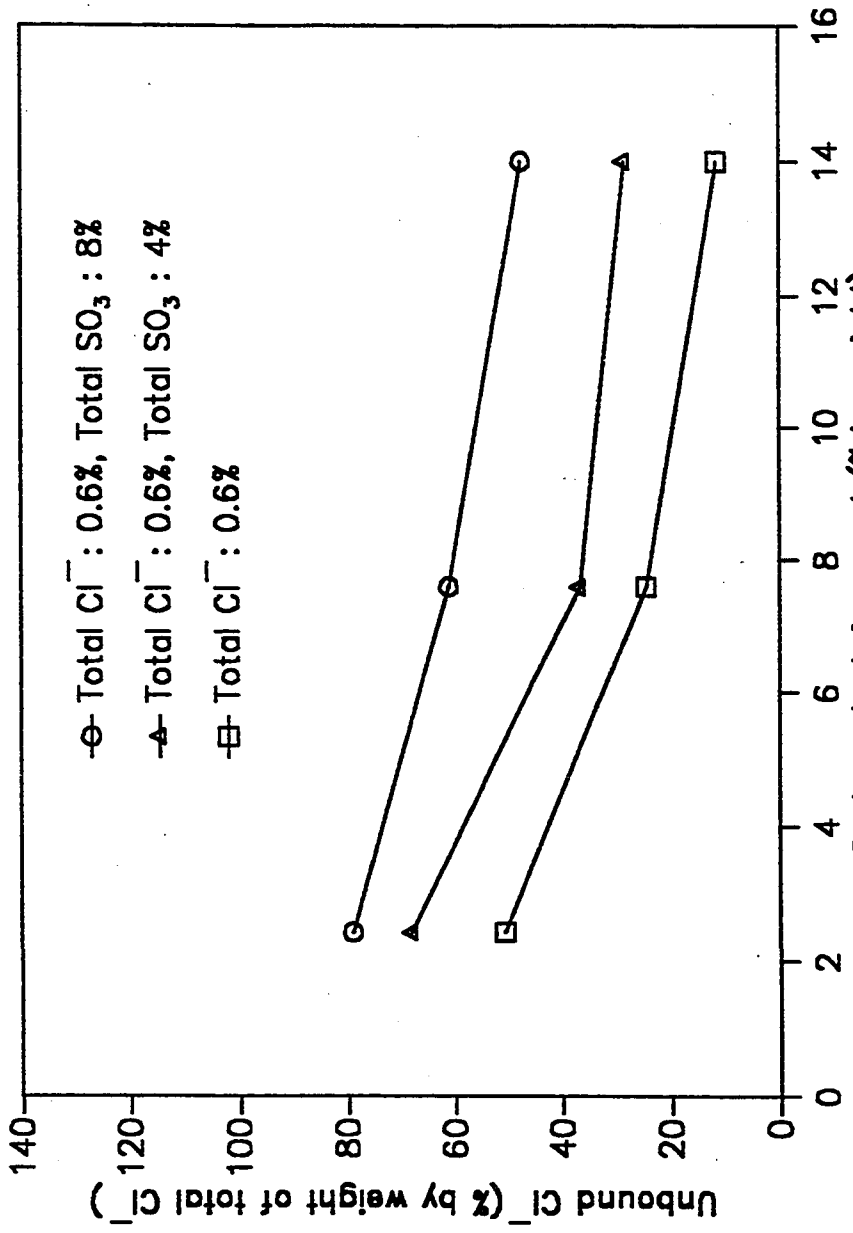

Fig. 4.2.1.17 Effect of C_3A Content on Unbound Chlorides in Pore Solutions of Cements Treated with 0.6% Chloride Level

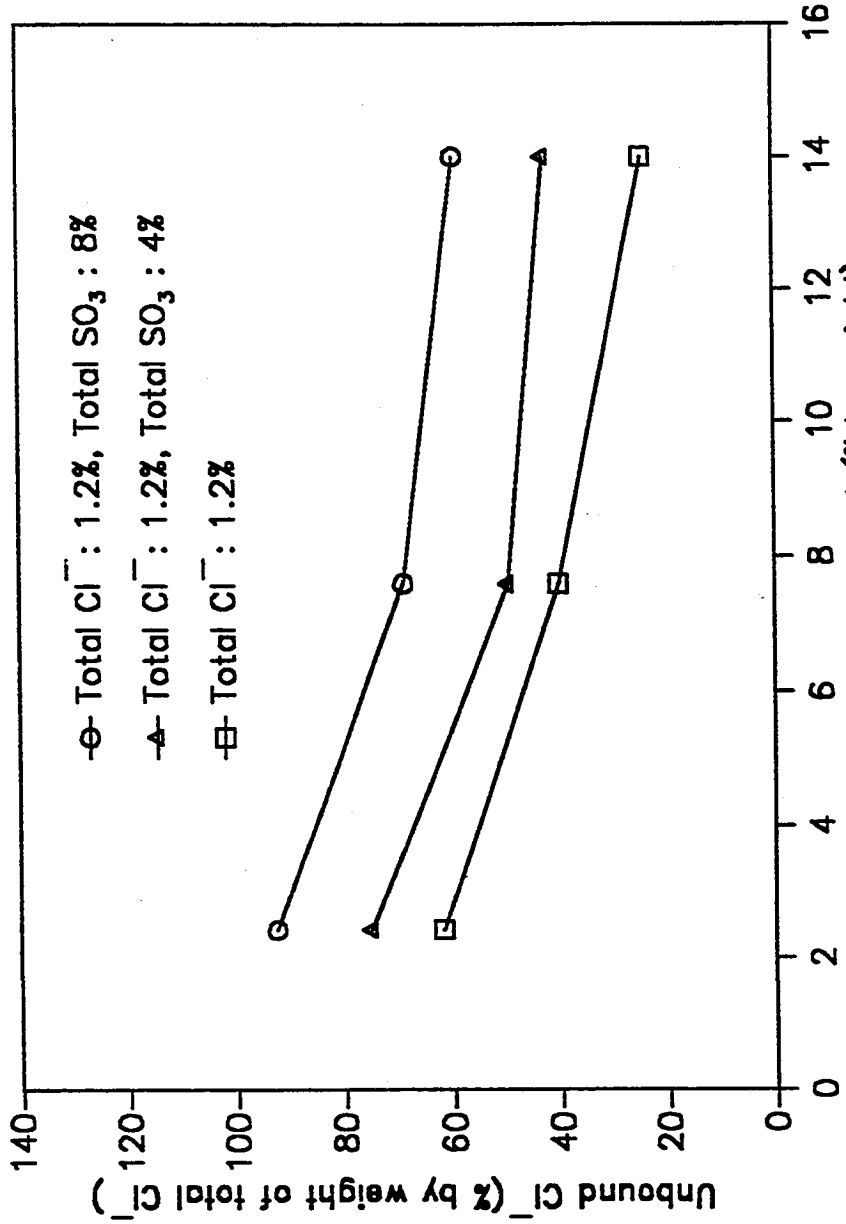

Fig. 4.2.1.18 Effect of C_3A Content on Unbound Chlorides in Pore Solutions of Cements Treated with 1.2% Chloride Level

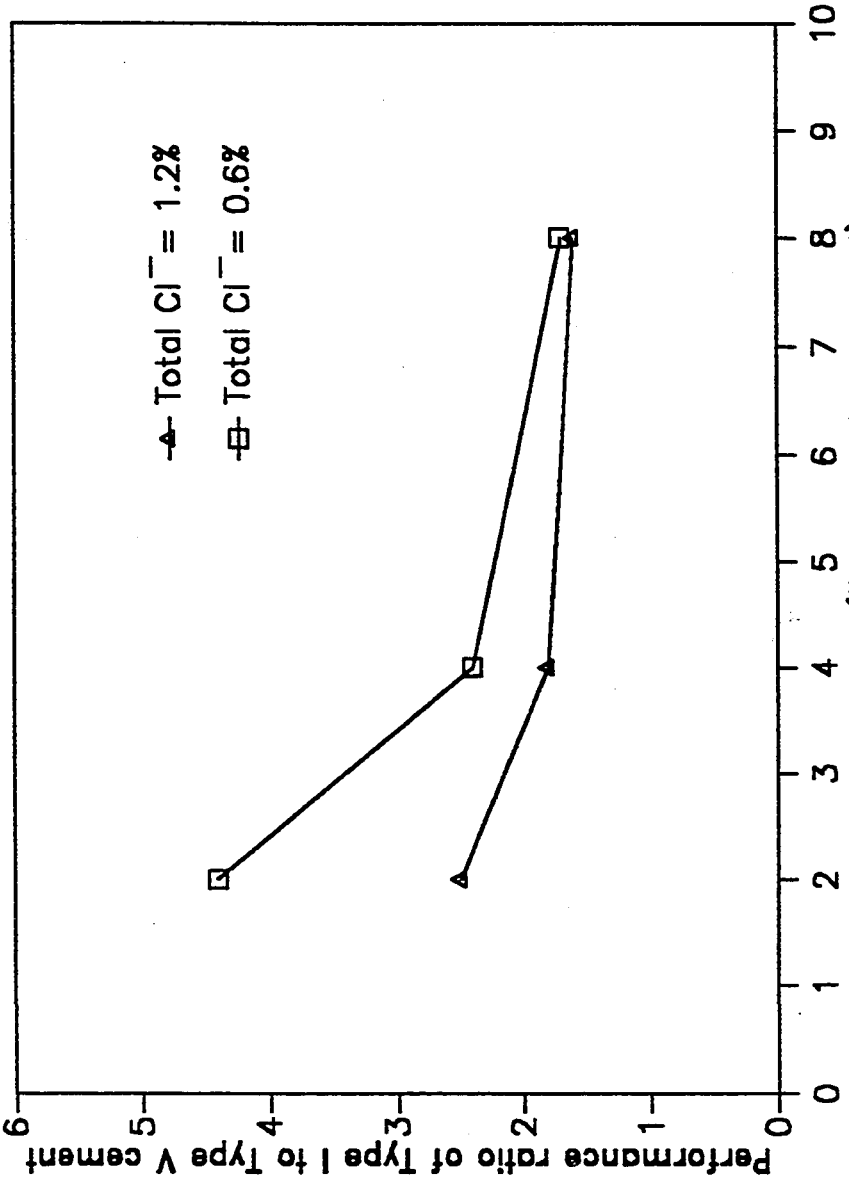

Fig. 4.2.1.19 Performance Ratio of Type I to Type V Cement

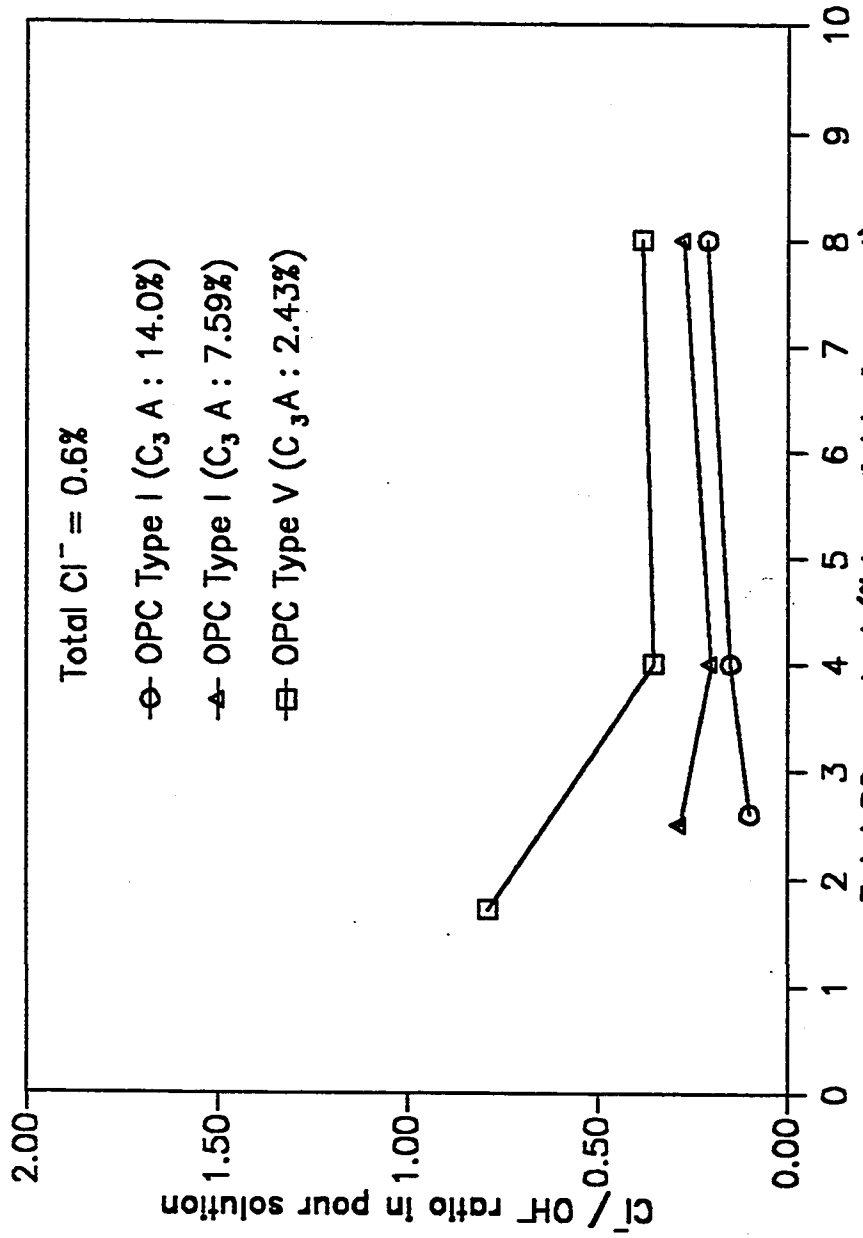

Fig. 4.2.1.20 Effect of Sulfate Addition on Cl^- PH Ratios in the Pore Solutions of Cements Treated with 0.6% Chloride Level

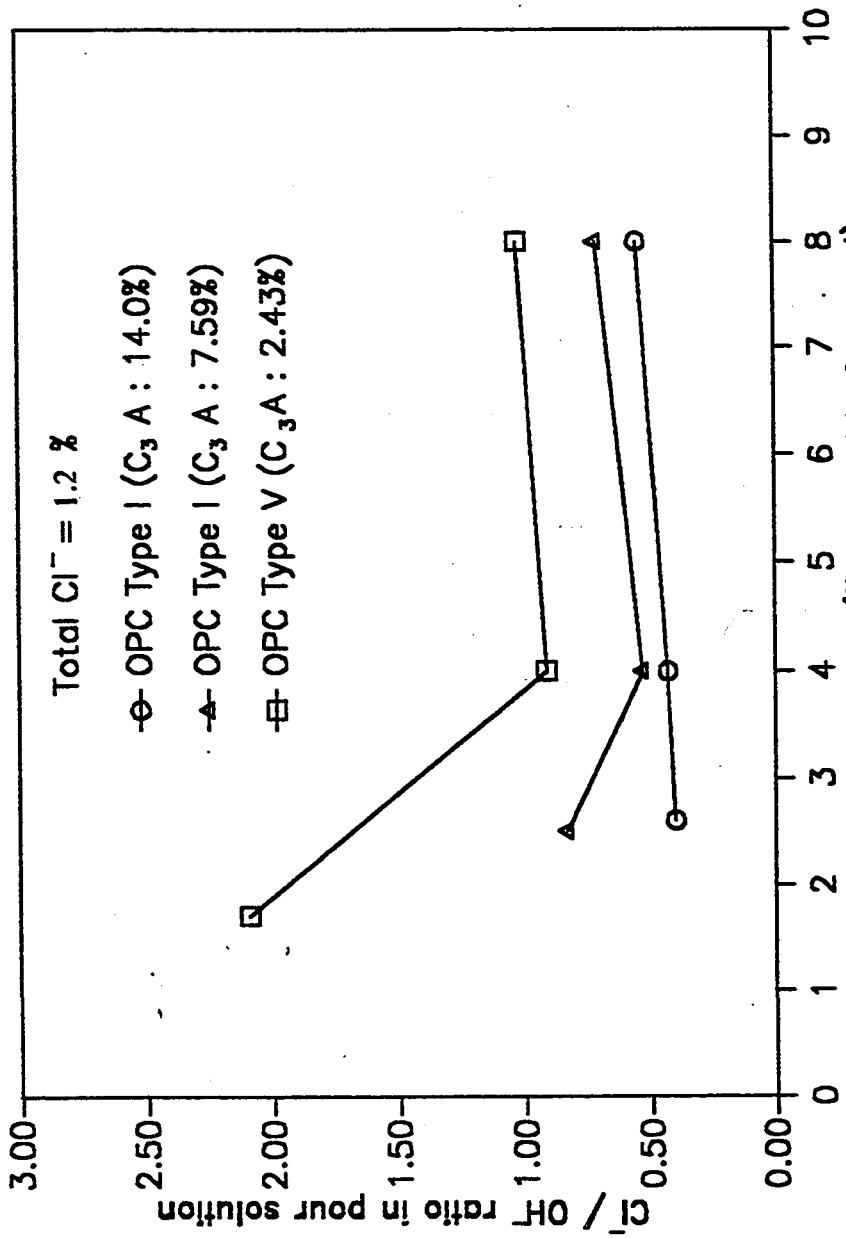

Fig. 4.2.1.21 Effect of Sulfate Addition on Cl^-/OH^- Ratios in the Pore Solutions of Cements Treated with 1.2% Chloride Level

cements. In view of the interplay of these several factors, the addition of sulfates in chloride-bearing concretes would not necessarily result in an increase in the Cl^-/OH^- ratio of pore solution. For given chloride and sulfate levels in concrete it would rather depend upon the interactive effect of the equivalent alkali content and the C_3A content of the cement.

4.2.1.4 Effect of Temperature

To study the effect of temperature on OH^- and Cl^- concentrations and hence Cl^-/OH^- ratio in the pore solution, cements 1, 2 and 4 (C_3A contents: 2.43, 7.59 and 14%) were used. Two levels of temperature, 20° C, which simulate room temperature, and 70° C, which simulates concrete surface temperature during a typical summer day in the Middle East, were used. Three levels of chloride addition, 0.3, 0.6, and 1.2% by weight of cement, were used. The chlorides were derived from NaCl.

(i) Chloride Ion Concentration in Pore Solution

Table 4.2.1.10 shows the equilibrium pore solution compositions of the three cement pastes treated with different chloride levels and cured at temperatures of 20 and 70° C. Figs. 4.2.1.22 through 4.2.1.24 show the chlorides remaining unbound in the pore solutions of the cement pastes cured at the two aforesaid temperatures. It is seen from the data of Table 4.2.1.10 and Figs. 4.2.1.22 through 4.2.1.24 that in all the three cements, free chlorides in the pore solution increase when the temperature is increased

from 20 to 70° C. This increase in unbound chlorides is more in high C_3A cements compared to low C_3A cements. For the 0.3% chloride treatment level, when the curing temperature is raised from 20 to 70° C the unbound chlorides increase by 2.2, 4.2 and 9.1 times for the 2.43, 7.59 and 14% C_3A cements. The corresponding values for the 1.2% chloride level are 1.2, 1.8 and 2.65 for the 2.43, 7.59 and 14% C_3A cements respectively. Arya et al (66) carried out a pore solution analysis study on a 9.9% C_3A cement cured at temperatures of 8, 20 and 38° C. His data show an increase in chloride binding of the cement with an increase in the curing temperature. They attribute this to faster reaction rates at higher temperatures. However, results contrary to those of Arya et al were observed by Roberts (33), whose data show that cements hydrated at elevated temperatures bound lesser chlorides compared to a cement which hydrated at the normal temperatures. Roberts conducted his tests on a Type V (C_3A: 1%) and a Type I (C_3A: 9%) cement. The tests involved shaking of the cements with $CaCl_2$ solution at 25, 50 and 90° C, then filtering at various periods up to 7 days and analysing the filtrates for chlorides. Equilibrium chloride concentrations were achieved after 4 days and for cement filtrates cured at 50 and 90° C free chlorides for Type I cement were found to be 2.3 and 3.7 times more than for the filtrates cured 25° C. However, the corresponding ratios for the Type V cement were significantly lower than those for Type I cement, both being equal to 1.1. Results of the present study are in good agreement with those of Roberts (33) which also show that the temperature effect of releasing additional free chlorides into the pore solution is more pronounced for the Type I than for Type V cement. The predominant phase of cement which complexes with chlorides is tricalcium aluminate (C_3A) forming either an insoluble calcium mono chloro aluminate ($3CaO.Al_2O_3.CaCl_2.10H_2O$) or calcium trichloro aluminate ($3CaO.Al_2O_3.3CaCl_2.10H_2O$), also called Friedel's salt. DTA results have shown the

formation of Friedel's salt in both 2.43 and 14% C_3A cements treated with 1.2% Cl^- (Fig. 4,2.1.4). An increase in the free chlorides of the pore solution due to an increase in the curing temperature can be attributed to the decomposition of Friedel's salt at higher temperatures such as 70° C temperature used in this study.

Roberts (33) tested the effect of temperature on the solubility of pure monocalcium chloroaluminate compound and found that the solubility in water and in solutions of calcium sulfate, calcium hydroxide and alkali hydroxides, increases with increasing temperature. The aforesaid solutions typically simulate concrete pore solution.

Fig. 4.2.1.25 shows the relationship between unbound chlorides and C_3A content of cement for curing temperatures of 20 and 70° C. Cement pastes cured at 20° C show a decrease in the unbound chlorides in the pore solution with increasing C_3A content. For chloride treatment level of 1.2%, the unbound chlorides reduce from 62 to 24% when the C_3A content is increased from 2.43 to 14% for the normal temperature curing. This shows for 1.2% chloride treatment, the 14% C_3A cement is 2.5 times more effective in removing chlorides than the 2.43% C_3A cement at the normal temperature curing of 20° C. However, for the cements cured at 70° C, the decrease in the unbound chlorides with an increase in the C_3A content from 2.43 to 14%is relatively much smaller, from 75.5 to 64.7%. This shows that at higher temperatures such as 70° C, the 14% C_3A cement is only 1.2 times more effective than the 2.43% C_3A cement in removing chlorides from the pore solution. The reduced differential in the unbound chlorides in the high and low C_3A cements at 70° C may be due to an increase in the solubility of Friedel's salt in the cement pastes cured at higher temperatures. Thus even in high C_3A cements, higher temperatures would possibly inhibit the formation of

Friedel's salt, thereby reducing their effectiveness in binding chlorides.

(ii) Hydroxyl Ion Concentration in Pore Solution

Figs. 4.2.1.26 through 4.2.1.28 show the hydroxyl ion concentrations in the pore solutions of the three cements cured at 20 and 70° C. Increase in curing temperature from 20 to 70° C causes a drop in the OH^- concentrations from 0.26 to 0.12 M/L for the 2.43% C_3A cement; from 0.40 to 0.15 M/L for the 7.59% C_3A cement; and from 0.50 to 0.20 M/L for the 14% C_3A cement. The effect of temperature in reducing OH^- concentrations may be ascribable to the hydroxyl ions entering into reaction to balance the anions removed due to the additional liberation of chloride ions into the pore solution.

(iii) Cl^-/OH^- Ratio in Pore Solution

The effect of temperature on Cl^-/OH^- ratio of the pore solution is shown in Fig. 4.2.1.29. The concomitant elevation of free chlorides and the depression of OH^- concentration with increase in temperature, raises the Cl^-/OH^- ratio of the pore solution significantly. As an example, for the 14% C_3A cement treated with 0.3% chlorides, the Cl^-/OH^- ratio increases 19 fold due to an increase in temperature from 20 to 70° C. Fig. 4.2.1.29 shows how the Cl^-/OH^- ratios multiply manifold for all the three chloride levels when cements are cured at 70° C instead of 20° C. The increase in Cl^-/OH^- ratio with temperature is observed to be most drastic for the lowest chloride treatment level of 0.3%. Also the increase in the Cl^-/OH^- ratio is more marked for the 14% C_3A cement than for the other two lower C_3A cements. This further

Table 4.2.1.10 Effect of Curing Temperature on Pore Soltuion Composition of 14% C_3A Cement Treated With Different Levels of Chloride

Cement No.	C_3A Content of Cement (% by weight)	Curing Temperature (^oC)	Total Cl^- Addition (% by weight of cement)	Pore Solution Composition				Evaporable Water (% by weight of cement)	Unbound Cl^- (% by weight of Total Cl^-)
				Cl^- (mM/L)	OH^- (mM/L)	pH	Cl^-/OH^-		
1	2.43	20	0.3	69.7	258	13.41	0.27	40.1	33.1
		70	0.3	140.6	120	13.08	1.17	43.4	72.2
		20	0.6	209.9	265	13.42	0.79	40.8	50.7
		70	0.6	279.0	128	13.11	2.18	43.6	72.0
		20	1.2	529.9	254	13.30	2.09	39.4	61.8
		70	1.2	571.2	116	13.06	4.92	44.7	75.5
2	7.59	20	0.3	35.0	385	13.59	0.09	38.7	15.9
		70	0.3	129.2	150	13.18	0.86	43.4	66.4
		20	0.6	109.0	391	13.59	0.28	38.2	24.6
		70	0.6	267.7	160	13.20	1.67	43.5	68.9
		20	1.2	342.0	413	13.62	0.83	39.8	40.3
		70	1.2	561.6	162	13.21	3.58	43.9	72.9
4	14.00	20	0.3	14.8	524	13.72	0.03	38.4	6.7
		70	0.3	125.5	222	13.35	0.57	41.1	61.0
		20	0.6	50.9	503	13.70	0.10	38.4	11.6
		70	0.6	260.1	198	13.30	1.31	40.0	64.3
		20	1.2	216.0	534	13.73	0.40	38.4	24.4
		70	1.2	533.6	194	13.29	2.75	41.0	64.7

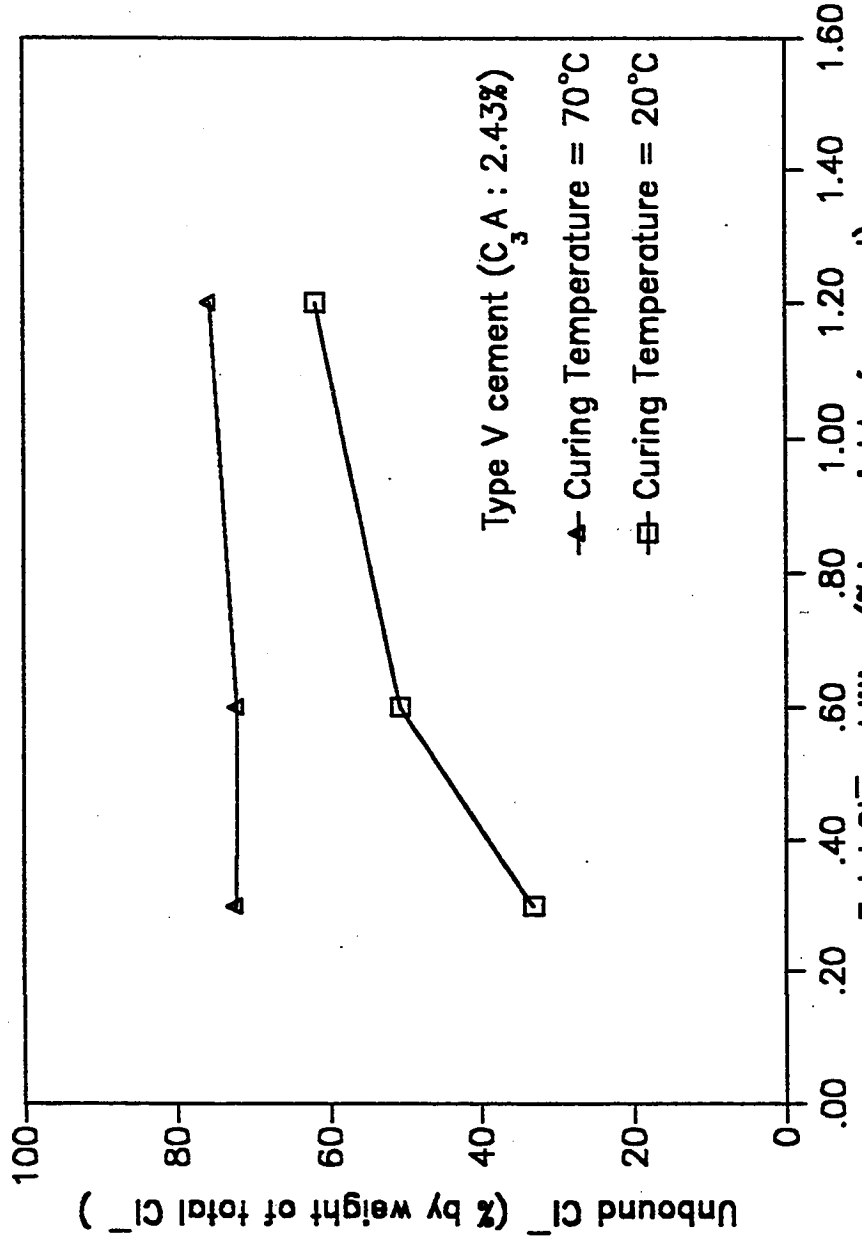

Fig. 4.2.1.22 Effect of Temperature on Unbound Chlorides in Pore Solutions of 2.43% C_3A Cement Treated with Different Levels of Chloride

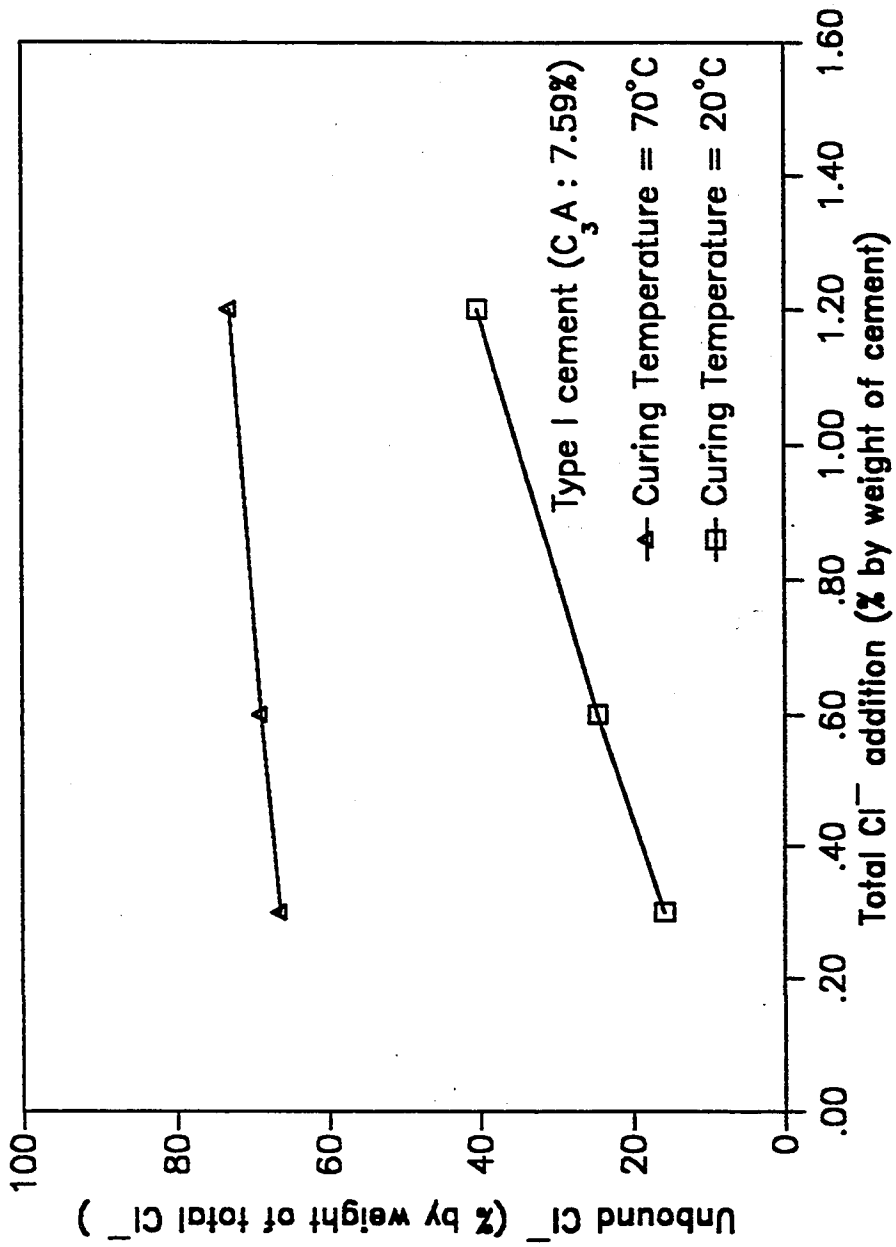

Fig. 4.2.1.23 Effect of Temperature on Unbound Chlorides in Pore Solutions of 7.59% C_3A Cement Treated with Different Levels of Chloride

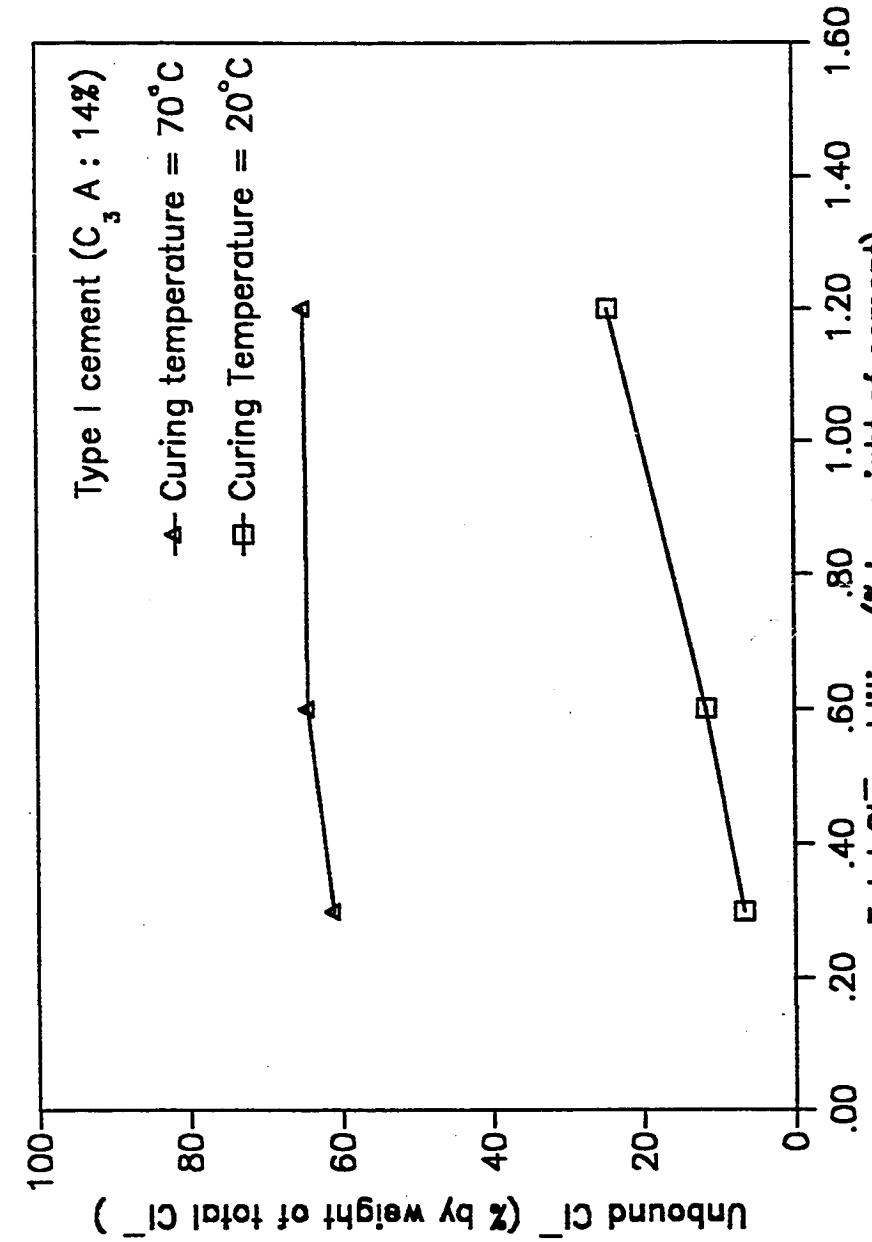

Fig. 4.2.1.24 Effect of Temperature on Unbound Chlorides in Pore Solutions of 14% C_3A Cement Treated with Different Levels of Chloride

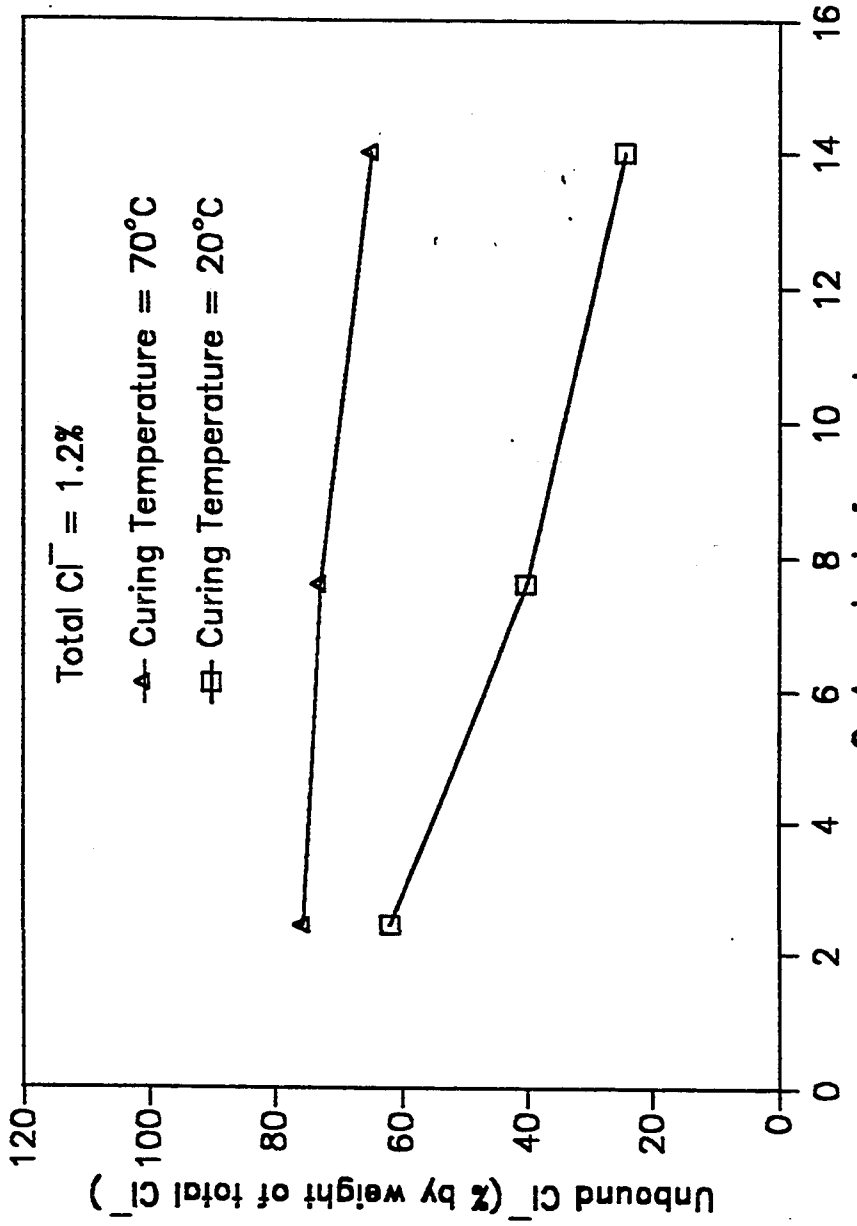

Fig. 4.2.1.25 Effect of Temperature on Unbound Chlorides in Pore Solutions of Different C_3A Cements

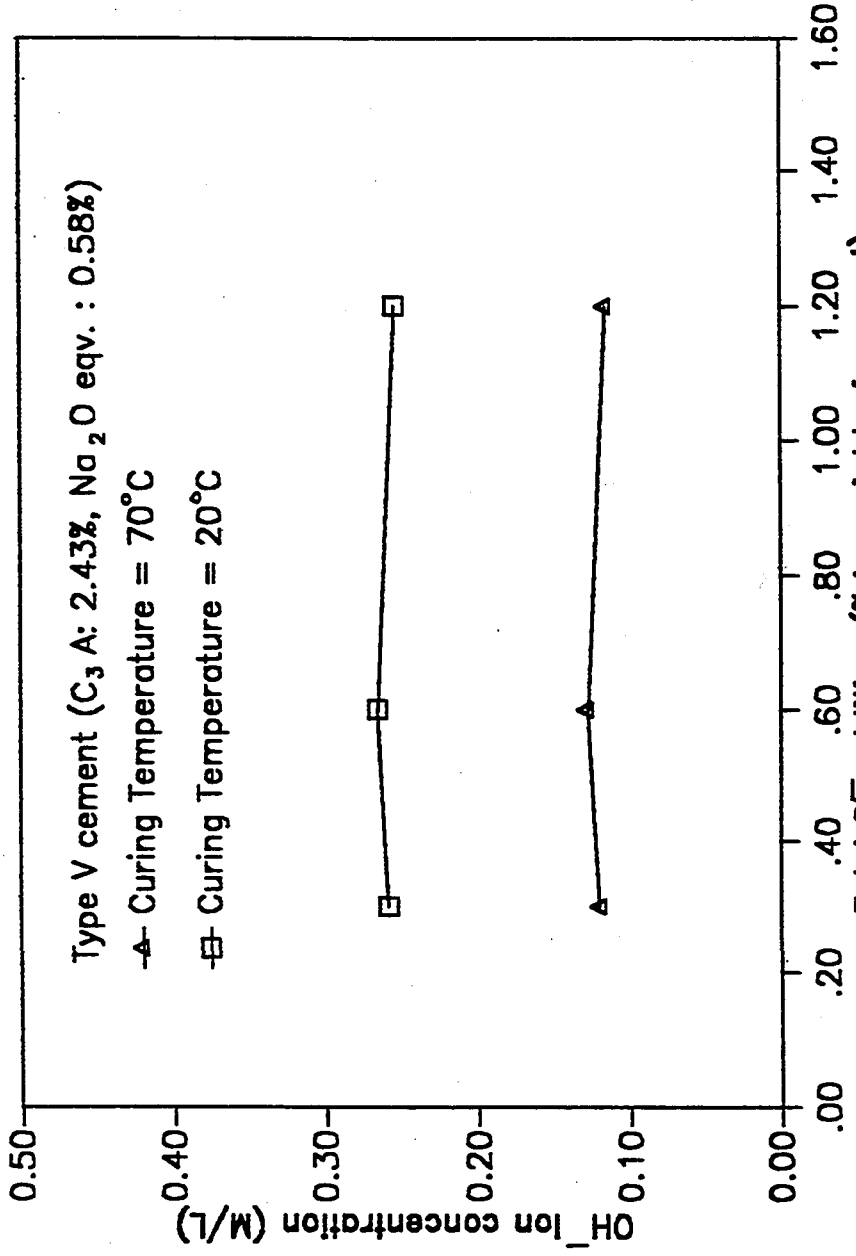

Fig. 4.2.1.26 Effect of Temperature on OH^- Concentration in Pore Solutions of 2.43% C_3A Cement Treated with Different Levels of Chloride

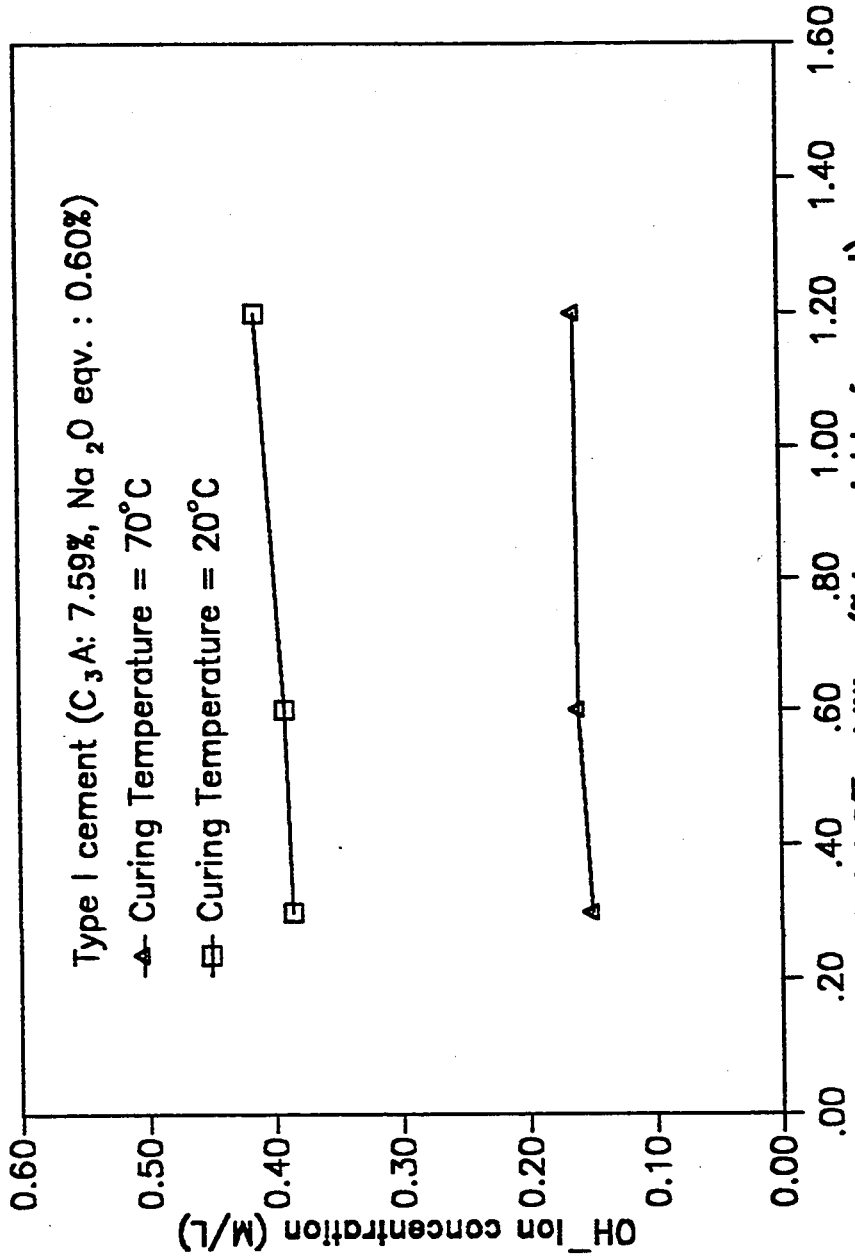

Fig. 4.2.1.27 Effect of Temperature on OH Concentration in Pore Solutions of 7.59% C_3A Cement Treated with Different Levels of Chloride

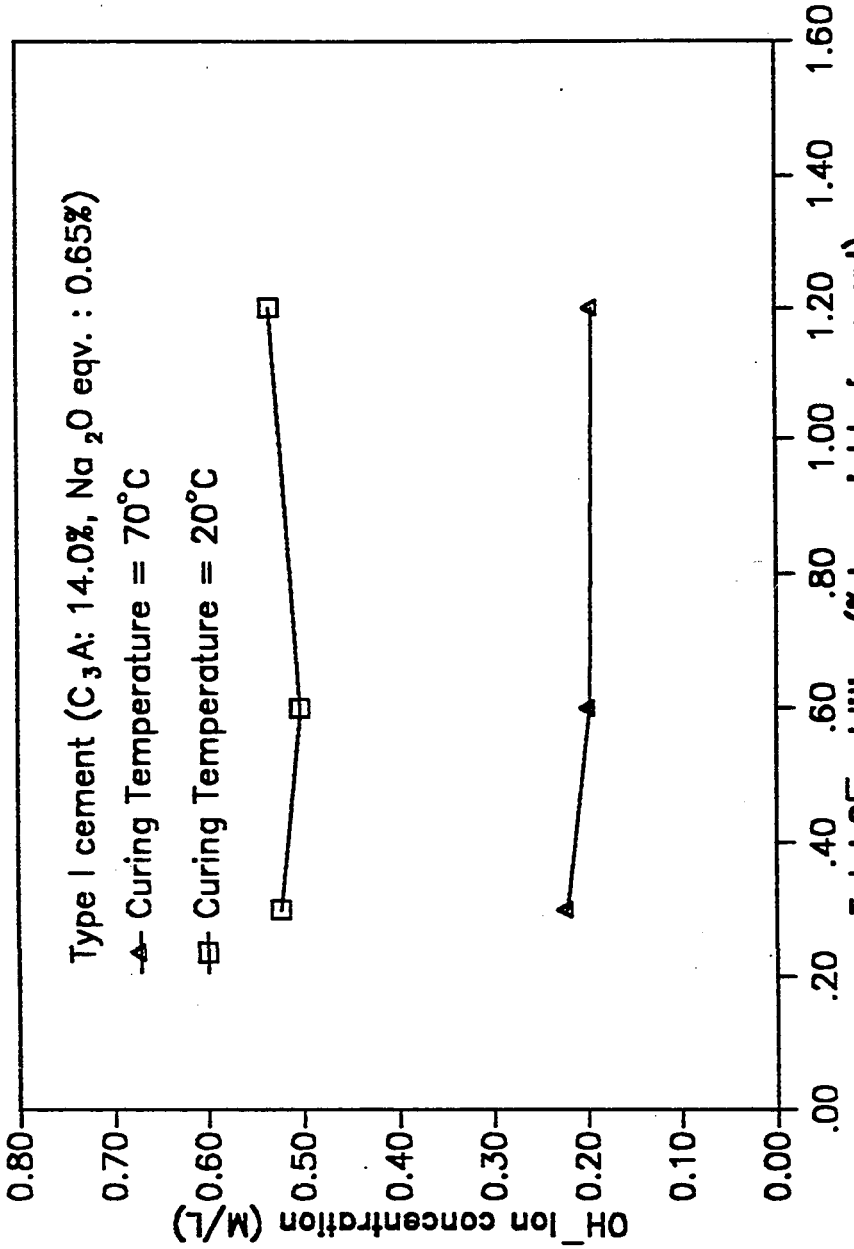

Fig. 4.2.1.28 Effect of Temperature on OH^- Concentration in Pore Solutions of 14% C_3A Cement Treated with Different Levels of Chloride

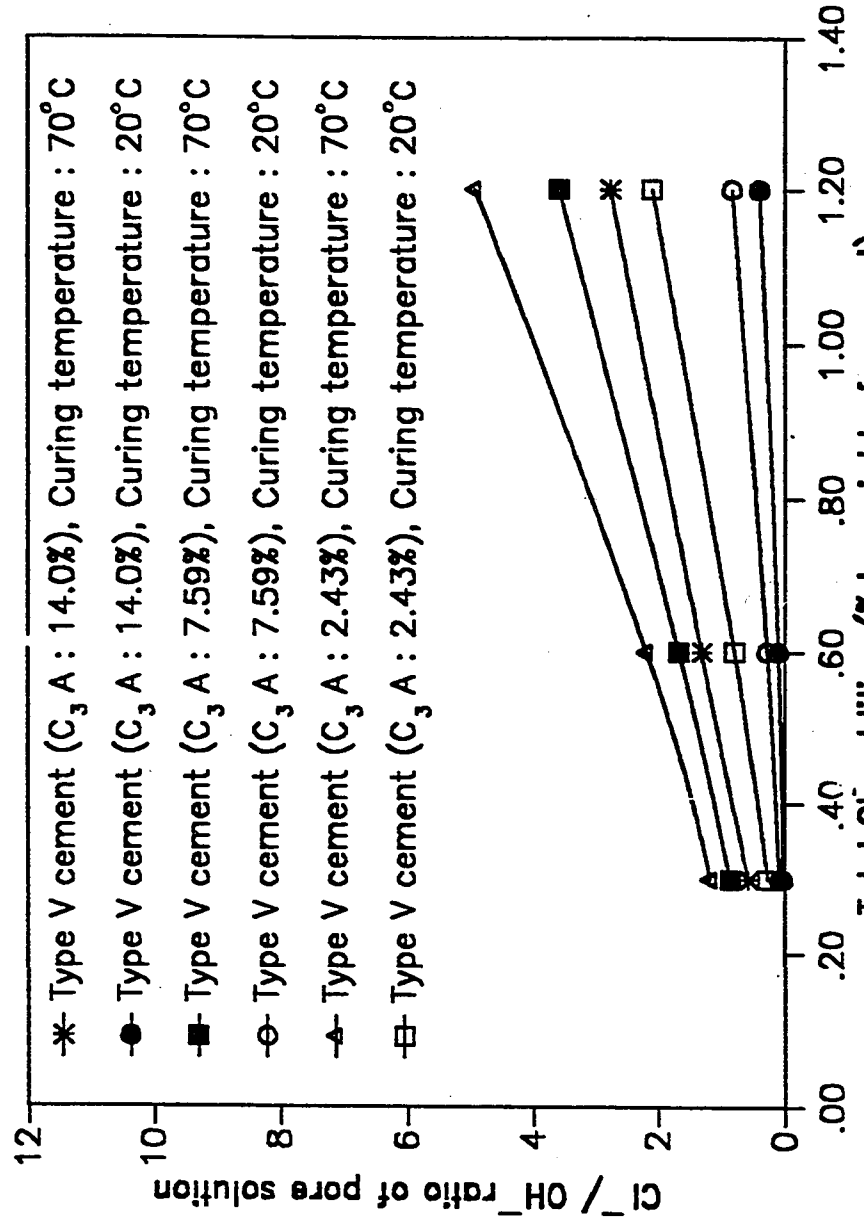

Fig. 4.2.1.29 Effect of Temperature on Cl^-/OH^- Ratio in Pore Solutions of Different C_3A Cements Treated with Different Levels of Chloride

emphasizes the point that in terms of corrosion environment the high C_3A cements are more adversely affected by temperature increase than the low C_3A cements.

The pore solution chemistry of cement pastes cured at higher temperature shows that the corrosion behavior of steel in concrete exposed to high temperature would be different as compared to concrete exposed to normal temperatures. The increase in Cl^-/OH^- ratio at higher temperatures indicates that the corrosion initiation time of steel in concrete would be decreased and corrosion rates would be increased significantly.

4.2.1.5 External Chlorides

To study the chloride-binding in plain cements when the chlorides are present as external chlorides, chloride was inducted into cement pastes after a hydration of 28 days. Plain cements 1,2 and 4 were used. Cement paste specimens were cast in 49x75 mm cylindrical PVC molds, without any chloride addition. The specimens were allowed to hydrate sealed in the molds and demolded after 28 days. 6 mm thick discs were cut from the cylindrical specimens. No lubricating liquid was employed for cutting. The discs were immersed in 10% NaCl solution, containing 0.5 M NaOH and crystalline $Ca(OH)_2$. The alkalies were added to the solution to avoid any leaching of alkalies from the samples, so that the unbound chlorides in the pore solution could be compared with those obtained in case of internal chlorides, at about equal pore solution alkalinity. Three discs were taken out after an immersion period of 10 days and pore solution extracted. The pore solution was analyzed for Cl^- and OH^- concentrations.

Another disc was used for finding the total soluble chlorides in the sample by acid digestion method.

The pore solution composition and the unbound chlorides are given in Table 4.2.1.11. The acid-soluble total chloride contents in the 2.43, 7.59 and 14% C_3A cements were 3.19, 3.18 and 2.87% by weight of cement respectively. As seen in Table 4.2.1.11, the unbound chlorides decrease with increasing C_3A content of cement. The unbound chlorides were 88.5, 82.9 and 79.3% for the 2.43, 7.59 and 14% C_3A cements respectively. To compare the chloride-binding of the cements for internal and external chlorides, the unbound and bound chlorides for internal and external chlorides are given in Table 4.2.1.12 and Fig. 4.2.1.30. The unbound chlorides for cements treated with internal chlorides are obtained from Fig. 4.2.1.2 by extrapolation for total chloride contents of 3.19, 3.18 and 2.87% for the 2.43, 7.59 and 14% C_3A cements. These values are 86, 63 and 59% for the 2.43, 7.59 and 14% C_3A cements respectively.

The OH^- concentrations in the pore solution of the 2.43, 7.59 and 14% C_3A cements treated with external chlorides were 382, 402 and 416 mM/L respectively. The average values of the OH^- concentrations for the 2.43, 7.59 and 14% C_3A cements for cements treated with internal chlorides were 260, 360 and 510 respectively (Table 4.2.1.1). It is seen that the pore solution alkalinity in the 2.43 and 7.59% C_3A cements were more for specimens treated with external chlorides compared to the specimens treated with internal chlorides. Since it is known that an increase in the pore solution alkalinity decreases chloride-binding (64,65), the increased pore solution alkalinity in the 2.43 and 7.59% C_3A cements would cause a decrease in the chloride-binding in the samples treated with external chlorides. The pore solution alkalinity in the 14% C_3A cement is less for the samples treated with external chlorides compared to those treated

with internal chlorides. This would cause an increase in the chloride-binding in the samples treated with external chlorides. However, it is seen from the data of Table 4.2.1.12 and Fig. 4,2.1.30 that the chloride-binding in all the three cements was less for the samples treated with external chlorides compared to those treated with internal chlorides. The ratios of bound chlorides in the samples treated with internal chlorides to those in the samples treated with external chlorides were 1.2, 2.2 and 2.0 for the 2.43, 7.59 and 14% C_3A cements. Such a difference in the bound chlorides for samples treated with internal and external chlorides is not expected from the difference in the pore solution alkalinity. It is also seen from Table 4.2.1.12 and Fig. 4.2.1.30 that whereas the bound chlorides increase by 2.9 times when the C_3A content of cement increases from 2.43 to 14% in the samples treated with internal chlorides, it increases by 1.8 times only, for the corresponding increase in the C_3A content in the samples treated with external chlorides. Thus, the removal of chlorides due to increasing C_3A content is less effective in situations when chlorides are inducted after significant degree of hydration. Arya et al (66) also found similar observation showing a decrease in chloride-binding differential between different C_3A cements when the chlorides were inducted externally after an initial curing period of 2 days compared to when the chlorides were inducted through mix water. They observed that the bound chlorides for the Type I (9.9% C_3A) and Type V SRPC were 38.5% and 28.3% respectively when the cements were treated with internal chlorides. When the chlorides were inducted after an initial curing of 2 days the bound chlorides were found to be almost equal, 50% and 47%, for the Type I and Type V cements respectively. It should be noted that the bound chlorides for cements treated with internal and external chlorides of the study of Arya et al (66) can not be compared with those of the present study, as the total chlorides were different for the samples treated with internal and external chlorides. In

their study, The total chloride content of the samples treated with internal chlorides were 1.0% whereas that for the samples treated with external chlorides was around 1.64%. The amount of total chlorides also has a significant effect on chloride binding (see Fig. 4.2.1.5); as the total chlorides increase the proportion of total chlorides which are bound decreases. In the study conducted by Arya et al, the chloride solution in which the specimens were immersed for induction of external chlorides, no alkalies were added to avoid the drop in the OH^- concentration due to leaching out of cement alkalies. Therefore, there is a strong possibility of cement alkalies being leached out, thereby considerably decreasing the pore solution alkalinity. Arya et al (66) did not report data on OH^- concentrations. Therefore the bound chlorides of samples treated with internal and external chlorides in the results obtained by Arya et al can not be compared since neither the total chlorides nor the pore solution alkalinity is the same for the cements treated with internal and external chlorides.

The decrease in the bound chlorides in samples treated with external chlorides compared to those treated with internal chlorides may be attributable to the formation of hydration products of C_3A namely mono sulfoaluminate and calcium aluminate hydrates, and possibly C-S-H gel, which has also been shown to bind chlorides (48), before the induction of chlorides. This possibly inhibits the formation of calcium chloroaluminates and chemisorption of chloride ions in the C-S-H gel. The data also show that the reduction in chloride-binding when the chlorides are subsequently inducted after hydration is more pronounced in high C_3A cements than in low C_3A cements, indicating a higher degree of inhibition of the Friedel's salt in the former.

Table 4.2.1.11 Unbound Chlorides in Pore Solution of Cements Containing External Chlorides

Cement No.	C_3A Content of Cement (% by weight)	Total Cl^- (% by weight of cement)	Pore Solution Composition				Evaporabe Water (% by weight of cement)	Unbound Cl^- (% by weight of Total Cl^-)
			Cl^- (mM/L)	OH^- (mM/L)	pH	Cl^-/OH^-		
1	2.43	3.19	1970	382	13.58	5.16	40.4	88.5
2	7.59	3.18	1858	402	13.60	4.62	40.0	82.9
4	14.00	2.87	1695	416	13.62	4.07	37.8	79.3

Table 4.2.1.12 **Unbound and Bound Chlorides in Cements Containing Internal and External Chlorides**

Cement No.	C_3A Content of Cement (% by weight)	Total Cl^- (% by weight of cement)	External Chlorides		Internal Chlorides	
			Unbound Cl^- (% by weight of Total Cl^-)	Bound Cl^- (% by weight of Total Cl^-)	Unbound Cl^- (% by weight of Total Cl^-)	Bound Cl^- (% by weight of Total Cl^-)
1	2.43	3.19	88.5	11.5	86*	14
2	7.59	3.18	82.9	17.1	63*	37
3	14.00	2.87	79.3	20.7	59*	41

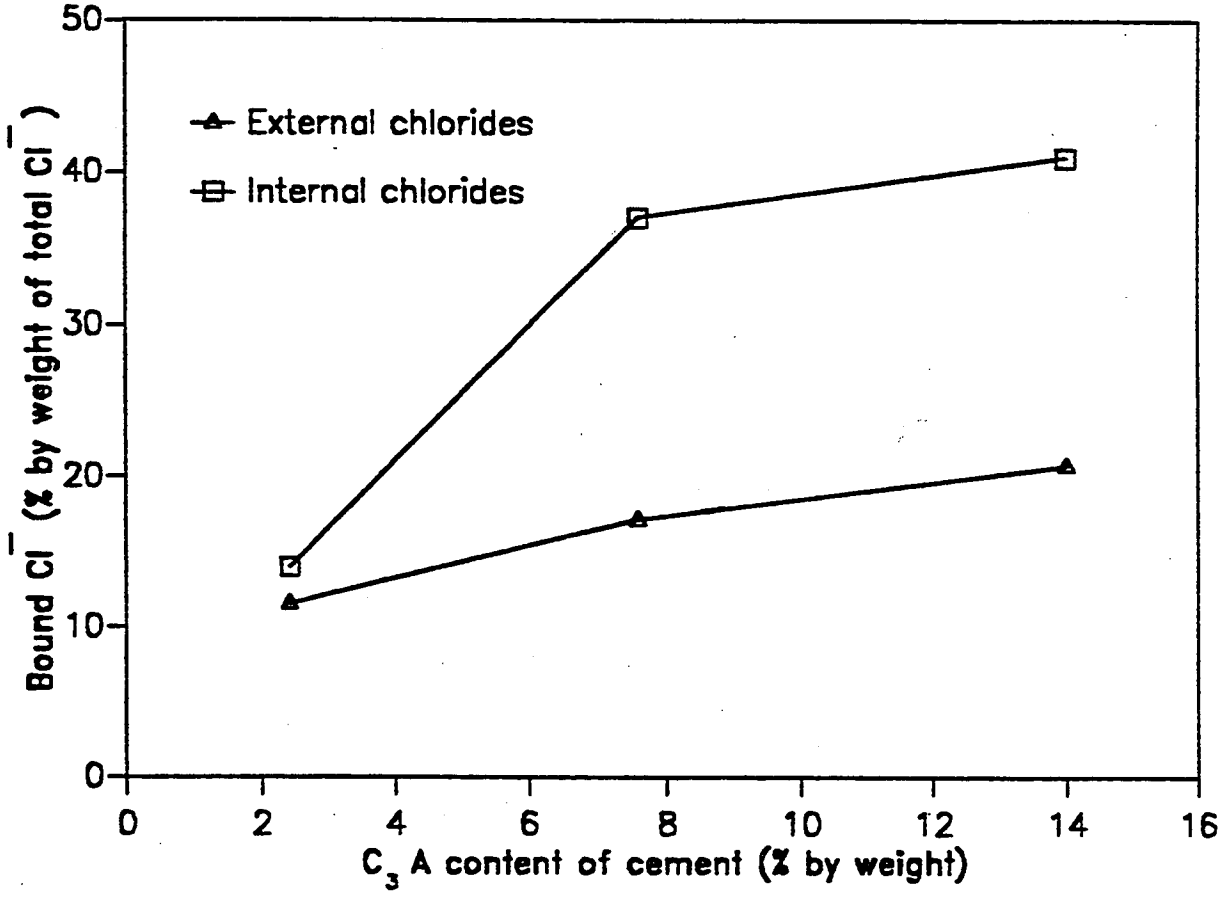

Fig. 4.2.1.30 Bound chlorides in different C_3A cements for internal and external chlorides.

4.2.2 CHLORIDE BINDING MECHANISM IN BLENDED CEMENTS

4.2.2.1 Microsilica Blended Cement

Two parent plain cements, cements 1 and 4, and two levels of microsilica,10 and 20% were used. The chloride additions used were 0.3, 0.6 and 1.2% by weight of cementitious material. OH^- and Cl^- concentrations, and hence Cl^-/OH^- ratio in the pore solution were measured after a curing period of 6 months.

(i) OH^- Concentration in Pore Solution

The OH^- concentrations in the pore solutions of the plain and the microsilica blended cement pastes made with 2.43% and 14% C_3A cements are shown in Table 4.2.2.1 and Figs. 4.2.2.1 and 4.2.2.2. It is seen from these data that the OH^- concentrations in the pore solutions of the microsilica blended cements are significantly lower compared to the parent plain cements.

The OH^- concentrations in the pore solutions of the 14% C_3A plain cement (equivalent Na_2O :0.65%) are 524, 503 and 534 mM/L for the chloride additions of 0.3, 0.6 and 1.2%. OH^- concentrations were also measured for the chloride-free plain and microsilica blended cements made with the 14% C_3A parent cement. The OH^- concentration in the chloride-free plain cement is 328 mM/L. This shows that the addition of NaCl in the range 0.3 to 1.2 chloride causes about 1.6 times increase in the

OH^- concentration in the pore solution of the plain cement. For the 10% microsilica blended cement paste, the OH^- concentrations in the pore solutions of both chloride-free and chloride-bearing hydrated cement pastes drop significantly with partial cement replacement by microsilica. The OH^- depression, however, is in general, more pronounced for chloride-bearing microsilica blended cement pastes, compared to chloride-free microsilica blended cement pastes. With 10% cement replacement by microsilica, in chloride-free paste, the OH^- concentration drops by 1.6 times, from 328 to 204 mM/L. However, for 0.3% chloride-bearing paste, the same 10% cement replacement by microsilica causes more reduction by 4.3 times the original value, from 524 to 121 mM/L. Doubling the cement replacement level from 10 to 20% causes a much steeper reduction in the OH^- concentration; it drops from 328 to 66 mM/L for the chloride-free paste, and to 10 times the original value, from 524 to 54 mM/L for 0.3% chloride-bearing paste. Increase in the chloride addition to 0.6 and 1.2% does not cause significant changes in the OH^- concentration in the plain cement. However increasing the chloride addition to 0.6 and 1.2% results in 46% and 80% increase in the OH^- concentrations of the 10% microsilica blended cement. In the 20% microsilica blended cement, the increase in the chloride addition to 0.6 and 1.2%, however, causes 67% and 54% reductions in the OH^- concentration.

Similar behavior is observed for the plain and microsilica blended cements made with 2.43% C_3A parent plain cement (equivalent Na_2O: 0.58%). OH^- concentrations were measured for the plain and microsilica blended cements in chloride-bearing cement only. The average OH^- concentration in the pore solution of the chloride-bearing cement pastes is 260 mM/L. 10% replacement of the cement by microsilica reduces the OH^- concentrations to 159, 154 and 110 mM/L for the chloride additions

of 0.3, 0.6 and 1.2%. Doubling the cement replacement by microsilica from 10 to 20% in the 2.43% parent plain cement causes a steep drop in the OH^- concentrations to 20, 12.5 and 14.8 mM/L for 0.3, 0.6 and 1.2% chloride treatment levels. These correspond to average drops in the OH^- concentration in the pore solution of the 10 and 20% microsilica blended cements by 1.9 and 16.5 times respectively compared to the plain cement.

The pH levels in the pore solutions of the 14% C_3A chloride-free plain cement is sustained at a value of 13.52. Additions of 0.3, 0.6 and 1.2% chlorides to the 14% C_3A plain cement increase the pore solution pH to 13.72, 13.70 and 13.73 respectively. 10% microsilica blending reduces the pore solution pH to 13.38, 13.08 and 13.25 for 0, 0.3, 0.6 and 1.2% chloride additions respectively. For the 20% cement substitution by microsilica the pH levels drop below that of saturated calcium hydroxide solution (12.5). Whereas, for the chloride-free and 0.3% chloride-bearing 20% microsilica blended cement pastes the pore solution pH values are slightly above that of saturated calcium hydroxide solution, 12.82 and 12.73 respectively, the pore solution pH values for the 0.6 and 1.2% chloride levels fall below that of saturated calcium hydroxide solution, 12.26 and 12.40 respectively. The pH levels in the pore solution of the 2.43% C_3A plain cement are 13.41, 13.42, and 13.40 for 0.3, 0.6 and 1.2% chloride levels. 10% microsilica blending reduces these values to 13.20, 13.06 and 13.04 respectively. However, the pH values for the 20% microsilica blended cement pastes made with the 2.43% parent plain cement fall well below that of saturated calcium hydroxide solution, the values being 12.11, 12.10 and 12.17 for 0.3, 0.6 and 1.2% chloride additions.

The drop in the pore solution alkalinity due to microsilica blending is attributable to the combination of silica, which constitutes about 95% of the microsilica, with alkali

hydroxides and calcium hydroxide. Diamond (55) and Page et al (37) measured alkali hydroxide concentrations in the pore solutions of plain and microsilica blended cements. Both the studies used cement replacement levels by microsilica of up to 30%. It was observed that the concentrations of Na^+ and K^+ reduced with increasing levels of microsilica. However, the drop in the hydroxyl ion concentration was far steeper compared to the drops in the Na^+ and K^+ concentrations. They also observed that the concentration of Ca^{2+} was very low for microsilica blending of up to 20%, thereafter an increase in the Ca^{2+} concentration was observed for 30% microsilica blending. The increase in the Ca^{2+} concentration in the 30% microsilica blended cement may be due to what is called common ion effect. At lower replacement levels up to 20%, the concentrations of NaOH and KOH are relatively high which inhibits the solubility of calcium hydroxide crystals. At higher levels of microsilica blending, of the order of 30%, the NaOH and KOH concentrations drop significantly, thereby allowing the calcium hydroxide crystals to dissolve in the pore solution.

Fig. 4.2.2.3 shows the DTA patterns of the plain and 10 and 20% microsilica blended cements. One of the dominant reasons for the steep decline in the OH^- ion concentration in the pore solution of the microsilica blended cement is the reduction in $Ca(OH)_2$ content with increasing addition of microsilica. This is shown by the clearly diminishing response of the $Ca(OH)_2$ endothermic peak at 520°C in the DTA pattern. TGA curves were also run to quantify $Ca(OH)_2$ consumption by microsilica. Computations show that the near 31% $Ca(OH)_2$ present in the plain parent cement, is reduced to about 18% by 10% microsilica, and is almost completely eliminated when microsilica content is doubled to 20%.

(ii) Cl^- Concentration in Pore Solution

The chloride ion concentration in the pore solution and the unbound chlorides for the plain and microsilica blended cements made with the 2.43% and 14% C_3A parent plain cements are shown in Table 4.2.2.1 and Figs. 4.2.2.4 through 4.2.2.6. These data show that the partial cement replacement by microsilica increases the unbound chlorides in the pore for both the parent cements.

In the case of the 14% C_3A parent cement, the substitution of cement by 10% microsilica increases the unbound chlorides by 3 times for 0.3% chloride addition and almost 2 times for 0.6% and 1.2% chloride additions. Increasing the microsilica blending to 20% further increases the unbound chlorides in the pore solution by 71% and 65% for 0.3 and 0.6% chloride addition, but only by 20% for 1.2% chloride addition over the respective chloride concentration values for the 10% microsilica blending. However, in the case of the 2.43% C_3A parent cement, the increase in the unbound chlorides due to microsilica blending is significantly lower than it is achieved in the case of the 14% C_3A parent cement. 10% microsilica blending to the 2.43% C_3A parent cement, causes a decrease of 14% in the unbound chlorides for 0.3% chloride addition. However, 10% microsilica blending causes almost negligible change for 0.6% chloride addition, and 13% increase for 1.2% chloride addition, in the unbound chlorides. A close inspection of the pore solution chloride concentrations of the plain and 10% microsilica blended cement made with 2.43% C_3A cement reveal that for 0.3, 0.6 and 1.2% chloride levels, the chloride concentration is in fact reduced by 24, 11 and 5% respectively due 10% microsilica blending. However, 20% microsilica blending to the 2.43% C_3A cement causes the unbound chlorides to increase by 40, 16 and 32% for 0.3, 0.6 and 1.2% chloride additions.

The data of Table 4.2.2.1 and Figs. 4.2.2.4 through 4.2.2.6 show that as the cement substitution by microsilica is increased there also is a systematic increase in the unbound chlorides except for 0.3 and 0.6% chloride bearing 10% microsilica blended cement pastes made with the 2.43% C_3A cement. Availability of more chlorides in the pore solutions of microsilica blended cement pastes is only possible when microsilica addition brings about a decomposition of the Friedel's salt which is known to be formed by complexing of C_3A phase of cement with chlorides in hydrated cement. This position is confirmed by the DTA patterns obtained for the 1.2% chloride-bearing plain and microsilica blended cements made with the 14% C_3A parent plain cement and shown in Fig.4.2.2.3. Whereas, there is a fairly well defined endothermic peak at about 320° C due to the formation of Friedel's salt in the plain cement, the response systematically weakens with increasing blending of the parent plain cement with microsilica, showing the progressive decomposition of Friedel's salt.

Page and Vennesland (37) attribute this decomposition to increased solubility of Friedel's salt at reduced pH levels of the pore solution. This explanation appears to contravene the observation by Rasheeduzzafar et al (83) and others (64) that a highly alkaline pore solution environment exerts a strong inhibiting effect on the chloride-binding capacity of a cement. However, as pointed out by Diamond (38) other Friedel's salt decomposition mechanisms are possible.

It is also noticed from the data developed on pore solution composition of microsilica blended cements made with low and high C_3A parent cements, that the increase in the unbound chlorides in the pore solution due to microsilica blending is more pronounced in the high 14% C_3A cement than in the low 2.43% C_3A Whereas the 20% microsilica brings about 5.4, 3.1 and 2.1 times increase in the unbound chlorides in the

14% C_3A cement for 0.3, 0.6 and 1.2% chloride additions respectively, the corresponding increases observed in the 2.43% C_3A cement are 1.4, 1.2 and 1.3. This clearly indicates that the increase in the unbound chlorides and hence the inhibition of the formation of Friedel's salt due to microsilica blending is proportional to the C_3A content of cement. Therefore, it is likely that the microsilica addition to a chloride-bearing cement paste may combine with C_3A phase of the cement, thereby inhibiting the availability of C_3A for the formation of Friedel's salt.

Since there appears to be a controversy in the reasons attributed to the increase in unbound chlorides due to microsilica addition, in terms of the effect of decreased pore solution alkalinity on chloride-binding, the effect of pore solution alkalinity on chloride-binding in 10 and 20% microsilica blended cements is also included in the present study. For this purpose, 14% C_3A cement pastes were prepared with sodium hydroxide additions to raise to equivalent Na_2O content of the cement from 0.65 to 1.2%. Chloride additions of 0.6 and 1.2% are used. The pore solution composition of the plain and the microsilica blended cements with equivalent Na_2O contents of 0.65% and 1.2% are shown in Table 4.2.2.2.

The OH^- concentrations and the unbound chlorides in the pore solution are shown in Figs. 4.2.2.7 through 4.2.2.9. Increasing the alkali content to 1.2% causes increase in the OH^- concentrations of 237, 113 and 2mM/L for the plain, 10 and 20% microsilica blended cements for chloride treatment level of 0.6%. For the 1.2% chloride level, the corresponding increases are 216, 116 and 1 mM/L. It has been shown that microsilica combines with alkali hydroxides in the pore solution (37,38) when used as partial cement replacement. The addition of alkalies, in the present study, causes an increase in the OH^- concentration in the pore solution of the 20% microsilica blended

cement by one half the increase caused in the plain cement, whereas, in the 20% microsilica the pore solution alkalinity is unaltered by the increase in the alkali content from 0.65% to 1.2%. This may be attributable to greater affinity of 20% microsilica blended cement to OH^- ions than that of the 10% microsilica blended cement. Figs. 4.2.2.8 and 4.2.2.9 show that the increase in the alkali content of the plain and the microsilica blended cements from 0.65 to 1.2% significantly increase the unbound chlorides in the pore solution. For 0.6% chloride level, increase in the alkali content from 0.65 to 1.2%, increases the unbound chlorides by about two fold in the plain and 10 and 20% microsilica blended cements. However, for 1.2% chloride level, the increase in the unbound chlorides, due to the increase in the alkalies are 1.8 fold for the plain and about 1.5 fold for both the microsilica blended cements. A close look at the pore solution data reveal that although the OH^- concentration of the pore solution remains unchanged, the unbound chlorides in the pore solution of the 20% microsilica blended cement pastes increase significantly due to an increase in the alkali content of the cement. This shows that in microsilica blended cements which have greater affinity for hydroxyl ions, it is the alkali content of the cement or the OH^- concentration prior to pozzolanic reaction which controls the chloride-binding of the cement. The more the alkali content of cement or the pore solution alkalinity before the pozzolanic reaction, the more will be the unbound chlorides in the pore solution. These results thus, contradict the theory proposed by Page and Vennesland (37) which states that decrease in the chloride binding in the microsilica blended cements is attributed to the increase in the solubility of Friedel's salt (calcium chloroaluminate) due to decrease in the pore solution alkalinity. Roberts(33) measured solubility of pure calcium chloroaluminate compound in solutions of varying alkalinity and found that the solubility of calcium chloroaluminate increased with increase in the alkalinity of the solution. The results of present study also confirm the observations made by others(64,65) using plain cements that the

unbound chlorides in the pore solution increase with an increase in the pore solution alkalinity. The data show that the mechanism of increase in the unbound chlorides due to increase in the pore solution alkalinity is operative not only in the plain cements but also in the microsilica blended cements. However, the increase in the unbound chlorides in the pore solution due to microsilica blending may be attributed to the increased binding of hydroxyl ions in the microsilica blended cement pastes, thereby releasing chloride ions to balance the cations present in the pore solution.

(iii) Cl^-/OH^- Ratio in Pore Solution

Cl^-/OH^- ratios in the pore solution of plain and microsilica blended cements are shown in Table 4.2.2.1 and Figs. 4.2.2.10. These data show that the Cl^-/OH^- ratios in the pore solutions of the 10 and 20% microsilica blended cements steeply increase due to the cumulative interactive effect of an increase in the free chlorides and a decrease in the OH^- concentrations in the pore solution of the microsilica blended cements. In the 14% C_3A cement, 10% microsilica blending causes 12, 5 and 4 fold increase in Cl^-/OH^- ratio for chloride levels of 0.3, 0.6 and 1.2%. In 2.43% C_3A cement, the increase in the Cl^-/OH^- ratio due to 10% microsilica blending is to a lesser extent, 1.2, 1.6 and 4.2 times for 0.3, 0.6 and 1.2% chloride additions respectively. However, when cement substitutions by microsilica is doubled to 20%, the Cl^-/OH^- ratios increases more steeply in both the parent cements. In the 14% C_3A parent cement, 20% microsilica blending causes 45, 76 and 39 fold increase whereas in the 2.43 C_3A parent cement, it causes 24, 21 and 19 fold increase in the Cl^-/OH^- ratios for 0.3, 0.6 and 1.2 chloride additions respectively. The steep increase in the Cl^-/OH^- ratios of the 20% microsilica blended cements is mainly attributed to the

Table 4.2.2.1 Pore Solution Composition of Plain and Microsilica Blended Cements Treated with Different Levels of Chloride

C_3A Content of Cement	Cement Replaced by Microsilica (% by weight)	Total Cl^- Addition (% by weight of cementitious material)	Pore Solution Composition				Evaporabe Water (% by weight of cementitious material)	Unbound Cl^- (% by weight of Total Cl^-)
			Cl^- (mM/L)	OH^- (mM/L)	pH	Cl^-/OH^-		
	0	0.3	69.7	258	13.41	0.2702	40.1	33.1
	10	0.3	52.7	159	13.20	0.3314	45.8	28.6
	20	0.3	81.9	20	12.11	6.3984	47.8	46.3
	0	0.6	209.9	265	13.42	0.7921	40.8	50.7
2.43	10	0.6	186.1	144	13.06	1.2924	46.3	50.9
	20	0.6	207.7	12.5	12.10	16.6200	48.0	59.0
	0	1.2	529.9	254	13.40	2.0862	39.4	61.8
	10	1.2	505.0	110	13.04	4.5909	46.6	69.6
	20	1.2	577.2	14.8	12.17	39.0000	47.9	81.8
	0	0.3	14.8	524	13.72	0.0282	38.4	6.7
	10	0.3	42.5	121	13.08	0.3512	42.0	21.1
	20	0.3	69.0	54	12.73	1.2778	44.2	36.1
14.00	0	0.6	50.9	503	13.70	0.1014	38.4	11.6
	10	0.6	91.2	177	13.25	0.5153	40.4	21.8
	20	0.6	139.7	18	12.26	7.7611	43.6	36.1
	0	1.2	216.0	534	13.73	0.4045	38.2	24.4
	10	1.2	356.0	218	13.34	1.6330	41.6	43.8
	20	1.2	395.0	25	12.40	15.8000	44.6	52.1

Table 4.2.2.2 Effect of Alkali Content of Cement on Pore Solution Composition of Microsilica Blended Cements Treated with Different Chloride Levels (Parent Cement C_3A: 14%)

Cement Replaced by Microsilica (% by weight)	Equivalent Na_2O Content of Cement (% by weight)	Total Cl Addition (% by weight of cementitious material)	Pore Solution Composition				Evaporable Water (% by weight of cementitious material)	Unbound Cl^- (% by weight of Total Cl^-)
			Cl^- (mM/L)	OH^- (mM/L)	pH	Cl^-/OH^-		
0	0.65	0.6	50.9	503	13.70	0.1014	38.4	11.6
0	1.20	0.6	93.8	740	13.87	0.1268	40.5	22.5
10	0.65	0.6	91.2	177	13.25	0.5153	40.4	21.8
10	1.20	0.6	163.0	290	13.46	0.5621	40.6	39.2
20	0.65	0.6	139.7	18	12.26	7.7611	43.6	36.1
20	1.20	0.6	249.2	20	12.30	12.4550	44.3	65.4
0	0.65	1.2	216.0	534	13.73	0.4045	38.2	24.4
0	1.20	1.2	362.8	750	13.88	0.4837	41.2	44.2
10	0.65	1.2	356.0	218	13.34	1.6330	41.6	24.4
10	1.20	1.2	430.2	334	13.52	1.2880	49.1	44.2
20	0.65	1.2	395.0	25	12.40	15.8000	44.6	52.1
20	1.20	1.2	541.2	26	12.40	20.8231	49.2	78.8

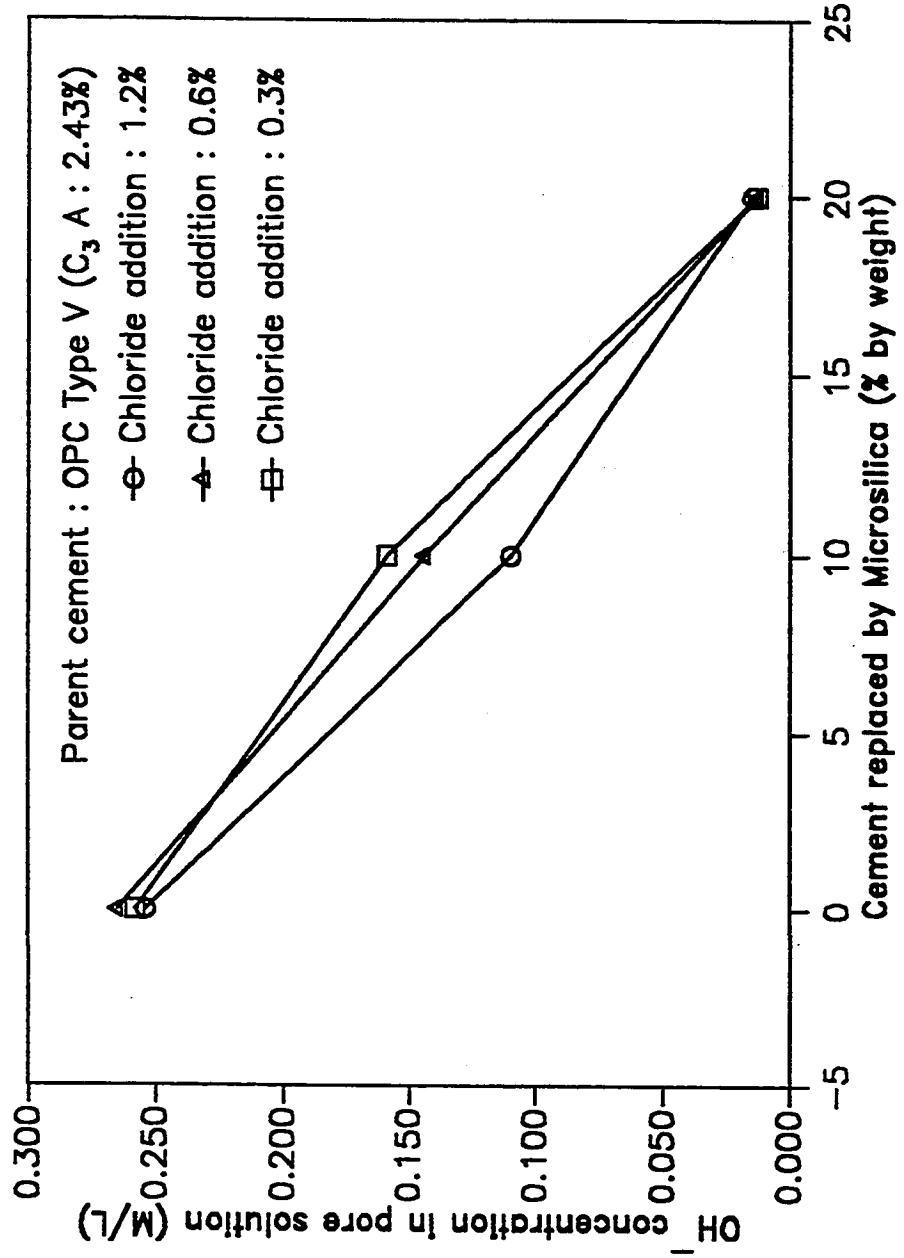

Fig. 4.2.2.1: OH^- Concentration in Pore Solutions of Plain and Microsilica Blended Cements Treated with Different Levels of Chloride

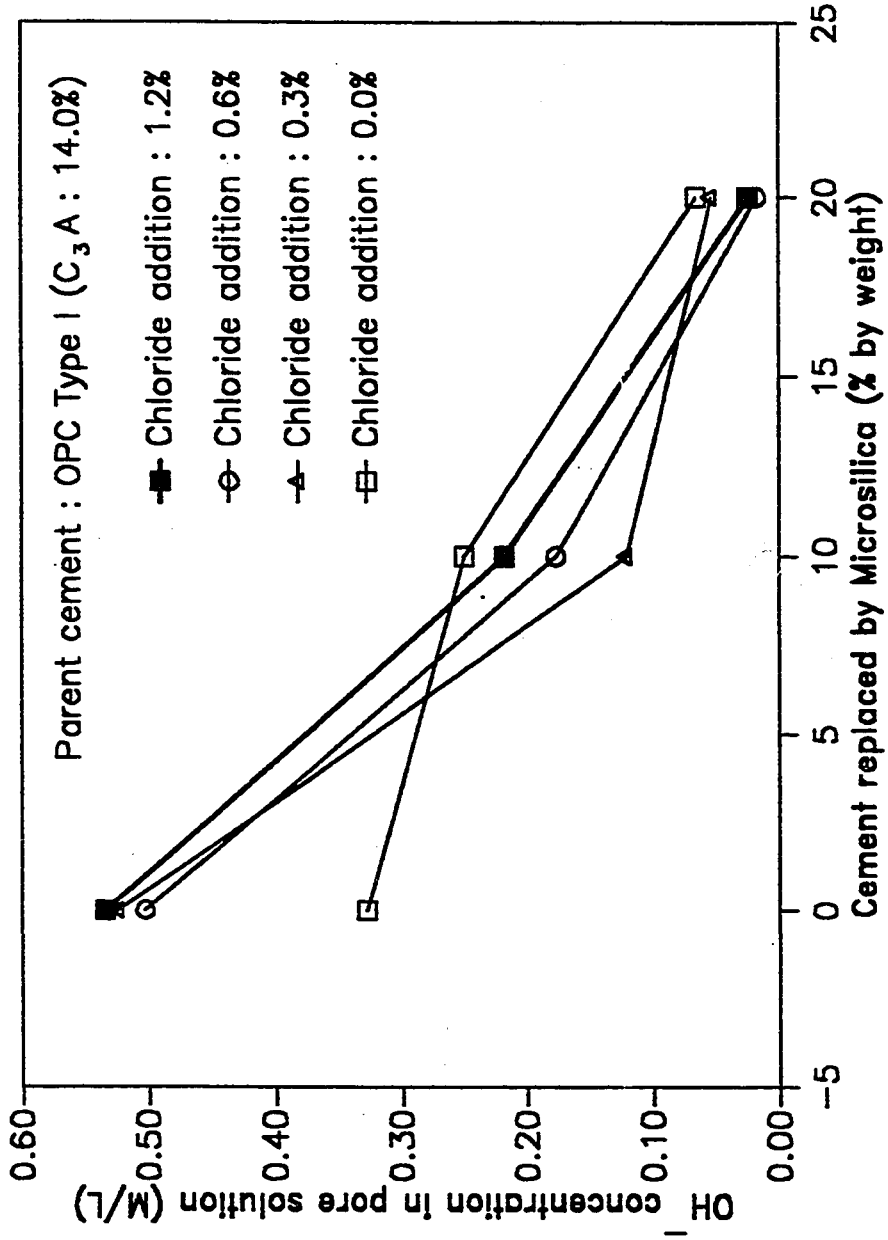

Fig. 4.2.2.2: OH^- Concentration in Pore Solutions of Chloride-Free and Chloride-Bearing Plain and Microsilica Blended Cements

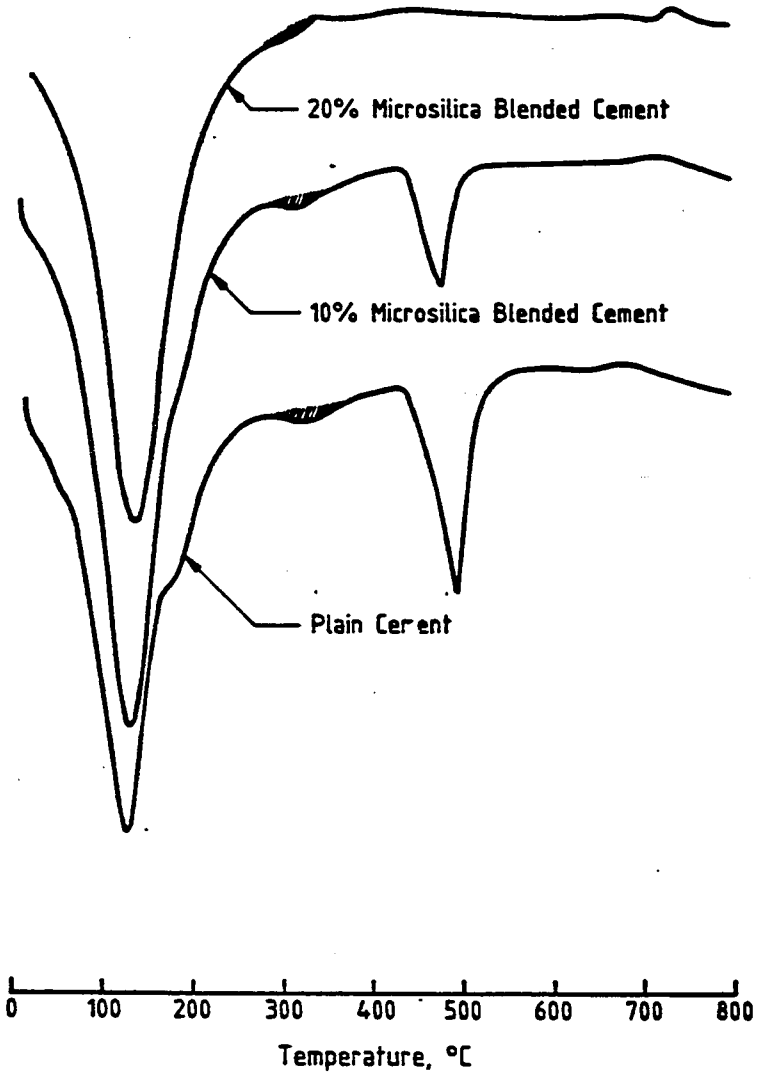

Fig. 4.2.2.3: DTA Curves For 1.2 Percent Chloride Bearing Plain & Microsilica Blended Cement Pastes

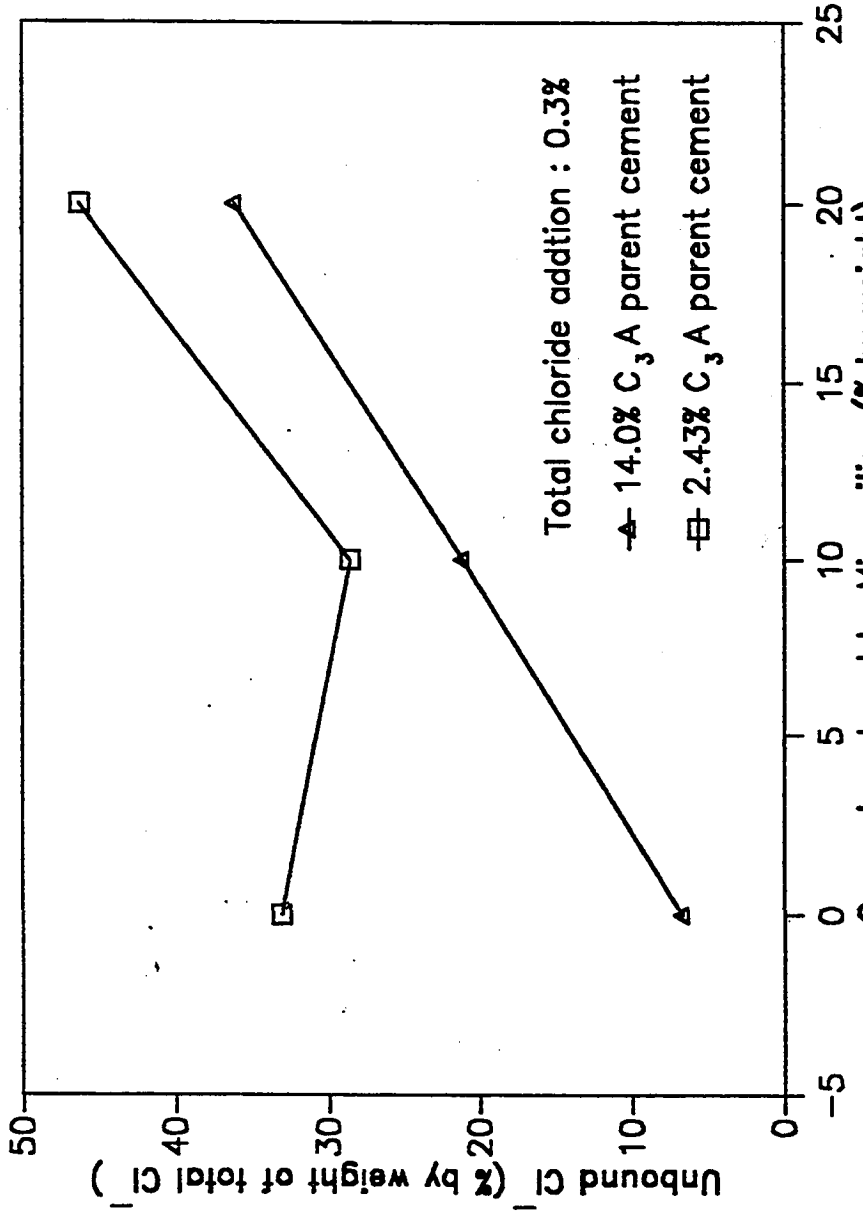

Fig. 4.2.2.4: Unbound Chlorides in Pore Solutions of Pore Solutions of Plain and Blended Cements Treated with 0.3% Chloride Level

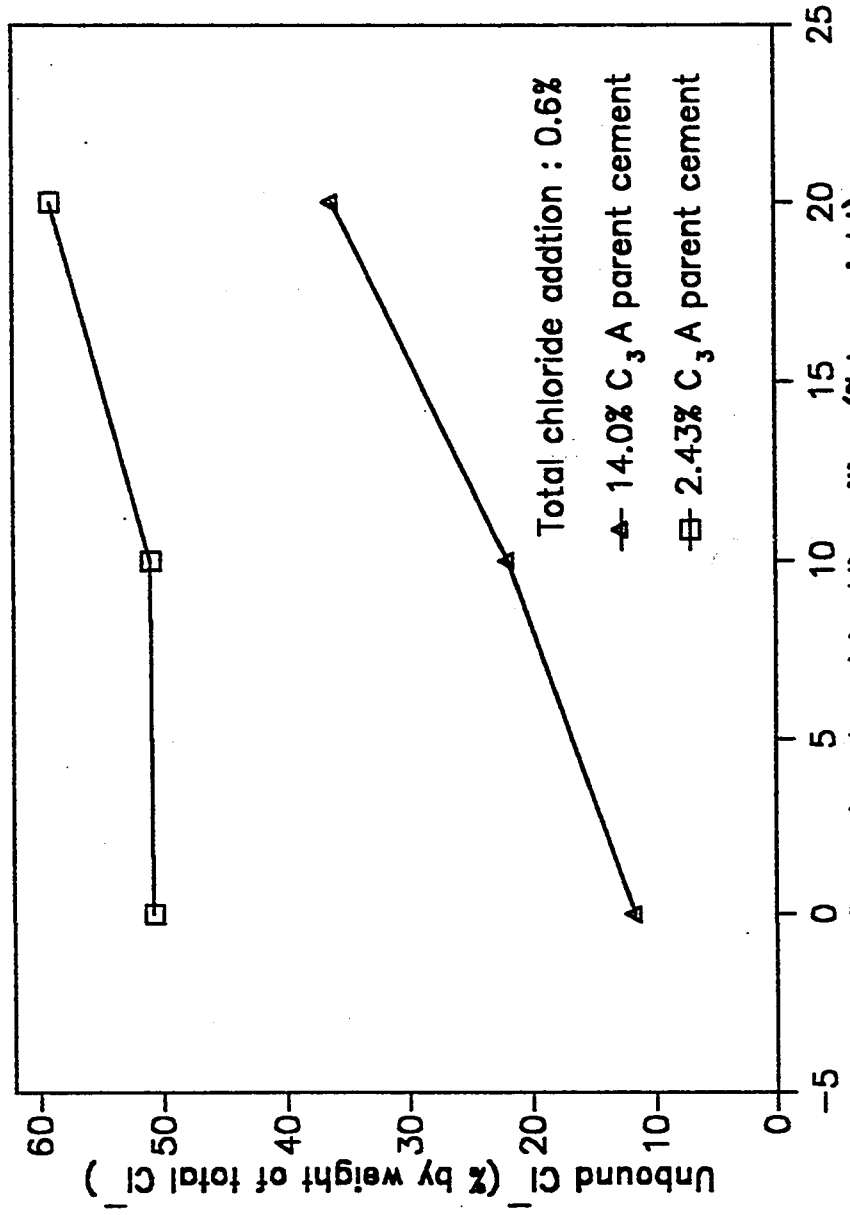

Fig. 4.2.2.5: Unbound Chlorides in Pore Solutions of Plain and Blended Cements Treated with 0.6% Chloride Level

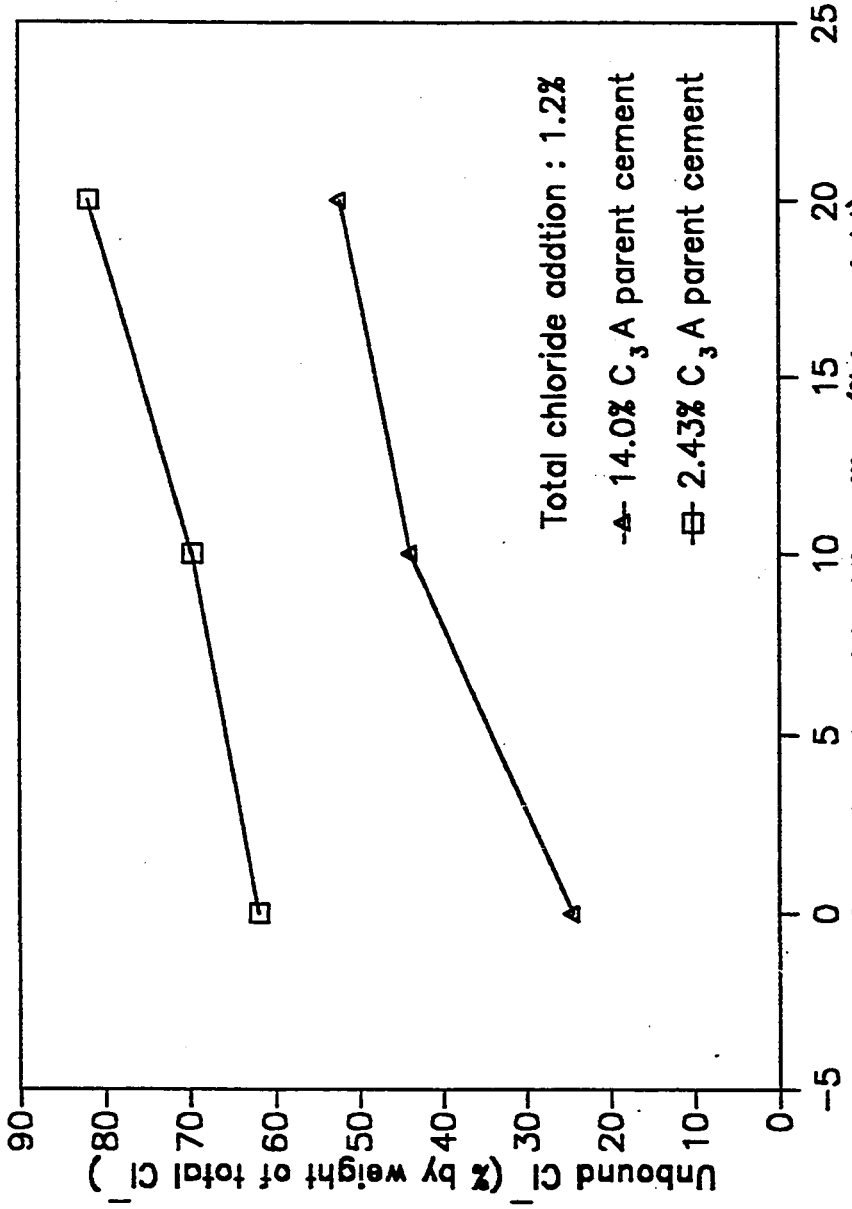

Fig. 4.2.2.6: Unbound Chlorides in Pore Solutions of Plain and Microsilica Blended Cements Treated with 1.2% Chloride Level

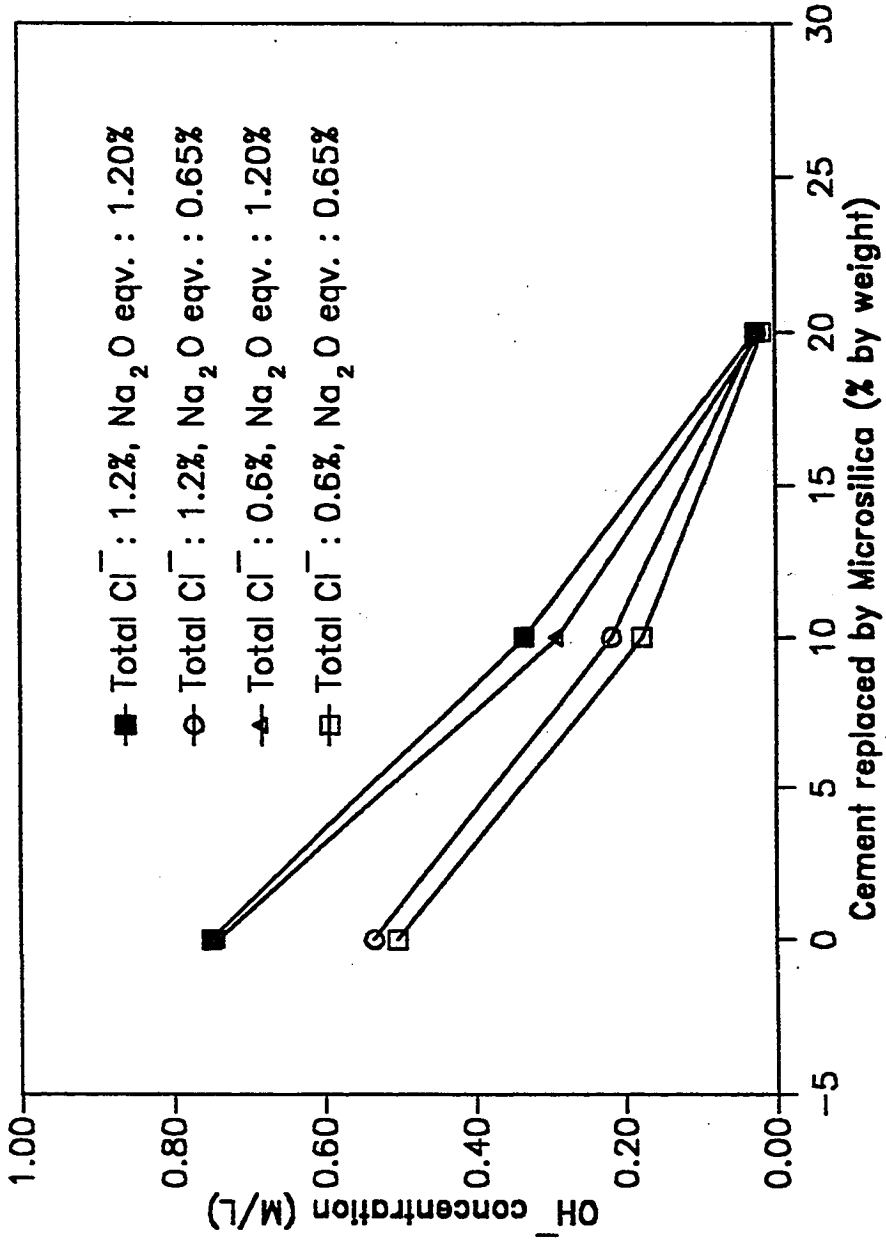

Fig. 4.2.2.7 Effect of Alkali content of Cement on OH^- Concentration in Pore Solution of Plain and Microsilica Blended Cements

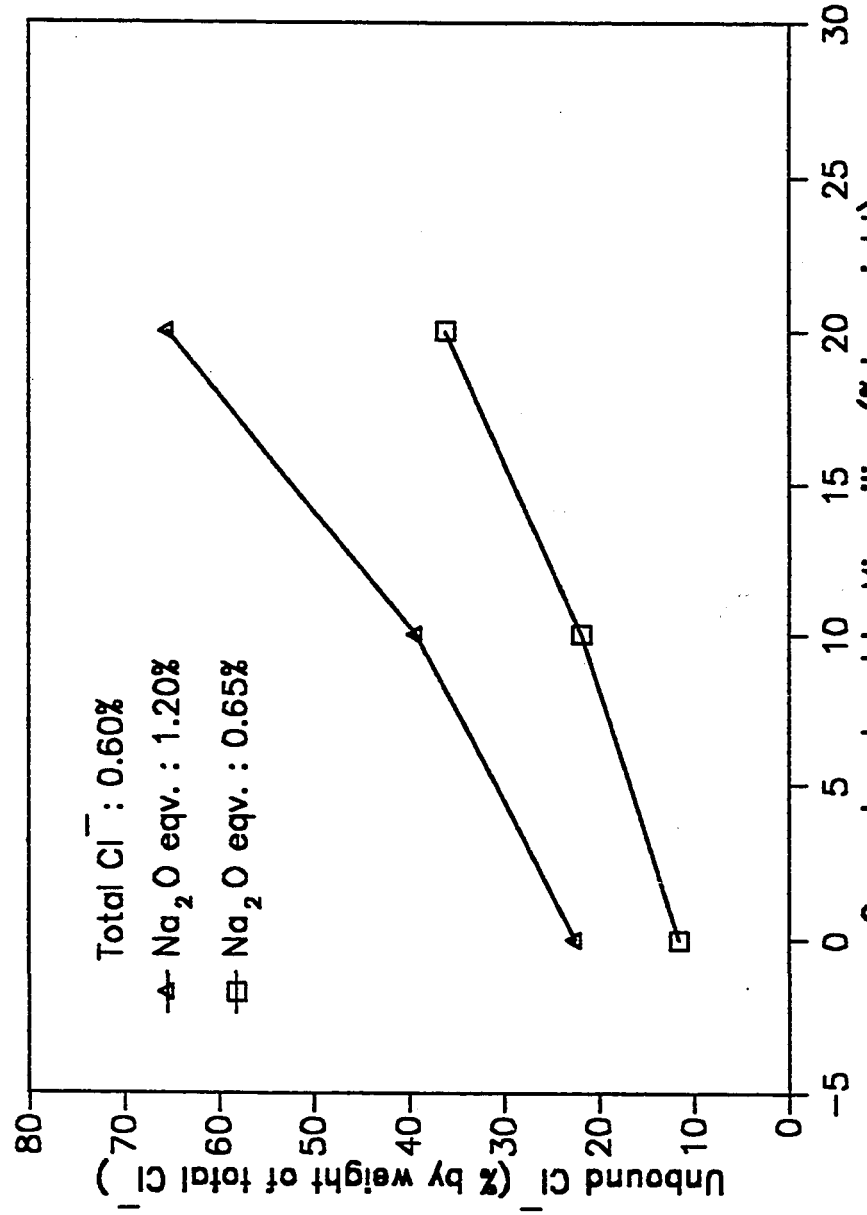

Fig. 4.2.2.8 Effect of Alkali content of Cement on Unbound Chlorides in Pore Solution of Plain and Blended Cements treated with 0.6% Chloride

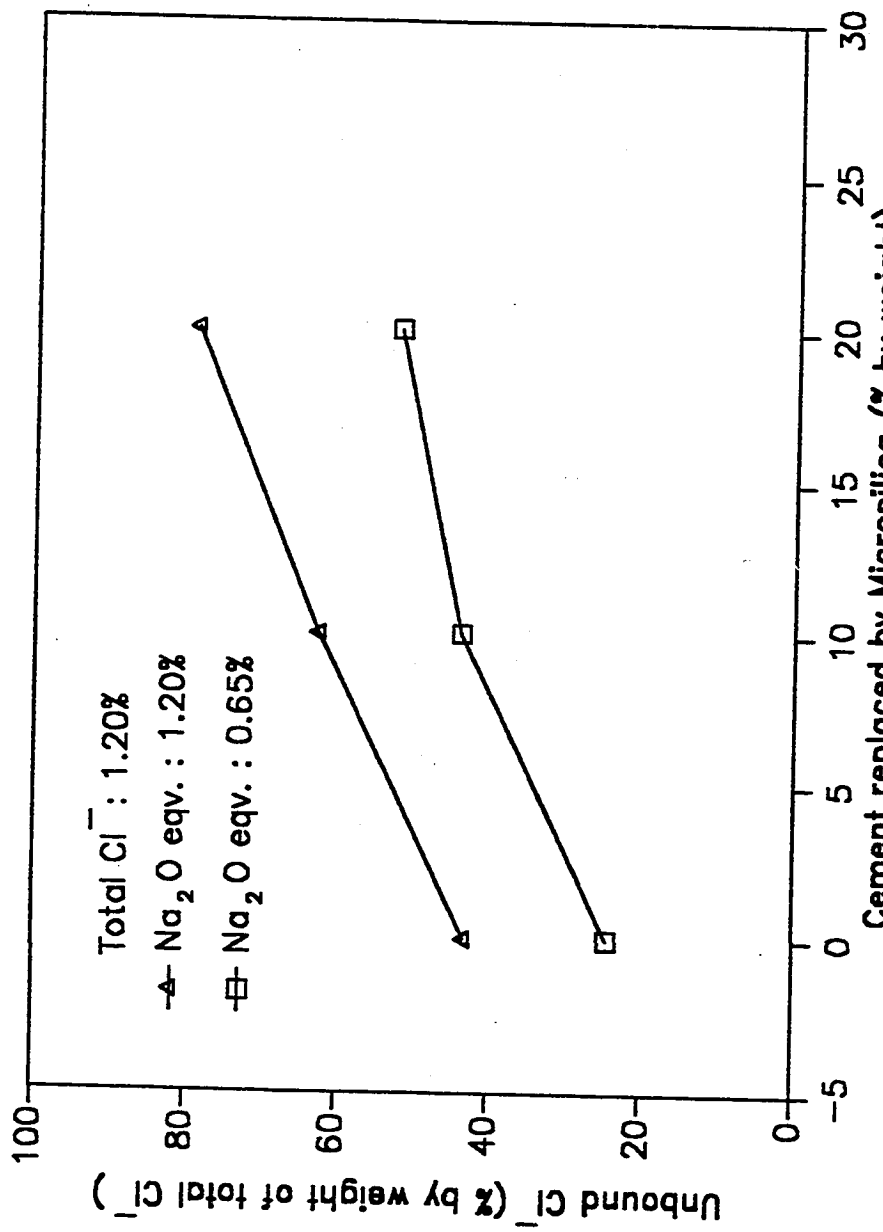

Fig. 4.2.2.9 Effect of Alkali content of Cement on Unbound Chlorides in Pore Solution of Plain and Blended Cements treated with 1.2% Chloride

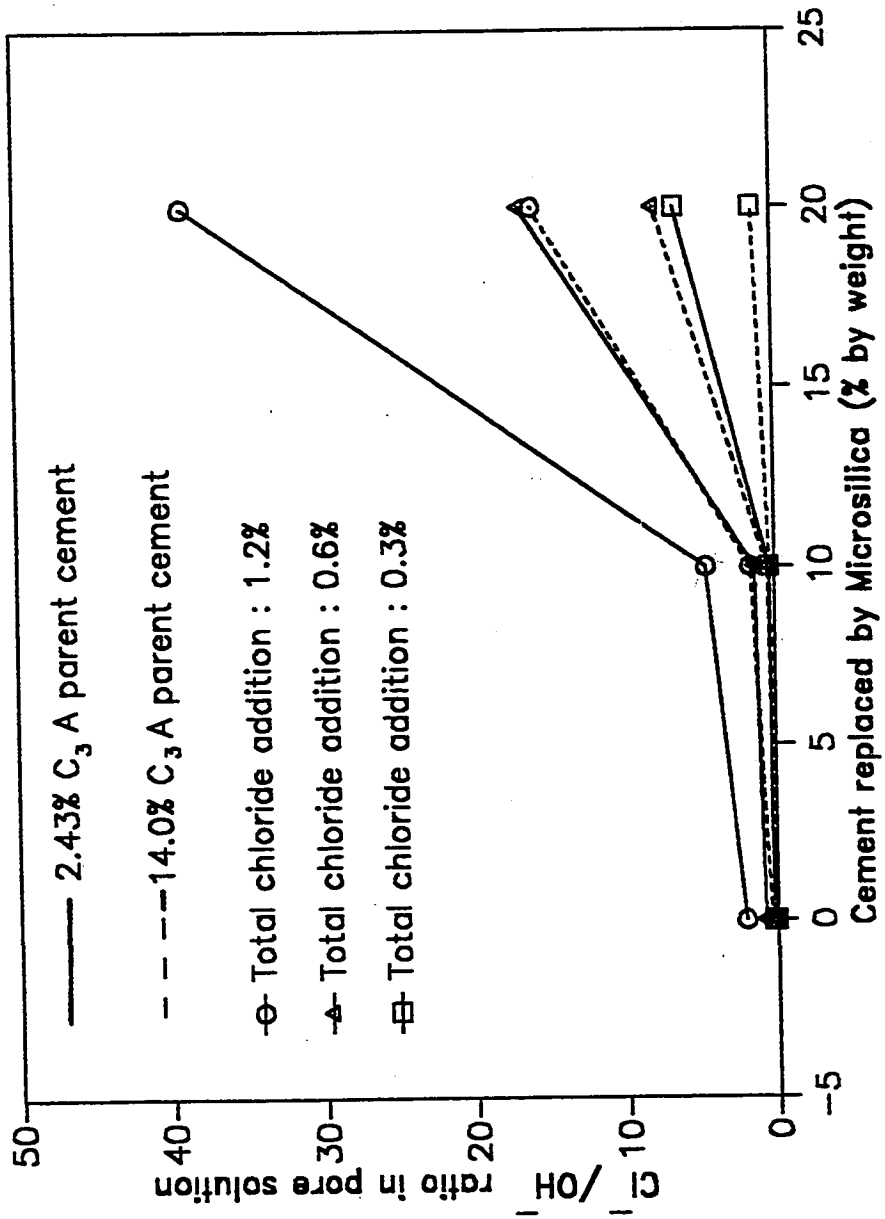

Fig. 4.2.2.10: Cl^-/OH^- Ratio in Pore Solutions of Plain and Microsilica Blended Cements Treated with Different Chloride Levels

sharp decline in the OH^- concentrations in the pore solutions.

The significantly lower chloride binding and the increased Cl^-/OH^- ratios in the pore solution of the microsilica blended cements compared to the plain cements indicate that there is an increased risk in the corrosion resistance characteristics of steel in the microsilica blended cement concrete. However, the corrosion behavior of steel does not depend only on the chemical environment of concrete but also depends greatly on its physical characteristics. Thus, it is the interactive effect of microsilica blending on the chemical environment and physical characteristics which control the corrosion performance of steel in microsilica blended cement concrete.

4.2.2.2 Blast Furnace Slag Cement

Two parent plain cements, cements 1 and 4, and one level of slag, 70% were used. The chloride additions used were 0.3, 0.6 and 1.2% by weight of cementitious material. OH^- and Cl^- concentrations, and hence Cl^-/OH^- ratio in the pore solution were measured after a curing period of 6 months.

(i) OH^- Concentration in Pore Solution

The effect of blast furnace slag blending with Type V (C_3A: 2.43%) and Type I (C_3A: 14%) cements on OH^- ion concentrations in the pore solution is shown in Table 4.2.2.3 (column 4) and Fig. 4.2.2.11. It is seen from these data that the OH^- concentration drops sharply as a result of 70% cement replacement by the slag for both types of cement. As an example, the OH^- concentration drops from an average value of 250 mM/L to 130 mM/L in the type V cement 1 and from 520 mM/L to 180

mM/L in the type I cement 4. It is also observed that for 70% replacement by slag (Na_2O: 0.46%) the drop in the OH^- concentration is significantly steeper for the Type I cement 4 compared to Type V cement 1; in the Type I (equivalent Na_2O:0.65 %) cement 4, the drop in the OH^- concentration is 2.9 times compared to 1.9 times for the Type V (equivalent to Na_2O: 0.58%) cement 1.

Fig 4.2.2.12 shows DTA patterns of plain and blast furnace slag cements treated with 1.2% chlorides. It can be observed that the calcium hydroxide peak formed at around 500° C is almost eliminated for the slag cement indicating that all the $Ca(OH)_2$ produced during cement hydration is consumed in the reaction with silica of the slag to form secondary C-S-H gel. This situation would significantly reduce the reserve alkalinity in the 70% slag cement which is otherwise present in portland cements due to the presence of crystalline $Ca(OH)_2$. Although the DTA results show no crystalline $Ca(OH)_2$ in hardened cement paste, the observed alkalinity of the pore solution is probably due to the dissolved $Ca(OH)_2$ and the alkali hydroxides present in the parent cement and the slag.

(ii) Cl^- Concentration in Pore Solution

Cl^- concentration in the pore solutions of the plain and the slag blended cements treated with 0.3, 0.6 and 1.2% chlorides are shown in Table 4.2.2.2 (column 4). The unbound chlorides remaining free in the pore solution are expressed as percentages of total chloride addition, and are shown in Table 4.2.2.2 (column 9) and in Fig. 4.2.2.13. It is observed from these data for both Type I cement 4 and Type V cement 1, blending with slag decreases the concentration of unbound chlorides of the pore solution, for

all three levels of chlorides. Pore solution studies carried out by Holden et al (26) and Arya et al (66) also show that slag blending decreases free chlorides in pore solution. Arya et al (66), used a 9.1% C_3A cement and 70% cement replacement by slag and observed 85% decrease in the unbound chlorides of the pore solution for a chloride level of 1%. However, Holden et al (26) using a parent cement with 14.1% C_3A content and a 65% cement replacement by slag observed a reduction of only 32% in the chloride ion concentration for a chloride level of 0.4%. In the present study, the reduction in chloride ion concentration of the 14% C_3A cement is 37% for the 0.3% chloride level, which is in good agreement with the results of Holden et al (26). However, the reductions in the unbound chlorides due to slag blending in both Type I and Type V cements 4 and 1 treated with 1.2% chlorides are observed to be 17% in the 2.43% C_3A cement and 21% in the 14% C_3A cement respectively. This is significantly less than the reduction observed by Arya et al (66).

The DTA pattern for slag cement blended with 14% C_3A parent cement and treated with 1.2% Cl^- does not show Friedel's salt peak, which appears around 300°C. However, an endothermic peak at around 360°C is observed which does not correspond to Friedel's salt. In the slag cement, the amount of C_3A is reduced to 4.2% due to the dilution effect of slag blending. It is therefore presumed that this reduced amount of C_3A would result in significantly reduced Friedel's salt formation and hence in reduced chloride binding. However, the pore solution data clearly show more chloride-binding in the slag cements compared to the plain cements. This indicates that in blast furnace slag cements the chloride-binding takes place by mechanisms other than the formation of Friedel's salt and the possibility that slag itself is capable of removing some of the chlorides from the pore solution can not be ruled out.

(iii) Cl^-/OH^- Ratio in Pore Solution

Cl^-/OH^- ratios in the pore solution of plain and slag cements treated with three levels of chlorides are shown in Fig 4.2.2.14. The reduction in the OH^- concentration outweighs the decrease in the free chlorides of the pore solution due to slag blending. The net effect, therefore, is an increase in the Cl^-/OH^- ratio of the pore solution in slag cements. In the 2.43% C_3A Type V cement 1, the Cl^-/OH^- ratio increases from 0.27 to 0.39 for 0.3% chloride treatment; from 0.79 to 0.94 for 0.6% chloride content; and from 2.09 to 2.84 for 1.2% chloride level. These values correspond to increases of 44, 20 and 36% for the 0.3, 0.6 and 1.2% chloride levels respectively. However, in the 14% C_3A Type I cement 4, the slag blending causes much bigger increases of 67, 80 and 105% increase in the Cl^-/OH^- ratios for 0.3, 0.6 and 1.2% chloride levels respectively. This significantly enhanced aggressivity for the pore solution of the 14% C_3A cement compared to the 2.43% C_3A cement is possibly attributable to a sharper drop in the OH^- concentration in former compared to the latter due to slag blending.

The increased Cl^-/OH^- ratios of the blast furnace slag cements are indicative of a higher level of aggressivity of the chemical environment of the slag cements in terms of reinforcement corrosion compared to plain portland cements.

Table 4.2.2.3 Pore Solution Composition of Plain and Blast Furnace Slag Blended Cement Treated with Different Levels of Chloride

C_3A Content of Cement	Cement Type	Total Cl^- Addition (% by weight of cementitious material)	Pore Solution Composition				Evaporabe Water (% by weight of cementitious material)	Unbound Cl^- (% by weight of Total Cl^-)
			Cl^- (mM/L)	OH^- (mM/L)	pH	Cl^-/OH^-		
	OPC*	0.3	69.7	258	13.41	0.2702	40.1	33.1
	BFSC**	0.3	50.5	130	13.11	0.3885	47.0	28.1
	OPC	0.6	209.9	265	13.42	0.7921	40.8	50.7
2.43	BFSC	0.6	121.8	130	13.11	0.9369	46.8	33.7
	OPC	1.2	529.9	254	13.40	2.0862	39.4	61.8
	BFSC	1.2	363.7	128	13.11	2.8414	47.7	51.3
	OPC	0.3	14.8	524	13.72	0.0282	38.4	6.7
	BFSC	0.3	9.3	172	13.24	0.0541	45.5	5.0
14.00	OPC	0.6	50.9	503	13.70	0.1014	38.4	11.6
	BFSC	0.6	33.0	187	13.27	0.1765	45.0	8.7
	OPC	1.2	216.0	534	13.73	0.4045	38.2	24.4
	BFSC	1.2	145.1	176	13.25	0.8244	45.0	19.3

* Plain Cement Concrete
** Blast Furnace Slag Blended Cement Concrete

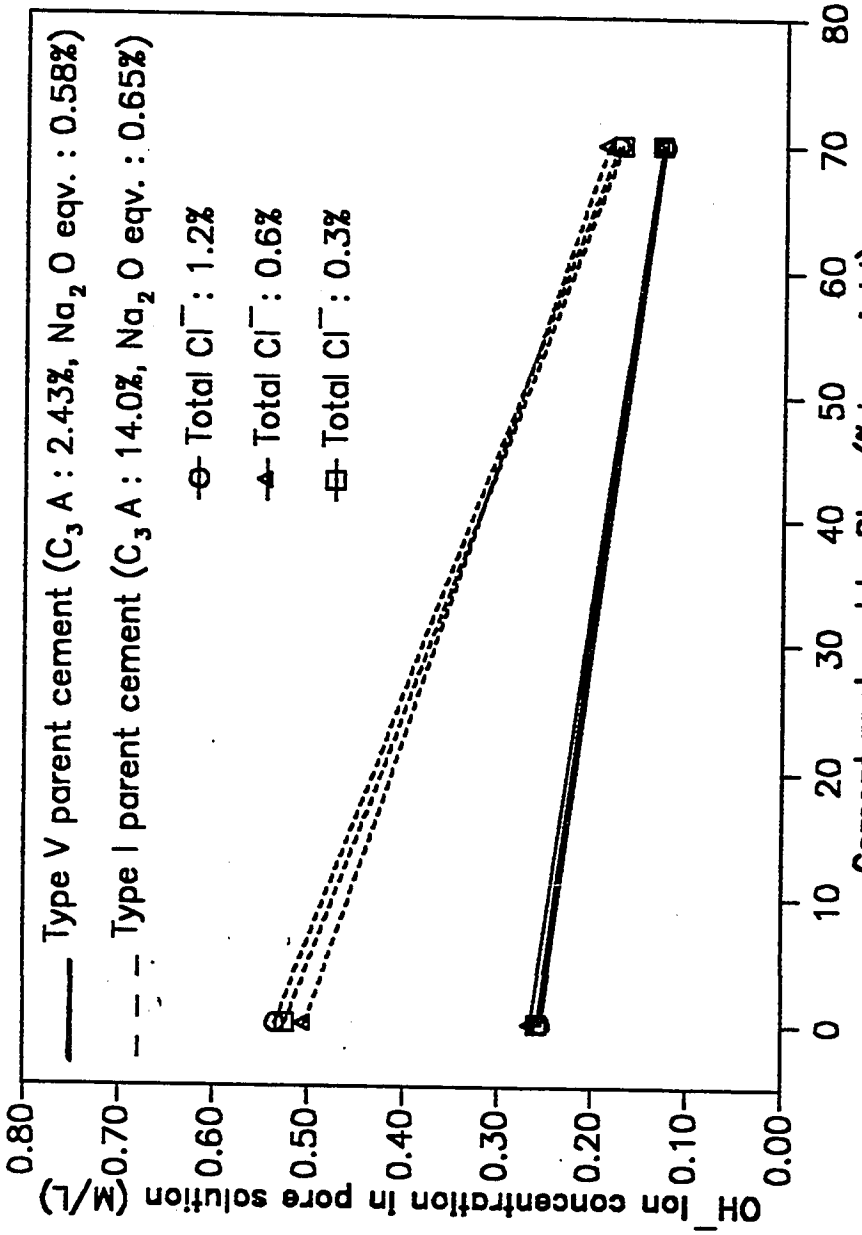

Fig. 4.2.2.11: OH^- Concentration in Pore Solutions of Plain and Blast Furnace Slag Cements Treated with Different Chloride Levels

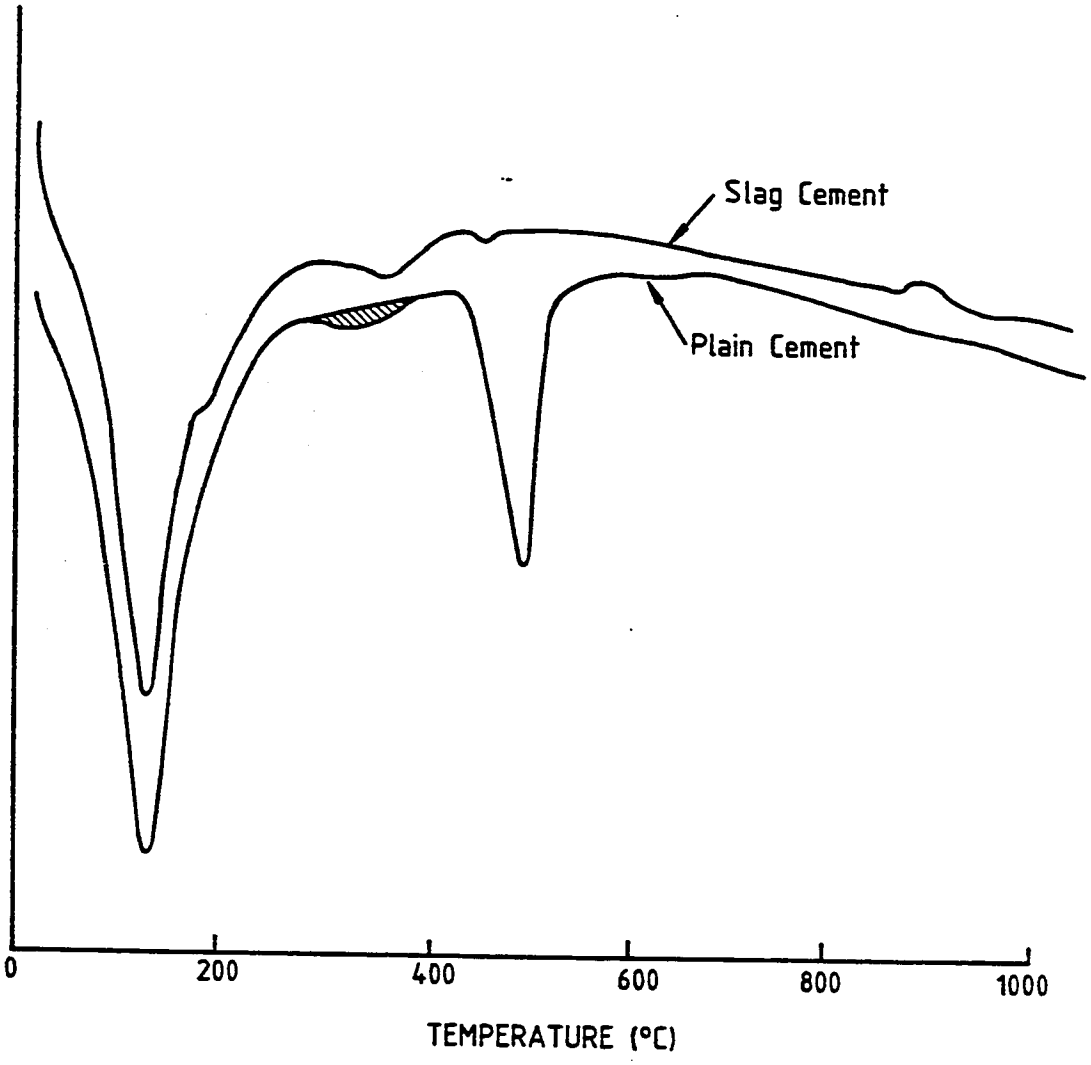

Fig. 4.2.2.12: DTA Curves of hydrated Plain and Slag Cement treated with 1.2% Cl^-

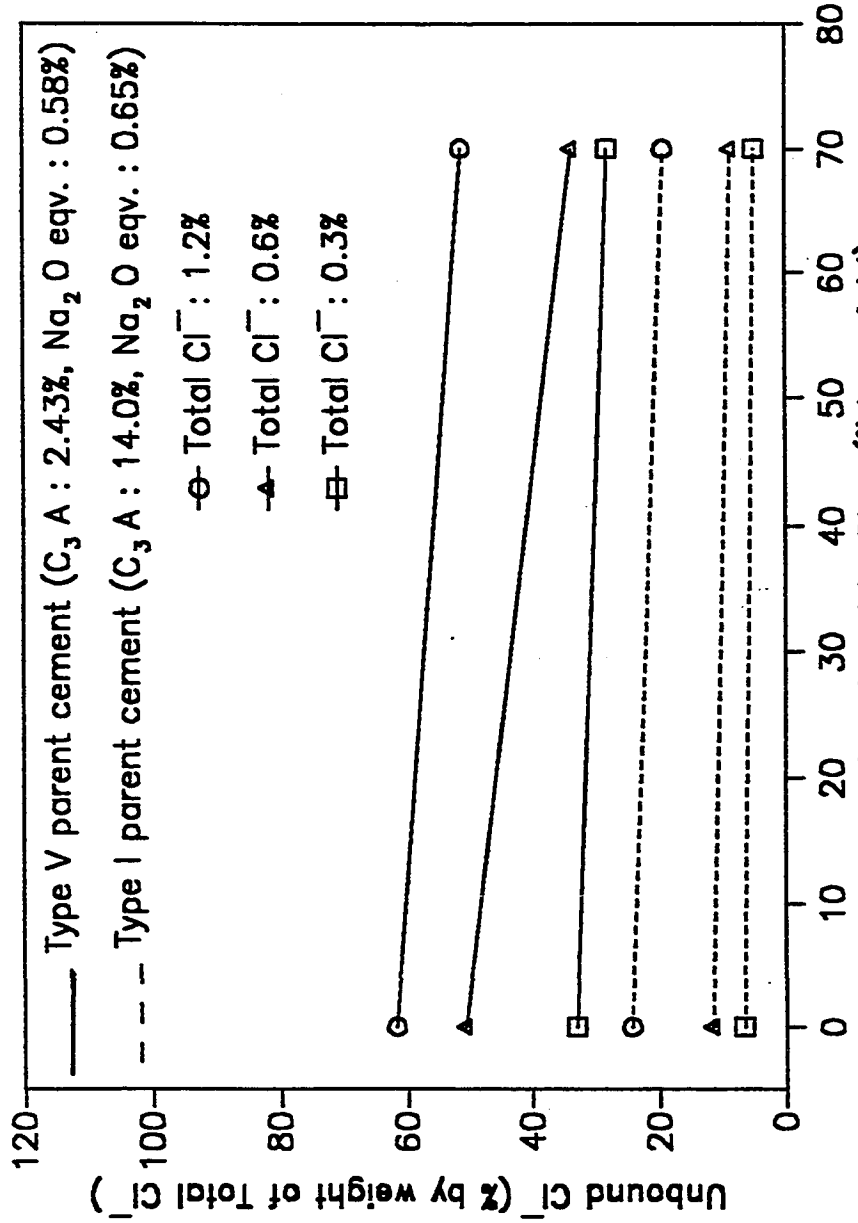

Fig. 4.2.2.13:Unbound Chlorides in Pore Solutions of Plain and Blast Furnace Slag Cements Treated with Different Chloride Levels

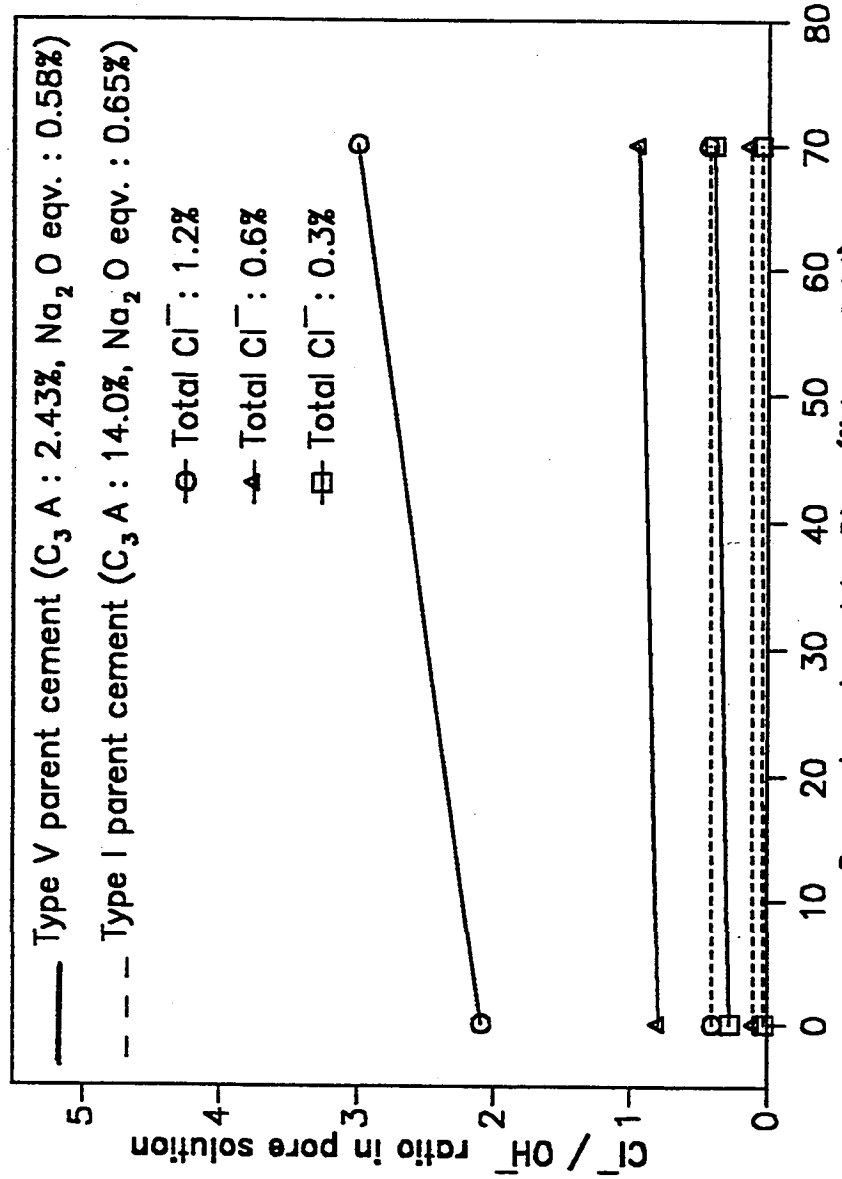

Fig. 4.2.2.14: Cl^-/OH^- Ratio in Pore Solutions of Plain and Blast Furnace Slag Cements Treated with Different Chloride Levels

4.2.2.3 Fly Ash Blended Cement

Two parent plain cements, cements 1 and 4, and one level of fly ash, 30%, were used. The chloride additions used were 0.3, 0.6 and 1.2% by weight of cementitious material. OH^- and Cl^- concentrations, and hence Cl^-/OH^- ratio in the pore solution were measured after a curing period of 6 months.

(i) OH^- Concentration in Pore Solution

Pore solution composition of hydrated cement pastes made with the plain and the fly ash blended cements, using 2.43% C_3A and 14% C_3A parent cements, are shown in Table 4.2.2.4. OH^- concentrations in the pore solutions for these cements are shown in Fig. 4.2.2.15, for chloride additions of 0.3%, 0.6% and 1.2%. It is seen that the cement replacement by 30% fly ash lowers the OH^- concentration of the pore solution, in both Type V and Type I cements 1 and 4, for all the three chloride levels. In the 2.43% C_3A cement 1, with alkali content of 0.58%, cement replacement by fly ash decreases the OH^- concentration from an average value of 260 mM/L(pH = 13.41) to an average value of 205 mM/L (pH = 13.31), for all three chloride levels. This corresponds to a drop of about 21%. However, in the 14% C_3A cement 4, with alkali content of 0.65%, the reduction in OH^- concentration is sharper, from an average value of 520 mM/L (pH: 13.72) to an average value of 315 mM/L (pH: 13.50), corresponding to a drop of about 40%.

Results of DTA test conducted on the 1.2% chloride-bearing plain and the fly ash

blended cement pastes, made with cement 4 (C_3A: 14%) is shown in Fig. 4.2.2.16. Calcium hydroxide ($Ca(OH)_2$) peaks can be noticed around 500° C. Calcium hydroxide contents in the hydrated cements were calculated from the TGA tests. Fly ash blending with 14% C_3A cement reduces the calcium hydroxide content from 30.6% to 13.1% by weight of cement. This corresponds to a reduction of about 55%. The alkalinity is reduced from an average value of 13.41 pH to an average value of 13.31 pH for the 2.43% C_3A cement 1 and from 13.72 pH to 123.50 pH for the 14% C_3A cement 4 due to fly ash blending.

(ii) Cl^- Concentration in Pore Solution

The data of Table 4.2.2.4 (column 5) show that the fly ash blending reduces the free chloride ion concentration of the pore solution in both the parent cements and for the three chloride levels inducted in the cement pastes. The amount of chlorides remaining unbound in pore solution, expressed as percentages of the total chloride added, are given in column 7 of Table 4.2.2.5. These values have been calculated based on evaporable water content of the samples, after making adjustment for the non-evaporable chemically bound water. The unbound chlorides for plain and fly ash blended cements for chloride levels of 0.3%, 0.6% and 1.2% are shown in Fig. 4.2.2.17. It can be seen that the unbound chlorides in the pore solution decrease with the fly ash blending in cements made with both Type V and Type I parent cements. The reduction in unbound chlorides, except for one case, varies from 21% to 35% with an average value of about 30%. It can also be seen that the unbound chlorides in the fly ash blended cement made with the 2.43% C_3A cement 1 are manifold more than those in the fly ash blended cement made with the 14% C_3A cement 4. DTA curves of the cements

(Fig. 4.2.2.16) show the formation of Friedel's salt in the plain as well as the fly ash blended cements with well defined peaks at around 300° C. However, the peaks are somewhat shallower for the fly ash blended cement compared to the plain cements, which may be attributable to a reduction in the C_3A due to the dilution effect as a result of fly ash blending. Hence, a reduced amount of Friedel's salt is detected in the fly ash blended cements as compared to the plain cement. The observation from the pore solution data that the unbound chlorides in the pore solutions of the fly ash blended cement are significantly less than in the pore solutions of plain cements indicates that fly ash itself may be effective in binding some of the chlorides.

(iii) Cl^-/OH^- Ratio in Pore Solution

The partial replacement of cement by the fly ash causes a decrease in OH^- concentration as well as Cl^- concentration in the pore solutions of both the cements. The Cl^-/OH^- ratio in the pore solution of the plain and the fly ash blended cement is shown plotted in Fig. 4.2.2.18. For the 2.43% C_3A Type V cement 1, the Cl^-/OH^- ratios of the fly ash blended cements are less than those of the plain cement. However, for the 14% C_3A Type I parent cement 4, the Cl^-/OH^- ratios in the pore solution of the fly ash blended cement are more than those for the plain cements; however, for the 0.3% and 0.6% chloride-bearing pastes the increase is only marginal. In fact the effect of the fly ash blending on Cl^-/OH^- ratio is relatively small compared to the other mineral admixtures such as microsilica. For example when microsilica blending is used only a 10% replacement increases the Cl^-/OH^- ratio from 0.10 to 0.52 for 0.6% chloride level. In the case of fly ash blending the maximum increase is about 41% in Type I 14% C_3A cement 4 and the maximum reduction is 32% in the 2.43% C_3A cement 1.

Kawamura et al (43), using a parent cement containing of 3.74% C_3A and 0.38% alkalies and 30% replacement by fly ash, have reported an increase in the Cl^-/OH^- ratio from about 1.3 to about 1.9 for a chloride addition of 1% as NaCl. Holden et al (26) have also reported an increase in the Cl^-/OH^- ratio. They used a 14.3% C_3A cement with 30% replacement by fly ash. In the present study for all chloride levels, the decrease in the Cl^- concentration in the pore solution of the 2.43% C_3A cement is observed to be more than the corresponding decrease in the OH^- concentration due to fly ash blending. The net result, is therefore, a decrease in the Cl^-/OH^- ratio. However, in the 14% C_3A cement 4, the fly ash blending increases Cl^-/OH^- ratio for all the three chloride levels, which is in agreement with the findings of the other investigators (26,43). If a threshold Cl^-/OH^- ratio of 0.6 is assumed for depassivation of steel reinforcement in concrete, as suggested by Hausmann (11), it is seen that the Cl^-/OH^- of the fly ash blended cements made with the 14% C_3A parent cement fall below the critical value, even for the 1.2% chloride addition.

Table 4.2.2.4 Pore Solution Composition of Plain and Fly Ash Blended Cement Treated with Different Levels of Chloride

C_3A Content of Cement	Cement Type	Total Cl^- Addition (% by weight of cementitious material)	Pore Solution Composition			
			Cl^- (mM/L)	OH^- (mM/L)	pH	Cl^-/OH^-
	OPC*	0.3	69.7	258	13.41	0.2702
	FAC**	0.3	38.9	212	13.33	0.1835
	OPC	0.6	209.9	265	13.42	0.7921
2.43	FAC	0.6	124.5	205	13.31	0.6073
	OPC	1.2	529.9	254	13.40	2.0862
	FAC	1.2	362.8	200	13.30	1.8140
	OPC	0.3	14.8	524	13.72	0.0282
	FAC	0.3	9.7	315	13.50	0.0308
14.00	OPC	0.6	50.9	503	13.70	0.1014
	FAC	0.6	33.1	300	13.48	0.1103
	OPC	1.2	216.0	534	13.73	0.4045
	FAC	1.2	188.5	330	13.52	0.5712

* Plain Cement
** 30% Fly Ash Blended Cement

Table 4.2.2.5 Unbound Chlorides in Pore Solution of Plain and Fly Ash Blended Cement Treated with Different Levels of Chloride

C_3A Content of Cement	Cement Type	Total Cl^- Addition (% by weight of cementitious material)	Cl^- Concentration in Pore Solution (% of Cl^- Concentration in Mix Water)	Evaporable Water (% by weight of cementitious mater-	Unbound Cl (% by weight of Total Cl^-)
2.43	OPC*	0.3	49.4	40.1	33.1
	FAC**	0.3	27.6	46.8	21.5
	OPC	0.6	74.4	40.8	50.7
	FAC	0.6	44.1	46.0	33.9
	OPC	1.2	94.1	39.4	61.8
	FAC	1.2	64.4	45.9	49.3
14.00	OPC	0.3	10.5	38.4	6.7
	FAC	0.3	6.8	42.00	4.8
	OPC	0.6	18.1	38.4	11.6
	FAC	0.6	11.7	42.6	8.3
	OPC	1.2	38.4	38.2	24.4
	FAC	1.2	33.5	41.3	23.0

* Plain Cement

** 30% Fly Ash Blended Cement

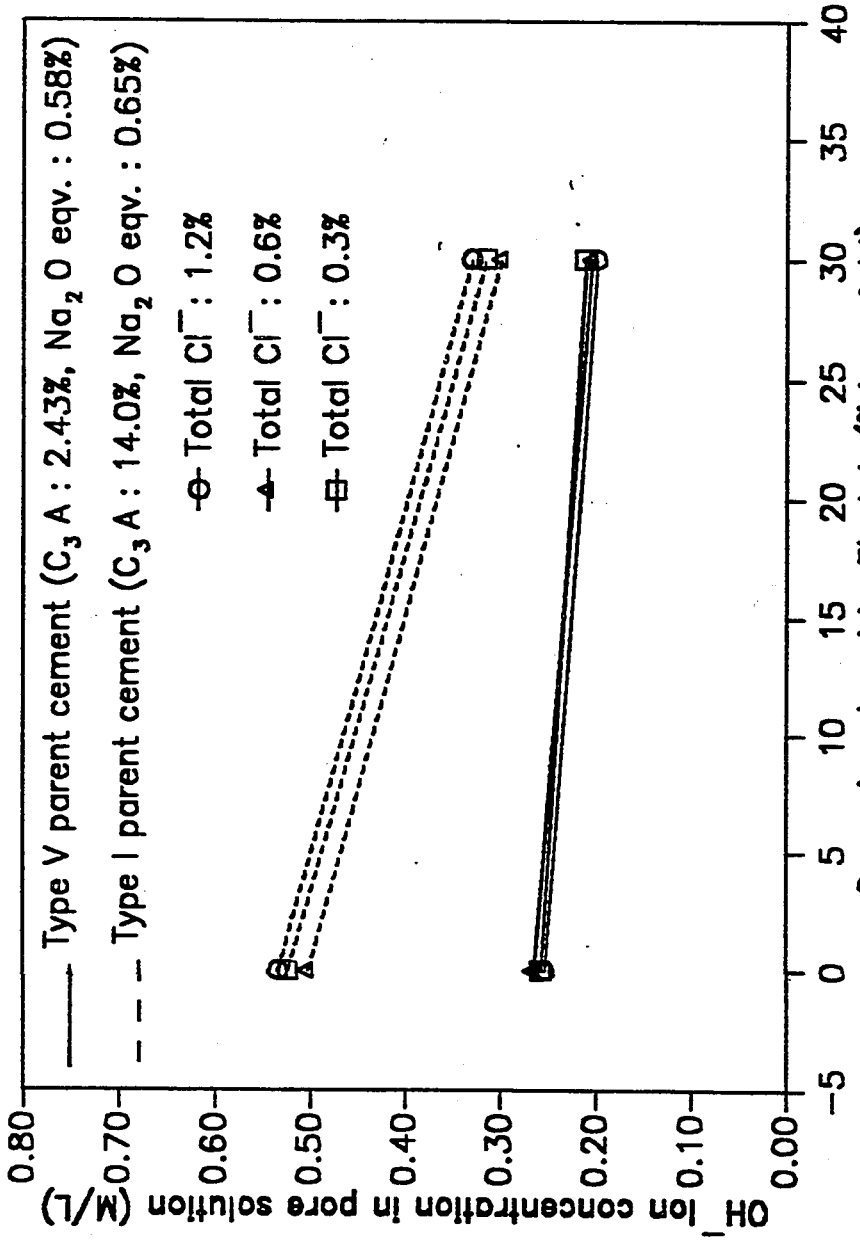

Fig. 4.2.2.15: OH^- Concentration in Pore Solutions of Plain and Fly Ash Blended Cements Treated with Different Chloride Levels

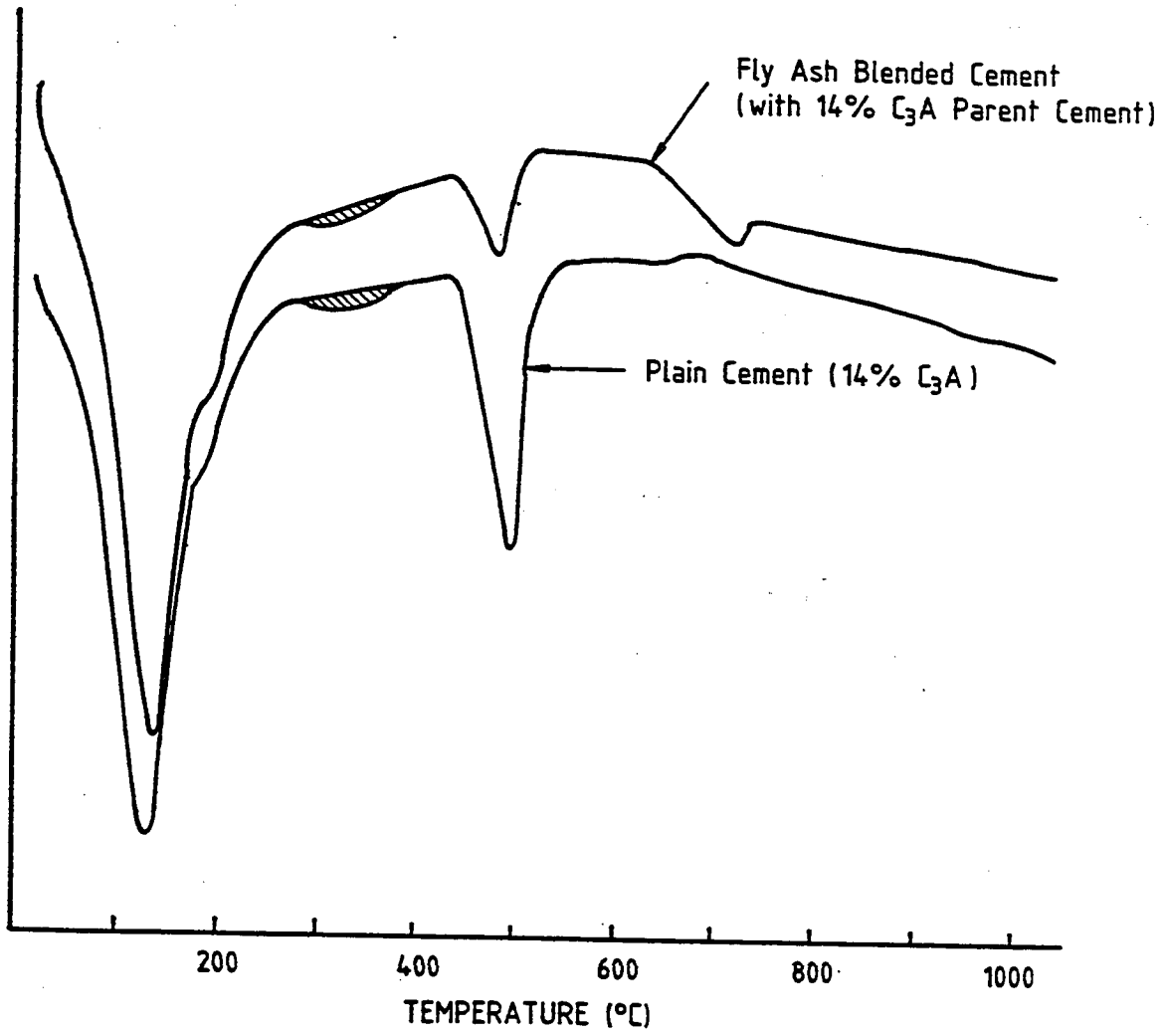

Fig. 4.2.2.16: DTA Curves of plain and fly ash Blended Cement with 14% C_3A Parent Cement (1.2% Cl^- Addition)

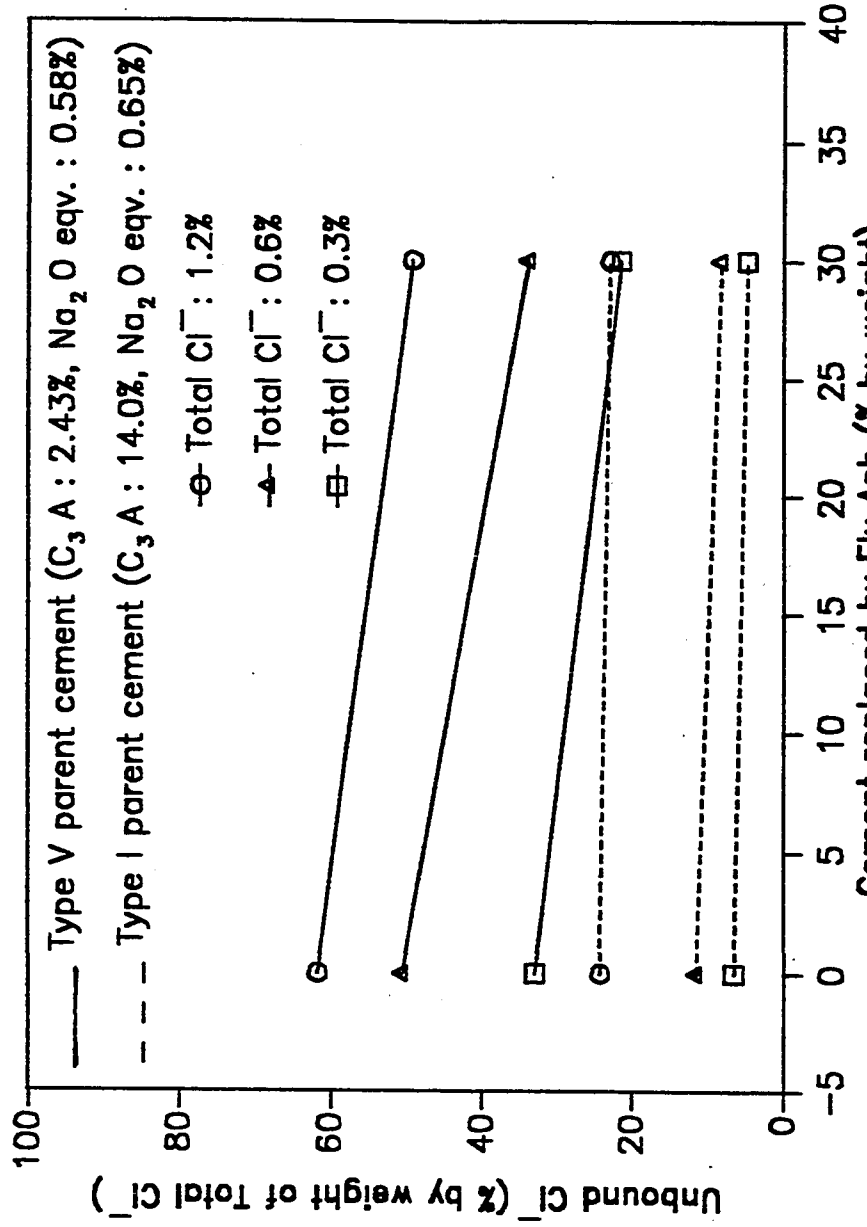

Fig. 4.2.2.17:Unbound Chlorides in Pore Solutions of Plain and Fly Ash Blended Cements Treated with Different Chloride Levels

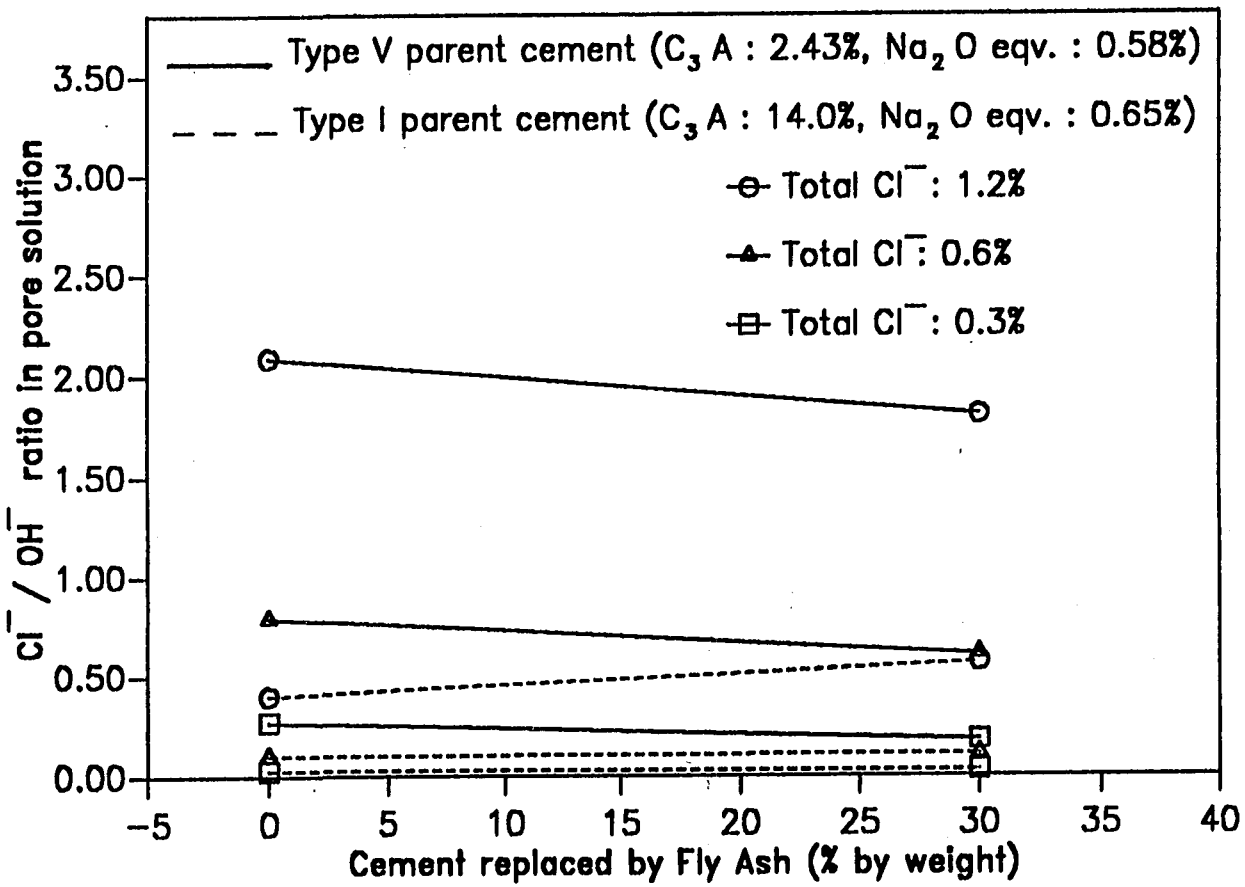

Fig. 4.2.2.18: Cl^-/OH^- Ratio in Pore Solutions of Plain and Fly Ash Blended Cements Treated with Different Chloride Levels

4.2.3 INFLUENCE OF MICROSILICA, BLAST FURNACE SLAG AND FLY ASH ON ALKALINE ENVIRONMENT OF HARDENED CEMENTS

The influence of microsilica, blast furnace slag and fly ash blending on pore solution alkalinity and calcium hydroxide contents which indicate reserve alkalinity, of hydrated cement pastes of the 14% C_3A plain (equivalent Na_2O: 0.65%) and the blended cements made with the same 14% C_3A cement are measured by DTA and TGA. The DTA and TGA patterns for the hydrated cement pastes of the plain and the blended cements are shown in Figs. 4.2.3.1 through 4.2.3.7. An endothermic peak of calcium hydroxide occurs at around 500° C. At this temperature the endothermic reaction involved is the dehydration of calcium hydroxide to form calcium oxide loosing one water molecule. The weight loss due to the dehydration of calcium hydroxide is recorded by the TGA curve, from which calcium hydroxide content is calculated. From the TGA curve total water content of the hydrated cement samples, which is the sum of evaporable and non-evaporable water, is also calculated from the loss in weight of the sample when heated to 1050° C. Knowing the total water content, ignited weight of the hydrated cement samples are calculated. The values of calcium hydroxide contents given in Table 4.3.2.1 are expressed as percentage of ignited weight of cement.

The effect of different cement replacement levels by microsilica, ranging from 5 to 25%, on the OH^- concentration in the pore solution are shown in Fig. 4.2.3.8. It is seen from these data that the OH^- concentration in the pore solution decreases significantly with increasing replacement levels of microsilica. The OH^- concentration in the pore solution decreases by 1.1, 1.8, 2.4, 5.0 and 25 times by 5, 10, 15, 20 and 25%

microsilica blending. Microsilica contains about 95% highly reactive silica glass. The reduction in the OH^- concentration with increasing microsilica blending is attributable to the combination of hydroxyl ions with silica present in microsilica. The calcium hydroxide contents of the plain and microsilica blended cements are shown in Fig. 4.2.3.9. It is seen from Fig. 4.2.3.9 that the calcium hydroxide content in cement drops steeply with increasing microsilica blending. For microsilica blending beyond 20% the calcium hydroxide content in the microsilica blended cement samples is completely absent. For 5 and 10% microsilica blending, the calcium hydroxide contents are reduced in the microsilica blended cements by 1.15 and 1.6 times compared to plain cement. The reduction in the calcium hydroxide content is attributable to the combination of silica with calcium hydroxide to form secondary C-S-H gel. The effect of partial cement replacement by blast furnace slag and fly ash on OH^- concentration in the pore solution and calcium hydroxide content of the hydrated cement are shown in Figs. 4.2.3.10 and 4.2.3.11. It is seen from these data that 60 and 70% cement replacement by blast furnace slag causes a decrease in the OH^- concentration in the pore solution by 1.4 and 1.9 times as compared to the plain cement. The calcium hydroxide content drops from 30.6 to 4.4% for 70% cement replacement by slag. 30% cement replacement by fly ash reduces the OH^- concentration and calcium hydroxide content of the plain cement by 1.4 and 2.4 times respectively. The reduction in the OH^- concentration and calcium hydroxide content due to slag and fly ash blending is attributable to the consumption of calcium hydroxide by slag and fly ash in pozzolanic reaction to form secondary C-S-H gel.

Although calcium hydroxide is not fully consumed by 30% cement replacement by fly ash and 70% cement replacement by slag, the pore solution pH drops significantly. This is attributable to the reaction of slag and fly ash with the alkali hydroxides present

Table 4.2.3.1: Pore Solution Alkalinity and Calcium Hydroxide Content in Hydrated Plain and Blended Cement Pastes

Cement Type	OH^- Concentration in Pore Solution (mM/L)	Pore Solution pH	$Ca(OH)_2$ Content (% by weight of cement)
OPC*	328	13.52	30.6
MS5*	306	13.49	26.6
MS10*	182	13.26	19.2
MS15*	135	13.13	-
MS20*	66	12.82	0.0
MS25*	13	12.11	0.0
BFS60*	240	13.38	-
BFS70*	170	13.23	4.4
FA*	234	13.27	12.6

*OPC : Plain Cement (C_3A:14%)
*MS5 : 5% Microsilica Blended Cement
*MS10 : 10% Microsilica Blended Cement
*MS15 : 15% Microsilica Blended Cement
*MS20 : 20% Microsilica Blended Cement
*MS25 : 25% Microsilica Blended Cement
*BFS60: 60% Blast Furnace Slag Blended Cement
*BFS70: 70% Blast Furnace Slag Blended Cement
*FA : 30% Fly Ash Blended Cement

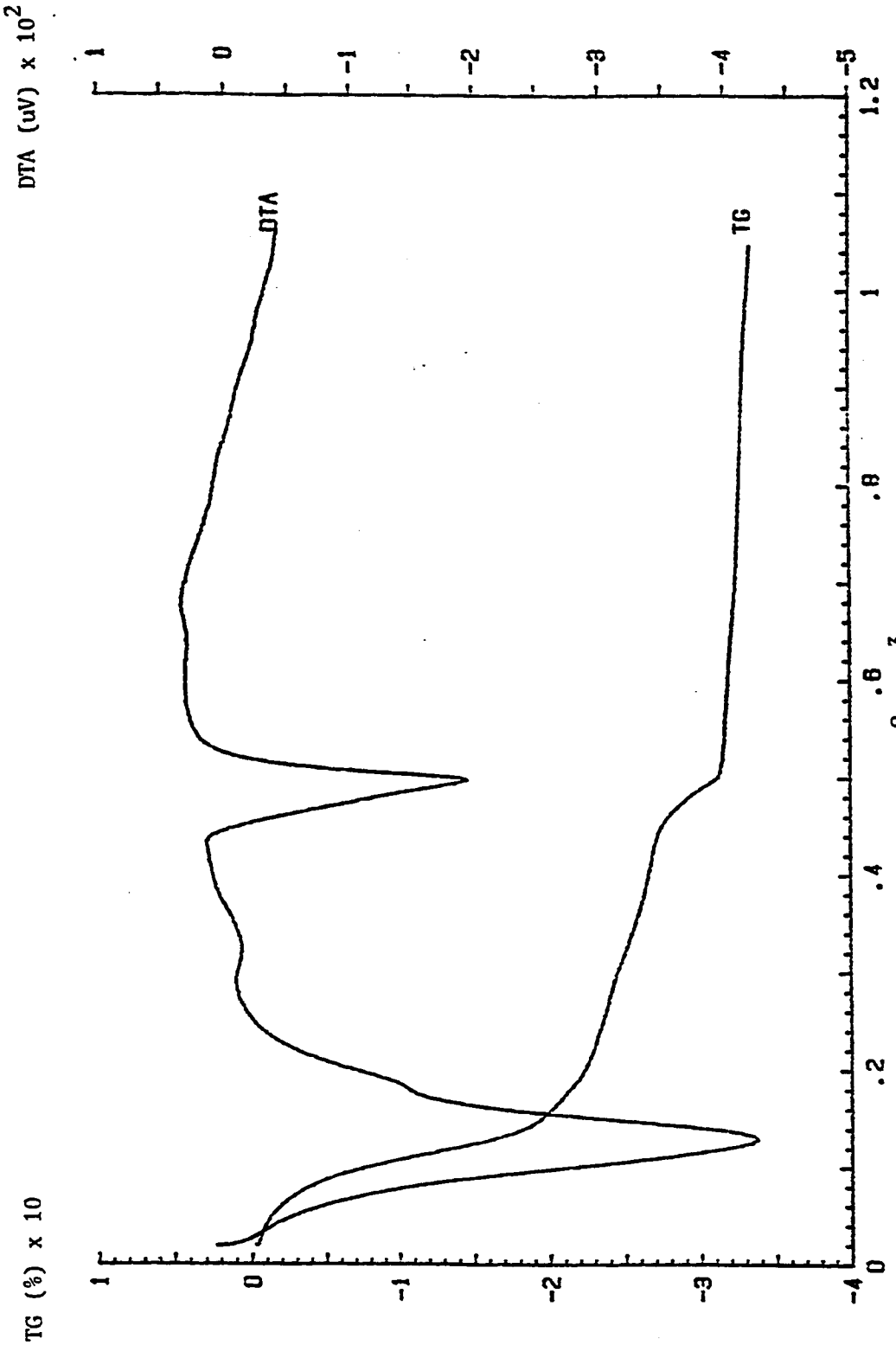

Fig. 4.2.3.1: DTA and TGA Curves for Hydrated Plain Cement Paste

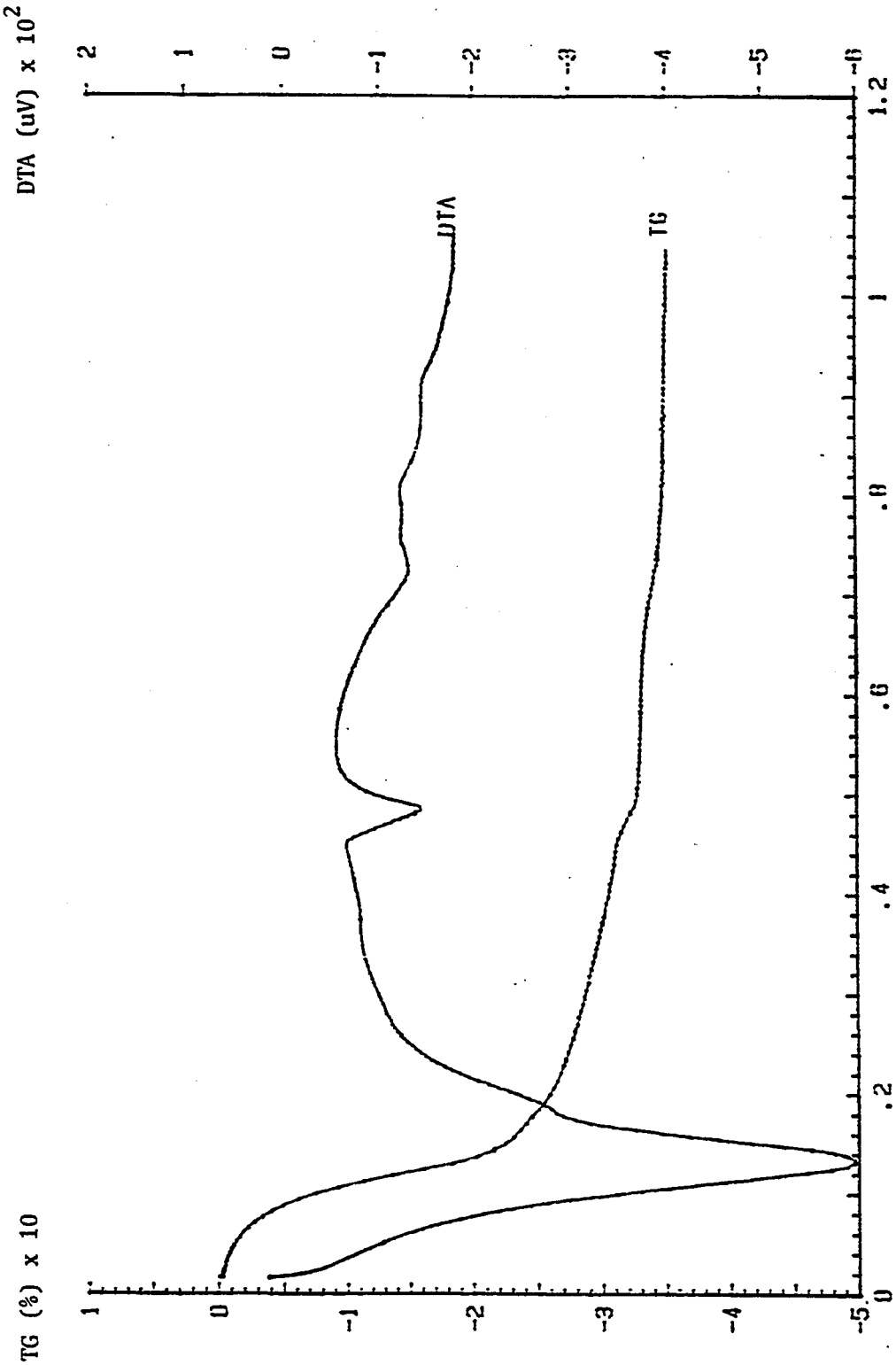

Fig. 4.2.3.2: DTA and TGA Curves for Hydrated Paste of 30% Fly Ash Blended Cement

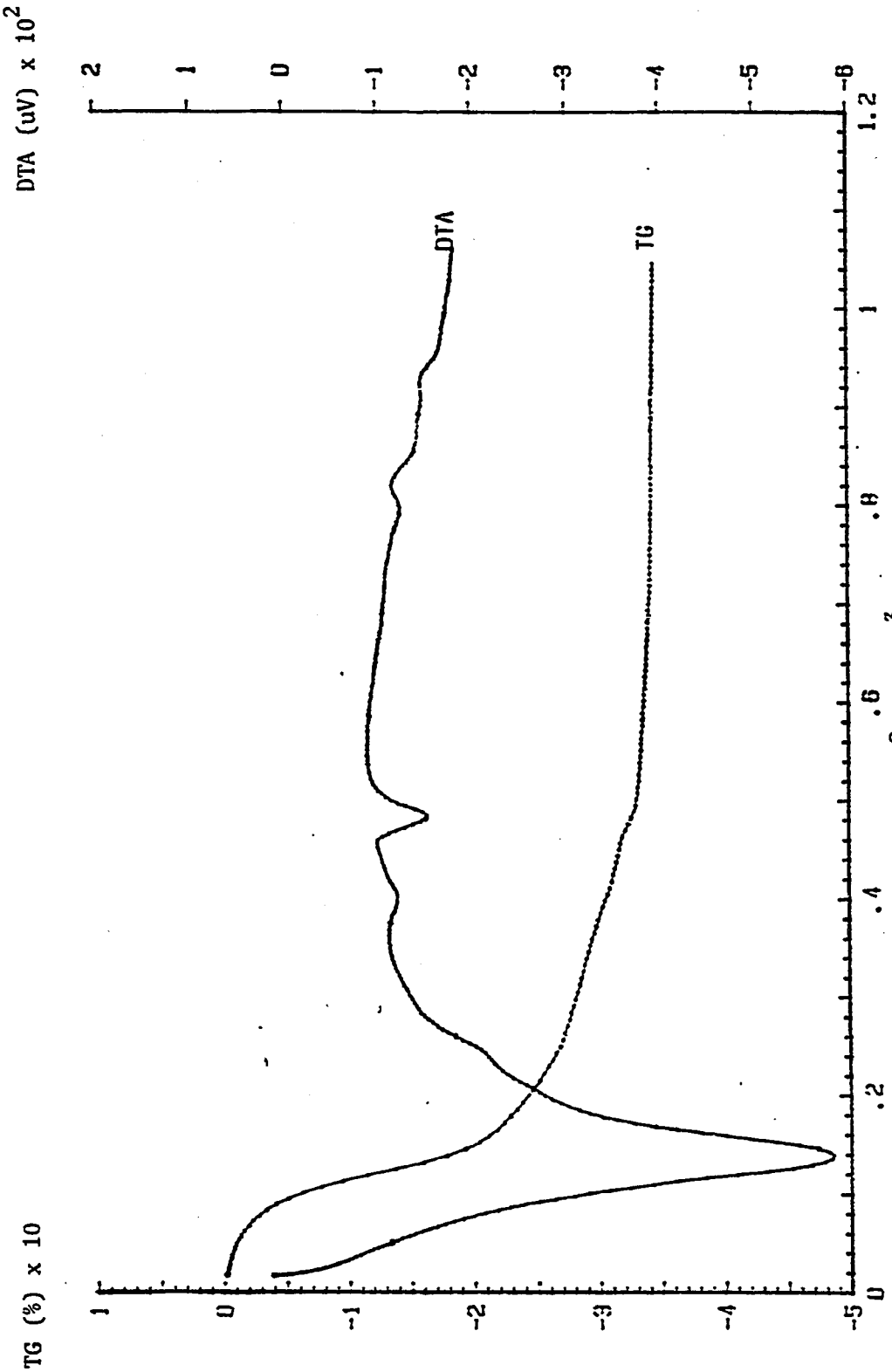

Fig. 4.2.3.3: DTA and TGA Curves for Hydrated Paste of 70% Blast Furnace Slag Blended Cement

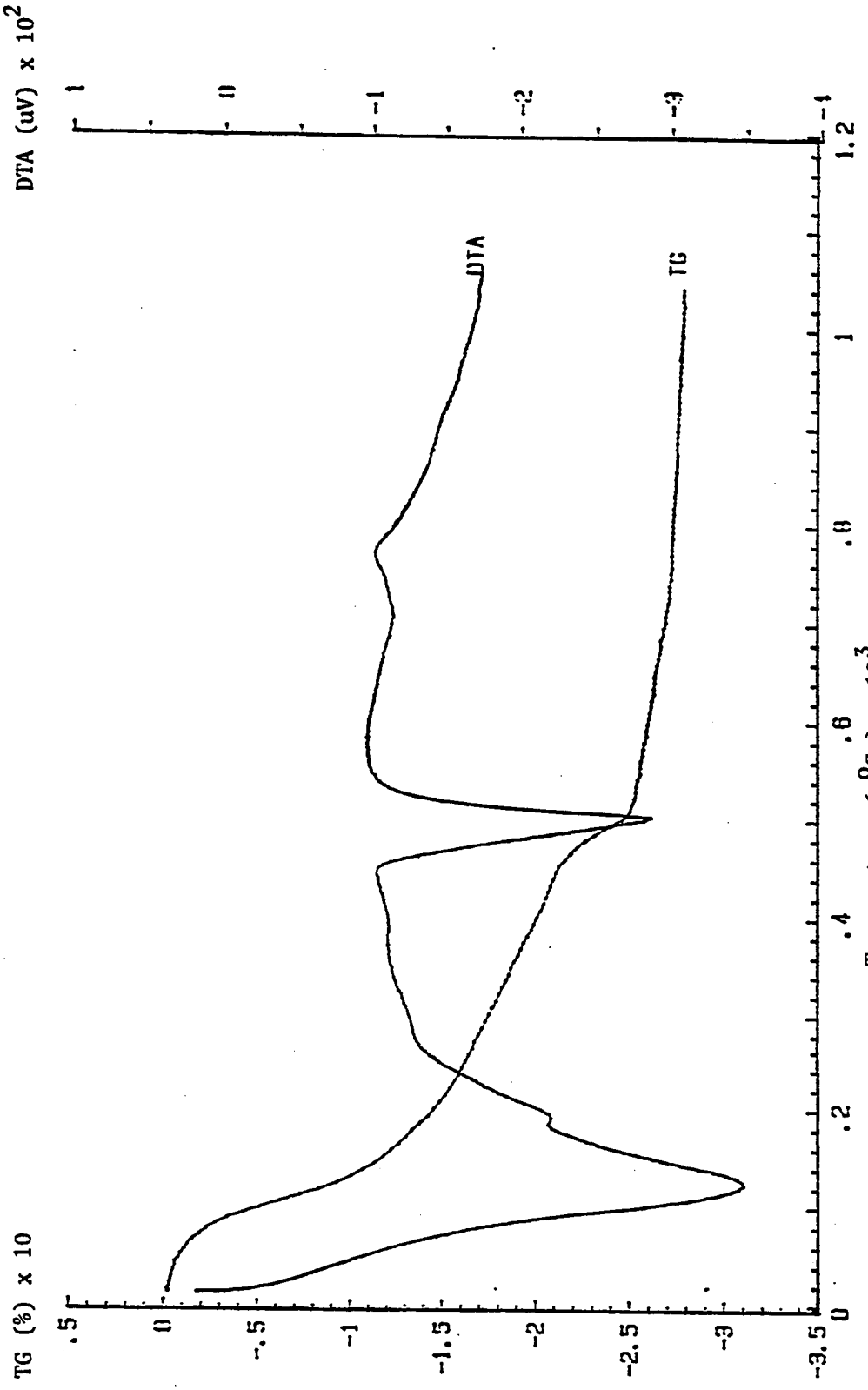

Fig. 4.2.3.4: DTA and TGA Curves for Hydrated Paste of 5% Microsilica Blended Cement

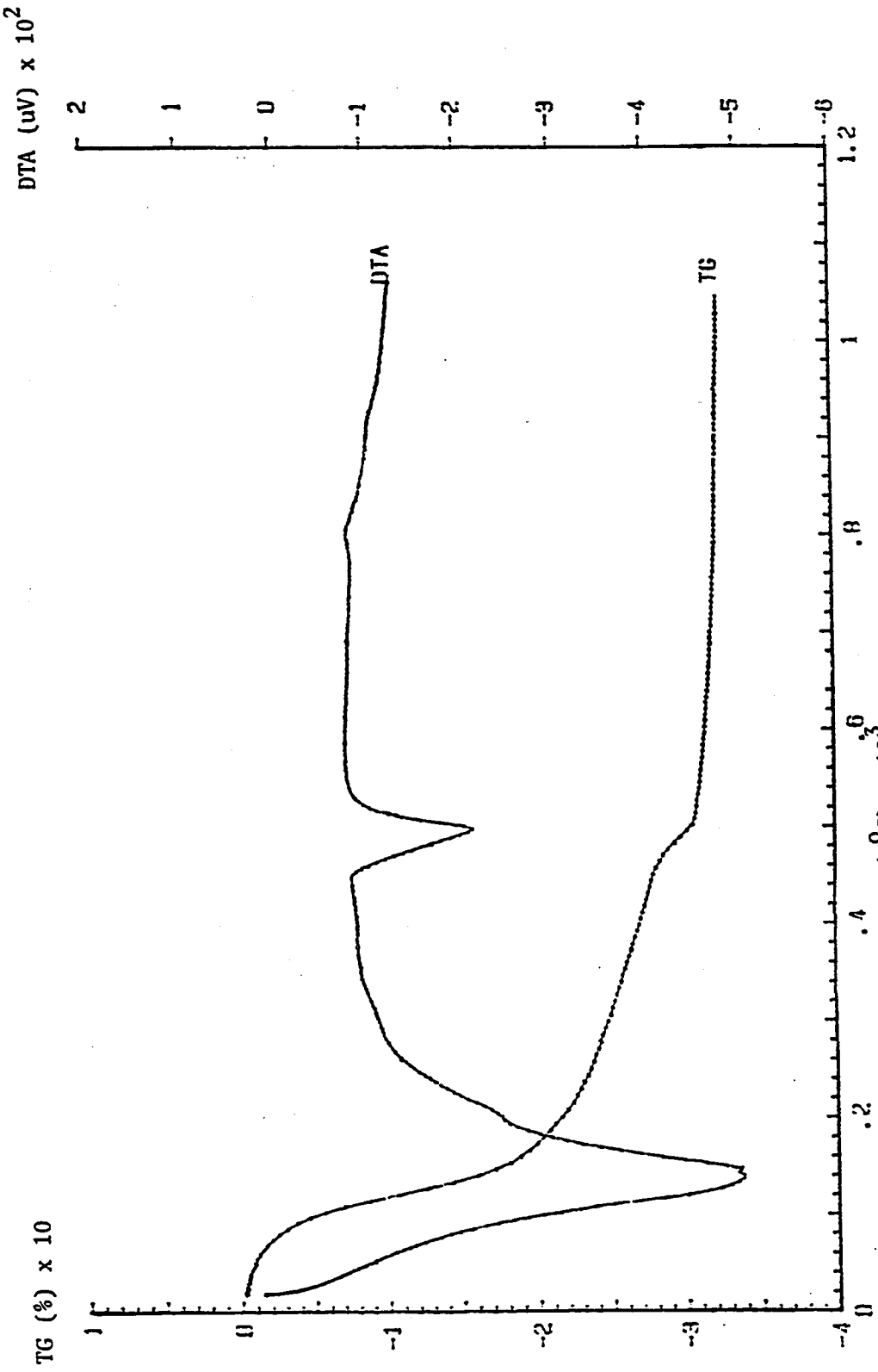

Fig. 4.2.3.5: DTA and TGA Curves for Hydrated Paste of 10% Microsilica Blended Cement

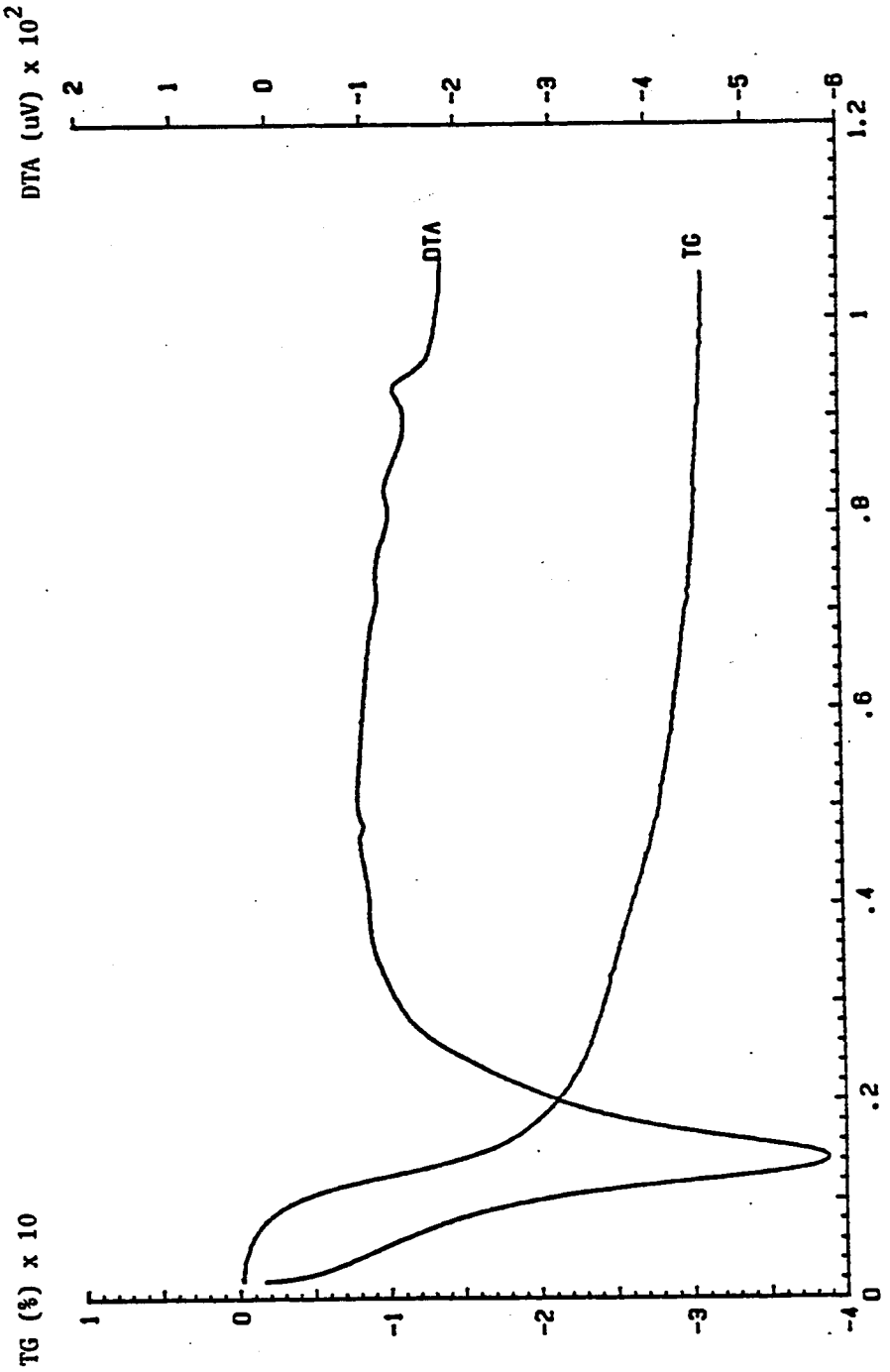

Fig. 4.2.3.6: DTA and TGA Curves for Hydrated Paste of 20% Microsilica Blended Cement

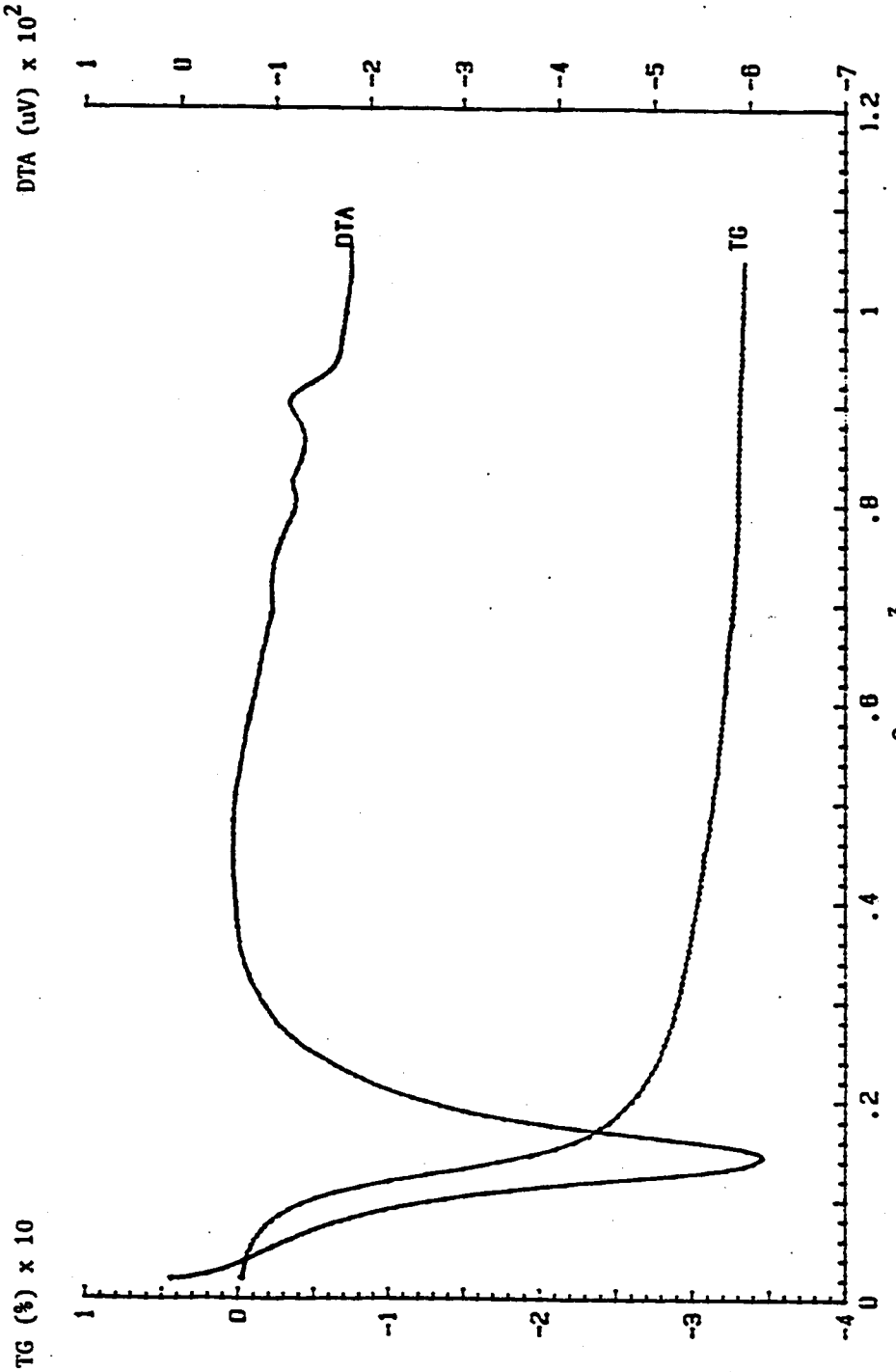

Fig. 4.2.3.7: DTA and TGA Curves for Hydrated Paste of 25% Microsilica Blended Cement

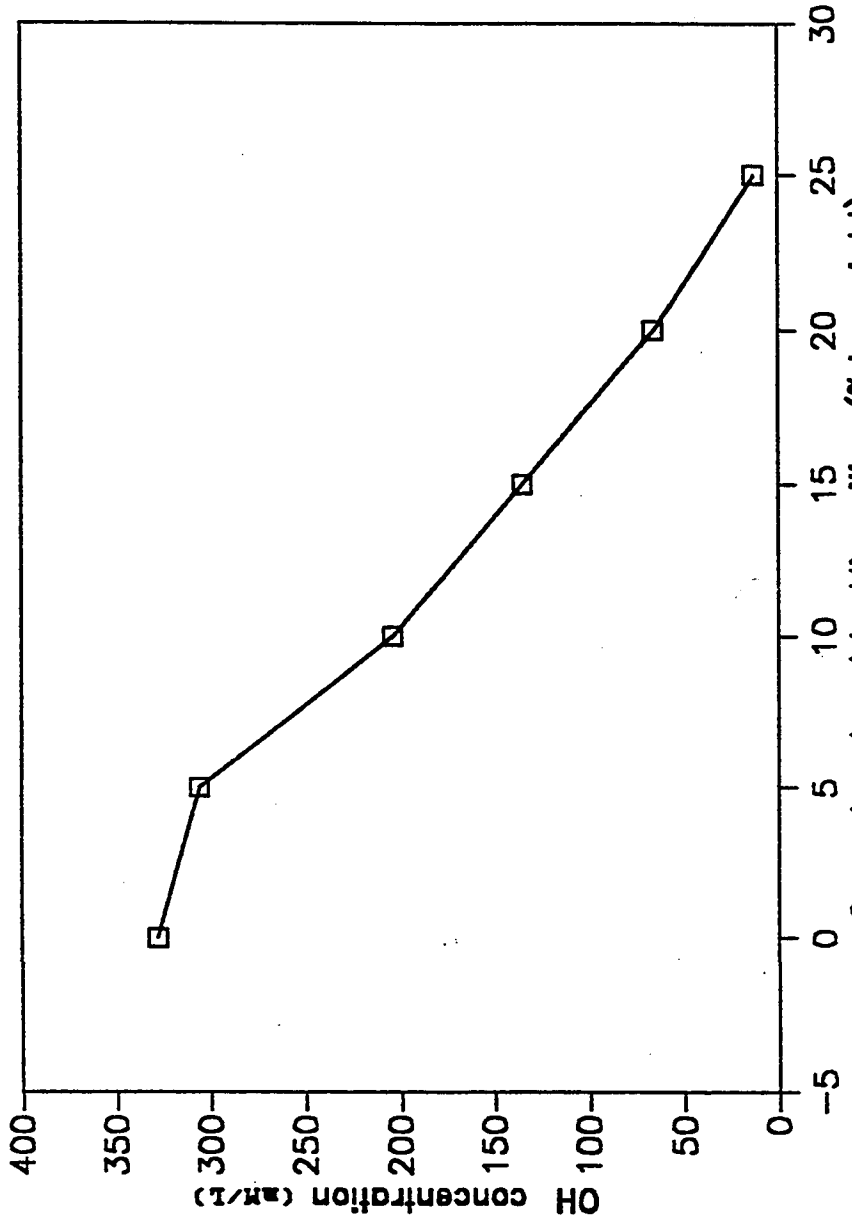

Fig. 4.2.3.8: Effect of Microsilica Addition on OH^- concentration in Pore Solution

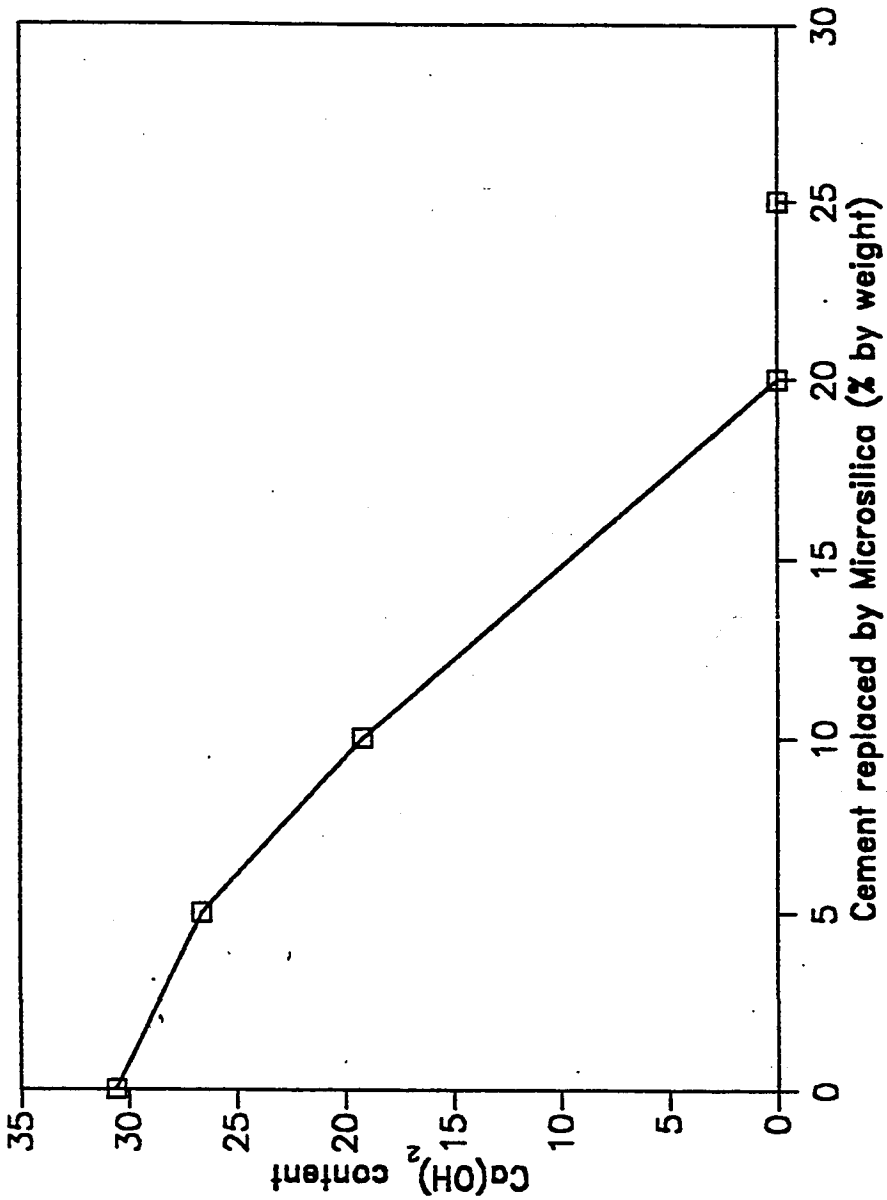

Fig. 4.2.3.9: Effect of Microsilica Addition on Calcium Hydroxide content in Hydrated Cement

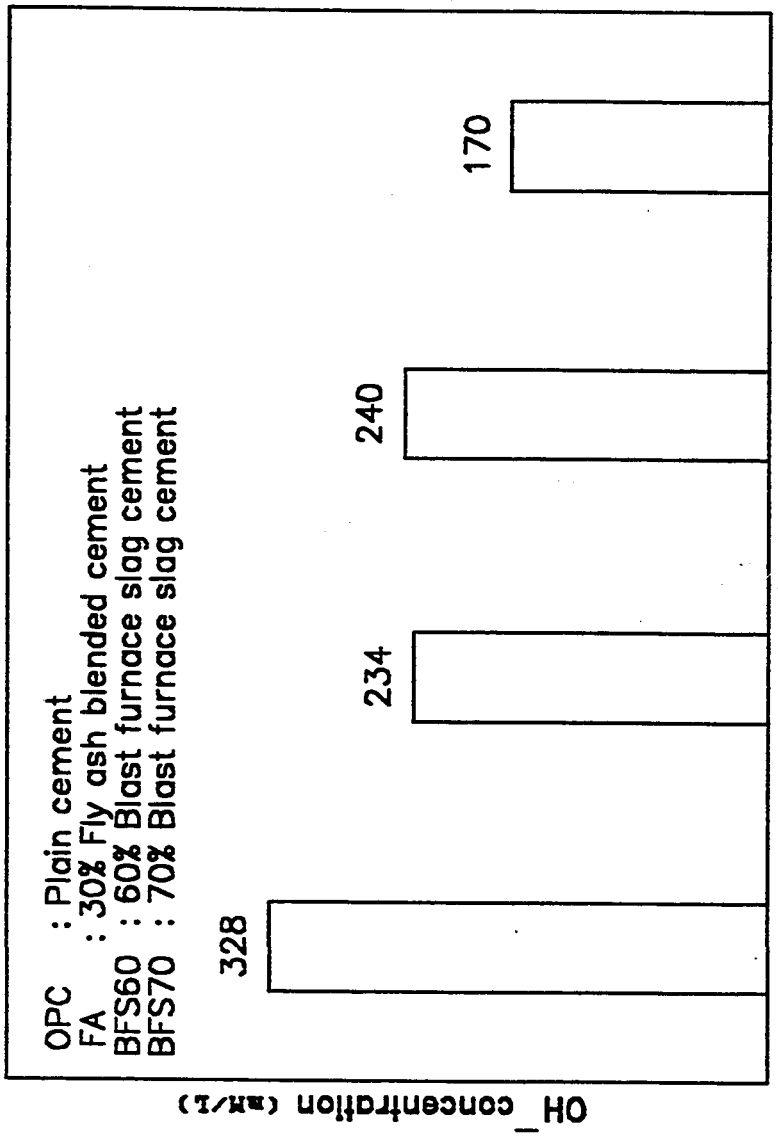

Fig. 4.2.3.10: Effect of Fly Ash and Blast Furnace Slag on OH^- concentration in Pore Solution

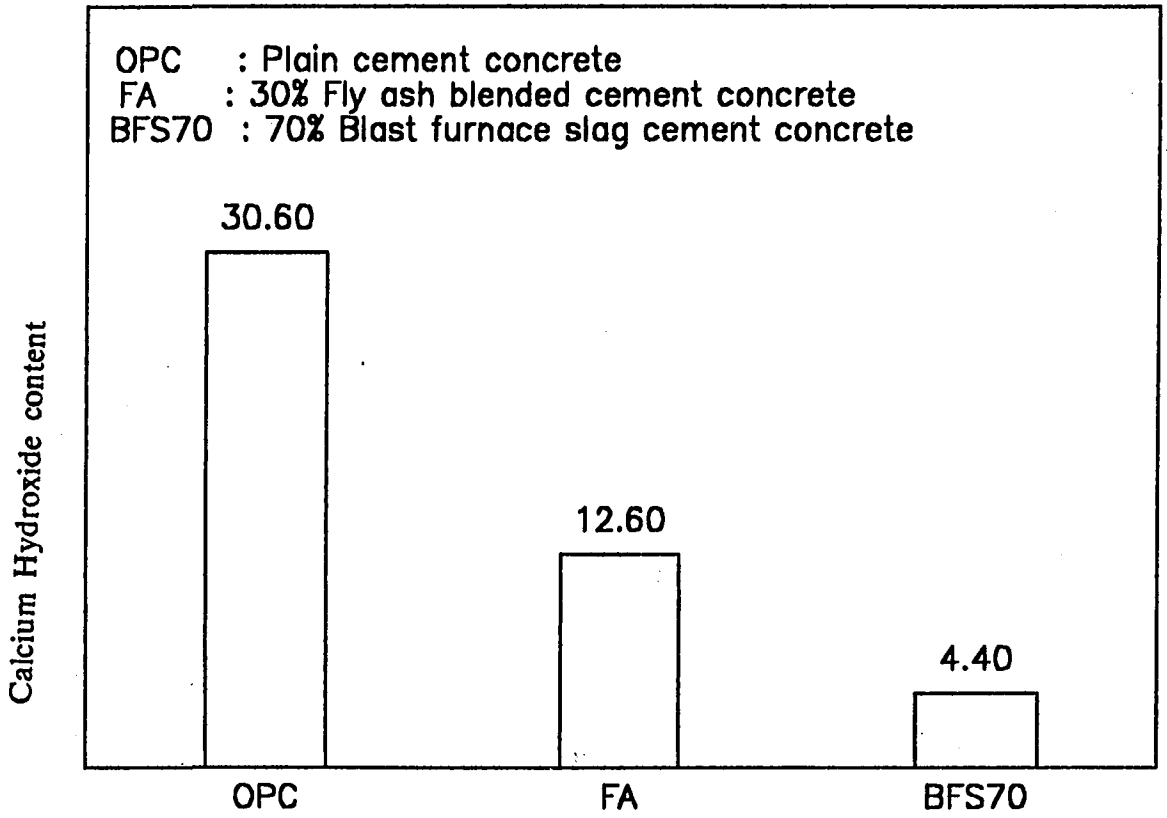

Fig. 4.2.3.11: Effect of Fly Ash and Blast Furnace Slag on Calcium Hydroxide content in Hydrated Cement

in the cement, which are responsible for high pH of the order of 13.5 in plain cements. In 20 and 25% microsilica blended cements, although the crystalline calcium hydroxide is completely depleted the alkalinity of the pore solution is due to alkali hydroxides of the cement and possibly of microsilica also, and soluble calcium hydroxide.

In concrete exposed to normal environment, reinforcing steel remains passive due to high alkalinity of concrete pore solution. Depassivation of reinforcing steel in concrete occurs when either the pore solution alkalinity is lowered or chloride ions enter into concrete. When Cl^-/OH^- ratio in the concrete pore solution reaches a threshold value, steel is depassivated and active corrosion starts. A threshold value of Cl^-/OH^- ratio of 0.6 is proposed by Hausmann (11) and a value of 0.3 is recommended by Diamond (38). The incorporation of the blending materials in cement would, therefore, increase the risk of corrosion of steel in concrete, due to their effect of reducing the pore solution alkalinity. However, the corrosion behavior of steel in concrete depends on factors other the pore solution alkalinity, for example chloride-binding capacity of cement and physical structure of cement matrix, which controls the mobility of aggressive ions into concrete.

4.2.4 DETERMINATION OF THRESHOLD Cl^-/OH^- RATIO IN PLAIN CEMENTS

Fig. 4.2.4.1 shows the potential measurement record of steel in the three cement mortars tested. Average values of at least two specimens have been plotted. The corrosion initiation times of steel in 2.43, 7.59 and 14% C_3A cement mortars were 24, 31 and 47 days. The superior performance with increasing C_3A content is due to increasing chloride binding capacity with increasing C_3A content of the cement.

Pore solution composition of mortar surrounding the steel reinforcement is shown in Table 4.2.4.1. It can be noticed that the OH^- concentrations recorded here are significantly less than those observed in the sealed cement paste specimens used for pore solution studies, for the same cements. This is probably due to leaching out of alkalies and calcium hydroxide from the cement mortar. The OH^- concentrations range from 90 to 158 mM/L (pH 12.95 to 13.2) for which the threshold chlorides range from 180 to 208 mM/L. Since the data covers a small range of OH^- concentration values, a definite relationship between OH^- concentration and threshold Cl^- concentration can not be established. However, the data clearly indicate that the threshold Cl^-/OH^- ratio is dependent on the OH^- concentration and is inversely proportional to it. As the OH^- ion concentration increases, the threshold Cl^-/OH^- ratio decreases. The data show an average value of threshold Cl^-/OH^- ratio of about 1.8 for a hydroxyl ion concentration value of about 110 mM/L (pH = 13.04). However, for a higher OH^- concentration of about 150 mM/L (pH = 13.2), the threshold Cl^-/OH^- was 1.3. It can noted that, for the range of OH^- concentrations tested, the threshold chlorides obtained are more than those given by Hausmann's (11) and Gouda's (54) criteria. This may be attributed to the fact that Hausmann's and Gouda's work involved tests on steel embedded in artificial alkaline pore solutions and not in actual concrete. The physical parameters such as high electrical resistivity and low ionic mobility in concrete may have an effect on threshold Cl^-/OH^- ratio. Yonezawa (67) et al conducted corrosion tests on steel in alkaline solution and on actual cement mortar. Their results showed that the threshold Cl^-/OH^- ratios for corrosion of steel in mortar is very high compared to the threshold Cl^-/OH^- ratio of steel in aqueous solutions. Thus, the results of the present study and those of Yonezawa (67) indicate that the threshold Cl^-/OH^- ratio for corrosion of steel in actual cement mortar/concrete are more than that

Table 4.2.4.1: Pore Solution Composition of Specimens Used For Threshold Cl^-/OH^- Ratio Determination

Cement No.	Specimen	C_3A Content of Cement (% by weight)	Pore Solution Composition			
			Cl^- (mM/L)	OH^- (mM/L)	pH	Cl^-/OH^-
1	A1	2.43	180	90	12.95	2.00
1	A2	2.43	186	100	13.00	1.86
2	B1	7.59	220	118	13.07	1.86
2	B2	7.59	196	115	13.06	1.70
2	B3	7.59	230	128	13.11	1.80
3	C1	14.00	203	158	13.20	1.28
3	C2	14.00	208	158	13.20	1.32

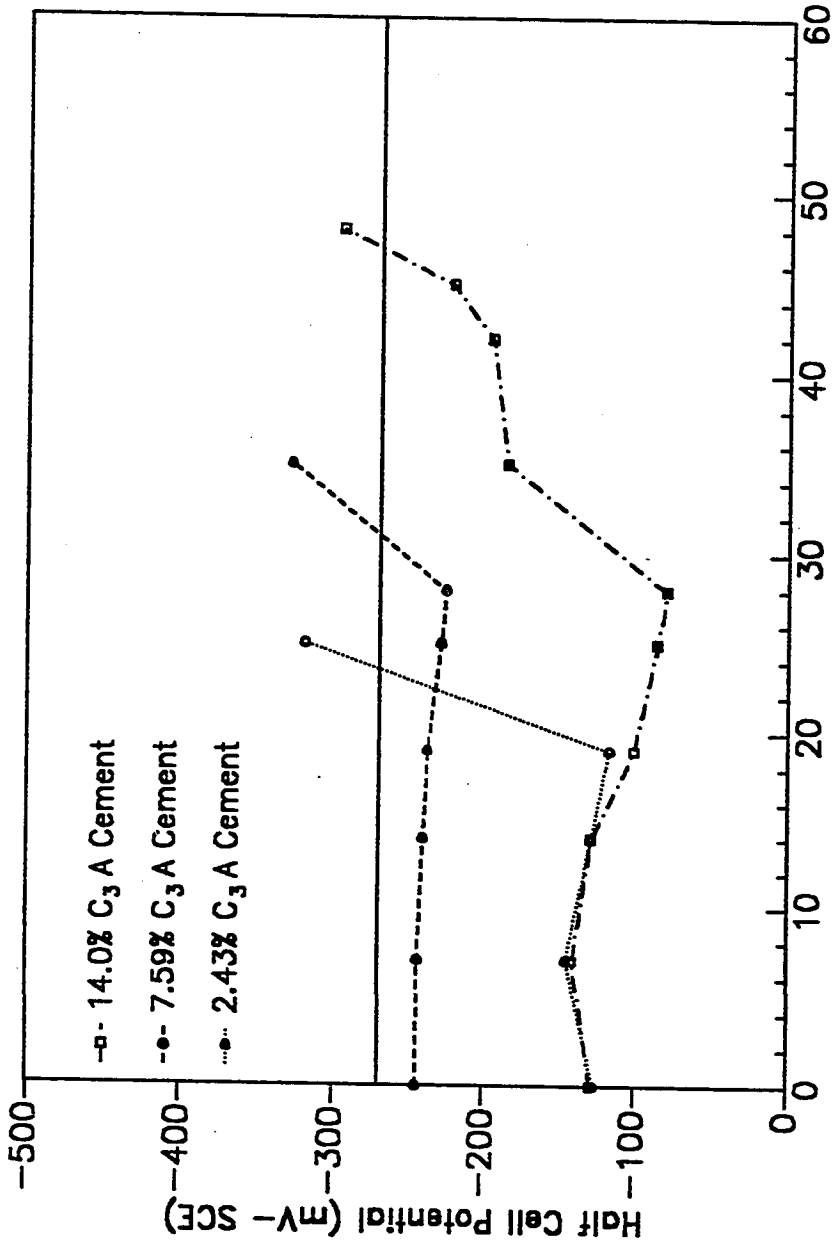

Fig. 4.2.4.1: Potential Measurement Record of Steel in Cement Mortars

measured in simulated pore solutions.

The results of the present study indicate that for pore solution pH of 13.0 and 13.2, the threshold Cl^-/OH^- ratios may be taken as 1.8 and 1.3 respectively.

4.3 PHYSICAL CHARACTERISTICS OF PLAIN AND BLENDED CEMENTS

4.3.1 PORE SIZE DISTRIBUTION OF HARDENED CEMENT PASTES

Pore size distribution for plain and blended cements for curing ages ranging from 3 days to 6 months are given in Table 4.3.1.1 through 4.3.1.5 and plotted in Figs. 4.3.1.1 through 4.3.1.5. In Table 4.3.1.6 and Fig. 4.3.1.6, the average pore radii of plain and blended cements for different curing periods is shown. Total pore volume are also tabulated in Tables 4.3.1.1 through 4.3.1.5.

The data shows that the pore size distribution of fly ash and blast furnace slag blended cements are coarser than that of the plain cements at early ages. The average pore radii in the fly ash blended cement is more than that in the plain cement up to a curing period of 14 days. The blast furnace slag cement shows a higher average pore radius than the plain cement up to 7 days. However, at later ages, the fly ash and the blast furnace slag blended cements show significantly refined pore structure than that of the plain cement. This behavior indicates that the fly ash and the slag blended cements have weaker structure at early ages and pore refinement occurs at later ages due to slow pozzolanic reaction. At 6 months age, the average pore radii of the fly ash and the blast furnace slag blended cements are about 70% of that of the plain cement.

Table 4.3.1.1 Pore Size Distribution of Plain Cement Paste

Age (days)	Total Pore Volume (mm^3/g)	Pore Radius (A^0)	48.5	80	140	250	440	780	1400	2500	4400
3	338	PV*	2	6	8	8	11	12	11	22	20
		CPV*	338	331	311	284	257	220	179	142	68
7	210	PV*	2	11	6	21	46	2	1	1	0
		CPV*	210	206	182	149	105	8	4	2	0
14	192	PV*	4	11	19	20	44	1	1	0	0
		CPV*	192	184	163	127	88	4	2	0	0
28	168	PV*	5	14	15	20	43	1	1	0	0
		CPV*	168	160	136	110	76	3	2	0	0
60	159	PV*	7	16	17	34	24	1	1	0	0
		CPV*	159	148	122	95	41	3	2	0	0
90	154	PV*	7	17	18	30	25	1	0	0	0
		CPV*	154	143	116	88	41	2	0	0	0
120	149	PV*	8	19	20	36	16	1	0	0	0
		CPV*	149	137	109	79	25	2	0	0	0
180	139	PV*	7	19	19	41	13	1	0	0	0
		CPV*	139	129	103	76	19	1	0	0	0

* PV : Pore Volume ($mm^3/g.$)
* CPV : Cummulative Pore Volume ($mm^3/g.$)

Table 4.3.1.2 Pore Size Distribution of 30% Fly Ash Blended Cement

Age (days)	Total Pore Volume (mm^3/g)	Pore Radius (A^0)	48.5	80	140	250	440	780	1400	2500	4400	7800
3	351	PV*	2	5	5	8	7	7	8	11	12	35
		CPV*	351	344	326	309	281	256	232	204	165	123
7	245	PV*	3	13	14	15	19	30	4	1	0	0
		CPV*	245	237	205	171	134	87	12	3	0	0
14	208	PV*	4	10	12	15	21	33	2	0	0	0
		CPV*	208	199	178	152	120	75	4	0	0	0
28	200	PV*	7	21	22	33	12	3	2	0	0	0
		CPV*	200	184	139	88	33	8	2	0	0	0
60	197	PV*	10	24	26	24	13	2	1	0	0	0
		CPV*	197	177	130	79	32	6	2	0	0	0
90	179	PV*	10	24	40	22	2	1	1	0	0	0
		CPV*	179	161	118	47	7	4	2	0	0	0
120	175	PV*	10	31	42	13	2	1	1	0	0	0
		CPV*	175	158	103	30	7	4	2	0	0	0
180	175	PV*	10	32	42	11	1	1	1	0	0	0
		CPV*	175	157	100	25	5	4	2	0	0	0

* PV : Pore Volume ($mm^3/g.$)
* CPV : Cummulative Pore Volume ($mm^3/g.$)

Table 4.3.1.3 Pore Size Distribution of Blast Furnace Slag Cement

Age (days)	Total Pore Volume (mm^3/g)	Pore Radius (A^0)	48.5	80	140	250	440	780	1400	2500	4400
3	308	PV*	3	8	11	11	12	9	10	25	10
		CPV*	308	299	274	240	207	168	140	109	34
7	280	PV*	6	10	15	19	31	18	1	0	0
		CPV*	280	263	235	193	140	53	2.8	0	0
14	261	PV*	5	11	18	26	34	2	1	0	0
		CPV*	261	248	218	170	100	8	2.7	0	0
28	218	PV*	7	14	21	33	23	0	0	0	0
		CPV*	218	202	171	125	51	0	0	0	0
60	182	PV*	7	17	28	40	7	0	0	0	0
		CPV*	182	169	138	86	13	0	0	0	0
90	175	PV*	7	18	29	40	5	0	0	0	0
		CPV*	175	163	131	80	9	0	0	0	0
120	162	PV*	8	23	28	36	4	0	0	0	0
		CPV*	162	149	111	65	7	0	0	0	0
180	133	PV*	10	22	37	26	2	0	0	0	0
		CPV*	133	119	89	38	3	0	0	0	0

* PV : Pore Volume ($mm^3/g.$)
* CPV : Cummulative Pore Volume ($mm^3/g.$)

Table 4.3.1.4 Pore Size Distribution of 10% Microsilica Blended Cement Concrete

Age (days)	Total Pore Volume (mm^3/g)	Pore Radius (A^0)	48.5	80	140	250	440	780	1400	2500	4400
3	258	PV*	5	11	15	16	24	27	1	1	0
		CPV*	258	245	217	178	137	75	5.2	2.6	0
7	198	PV*	5	14	21	23	34	3	0	0	0
		CPV*	198	188	160	119	73	6	0	0	0
14	154	PV*	7	14	19	25	34	1	0	0	0
		CPV*	154	143	122	92	54	1.5	0	0	0
28	140	PV*	9	17	22	47	2	2	0	0	0
		CPV*	140	127	103	72	5.6	2.8	0	0	0
60	140	PV*	9	18	22	41	6	1	0	0	0
		CPV*	140	127	101	69	10.1	1.4	0	0	0
90	130	PV*	9	19	127	41	3	0	0	0	0
		CPV*	130	118	93	58	4	0	0	0	0
120	127	PV*	9	20	27	40	2	0	0	0	0
		CPV*	127	115	89	54	2.6	0	0	0	0
180	122	PV*	9	21	27	40	1	0	0	0	0
		CPV*	122	111	85	51	1.2	0	0	0	0

* PV : Pore Volume ($mm^3/g.$)
* CPV : Cummulative Pore Volume ($mm^3/g.$)

Table 4.3.1.5 Pore Size Distribution of 20% Microsilica Blended Cement Concrete

Age (days)	Total Pore Volume (mm^3/g)	Pore Radius (A^0)	48.5	80	140	250	440	780	1400	2500	4400
3	254	PV*	5	15	19	15	40	4	1	1	0
		CPV*	254	241	207	155	117	15	5.1	2.5	0
7	214	PV*	7	16	18	18	37	1	1	0	0
		CPV*	214	199	164	124	85	4	2	0	0
14	174	PV*	10	16	21	27	24	1	0	0	0
		CPV*	174	156	128	91	44	1.8	0	0	0
28	129	PV*	13	20	21	38	4	1	0	0	0
		CPV*	129	112	85	57	6.6	1.3	0	0	0
90	120	PV*	13	21	22	31	9	0	0	0	0
		CPV*	120	104	78	50	11	0	0	0	0
120	120	PV*	16	27	22	28	2	0	0	0	0
		CPV*	120	99	65	38	2.5	0	0	0	0
180	118	PV*	18	31	21	26	1	0	0	0	0
		CPV*	118	96	58	33	1.2	0	0	0	0

* PV : Pore Volume ($mm^3/g.$)
* CPV : Cummulative Pore Volume ($mm^3/g.$)

Table 4.3.1.6 Average Pore Radius of Plain and Blended Cements

Cement Type	Average Pore Radius (A°)							
	3 days	7 days	14 days	28 days	60 days	90 days	120 days	180 days
Plain cement	1763	342	303	299	252	240	215	213
30% Fly Ash Blended Cement	3762	472	455	238	207	166	152	146
70% Blast Furnace Slag Cement	1413	370	289	232	189	182	171	153
10% Microsilica Blended Cement	427	274	261	193	192	175	170	167
20% Microsilic Blended Cement	325	277	230	177	---	155	146	136

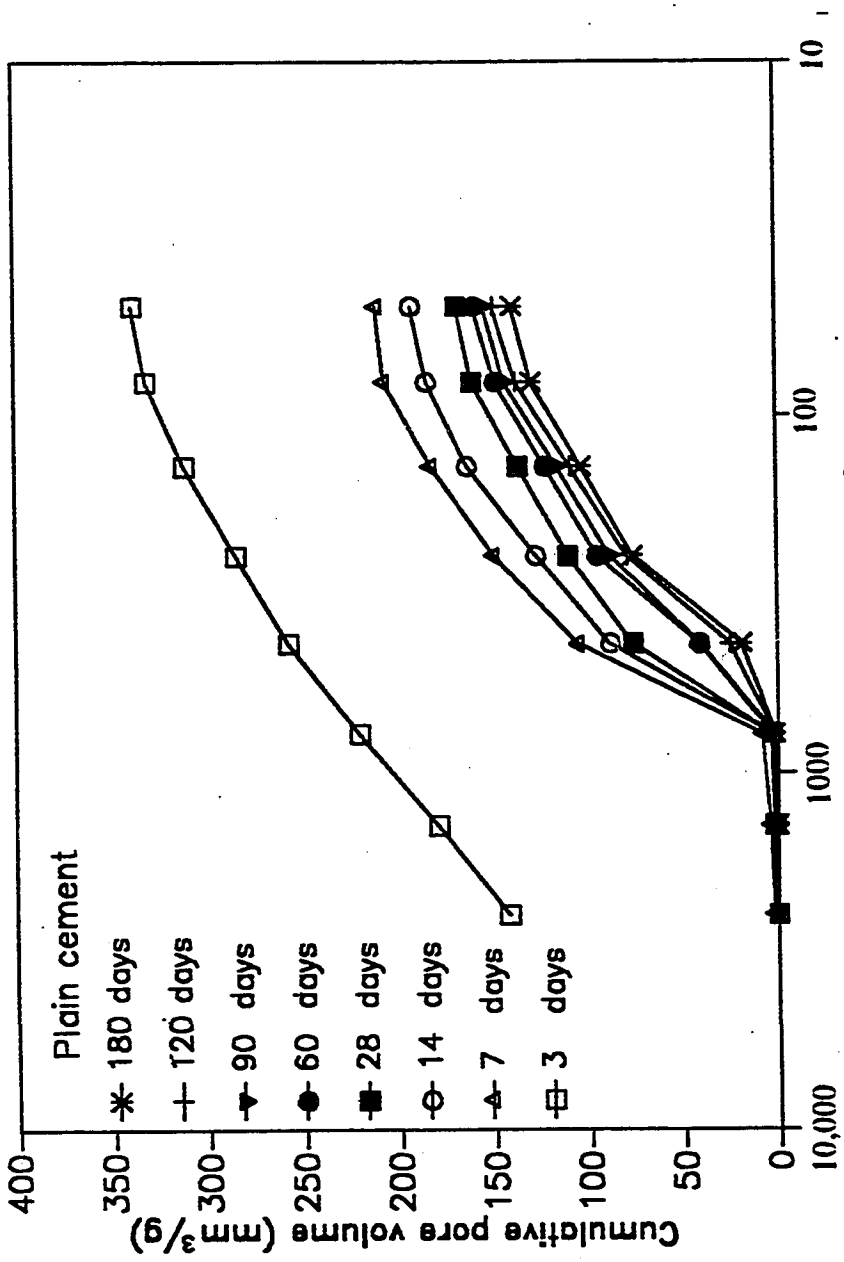

Fig 4.3.1.1 : Pore Size Distribution of Plain Cement

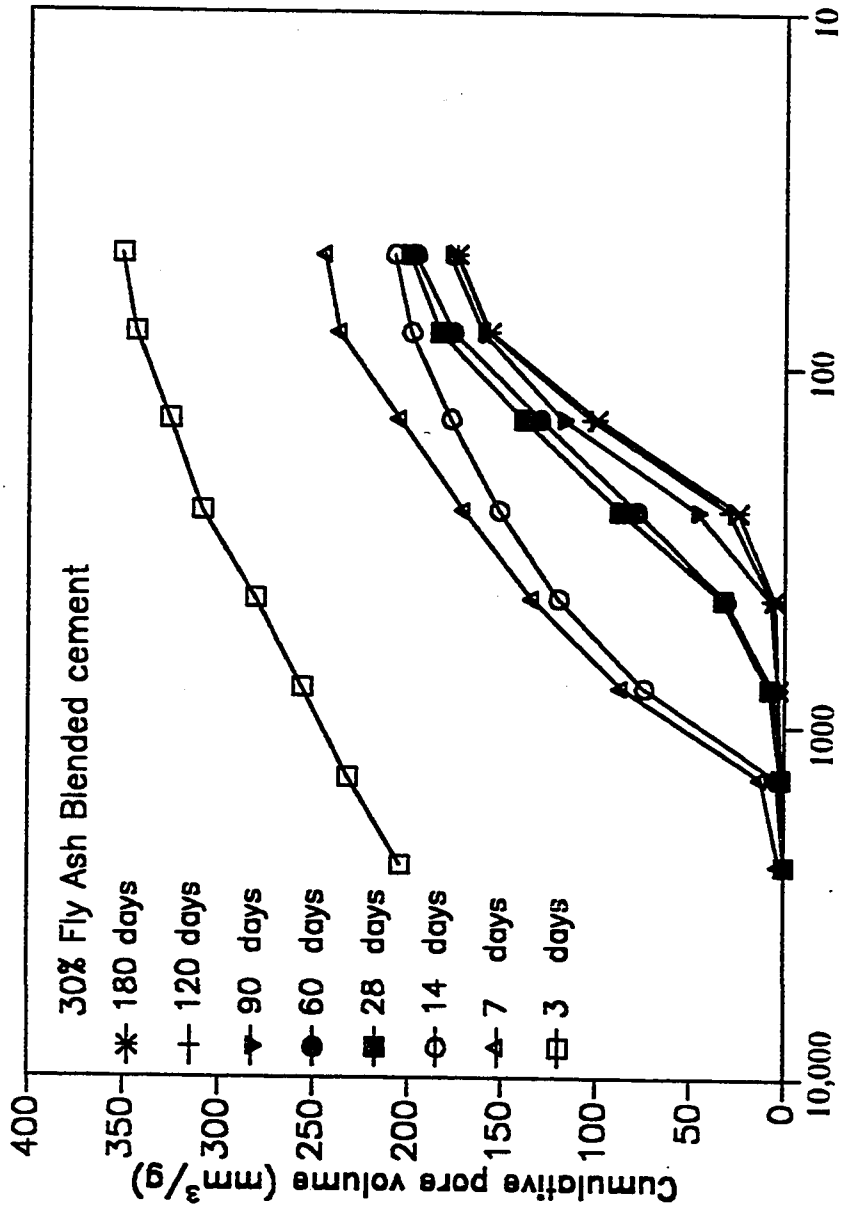

Fig. 4.3.1.2 : Pore Size Distribution of Fly Ash Blended Cement

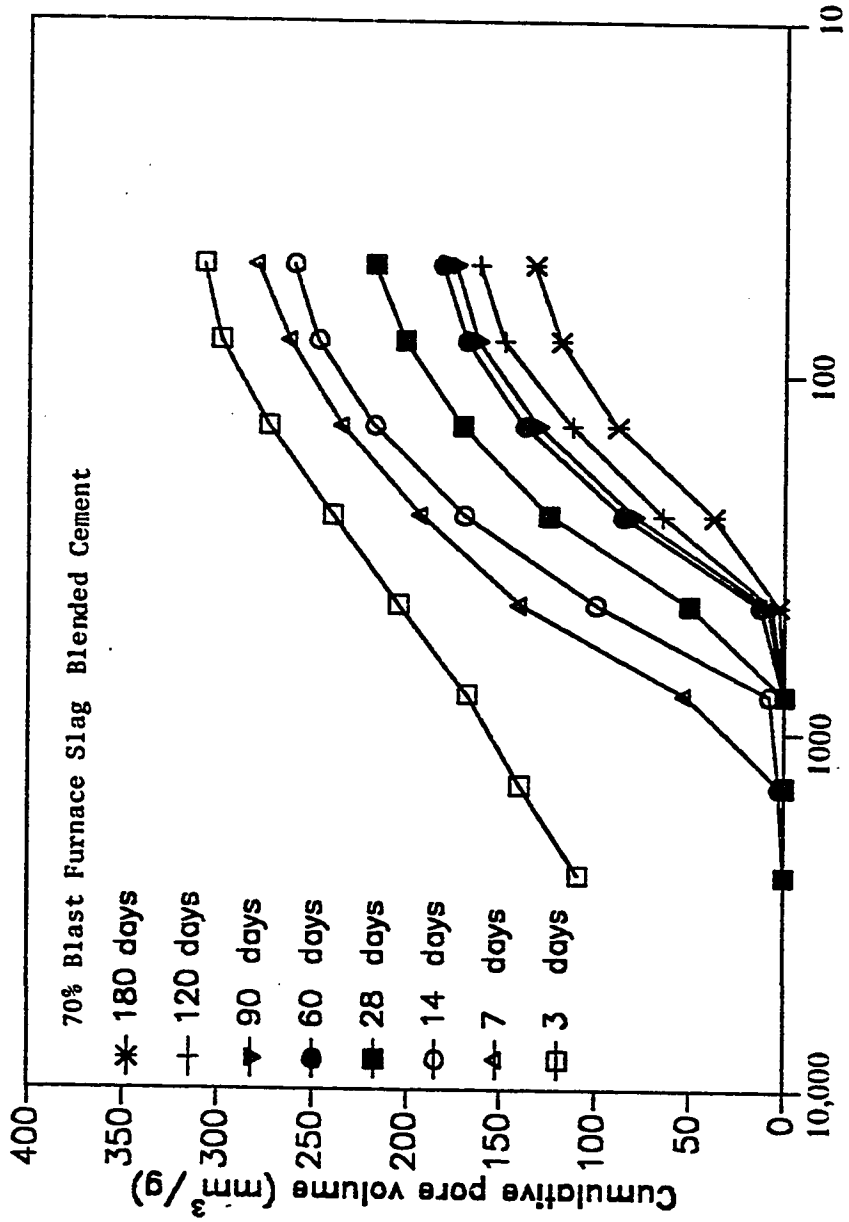

Fig. 4.3.1.3 : Pore Size Distribution of Blast Furnace Slag Cement

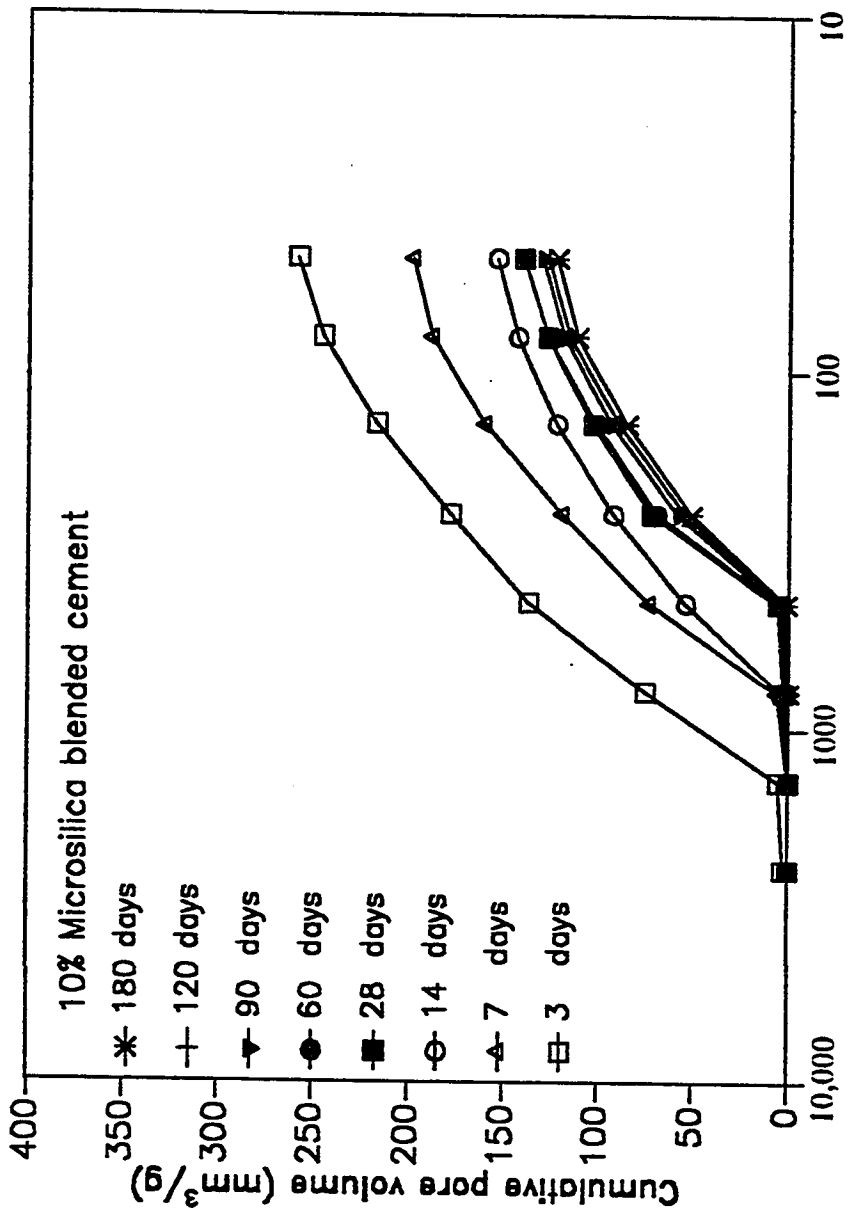

Fig. 4.3.1.4 : Pore Size Distribution of 10% Microsilica Blended Cement

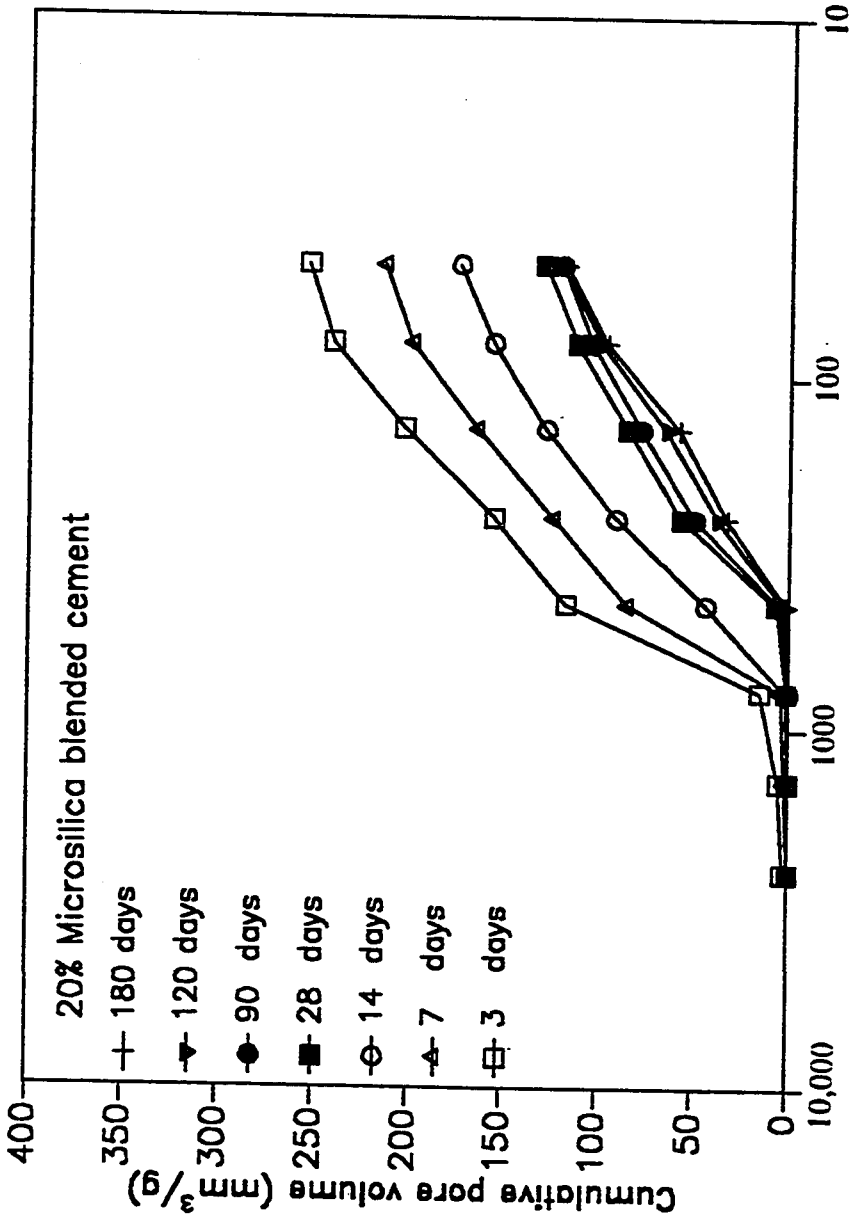

Fig.4.3.1. 5: Pore Size Distributionof 20% Microsilica Blended Cement

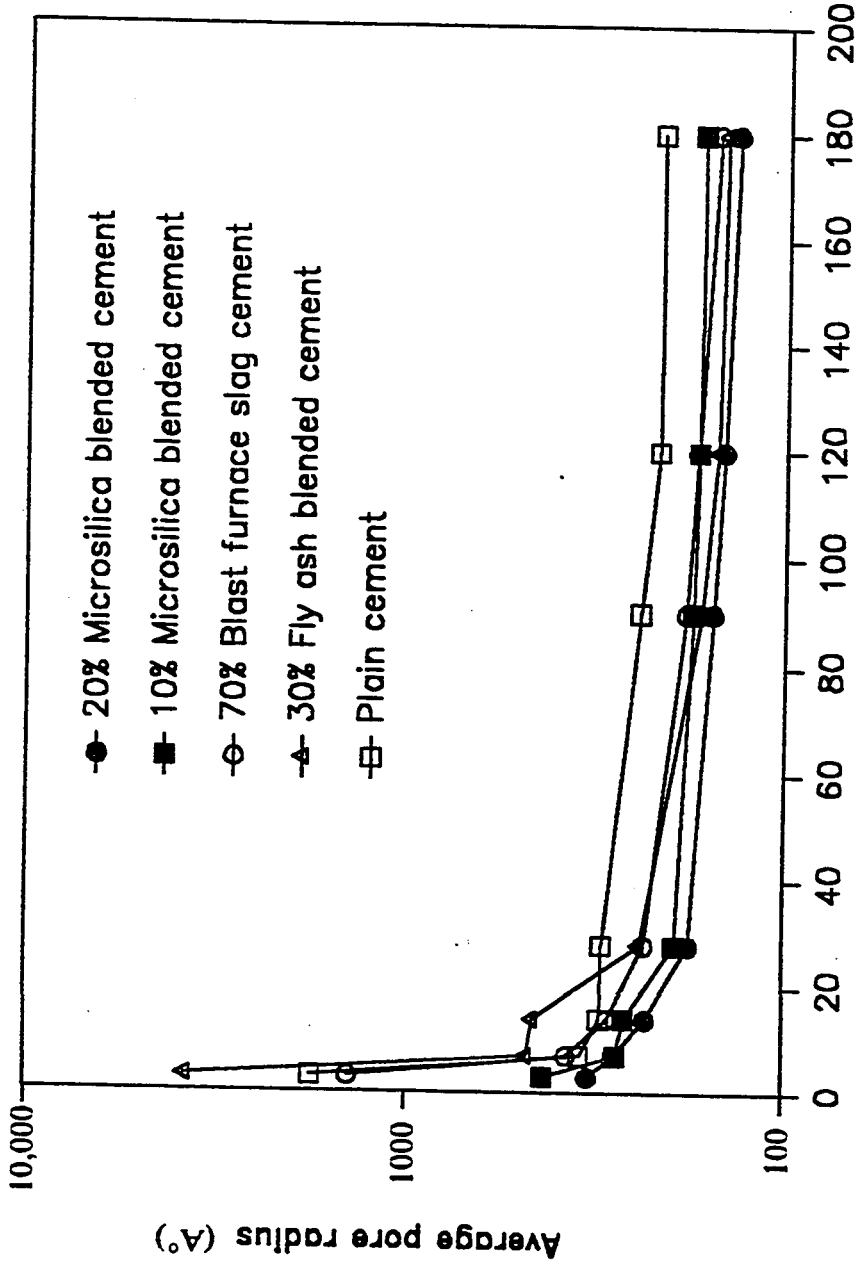

Fig.4.3.1.6 : Average Pore Radius of Plain and Blended Cements

Both the 10 and 20% microsilica blended cements show a more refined pore structure than the plain cements for all the ages. Even at 3 days age, the average pore radii of the 10 and 20% microsilica blended cements are 4 and 5.5 times less than that of the plain cement. Among all the blended cements tested, 20% microsilica showed the smallest average pore radius. At 6 months age, the average pore radius of 20% microsilica blended cement is 136 A° as compared to 213 A° for the plain cement. For the 10% microsilica blended cement, this value is 167 A°.

Data of Table 4.3.1.1 through 4.3.1.5 show that the total pore volume of the fly ash blended cement is more than that of the plain cement at all the ages. For the blast furnace slag, the total pore volume is more than that of the plain cements in all the ages except 3 and 180 days. However, according to Manmohan and Mehta (29), it is the pore size distribution and not the total pore volume which determines the permeability characteristics of a cement. 10 and 20% microsilica blended cements showed less total pore volume than the plain cement for all the ages.

4.3.2 PERMEABILITY TO WATER

4.3.2.1 Permeability of Plain Cement Concrete

To verify the validity of results of the high pressure permeability test method developed in this study, permeability of concrete was measured for three different water cement ratios at three different ages. A pressure of 300 psi was used. Figs. 4.3.2.1 through 4.3.2.9 show water injected into the specimen "q" versus time "t" curves for the different specimens tested. Coefficients of permeability were calculated from the steady-state portion of these curves. The coefficients of permeability of the concrete mixes

tested are shown in Table 4.3.2.1 and Figs. 4.3.2.10 and 4.3.2.11. The values reported are average of values obtained from two tests. The results show a decrease in the coefficient of permeability with increasing age for a given water cement ratio. Also, the coefficient of permeability increased as the water cement ratio increased for all the three ages. These data confirm the validity of results of the high pressure permeability test method used in this investigation. It can also be noted from Table 4.3.2.1 that the variability in the coefficient of permeability values of the two replicates tested for each mix is very small compared to the high variability generally associated with permeability testing.

The increase in coefficient of permeability with increasing water cement ratio is maximum for 7 days age. This can be explained by the fact that at early ages, the degree of hydration is less and therefore, the difference in capillary pores of different water cement ratio concretes is more. Also, Fig. 4.3.2.11 shows that the rate of change of coefficient of permeability with curing period decreases as water cement ratio decreases. For the 0.35 water cement ratio concrete, the effect of curing period on coefficient of permeability is almost negligible. The decreasing effect of curing period on permeability with decreasing water cement ratio is due to the fact that, as water cement ratio is decreased, capillary pores are also decreased. At early curing periods, high water cement ratio concretes contain more capillary pores to be filled up by hydration products than in low water cement ratio concretes. Therefore, the effect of curing period on filling empty capillary pores with hydration products and hence, a decrease in permeability, is more pronounced in high water cement ratio concretes than in low water cement ratio ones.

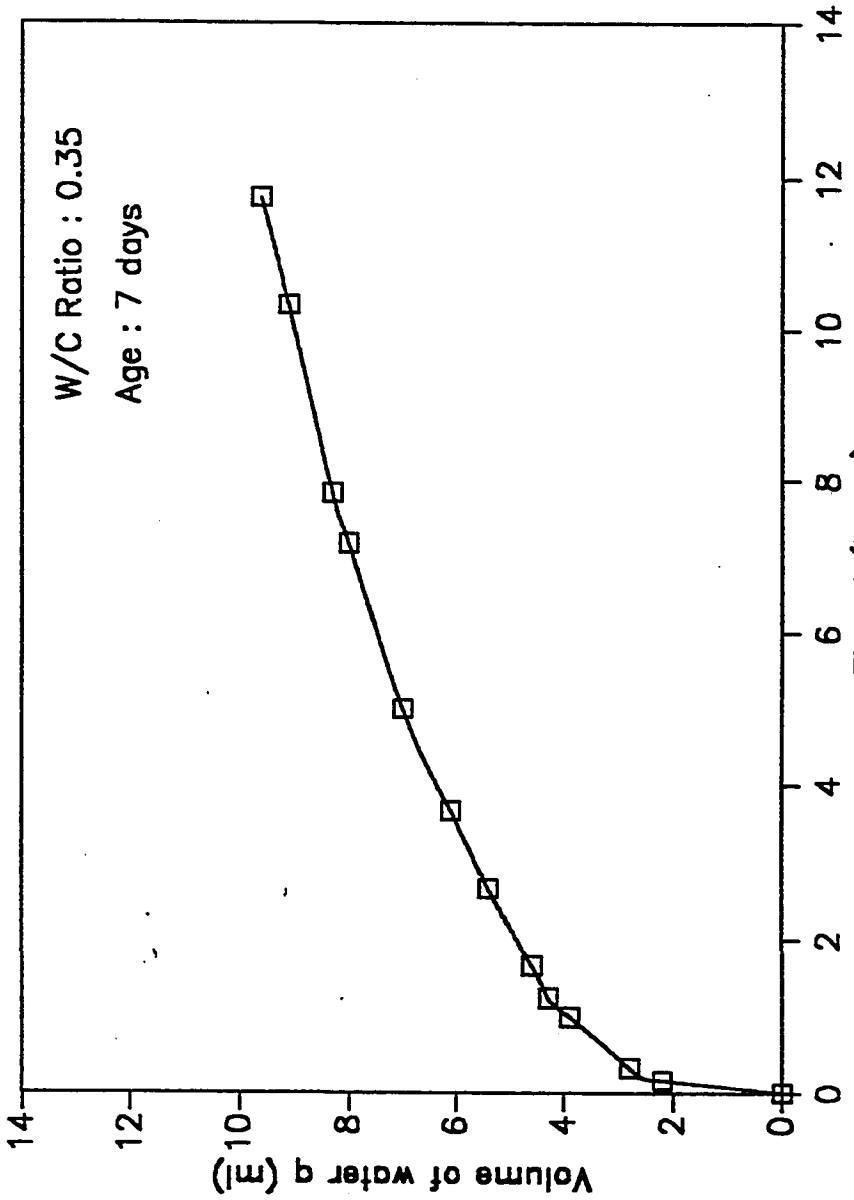

Fig 4.3.2.1: 'q' vs 't' curve for Plain Cement Concrete (W/C: 0.35; Age: 7days)

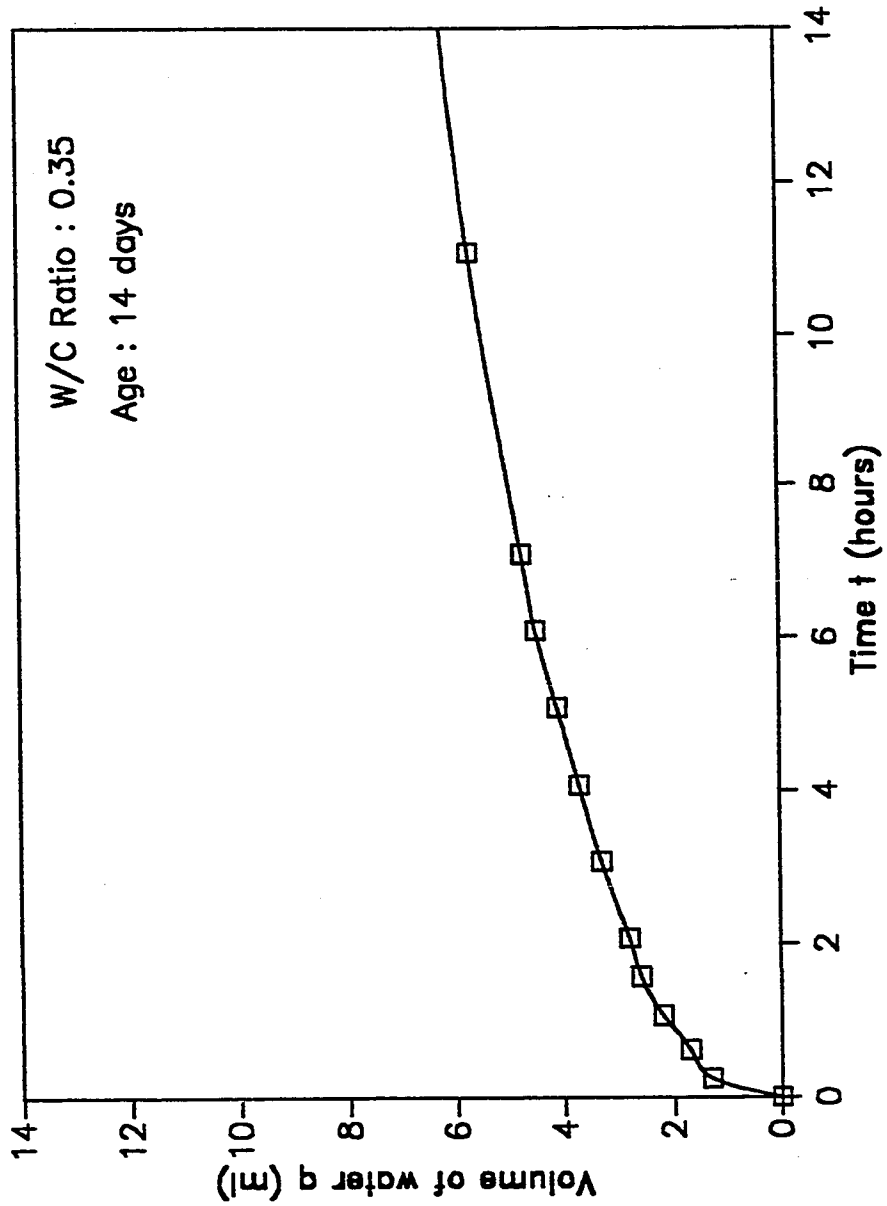

Fig 4.3.2.2: 'q' vs 't' curve for Plain Cement Concrete (W/C: 0.35; Age: 14days)

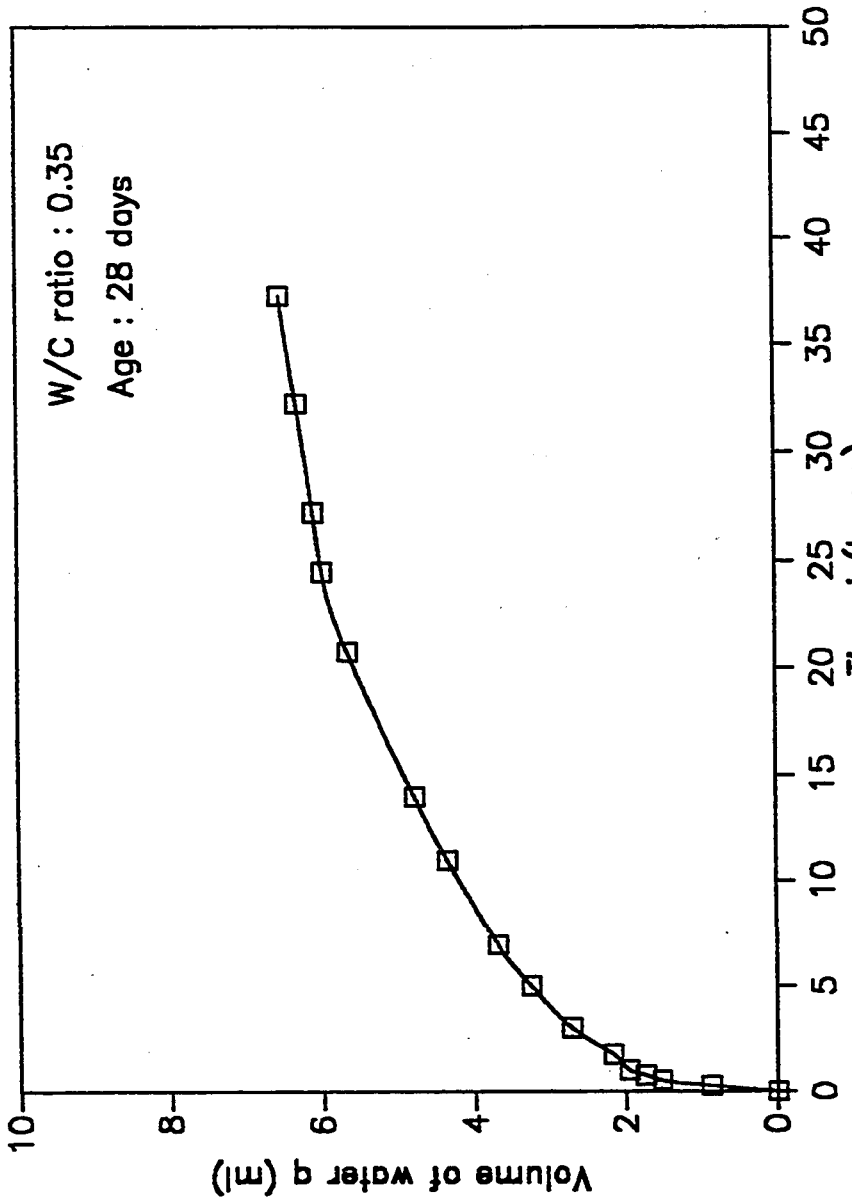

Fig 4.3.2.3: 'q' vs 't' curve for Plain Cement Concrete (W/C: 0.35; Age: 28days)

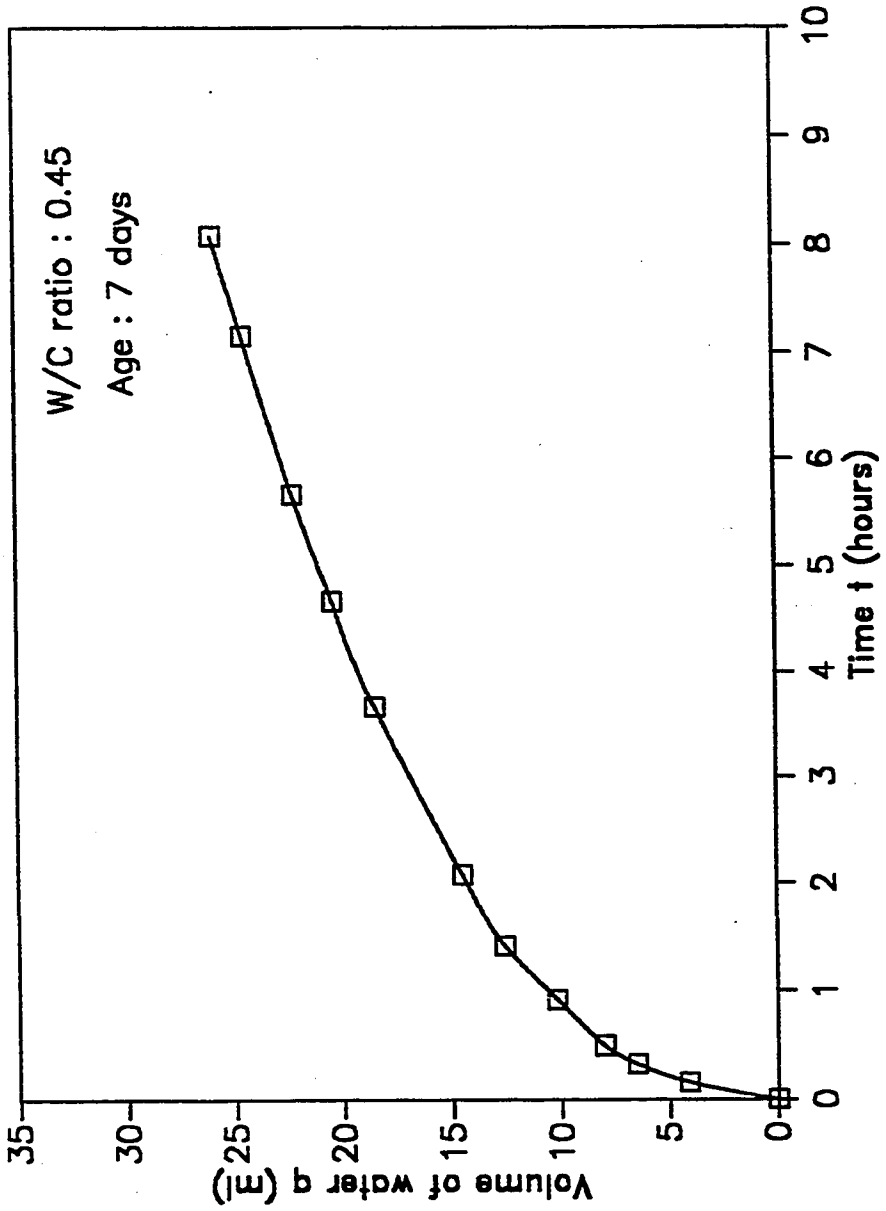

Fig 4.3.2.4: 'q' vs 't' curve for Plain Cement Concrete (W/C: 0.45; Age: 7days)

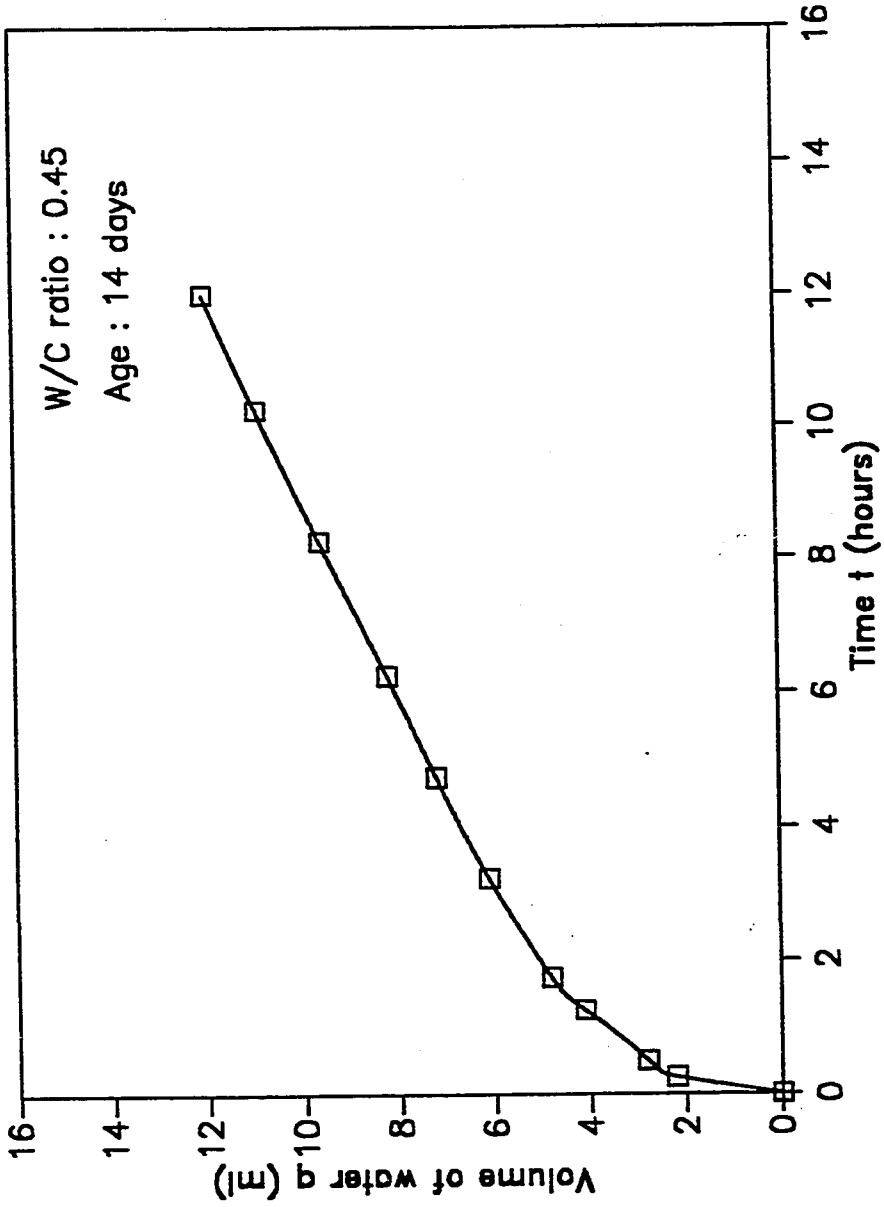

Fig 4.3.2.5: 'q' vs 't' curve for Plain Cement Concrete (W/C: 0.45; Age: 14days)

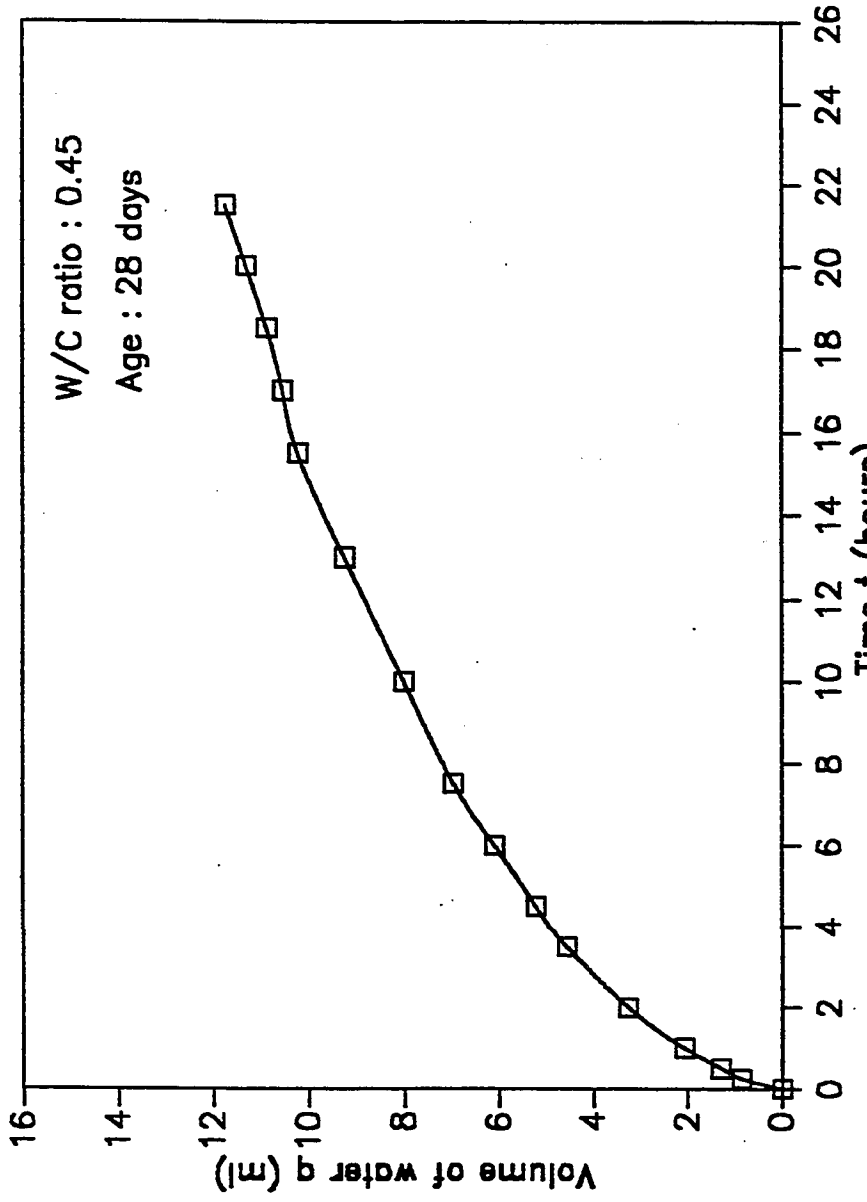

Fig 4.3.2.6: 'q' vs 't' curve for Plain Cement Concrete (W/C: 0.45; Age: 28days)

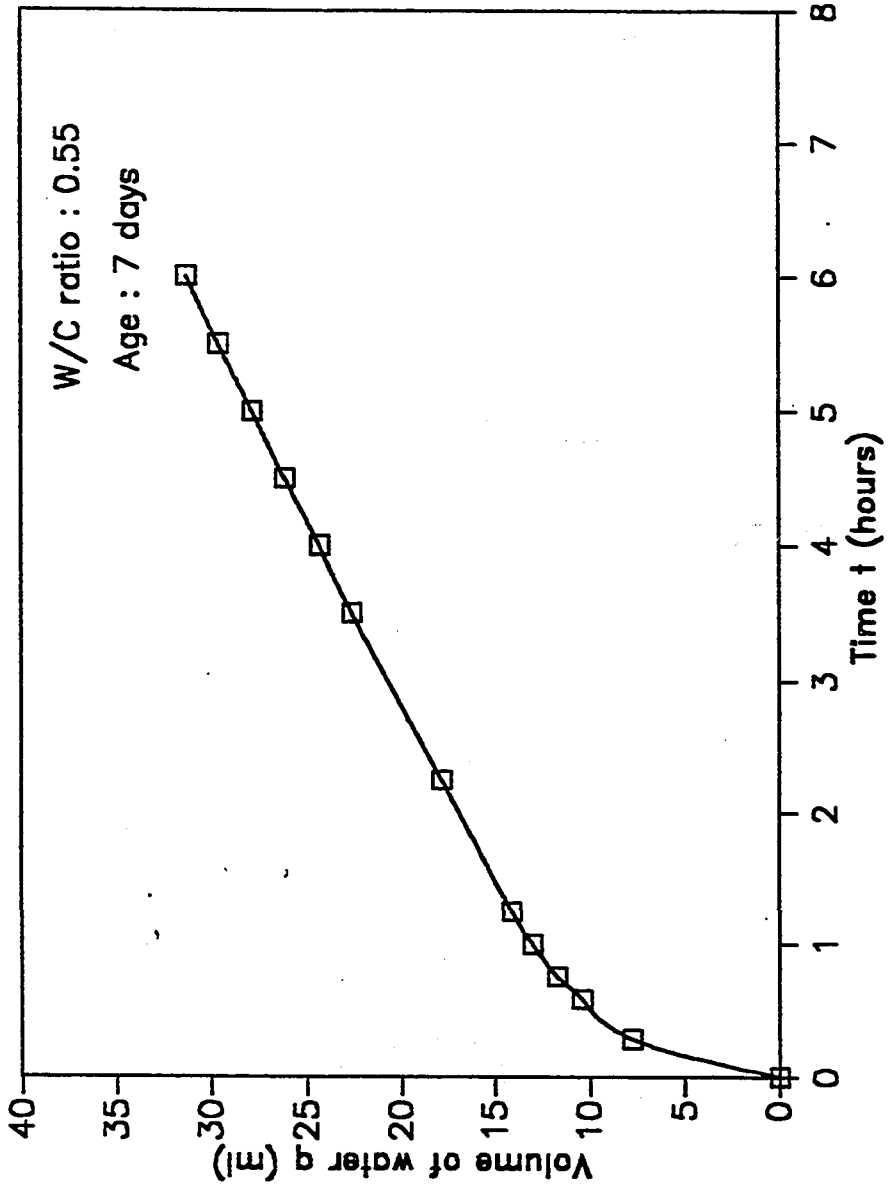

Fig 4.3.2.7: 'q' vs 't' curve for Plain Cement Concrete (W/C: 0.55; Age: 7days)

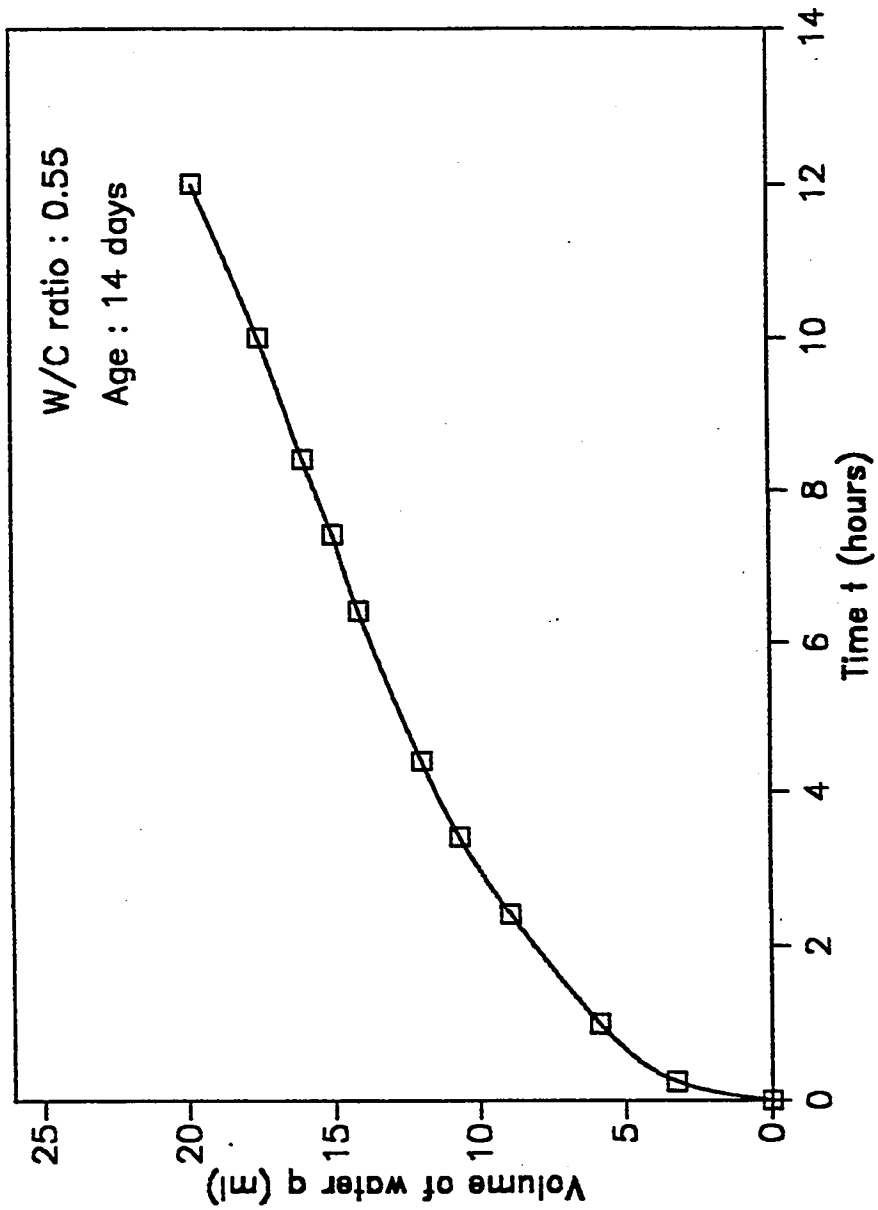

Fig 4.3.2.8: 'q' vs 't' curve for Plain Cement Concrete (W/C: 0.55; Age: 14days)

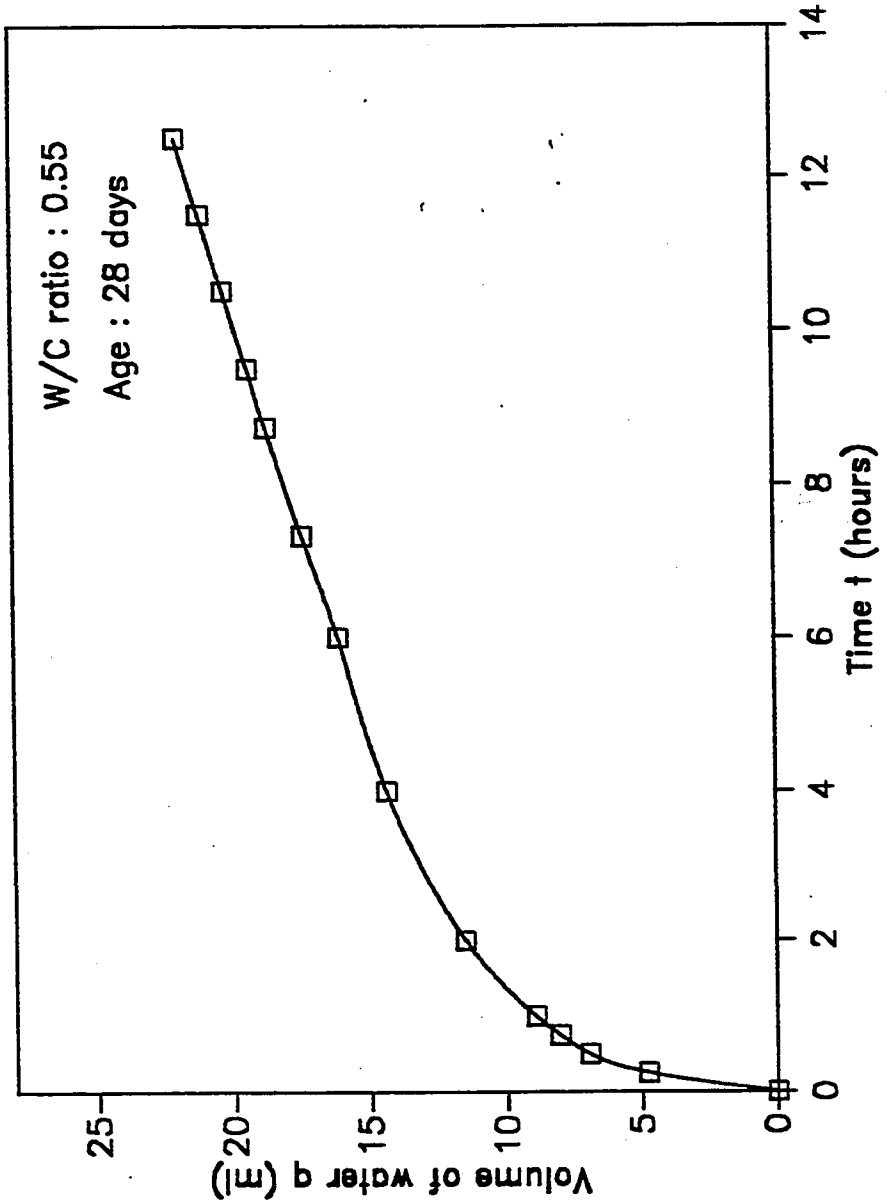

Fig 4.3.2.9: 'q' vs 't' curve for Plain Cement Concrete (W/C: 0.55; Age: 28days)

Table 4.3.2.1: Effect of Water Cement Ratio and Age on Coefficient of Permeability of Plain Cement Concrete

W/C Ratio	Age (days)	Coefficient of Permeability K(10^{-11} cm/sec)		
		(1)	(2)	mean
0.35	7	7.17	5.23	6.20
0.35	14	3.68	6.60	5.14
0.35	28	1.00	0.95	0.98
0.45	7	44.50	48.80	46.70
0.45	14	9.28	15.10	12.20
0.45	28	3.74	5.61	4.70
0.55	7	127.00	75.30	101.20
0.55	14	23.80	24.20	24.00
0.55	28	19.80	-	19.80

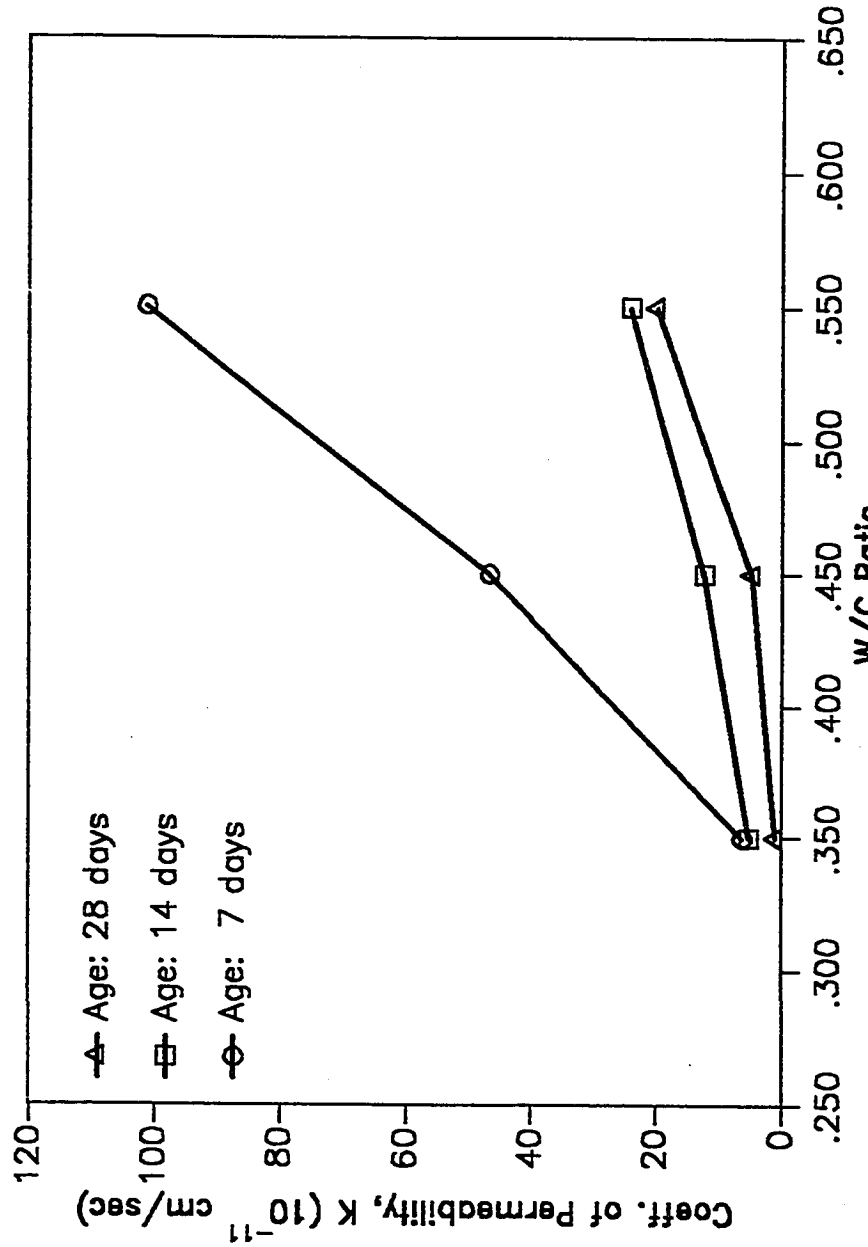

Fig. 4.3.2.10: Effect of W/C Ratio on Coefficient of Permeability of Plain Cement Concrete

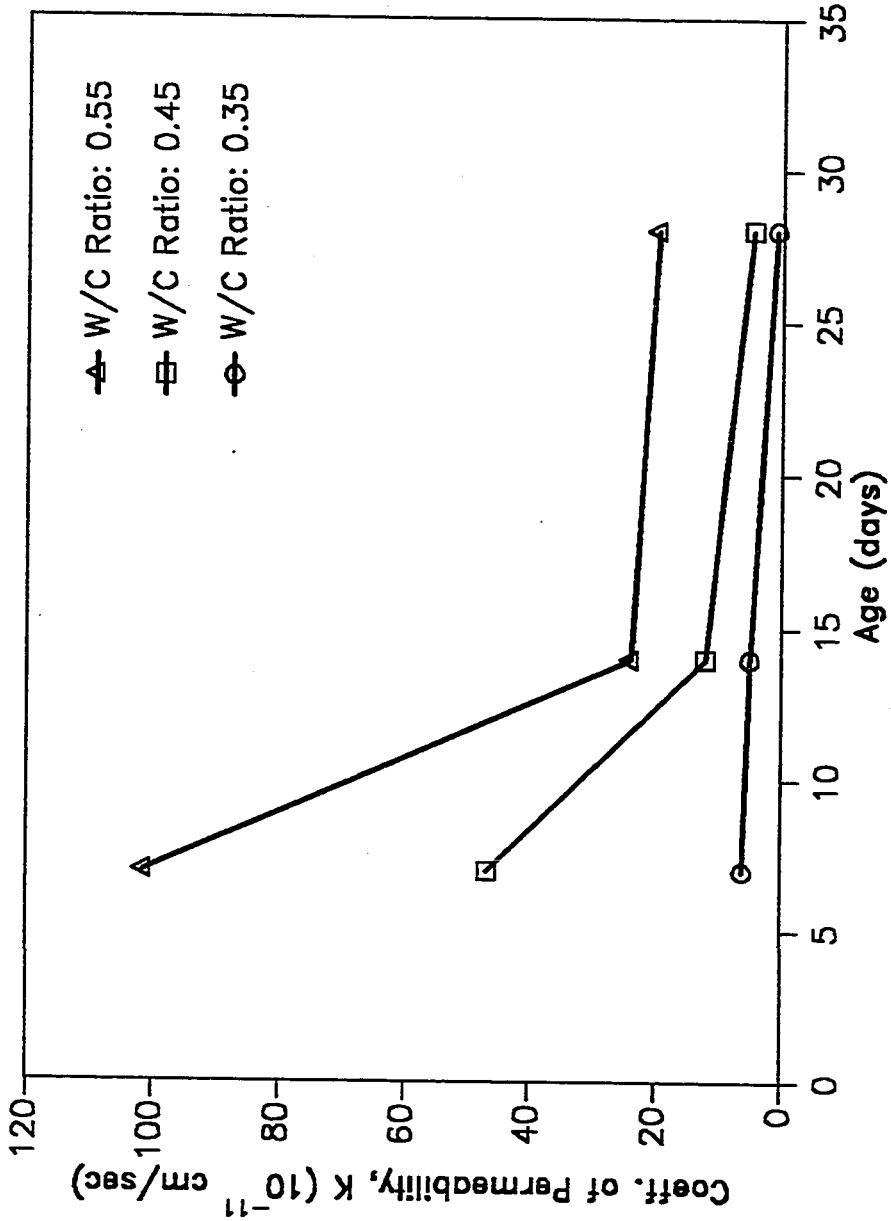

Fig. 4.3.2.11: Effect of Age on Coefficient of Permeability of Plain Cement Concrete

4.3.2.2 Permeability of Blended Cement Concretes

Figs. 4.3.2.9 and 4.3.2.12 through 4.3.2.25 show q versus t curves for the plain (control) and the blended cement concrete test at three different ages of 28, 90 and 180 days. The coefficients of permeability are computed from the steady-state portions of the q-t curves. A pressure of 300 psi was used for the specimens tested at 28 days and 60 days, whereas a pressure of 600 psi was used for specimens tested at 180 days to reduce the time of the test. Coefficients of permeability for the plain and the blended cements are shown in Table 4.3.2.2 and Fig. 4.3.2.26.

The data show that the coefficient of permeability drops steeply when the curing period is increased form 28 to 90 days in the plain, fly ash and slag cement concretes. From 90 to 180 days the rate of decrease in permeability reduces for these cements. For the 10 and 20% microsilica blended cement concretes, the rate of decrease in the coefficient of permeability is less than the other cements. This implies that the structure of the microsilica blended cements is developed better than other cements even at the age of 28 days. Further increase in curing period decreases permeability at a lower rate than the plain, fly ash and slag cements. A comparison of coefficients of permeability of the blended cements show that, all the blended cement concretes showed lower permeability than the plain cement concrete for all the ages. The permeability was found to be least in the 20% microsilica blended cement concrete followed by the 10% microsilica, blast furnace slag and fly ash blended cement concrete. At 6 months, the coefficient of permeability of the 20 and 10% microsilica, slag and fly ash blended cement concrete were 16, 12, 10 and 5 times less than that of the plain cement concrete respectively.

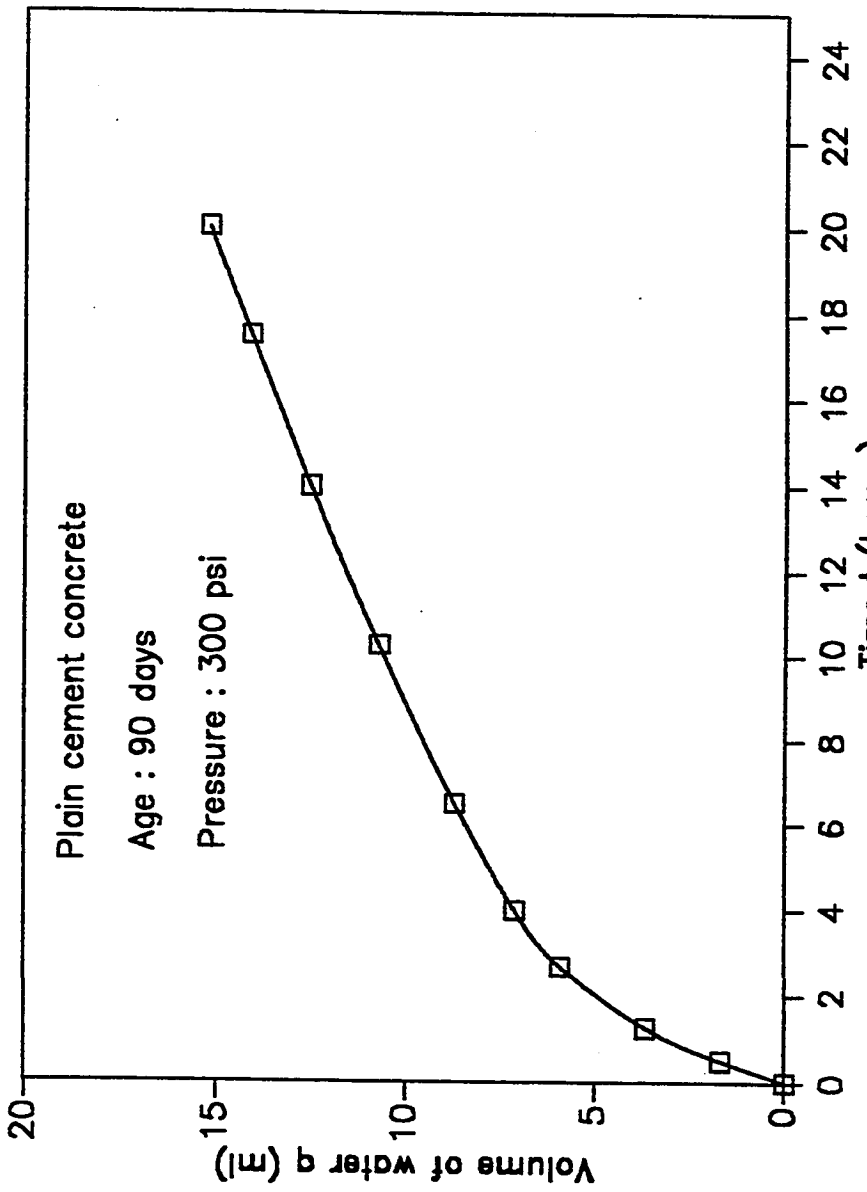

Fig 4.3.2.12: 'q' vs 't' curve for Plain Cement Concrete (Age: 90 days)

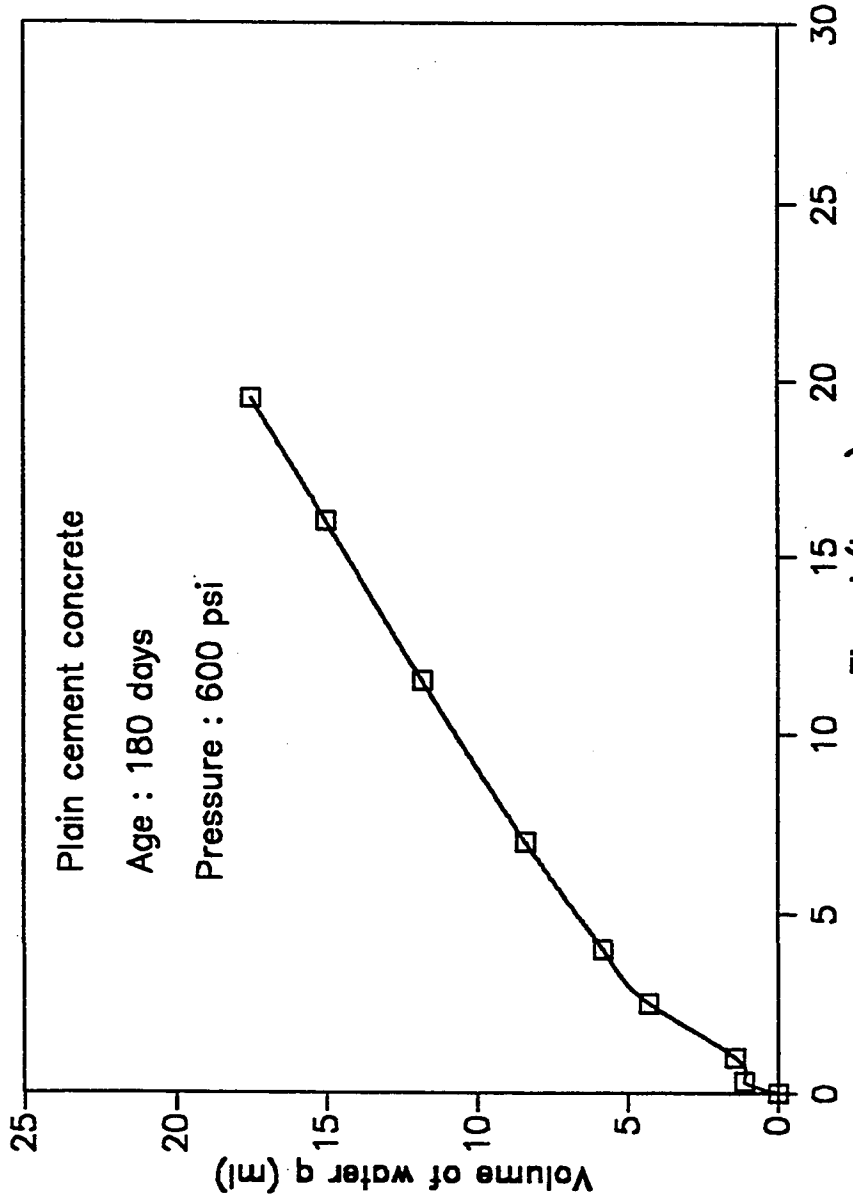

Fig 4.3.2.13: 'q' vs 't' curve for Plain Cement Concrete (Age: 180 days)

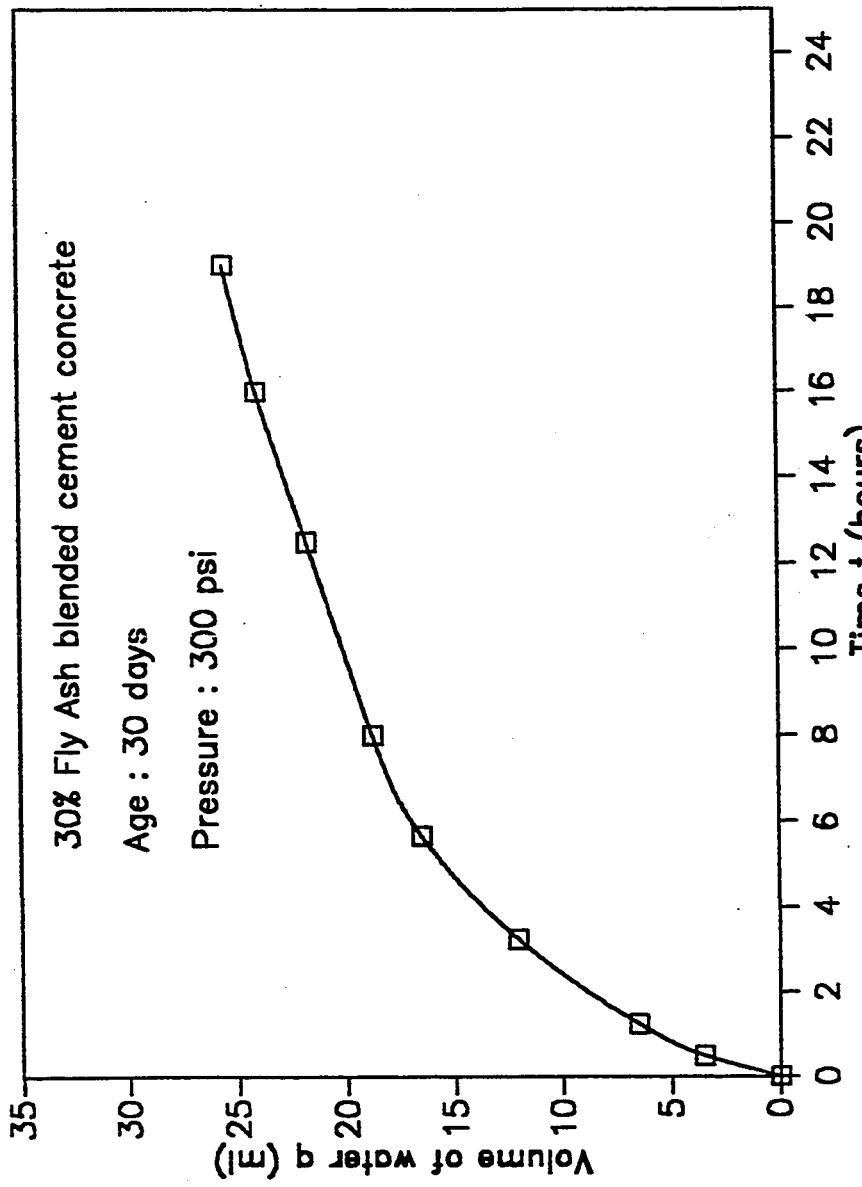

Fig 4.3.2.14: 'q' vs 't' curve for Fly Ash Blended Cement Concrete (Age: 28 days)

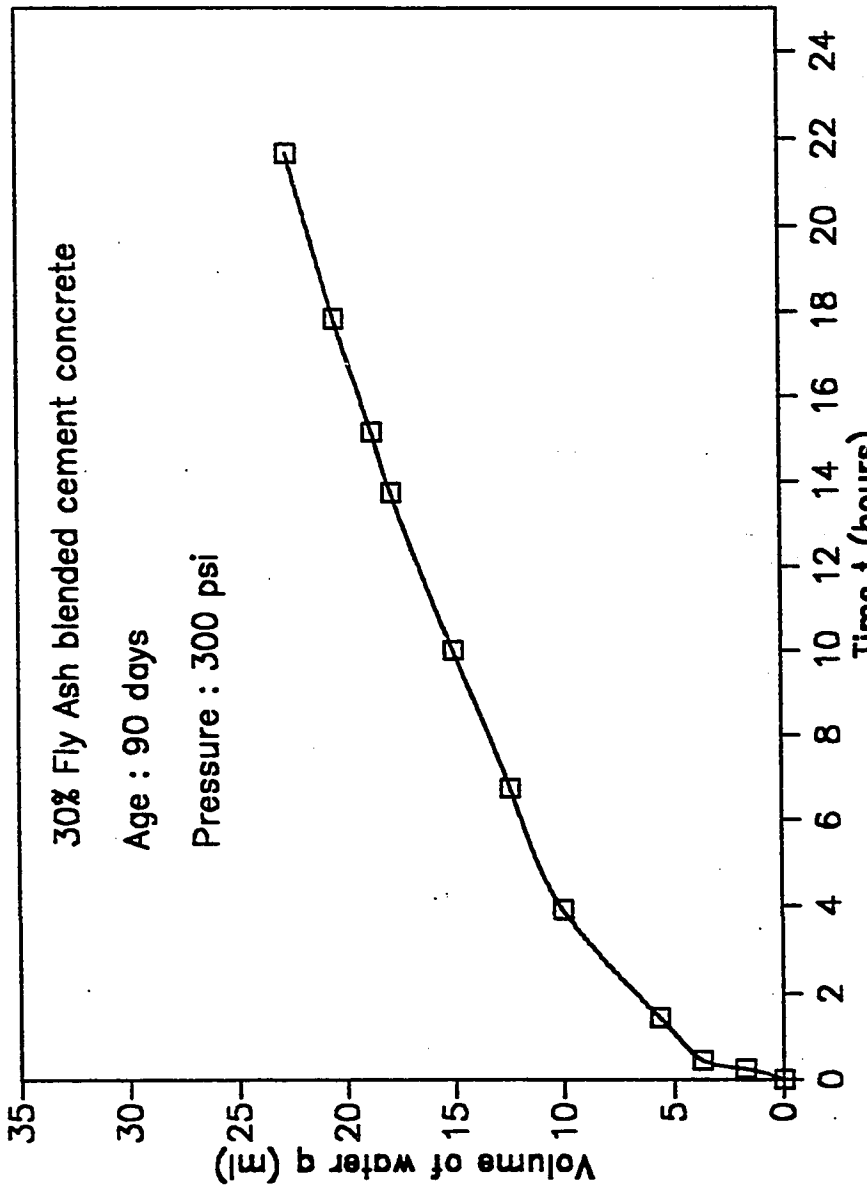

Fig 4.3.2.15: 'q' vs 't' curve for Fly Ash Blended Cement Concrete (Age: 90 days)

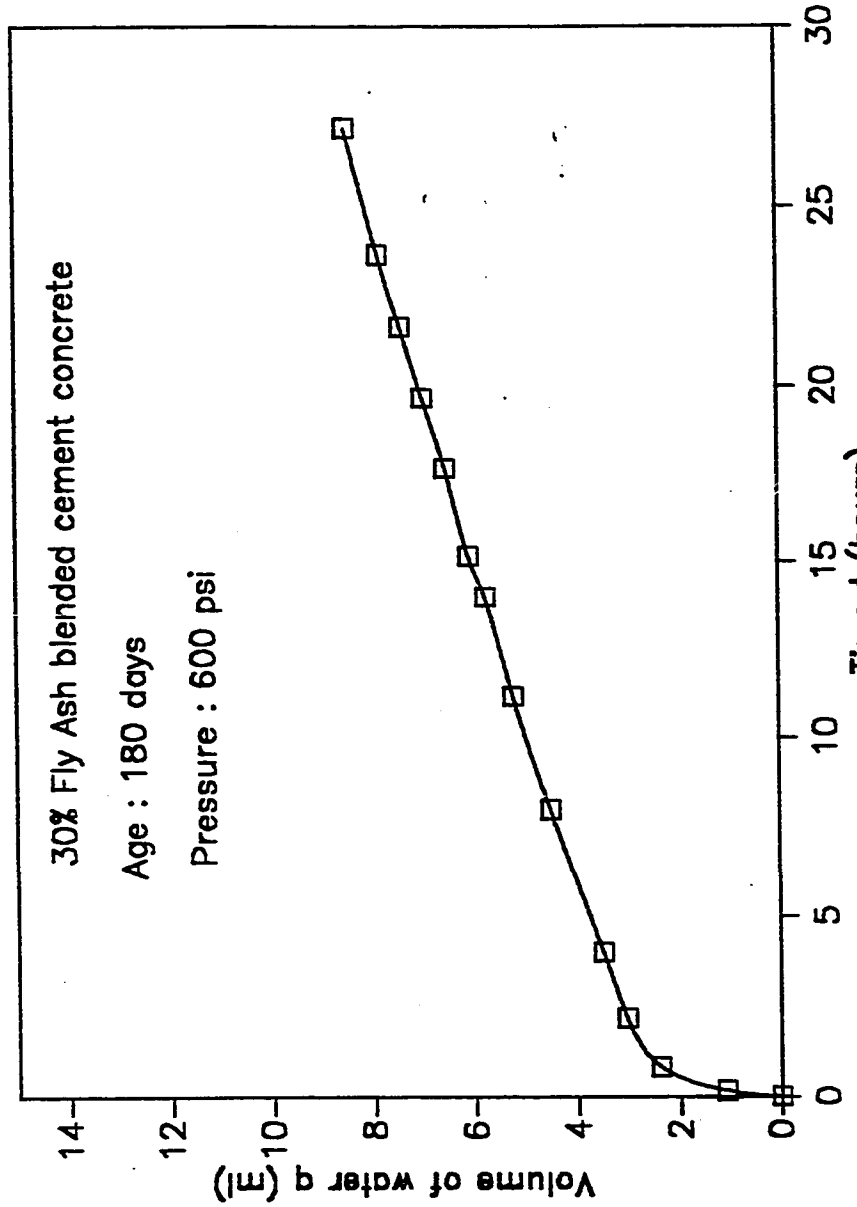

Fig 4.3.2.16: 'q' vs 't' curve for Fly Ash Blended Cement Concrete (Age: 180 days)

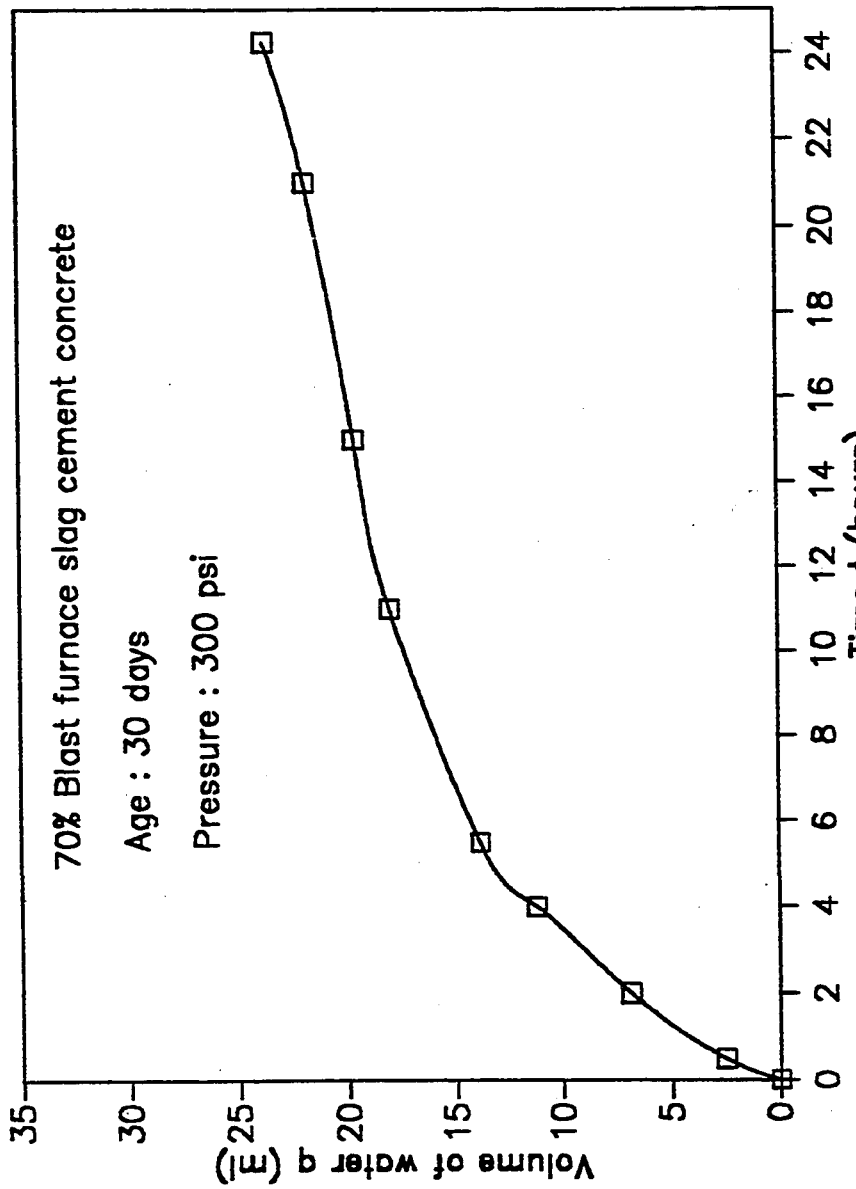

Fig 4.3.2.17: 'q' vs 't' curve for Blast Furnace slag Cement Concrete (Age: 28 days)

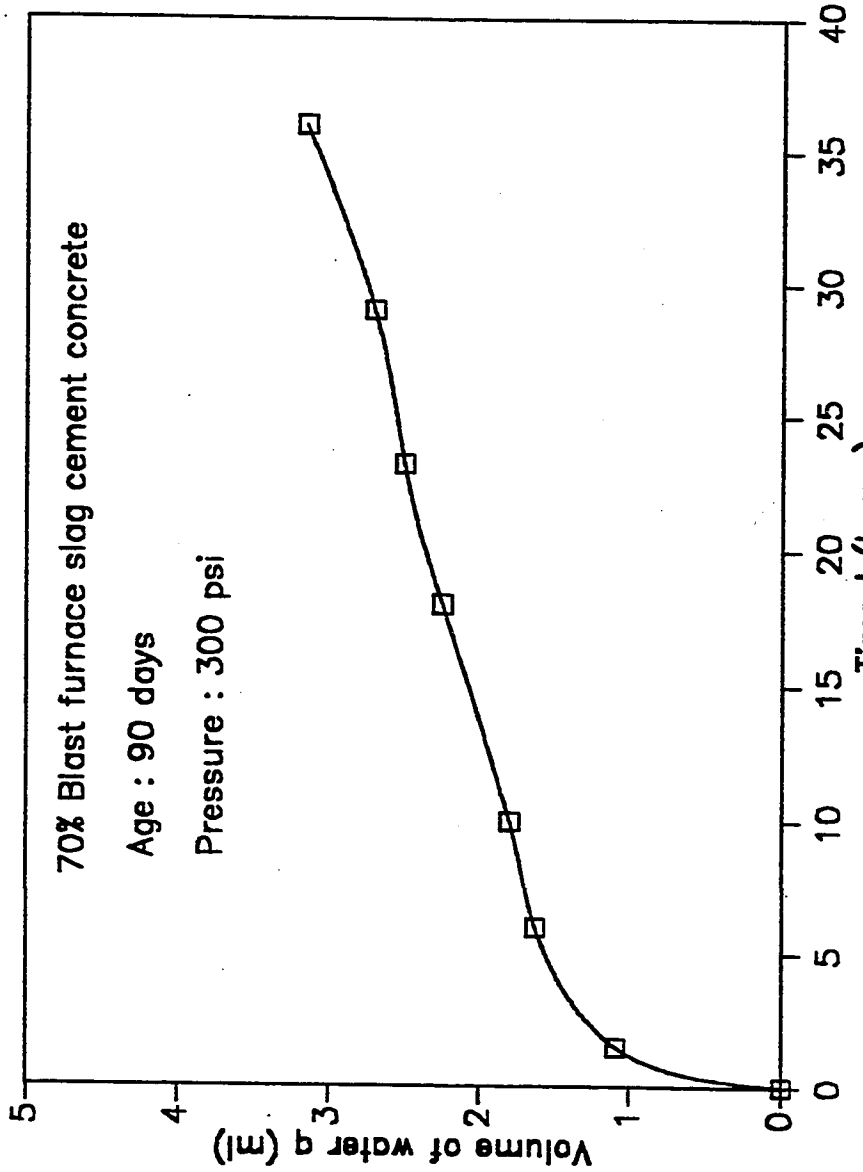

Fig 4.3.2.18: 'q' vs 't' curve for Blast Furnace slag Cement Concrete (Age: 90 days)

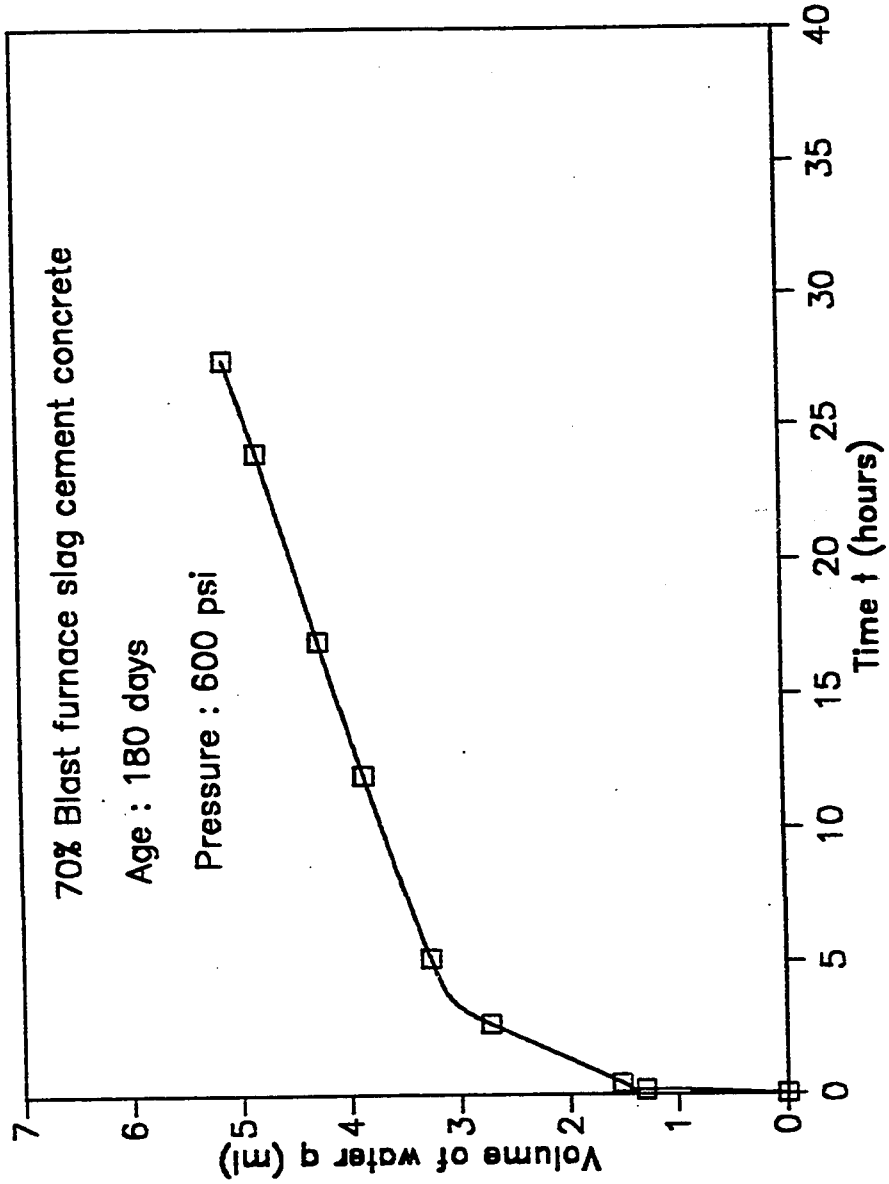

Fig 4.3.2.19: 'q' vs 't' curve for Blast Furnace slag Cement Concrete (Age: 180 days)

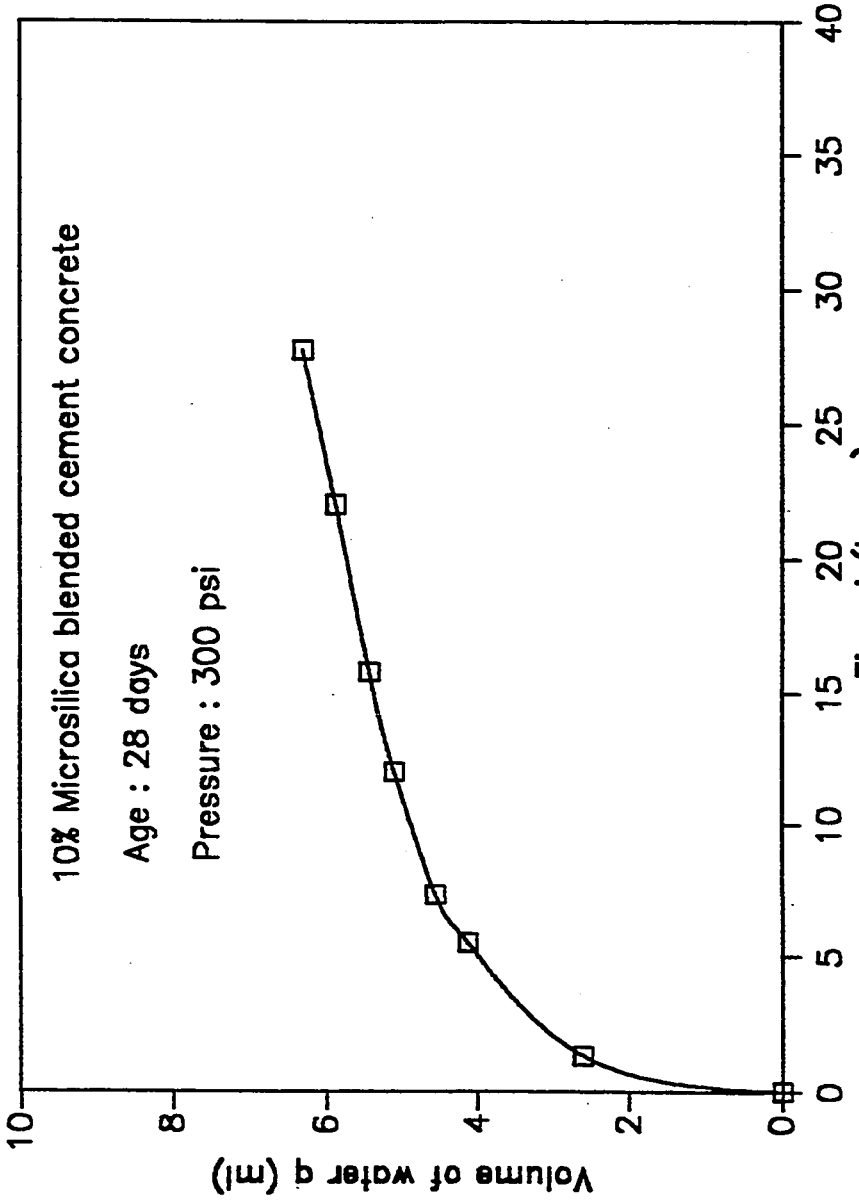

Fig 4.3.2.20: 'q' vs 't' curve for 10% Microsilica Blended Cement Concrete (Age: 28 days)

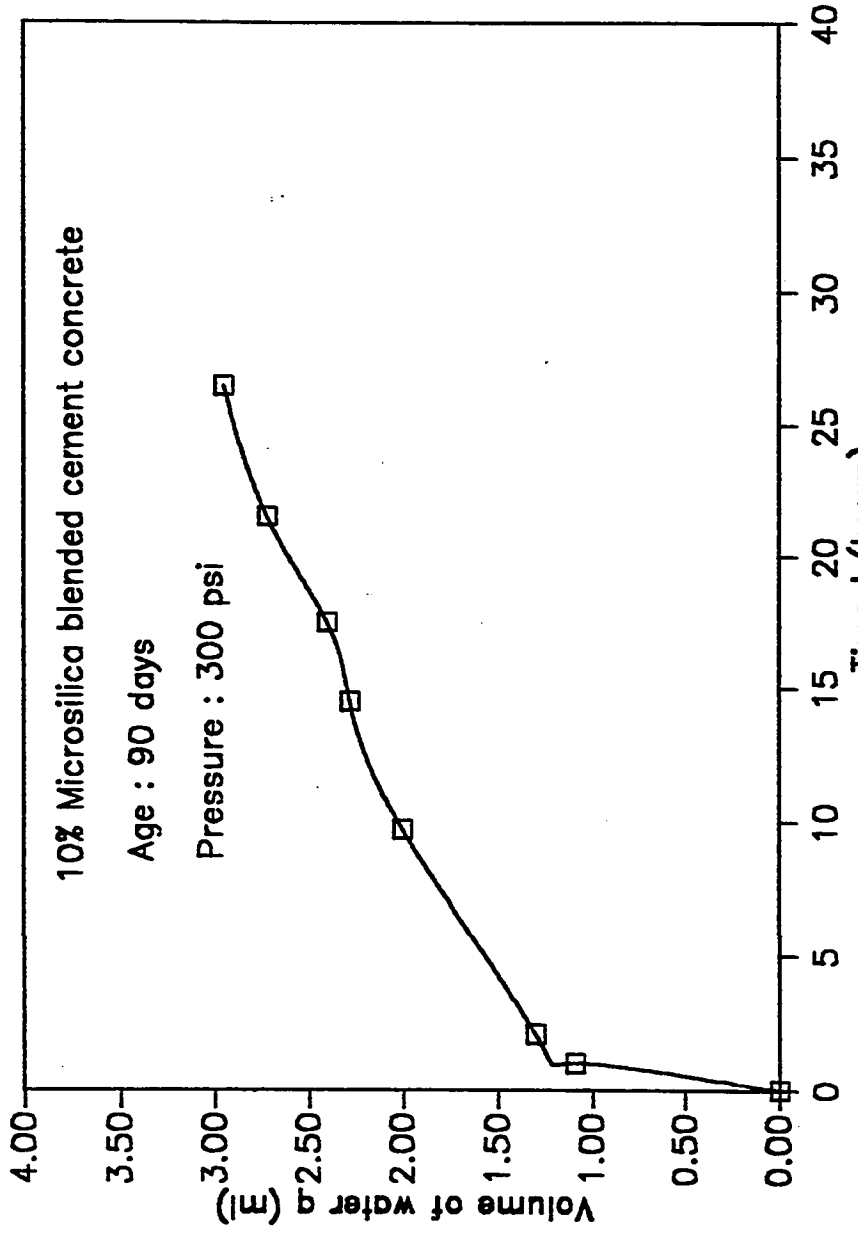

Fig 4.3.2.21: 'q' vs 't' curve for 10% Microsilica Blended Cement Concrete (Age: 90 days)

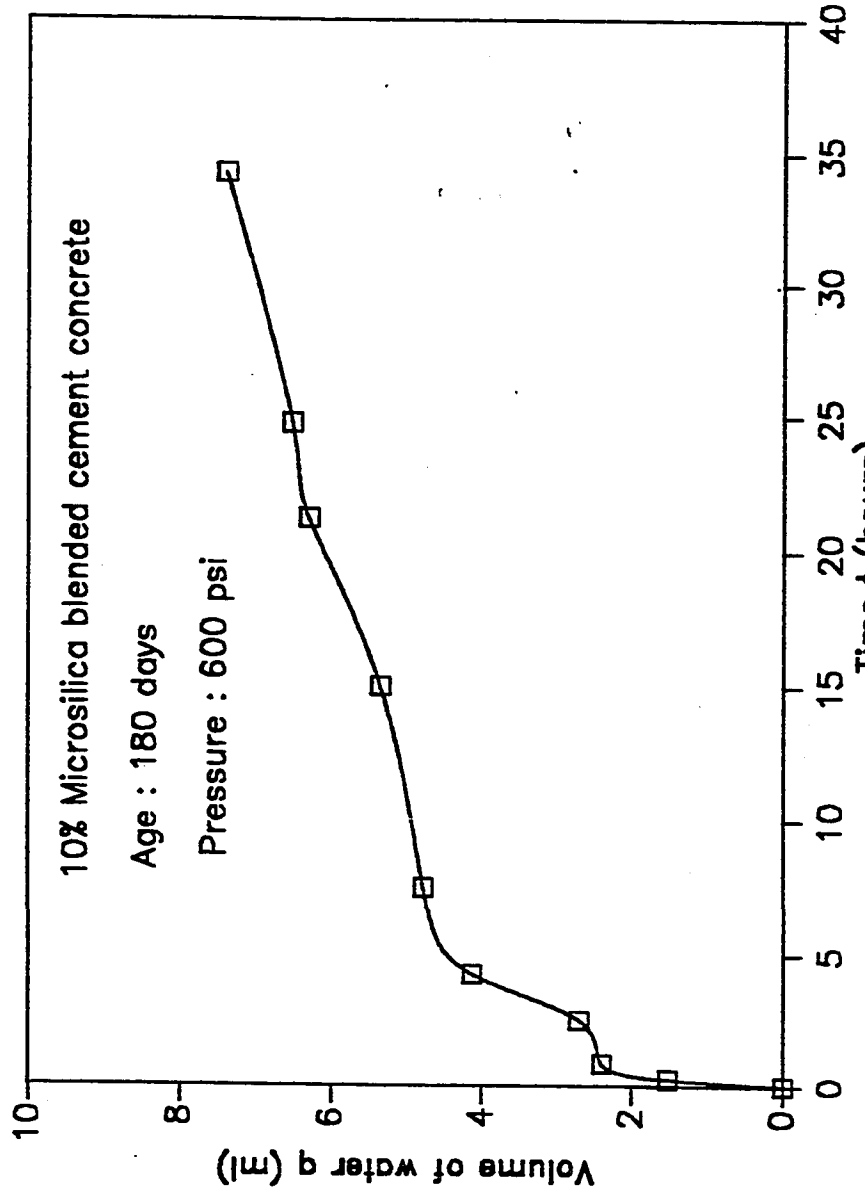

Fig 4.3.2.22: 'q' vs 't' curve for 10% Microsilica Blended Cement Concrete (Age: 180 days)

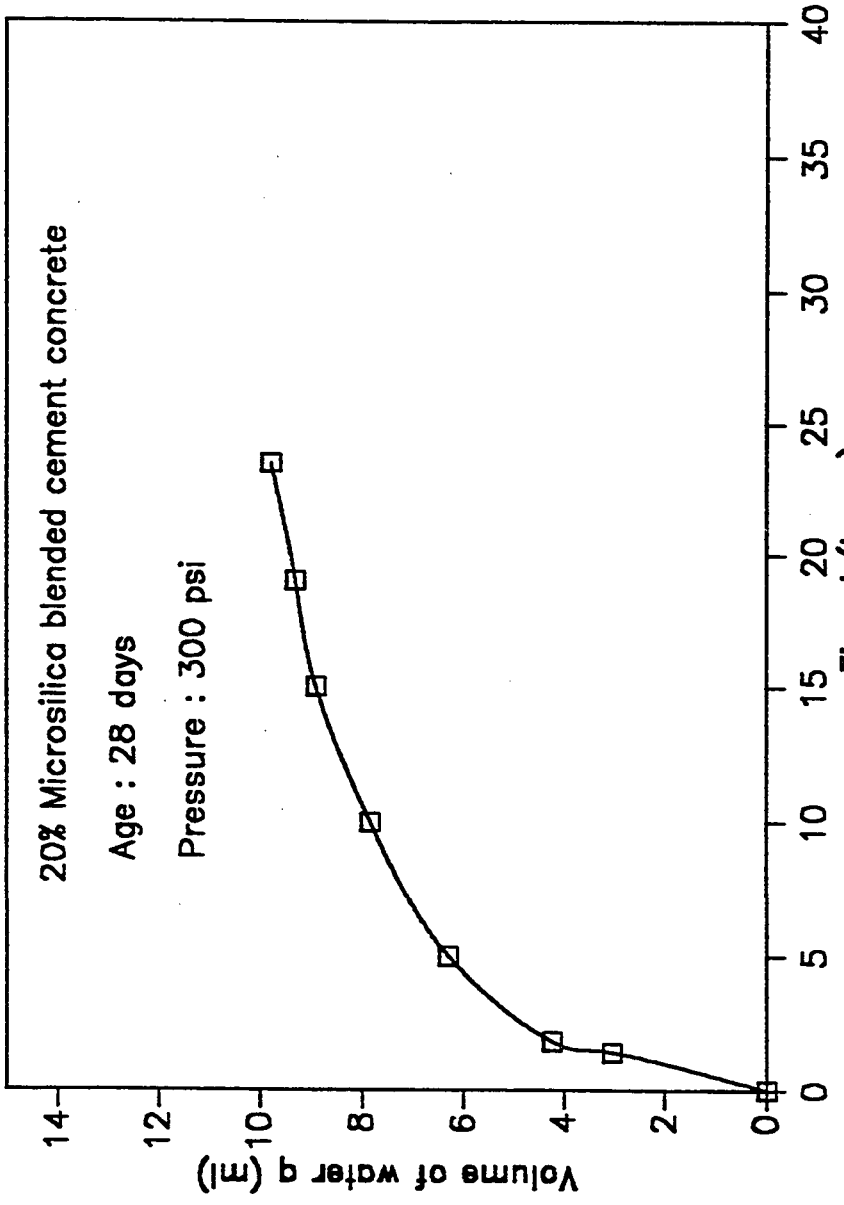

Fig 4.3.2.23: 'q' vs 't' curve for 20% Microsilica Blended Cement Concrete (Age: 28 days)

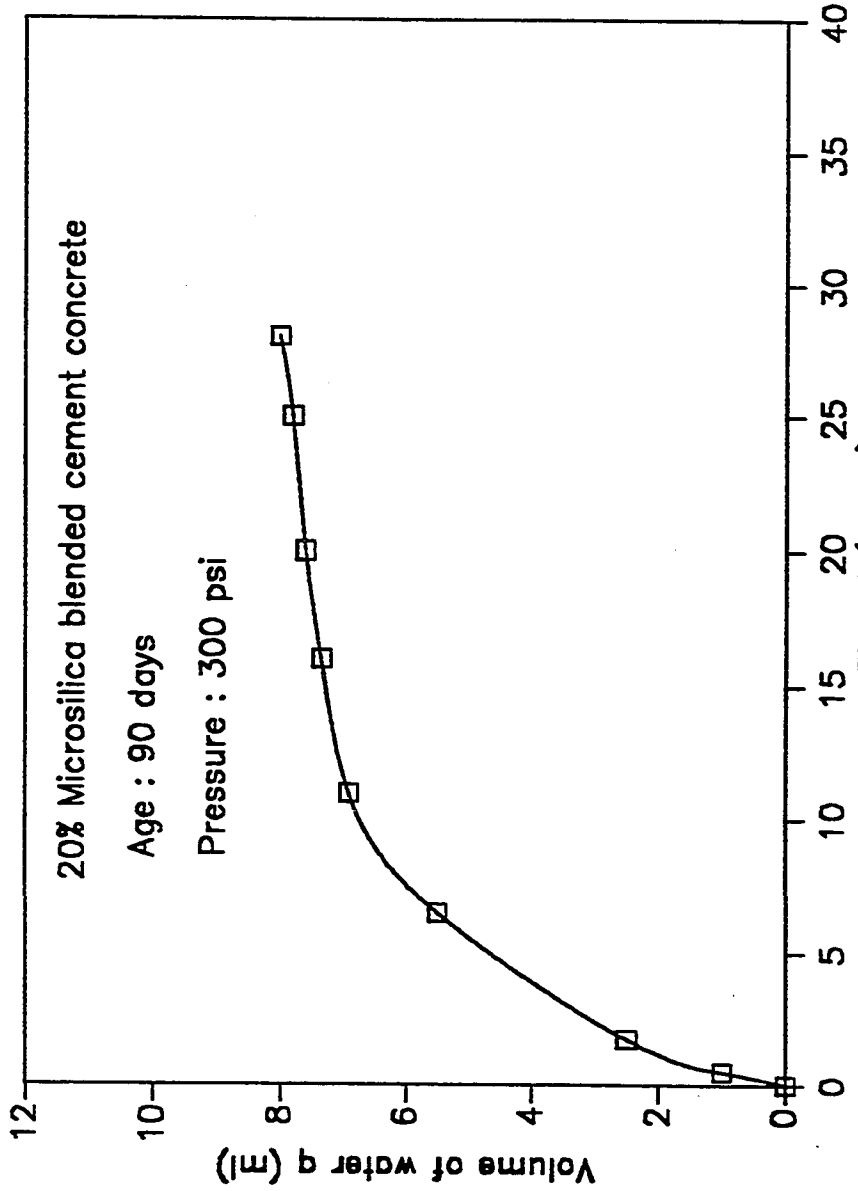

Fig 4.3.2.24: 'q' vs 't' curve for 20% Microsilica Blended Cement Concrete (Age: 90 days)

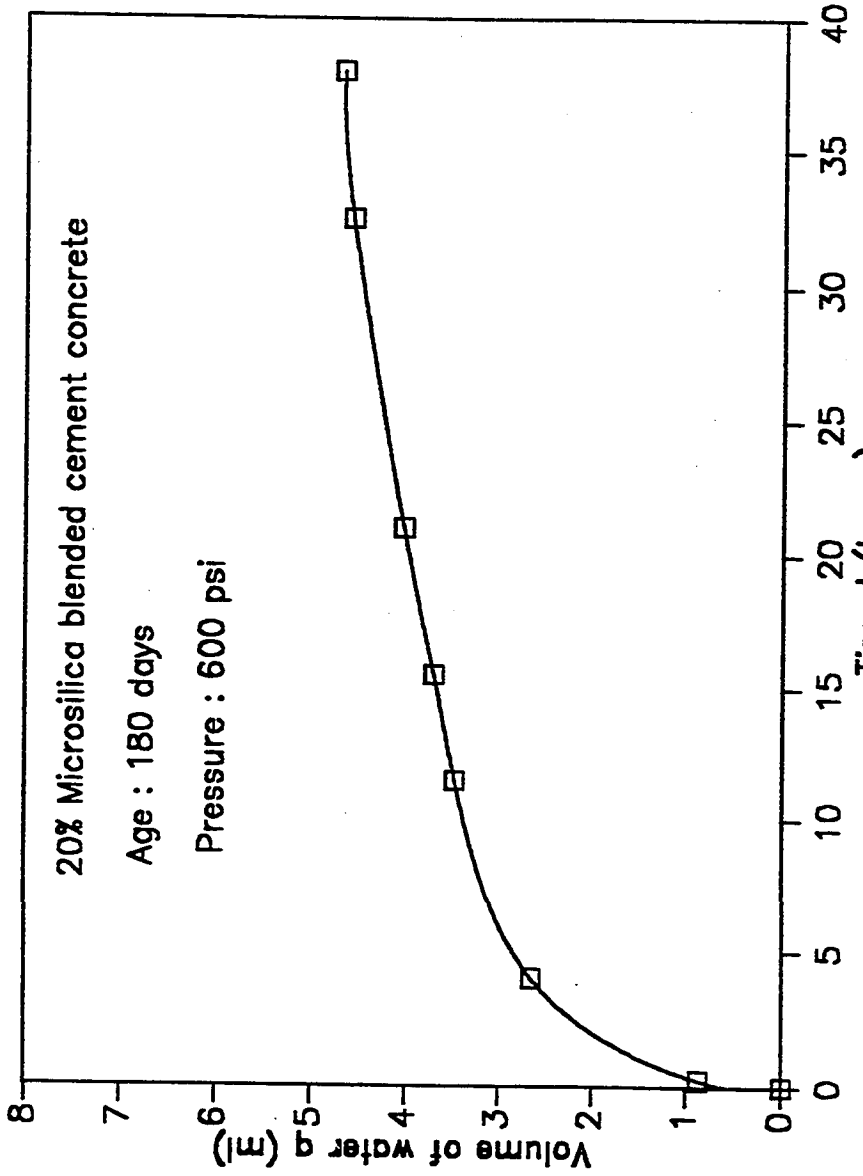

Fig 4.3.2.25: 'q' vs 't' curve for 20% Microsilica Blended Cement Concrete (Age: 180 days)

Table 4.3.2.2: Coefficient of Permeability of Plain and Blended Cement Concrete

Cement Type	Coefficient of Permeability K(10^{-11} cm/sec)		
	28 days	60 days	120 days
OPC*	19.80	9.30	8.70
FA*	11.20	4.00	1.77
BFSC*	7.39	1.58	0.86
MS10*	2.37	1.18	0.72
MS20*	2.31	1.00	0.53

* OPC : Plain Cement Concrete
* FA : 30% Fly Ash Blended Cement Concrete
* BFSC: 70% Blast Furnace Slag Cement Concrete
* MS10: 10% Microsilica Blended Cement Concrete
* MS20: 20% Microsilica Blended Cement Concrete

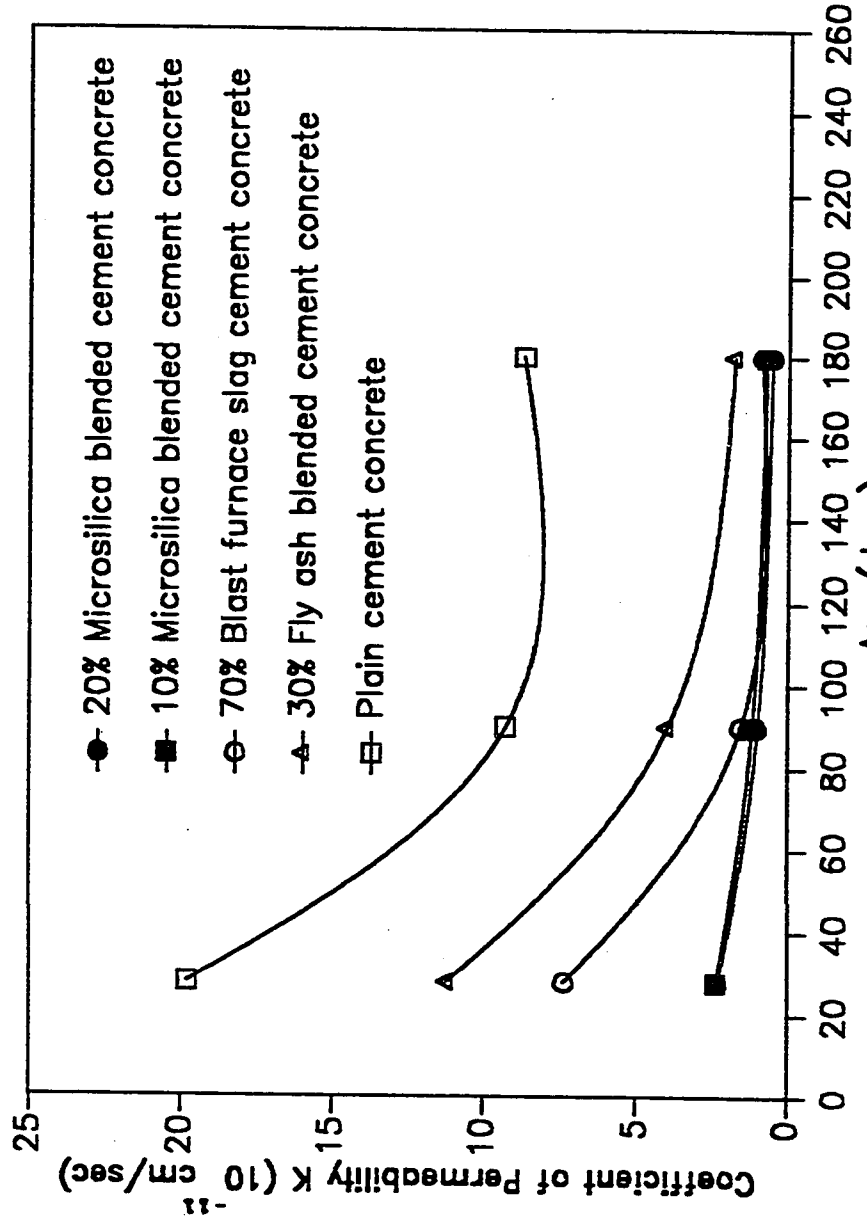

Fig 4.3.2.26: Coefficient of Permeability of Plain and Blended Cement Concrete

The improved impermeability in blended cement concretes is a direct consequence of pore refinement . In recent years there have been attempts to correlate pore structure with permeability. Mehta and Manmohan (68), Hughes (69) and Nyame and Illston (70) have developed correlations between pore structure and permeability using cement pastes. Mehta and Manmohan (68) correlated coefficient of permeability with pore volumes corresponding to arbitrary pore radii of 300 and 1350 A°. Hughes (69) used Poisueille 3-D flow equation to correlate coefficient of permeability with pore radius. He eliminated the restrictive nature of gel pores by neglecting pores with radius less than 75 A° and considering only the continuous pore system by using the second intrusion curve. Nyame and Illston (70) found a good correlation between coefficient of permeability and the smallest pore radius for which there is a continuous capillary pore system through which Darcy's flow can occur. Since the permeability tests were carried out on concretes whereas pore size distribution measurements were conducted on cement pastes, no attempt has been made to correlate the pore size distribution parameters with coefficient of permeability in this study. However, a general correlation/relationship can be observed between the average pore radius and the coefficient of permeability.

4.3.3 CHLORIDE ION DIFFUSION

Chloride ion diffusion tests were conducted on 8mm thick cement paste discs cut from 4x6 inch (100x150 mm) cylindrical specimens cured in saturated calcium hydroxide solution for 90 days. Figs. 4.3.3.1 and 4.3.3.2 show the rate of increase in chloride concentration in chamber B containing saturated calcium hydroxide solution, for the plain and the blended cement pastes. It is seen from Fig. 4.3.3.1 that the rate of increase of chloride ion concentration in chamber B is higher for the type V 2.43%

C_3A cement compared to the Type I 14% C_3A cement. Also, it is seen from the comparison of Figs. 4.3.3.1 and 4.3.3.2 that the rate of increase of chloride ion concentration in chamber B is significantly lower for the blended cements compared to the plain cements.

Chloride diffusion through hardened cements can be described by Fick's law which states that

$$J = D\ \frac{(C_1 - C_2)}{l}$$

where J = Flux of chloride ion entering chamber B (mole/cm^2-sec),

D = Diffusion constant (cm^2/sec),

C_1 = Chloride concentration in chamber A ,

C_2 = Chloride concentration in chamber B ,

l = Thickness of cement disc (cm).

The solution concentrations C_1 and C_2 are assumed to be equal to the surface activities of chloride ion in moles/cm^3. Hence,

$$\log_e\ [1 + \frac{C_2}{C_1 - C2}] = \frac{DA(t\text{-}t_0)}{Vl}$$

where A = area of cross section of the disc,

t_o = time before establishment of equilibrium of flow across the disc,

V = volume of solution in chamber B.

For $t > t_o$, $C_1 > C_2$, $D = (C_2Vl)/AC_1(t\text{-}t_o) = \frac{Vl}{AC_1}$(slope of C_2 vs t curve).

Thus, the diffusion coefficient D can be calculated form the slopes of ' C_2 ' verses 't' curves given in Figs 4.3.3.1 and 4.3.3.2. The diffusion coefficients, calculated so, are tabulated in Table 4.3.3.1. It is seen that the diffusion coefficient of Type V cement is more than that of the Type I cement. It is tempting to assume that the lower chloride ion diffusivity in the high C_3A cement compared to the low C_3A cement is due to the difference in chloride binding capacity of these cements. However, the effect of chloride-binding in the cement disc is present only in initial stages when the amount of chloride-binding diffused into the discs is small. Due to the limiting chloride-binding capacity of C_3A content of the cements compared to the chloride concentration of the solution in chamber A, difference in the diffusion of chloride ions present is in the initial stage only and once the chloride-binding capacity of the cement is exhausted, a steady-state of diffusion of chloride ions into chamber B is achieved. The time t_o required to achieve a steady-state of diffusion is not only dependent on the chloride-binding of the cement but also on its pore structure. Page et al (61) have also observed a lower diffusion coefficient for Type I cement compared to SRPC Type V cement. They conclude that the low C_3A content of the Type V cement was not solely responsible for the higher chloride diffusion. They rather attribute this to the coarser pore structure of the Type V cement as measured by mercury intrusion porosimeter.

Table 4.3.3.1 also shows that the chloride ion diffusion coefficients are significantly lower for the blended cements compared to the plain cement. The diffusion coefficients for the 30% fly ash, 70% blast furnace slag and 10 and 20% microsilica blended cements are 6, 39, 150 and 300 times less than that for the plain cement. Page et al(61) used a 3 mm thick cement paste disc and found that the diffusion coefficient for 30% fly ash and 65% blast furnace slag cements, cured for 60 days prior testing, were 3 and 11 times less than that for the plain cement. Preece et al(71) found that the chloride

diffusion for 65% blast furnace slag cement was 26 times less than that of the plain cement. Chloride diffusion tests conducted by Byfors (72) on 10 and 20% microsilica cements showed the chloride diffusion for these cements to be 2 and 11 times less than that of the plain cement, for cement paste specimens cured for 14 weeks. The chloride diffusion results for the fly ash and the slag cements in the present study are in good agreement with those of others(61,71). However, the chloride diffusion coefficients of microsilica blended cements obtained in the present study are less than those obtained by Byfors (72) by an order of 2.

The significant reduction in the chloride diffusion in the blended cements compared to the plain cement is a direct consequence of the pore refinement in the blended cements. The average pore radii of the plain, 30% fly ash, 70% blast furnace slag and 10 and 20% microsilica blended cements were 240, 166, 182, 175 and 155 A^0 at an age of 3 months. Apart from the pore refinement, as measured by the mercury intrusion porosimeter, blending by microsilica, blast furnace slag and fly ash may also cause pore blocking resulting from the formation of secondary C-S-H gel, thereby making the pores discontinuous. If the pore structure is discontinuous, the diffusion of chloride ions is hindered. This phenomenon of pore blocking may be responsible for the drastic decrease in the coefficient of chloride diffusion in case of 10 and 20% microsilica blended cements.

The significantly reduced chloride diffusion in the blended cements would be reflected in delayed corrosion initiation times of steel embedded in the blended cements concretes. Even if the chloride-binding capacity of the blended cement is lower than that of the plain cement, as in the case of microsilica blended cements, the significantly lower chloride diffusion would tend to increase the corrosion initiation time of steel in concretes made from such cements.

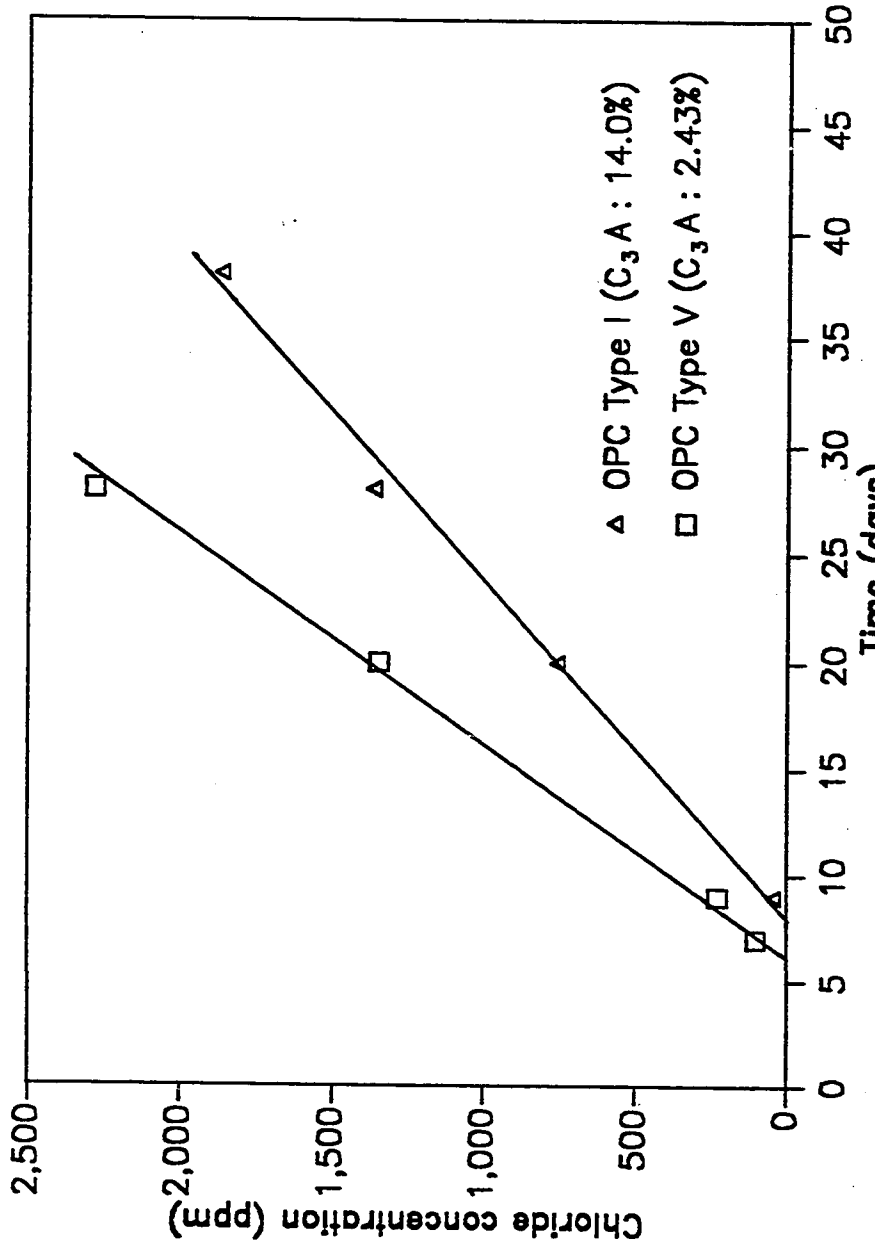

Fig 4.3.3.1: Rate of Increase in Chloride Concentration in Chamber B for Plain Cements

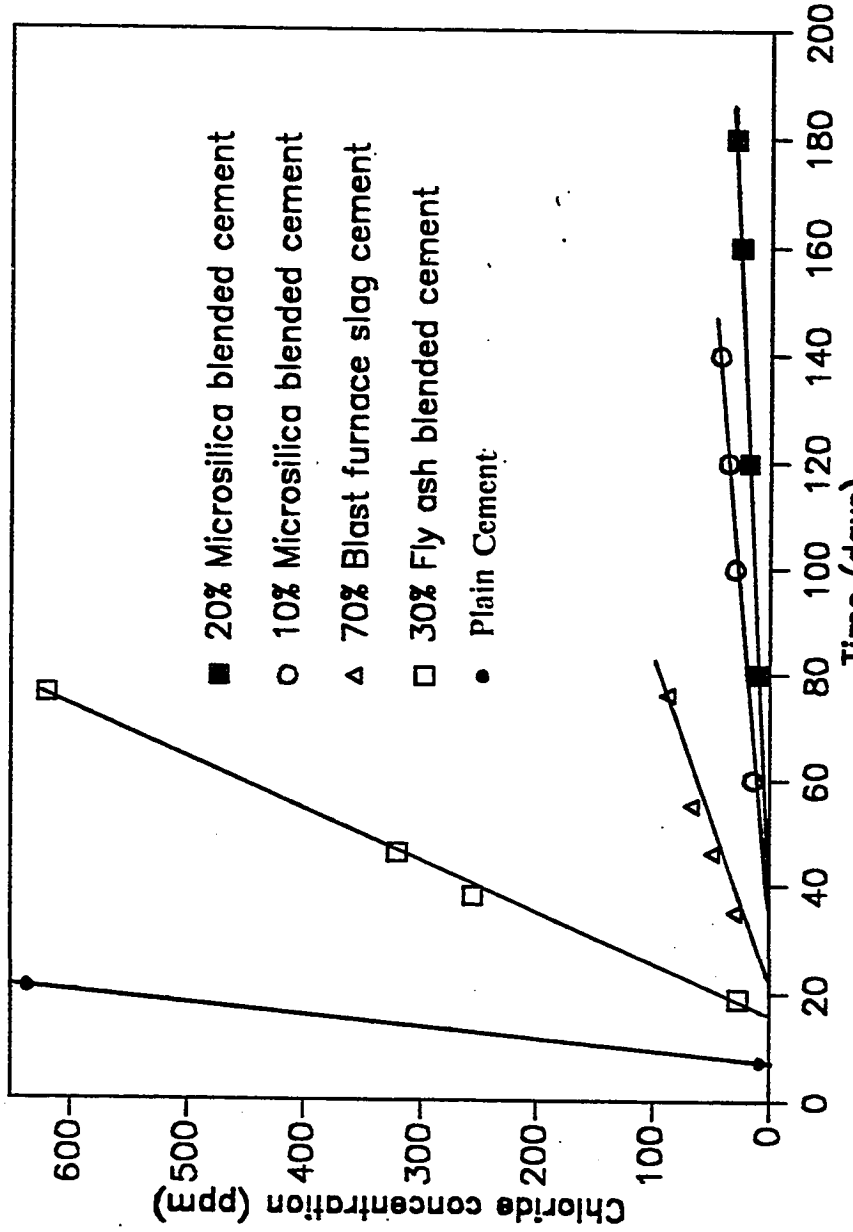

Fig 4.3.3.2: Rate of Increase in Chloride Concentration in Chamber B for Blended Cements

Table 4.3.3.1 Chloride Diffusivity of Plain and Blended Cement Concrete

Cement Type	Chloride Diffusivity (10^{-11} cm /sec)
OPCV*	3300.0
OPCI*	2450.0
FA*	408.0
BFSC*	60.0
MS10*	16.3
MS20*	8.2

* OPCV: Plain Type V Cement Concrete (C_3A:2.43%)
* OPCI: Plain Type I Cement Concrete (C_3A:14%)
* FA : 30% Fly Ash Blended Cement Concrete
* BFSC: 70% Blast Furnace Blended Cement Concrete
* MS10: 10% Microsilica Blended Cement Concrete
* MS20: 20% Microsilica Blended Cement Concrete

4.3.4 ELECTRICAL RESISTIVITY

Electrical resistivity R of concrete was calculated from the values of resistance of the 3x6 inch cylindrical specimens measured by the resistivity meter as follows:

$$R = \frac{rA}{L}$$

where r = resistance value recorded by the resistivity meter (k ohm),

A = area of cross-section of the specimen, ($cm^{2)}$

L = length of the specimen (cm).

The values of the resistivity of saturated samples of the plain and the blended cement concrete for curing ages of 28, 60 and 120 days are shown in Table 4.3.4.1 and Fig. 4.3.4.1. It is seen that the resistivity increases with the curing age for the plain and all the blended cement concretes. The resistivity of the blended cement concretes is more than that of the plain cement concrete at all the three ages. At an age of 120 days, the resistivity values for the fly ash, blast furnace slag and 10 and 20% microsilica blended cement concrete are 2.2, 2.6, 3.2 and 5.7 times more than that for the plain cement concrete. Vennesland and Gjorv (31) measured electrical resistivity of microsilica blended cement concrete using cement factors of 100, 200 and 400 kg./m^3 concrete. They found that at four months age, 10 and 20% microsilica blending increased the resistivity of concrete by 1.6 and 3 times for the cement factor of 100 kg./m^3, 3.1 and 7.2 times for the cement factor of 200 kg./m^3, and 6.5 and 14.3 for the cement factor of 400 kg./m^3.

In the corrosion process of reinforcing steel in concrete, once corrosion of steel is initiated due to depassivation, the corrosion propagation rate is controlled by rate of

Table 4.3.4.1: Electrical Resistivity of Plain and Blended Cement Concrete

Cement Type	Resistivity (K ohm-cm)		
	28 days	60 days	120 days
OPC*	6.68	10.52	13.14
FA*	6.86	14.38	29.08
BFSC*	9.10	18.10	34.53
MS10*	10.44	22.48	42.23
MS20*	26.92	52.53	74.31

* OPC : Plain Cement Concrete
* FA : 30% Fly Ash Blended Cement Concrete
* BFSC: 70% Blast Furnace Slag Blended Cement Concrete
* MS10: 10% Microsilica Blended Cement Concrete
* MS20: 20% Microsilica Blended Cement Concrete

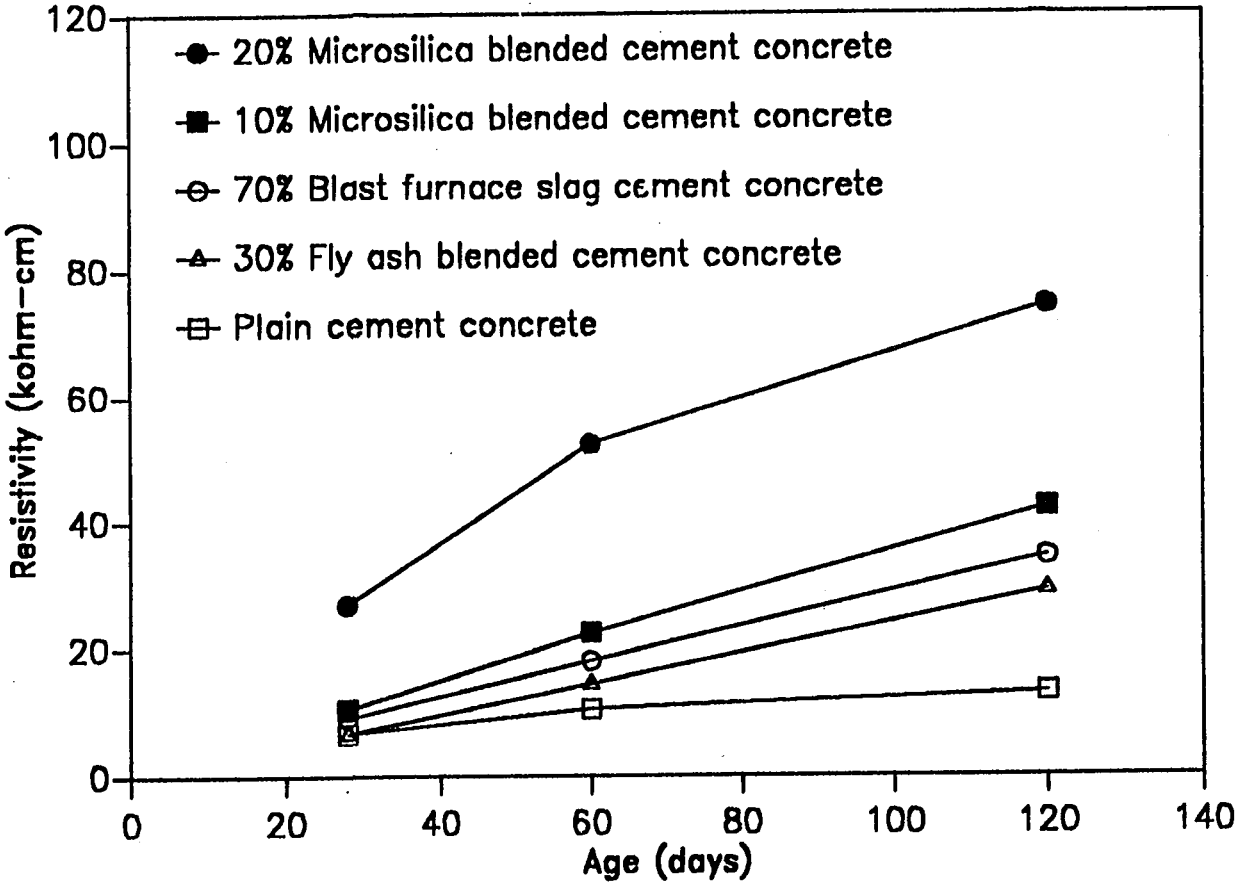

Fig 4.3.4.1: Electrical Resistivity of Plain and Blended Cement Concrete

diffusion of oxygen and moisture to the steel surface, composition of concrete pore solution in terms of Cl^-/OH^- ratio, and resistivity of concrete. The more the resistivity the less will be the corrosion rate. In a corrosion study carried out by Gewertz (73) on a California bridge, the corrosion deterioration of reinforcing steel bars was found to be inversely proportional to the electrical resistivity of the concrete. Thus, the increased resistivity of the blended cement concrete would result in a significant reduction in corrosion rate of the reinforcing steel.

4.3.5 OXYGEN DIFFUSION

The principle used in the measurement of diffusion of oxygen through concrete is that when a potential in the range of -650 to -900 mV SCE is applied to a steel plate embedded in concrete by means of a potentiostat, the most likely reaction on the steel surface is the oxygen reduction according to the following equation:

$$\frac{1}{2}O_2 + H_2O + 2e^- \longrightarrow 2OH^-$$

The current caused by this reaction is therefore a direct measure of the amount of oxygen reacting at the embedded steel plate. The oxygen flux was calculated from the I-time curves, when a steady-state current is reached using Faraday's law:

$$J(O_2) = \frac{I}{nF},$$

where I = steady state current density,

n = 4 and

R = Faraday's constant (96494 Coulombs/mole).

The steady state current values are recorded for the plain and blended cement concrete specimens and oxygen diffusion is calculated using Faraday's law. The calculated

oxygen flux values are given in Table 4.3.5.1. The values given in Table 4.3.5.1 represent average values obtained from two specimens. Oxygen flux for the plain and the blended cements are also shown in Fig. 4.3.5.1.

The data of Table 4.3.5.1 and Fig. 4.3.5.1 show that the plain cement concrete shows maximum and the fly ash blended cement concrete shows minimum oxygen flux. In the fly ash cement concrete, the oxygen flux is about 100 times less than that in the plain cement concrete. However, the other three blended cements showed a moderate reduction in oxygen flux values. The slag cement concrete and the 10 and 20% microsilica blended cement concretes show oxygen flux values 5, 1.5 and 2.1 times less than that in the plain cement. The data show that the fly ash blending drastically decreases oxygen flux through concrete and the blast furnace slag blending is also significantly effective in reducing oxygen flux. However, both 10 and 20% microsilica blending are moderately effective in reducing oxygen flux through concrete. Results on the effect of fly ash and slag are not available in the literature. However, studies carried out by Vennesland and Gjorv (31) on microsilica blended cement concrete also show that 10 and 20% microsilica blending to cement caused little change in the oxygen flux through concrete.

Table : 4.3.5.1 : Oxygen Flux of Plain and Blended Cement

Cement Type	Oxygen Flux (10^{-10} mole/cm^2-sec)
Plain	9.42
Fly Ash Blended Cement	0.10
Blast Furnace Slag Cement	1.89
10% Microsilica Blended Cement	6.44
20% Microsilica Blended Cement	4.40

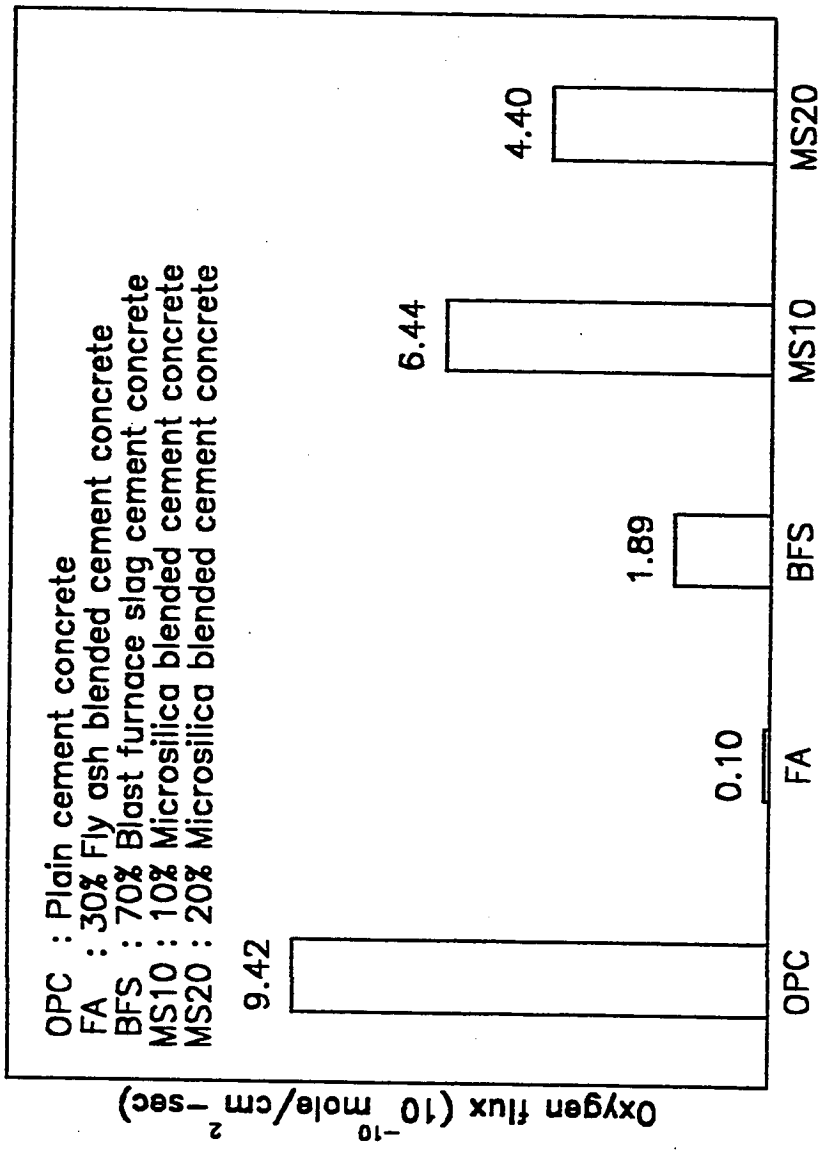

Fig 4.3.5.1: Oxygen Flux for Plain and Blended Cement Concrete

4.4 CONTROL OF ALKALI-SILICA REACTIONS IN BLENDED CEMENT CONCRETE

Mortar-bar expansion data up to a period of six months for the plain parent cement (control) and the microsilica, slag and fly ash blended cements are plotted in Fig.4.1.2.1. The final six-month expansions are shown in Fig. 4.1.2.2 to facilitate quantitative comparison.

The hydroxyl ion concentrations and the pH values of the pore solutions extruded from various plain and blended cements containing different levels of alkalies are given in Table 4.1.2.1.

It must be noted that the measured values represent changes in the OH^- concentrations only, without taking into account the volume of pore solution due to its chemical consumption during the formation of chemical hydrates. The proportion of chemically bound water in mature hydrated cement pastes of constant water/solids ratio decreases in blended cements. Also, the "evaporable water", which is the residual capillary water after its progressive reduction by the ongoing process of cement hydration, increases as the replacement level by blend material increases.

The mortar-bar expansion results show that for the plain parent cement (equivalent Na_2O 1.2%), the expansions began immediately with no incubation period with the highest rate obtainable for the first 20 days, thereafter decreasing gradually to a low value. A highly unacceptable final value of 0.865%, 8.65 times the allowable 0.1% value, was measured at the end of the six-month period for the plain cement. Replacement by 10% and 20% microsilica (1.11 and 1.02% alkalies) decreased the six-month

expansion values to 0.023% and 0.009% respectively. For the 60% and 70% blast furnace slag cements (equivalent Na_2O values 0.76% and 0.69% respectively), the corresponding values were 0.04% and 0.028%. Expansion with 30% fly ash blended cement is at the 6 months permissible limit (0.1%) and in view of the fact that the reactivity of the aggregate is unusually high and the alkali content is also high, this performance of fly ash should be acceptable.

The measured OH^- concentrations in the pore solution ranged from a maximum of 946 mM/L for the high 1.5% alkali content to a low of 13 mM/L for the 25% microsilica blended cement with 0.65% alkali content. The corresponding pH levels ranged from 13.98 to 12.82.

Microsilica, slag and fly ash inductions reduced hydroxide ion concentrations significantly. The reduction, however, was drastic (for example, from 946 mM/L to 16 mM/L for the 1.5% alkali cements) with 25% microsilica. Also, in medium 0.9% alkali cements, 60% blast furnace slag appears to be an alkali remover comparable to 10% microsilica. However, in the case of high 1.5% alkali cements, 10% microsilica is appreciably more effective in removing hydroxide ions than 60% slag. It is seen that in the case of 1.5% alkali plain and blended cements, whereas 10% microsilica reduces OH^- concentration from 946 mM/L to 533 mM/L, 60% slag reduces it only to a level of 708 mM/L. 20% microsilica is manifold more effective as an alkali oxide remover than even 70% slag for the whole range of alkali contents included in this program. This is specially so for the high 1.5% alkali cement where 25% microsilica is 37 times as effective as 70% slag.

The rapid accumulation of hydroxide ions in the pore solution as a cation charge balancing mechanism provides the driving force for ASR. The removal of these

hydroxide ions from the pore solution is a key factor in the ASR prevention mechanism.

The data developed in this study confirms the broad correlation reported earlier by others between the hydroxide ion concentration and the ASR generated expansions. However, within this broad correlation there are obvious deviations which are strongly indicative of other possible mechanisms also being concurrently operative in conjunction with alkali removal action. For example, 60% slag cement with 0.76% alkali content showed about twice as much expansion as 10% microsilica cement with 1.11% alkali content, even though the hydroxide ion concentration in the pore solution of the former is only 37% of the concentration measured in the pore solution of the latter. Also, for about equal alkali contents, 10% microsilica cement suffered only $2\frac{1}{2}$ times more expansion compared to 20% microsilica, although the OH^- concentration in 10% microsilica cement paste is $5\frac{1}{2}$ times higher than in the 20% microsilica cement paste.

Blast furnace slag, when inducted in large dosages of 60 to 70% would obviously act as an alkali diluent if its own alkali content is lower than that of the parent cement, as was the case in this study. For the same water to solids ratio, a higher evaporable water content would further facilitate this dilution mechanism. However, apart from these considerations, the data in this study show that the slag acts as an active remover of alkalies, and is specially effective in medium alkali cements, where the performance of 60% blast furnace slag cement as an alkali remover was found to be parallel to 10% microsilica cement. This is also indirectly shown by the data of Longuet et al (52) and explicitly by the data of Canham, Page and Nixon (74), although they state that slags were not found to be particularly efficient as alkali removers when compared with

other cement extenders that are used to control ASR, such as fly ash and microsilica. However, our data also show that this effectiveness decreases as the alkali content of the cement increases. The effectiveness of 70% blast furnace slag is found to be 4.5, 2.1 and 1.5 for the 0.9, 1.2 and 1.5% alkali cements respectively.

The data also show that 30% fly ash blended cement removes alkalies more than 60 and 70% slag blended cement. For example, for 1.5% alkali content, the hydroxyl ion concentrations in fly ash, and 60 and 70% slag cements were found to be 440, 708 and 600 mM/L respectively. However, due to high alkali content of the fly ash, blending of 30% fly ash with a 1.2% alkali cement resulted in the blended cement with alkali content of 1.5%, which is the maximum alkali content in the blended cements used for mortar bar expansion tests. This high alkali content in the fly ash blended cement may be responsible for expansions greater than those in slag and microsilica blended cements.

In order to evaluate the effectiveness of slag as an ASR suppressor, a reference threshold value corresponding to a minimum hydroxide concentration of 250 mM/L (concentration defined pH = 13.4) to initiate and sustain alkali-silica reaction has been proposed by Diamond (75). It is seen that purely on the basis of pore solution chemistry, 70% slag would effectively control ASR for cement alkalies up to 1%. It is only in the case of 1.2% and 1.5% alkalies that the residual OH^- concentrations in 70% slag cements exceed the reference value of 250 mM/L. This discussion specifically pertains to the slag type used in this study. Obviously, slags of other reactiveness and compositions in terms of glass content and C/S ratio may react significantly differently.

Pore solution data show that incorporation of 25% microsilica virtually sweeps nearly all the hydroxide ions from the pore solution even in the high 1.5% alkali con-

tent cements. There are, however, questions about the wisdom of using this relatively high dosage. Apart from the two-fold drying shrinkage, the chemical environment for reinforcing steel corrosion is rendered significantly adverse. Tests carried out by Page and Vennesland (37) show that the pH is reduced from 13.32 to 12.60 and Cl^-/OH^- ratio is increased from 2.83 to 16.64 if microsilica is doubled from 10 to 20%. Results of this study also confirm this position. As the microsilica dosage was doubled from 10 to 20%, the Cl^-/OH^- ratio increased from 1.63 to 15.80 and pH was reduced from 13.34 to 12.40. These Cl^-/OH^- ratios are one order higher than the threshold value of 0.60 proposed by Hausmann (11) for concrete simulated calcium hydroxide solution (pH = 12.5) and a value of 0.30 suggested by Diamond (38) for actual concrete environment where pH is usually in excess of 13.5.

Accelerated corrosion tests (23) also show that there is not much to be gained in terms of time to initiation of corrosion due to the ingress of external chlorides when cement replacement by microsilica is doubled from 10 to 20%.

These data indicate the desirability of keeping microsilica dosage to a minimum, consistent with the achievement of desired goals.

The pore solution data show that 10% addition is sufficient to bring down the OH^- concentration close to the threshold value of 250 mM/L in medium 0.9% alkali cements. However, for higher alkali contents of 1.2% and 1.5%, 10% microsilica does not bring the OH^- ion concentrations below the postulated threshold value of 250 mM/L. That these higher than 250 mM/L concentration do not cause expansions anywhere near the permissible value of of 0.1% is strongly indicated by our expansion data. The 10% microsilica cement (1.11% alkali content) having a hydroxide concentration of 368 mM/L shows 0.023% final expansion which is only one-quarter of the

permissible 0.1% value. This indicates that for blended cements a threshold value of 250 mM/L is excessively conservative. This is possibly ascribable to the fact that in blended cements, preventive mechanisms other than hydroxide ion removal may also be operative concomitantly. There is considerable evidence (76,77) to suggest that the beneficial role of microsilica in mitigating ASR expansion could also be partly explained by the fact that microsilica addition causes a reduction of global C/S ratio of the paste. A microsilica blended cement paste is relatively silica-rich compared to an identical paste without microsilica. It has been shown (77) that silica-rich CSH has a higher sorptive capacity for alkalies. CSH formed in microsilica blended cements would therefore entrap more alkalies leaving less concentrations in the pore fluid. This mechanism would also be operative in blast furnace slag cements if sufficient quantity of reactive slag is added to cement.

Apart from these significant chemical factors, the addition of reactive silica in the form of microsilica, fly ash or slag also brings about very significant changes in the physical structure of blended cements. Incorporation of such blend materials markedly refines pore structure and densifies binder matrix; this results in blocking and segmentation of the pores. Such physical changes effectively retard the transportation of alkalies to reaction sites, thereby mitigating ASR. Bakker (17) has explicitly modelled this mechanism for blast furnace slag cements. With its proven pore refining characteristics, there is no reason why a similar type of mechanism would not be operative for fly ash and microsilica blended cements.

With these preventive mechanisms acting concurrently with favourable chemical factors, the threshold for hydroxide ions should be significantly higher for blended cements than the postulated 250 mM/L. It appears that, at least for microsilica blended cements, it would certainly be in excess of 400 mM/L.

Chapter 5

DURABILITY MECHANISMS

5.1 CORROSION OF REINFORCING STEEL

The corrosion process comprises two distinct phases (62,63) the corrosion initiation period (t_o) and the corrosion propagation time (t_1) as shown in Fig. 5.1. The initiation time (t_o) is the time for the diffusion of aggressive substances through concrete to steel-concrete interface to cause activation of the corrosion process; corrosion initiation time predominantly depends on the physical characteristics of concrete which control the mobility of aggressive ions to the steel level. The propagation time (t_1) represents the period before unacceptable corrosion damage has occurred and is dependent on a complex interplay of numerous factors such as oxygen flow, temperature, resistivity of concrete, cover thickness and quality, size and spacing of bars, moisture content and tensile strength of concrete.

5.1.1 Passivation of Steel in Concrete

The usual chloride free environment of uncarbonated concrete is highly protective against corrosion of embedded steel for three reasons. Firstly, the aqueous environment within concrete matrix is characterized by significant presence of highly alkaline uncombined water in the well-distributed pores or voids of concrete. This environment

passivates steel against corrosion by the formation of a protective submicroscopically thin oxide film comprising predominantly of Fe_2O_3 or Fe_3O_4 (8). Secondly, concrete cover over reinforcement forms a defensive shield against the ingress of substances from the external environment which may destroy the passivation of reinforcement. Thirdly, concrete offers high resistivity to the flow of corrosion current.

5.1.2 Loss of Passivation

For initiation of reinforcement corrosion, the protective oxide film on steel surface must decompose; in practice it may be disrupted by two specific circumstances which are of considerable significance to rebar corrosion mechanism in concrete. First, when the atmospheric carbon dioxide makes an ingress into the concrete matrix and its penetrating front advances deep enough to intercept the steel reinforcement. The ready combination of carbon dioxide with calcium hydroxide of hydrated cement paste signifies consumption of hydroxyl ions thereby tending to lower pH of the pore solution phase below the value needed to maintain the reinforcement in a passive condition. Second, the presence of chlorides in concrete is specially effective in eliminating passivity, because chloride ion has been described as a "specific and unique destroyer" of the passivating film.

5.1.3 Significance of Chloride-Induced Corrosion

The kinetics of carbonation of various types of concrete in different environments has been extensively studied. It has been found that the rate of carbonation decreases with increasing time of exposure to air, and for concrete kept continuously dry at normal relative humidities, the depth of carbonation is approximately proportional to the

square root of the time of exposure. For a suitable grade of concrete the rate of advance of carbonation declines within a fairly short time to a low level of less than 1 mm/year. Several investigators (78,79) have reported the depth of carbonation not to exceed 5-8 mm after 10 years which may increase to 10-15 mm after fifty years of exposure to normal outdoor environment. Thus for an adequate cover to reinforcement of normal density structural concrete, carbonation is not expected to penetrate to an extent which may endanger the passivity of the steel during the design life of a structure. This makes problems of corrosion arising from carbonation normally avoidable in a good quality concrete.

However, chloride-related depassivation of reinforcement and subsequent corrosion is more widespread. Chlorides may be inducted into concrete as primary chlorides during manufacture or as secondary chlorides during service. They may be introduced deliberately as cement hydration accelerating admixture, or as deicing salts in bridge decks or through sea water in marine structures. Concrete construction in the Middle East is continually exposed to ground and atmosphere charged with chloride salts. Chlorides are introduced into concrete through mix ingredients such as aggregates and mix water, salt contaminated reinforcement, brackish service water used for curing, and the frequent layers of salt-laden moisture precipitated in the form of dew on exposed surfaces. Concrete substructures on the Arabian Gulf Seaboard, where much of the development is founded and where the water table is relatively high, are almost constantly exposed to soils and ground water characterized by a high concentration of chloride salts.

In all such situations, the high incidence of corrosion against the backdrop of a highly chloride-polluted environment puts the chloride ion as the most important and prevalent cause of reinforcement corrosion.

5.2 MECHANISM OF CHLORIDE-INDUCED CORROSION OF STEEL IN CONCRETE

The usual chloride free environment of uncarbonated concrete is intrinsically protective against corrosion of embedded steel because it comprises a highly alkaline aqueous phase (pH = 13.5) contained in a continuous network of pores of varying shape and sizes within solid cement hydration products. The appropriate parameter of concern in chloride-induced steel corrosion is not the "total" chloride present in concrete, nor even the "dissolvable" fraction of the "total" chloride, but that part of the "dissolvable" chloride concentration which actually resides in the pore solution, and is permanently in contact with the steel surface. In spite of their critical importance, chloride concentrations alone do not determine decisive corrosion risk. It is now well recognized that depassivation of steel is a function of the Cl^-/OH^- ratio in the pore solution rather than chloride concentrations alone, and this parameter can be regarded as a rough measure of relative corrosion risk in the alkaline chloride bearing pore solutions of concrete. Hausmann (11) on the basis of mild steel corrosion tests in concrete-simulated artificial $Ca(OH)_2$ solution of pH around 12.5, has proposed a threshold depassivation Cl^-/OH^- ratio of 0.60. However, this value cannot be considered to be adequately representing conditions in real concrete, primarily because the pH levels of real concrete pore solutions are significantly higher than 12.5. In a later work, Gouda (54) carried out tests similar to Hausmann's in solutions where maximum NaCl threshold concentrations have been evaluated for six pH values ranging from 11.8 to 13.95. Diamond (38) has carefully scaled these data and has converted the results into Cl^-/OH^- ratios for easier comparison. These data showing Cl^-/OH^- ratio of 0.57 for pH 11.75 and 0.78 for a pH of 12.1 indicate reasonably good agreement with Hausmann's value of 0.6 for a pH of 12.5. However, the alkaline conditions of a typical concrete pore solu-

tion are much more closely represented by a pH of 13.3, which corresponds to a Cl^-/OH^- value of 0.30.

Once the corrosion is initiated, the corrosion rate is determined amongst other factors by the diffusion of moisture and oxygen to the steel level, electrical resistivity of concrete and pore solution aggressivity characterized by Cl^-/OH^- ratio of the pore solution. Goni et al (80) have also shown that after depassivation, the corrosion rate of steel in simulated concrete pore solution also depends upon the pore solution aggressivity in terms of Cl^-/OH^- ratio. Since oxygen diffusion and resistivity of concrete are a function of the physical structure of cement matrix, corrosion rate depends on the pore structure characteristics of cement matrix in concrete as well as on the chloride binding capacity and pore solution alkalinity of concrete.

Since corrosion initiation requires ingress of sufficient quantity of chloride ions through concrete cover to the steel surface, the corrosion initiation time of reinforcing steel in concrete exposed to a given environment depends upon the pore structure and permeability of concrete in general and chloride ion diffusion in particular. All the chloride ions entering into concrete are not available as free chlorides. A proportion of the chlorides entering into concrete are bound by C_3A phase of the cement to form insoluble Friedel's salt and possibly by C_3S phase of the cement. The steel is depassivated once the free chlorides exceeds the quantity required to reach the threshold Cl^-/OH^- ratio of the pore solution. Thus, apart from the physical structure of hardened cement matrix, corrosion initiation time of steel in concrete depends upon the chloride binding capacity and pore solution alkalinity of the concrete.

Corrosion rate of steel in concrete in an active state of corrosion depends upon oxygen diffusion, electrical resistivity and pore solution aggressivity of concrete. Diffu-

sion of oxygen determines the depolarization of cathode whereas electrical resistivity determines the magnitude of the corrosion current. The corrosion of steel results in cracking and spalling of concrete which often leads to serviceability failure of the structure.

5.3 MECHANISM OF CORROSION RESISTANCE OF STEEL IN PLAIN CEMENT CONCRETE

As discussed earlier, corrosion initiation time of steel in concrete depends upon the physical structure of the hardened cement paste as well as upon the chloride-binding capacity and pore solution alkalinity. Since the physical structure of concrete made with different plain cements is independent of the cement composition, corrosion initiation time of reinforcing steel in plain cement concrete depends predominantly upon the pore solution composition characterized by the concentrations of unbound chlorides and hydroxide ions. Pore solution composition of plain cements would be significantly affected by cement composition in terms of C_3A and alkali content of the cement as well as by the presence of sulfates and exposure temperature. Effect of these factors on chloride-binding, pore solution alkalinity and corrosion resistance performance is therefore the subject of present study and is discussed in the following sections.

5.3.1 C_3A Effect

Results of pore solution study conducted on plain cements with C_3A contents of 2.43, 7.59, 8.52 and 14% show that the unbound chlorides in the pore solution decrease with increasing C_3A content. For the four chloride additions of 0.3, 0.6, 1.2 and 2.4% there is 4.94, 4.37, 2.53 and 1.51 fold decrease in the free unbound chloride content of

the pore solution with an increase in the C_3A content from 2.43 to 14%.

Using the threshold Cl^-/OH^- ratio of 0.3 for the **initiation of corrosion** as suggested by Diamond(38), the tolerable chlorides for the 8.52 and 14% C_3A cements are 1.9 and 2.8 times the tolerable chloride for the 2.43% C_3A cement. It is noteworthy that the C_3A effect is specially beneficial for binding chlorides in the range of 0.3% to 0.6%, which is well within the range of chloride induction through inadequately prepared constituent concrete materials and brackish curing water.

The increase in chloride-binding capacity with increasing C_3A content would mean that the corrosion initiation time increases with increasing C_3A content of cement. Results of corrosion tests conducted in the same laboratory by Rasheeduzzafar et al (23) clearly show this expected behavior of increasing corrosion initiation time with increasing C_3A content of cement. These results show that the **corrosion initiation times** for steel in 9 and 14% C_3A cement concrete are 1.75 and 2.45 times more than that in the 2% C_3A cement concrete. The straight-line correlation between tolerable chlorides and corrosion initiation times (Fig. 5.2) show that the increase in corrosion initiation times of steel in plain cement concrete with increasing C_3A content is a direct consequence of the increasing chloride-binding with increasing C_3A content of the cement.

Corrosion rates of steel in plain cement concrete when the steel is in active state of corrosion depends on the Cl^-/OH^- ratio of the pore solution only, since the difference in physical structure of concrete made with cements of varying composition is negligible. This means that the corrosion rate of steel in high C_3A cements would be less than that in low C_3A cements. However, data developed on corrosion rates of

steel in concrete made with different C_3A cements show no correlation with the C_3A content of the cement. This is possibly because the corrosion rates were measured after 1200 days of immersion in 5% sodium chloride solution. Therefore, the total chlorides ingressed into concrete at the time of corrosion rate measurement are expected to be very high compared to the chloride binding capacity of even the high 14% C_3A cement. Results of pore solution study also indicate that with increasing level of chloride addition, although the absolute quantum of bound chloride increases, the rate of chloride binding decreases. For example, in the 14% C_3A cement the ratio of bound to unbound chloride is 14.4 times more for the lower level of 0.3% chloride addition compared to 2.4% chloride addition. This behavior in terms of chloride binding is explained by the fact that C_3A or any other cement hydrate can complex only with a limited amount of chlorides. As the quantity of chlorides progressively exceeds this complexing capacity, more and more chlorides would be left uncombined. Also, as the chloride content increases, the chloride-binding performance ratio between higher and lower C_3A cements decreases significantly. For example, in terms of bound to unbound chloride ratio the 6.9 fold superiority of the 14% C_3A cement over the 2.43% C_3A cement at the 0.3% chloride addition level drops to 3.2 for the 2.4% chloride addition. This indicates that C_3A is effective in binding only a limited amount of chlorides. Thus, it can be expected that high chloride content in concrete at the time of corrosion rate measurement are responsible for about the same corrosion rates of steel observed in different C_3A cement concretes.

5.3.2 Chloride-Sulfate Interaction

Concrete construction on the Arabian Gulf seaboard is characterized by concomi-

tant presence of high chloride and sulfate concentrations in soils and groundwater. Foundations are concurrently subjected to sulfate attack and chloride-induced rebar corrosion. In such a situation the reduction in the chloride-binding capacity of C_3A by sulfates is of considerable significance.

Pore solution data developed in this study show that the unbound chlorides in the pore solution increase with the addition of sulfates derived from sodium sulfate. 8% sulfate addition increases the unbound chlorides in the pore solution by 1.5, 2.5 and 4.1 times for 2.43, 7.59 and 14% C_3A cements for 0.6% chloride addition. In addition to the increase in the unbound chlorides, the addition of sulfates, derived from sodium sulfate, brings about increase in the OH^- concentration of the pore solution. The interactive combined effect of increase in alkalinity and chloride ion concentration with sulfate addition is not a consistent and well defined increase or decrease in the Cl^-/OH^- ratio of the pore solution. For a given chloride level, whether sulfate addition increases or decreases the Cl^-/OH^- ratio of the pore solution depends upon the interactive effect of equivalent alkali content and C_3A content of the cement. Therefore, in concrete structures exposed to chlorides and sulfates simultaneously, as in the substructures in the Middle East, the corrosion behavior of steel in concrete would depend on an interplay of the aforesaid factors.

5.3.3 Temperature Effect

The climatic conditions in the Arabian Gulf Seaboard during summer are characterized by extremely high temperatures of the order of 48° C in conjunction with high humidity. The extreme hot and humid climatic conditions of the coastal hot-arid regions are almost ideal for accelerated rebar corrosion. Temperatures as high as 70° C

may be achieved on concrete surfaces due to solar radiation effects.

Results of pore solution tests conducted in this study on 2.43, 7.59 and 14% C_3A plain cements exposed to two different temperatures of 20 and 70° C show that free chlorides in the pore solution increase when the temperature is increased from 20 to 70° C. The adverse effect of temperature on unbound chlorides in the pore solution is more pronounced in high C_3A cements than in low C_3A cements. For the 0.3% chloride treatment level, when the curing temperature is raised from 20 to 70° C the unbound chlorides increase by 2.2, 4.2 and 9.1 times for the 2.43, 7.59 and 14% C_3A cements. The corresponding values for the 1.2% chloride level are 1.2, 1.8 and 2.65 for the 2.43, 7.59 and 14% C_3A cements respectively. At 20° C the effectiveness of 14% C_3A cement in removing chlorides from the pore solution is 2.5 times more compared to 2.43% C_3A cement. However, at 70° C, 14% C_3A cement is only 1.2 times more effective in removing chlorides from the pore solution than 2.43% C_3A cement. An increase in the free chlorides in the pore solution may be attributed to an increase in the decomposition of Friedel's salt at higher temperatures such as 70° C temperature used in this study.

In addition to increasing the unbound chlorides in the pore solution, increase in curing temperature from 20 to 70° C also results a drop in the OH^- concentrations from 0.26 to 0.12 M/L for the 2.43% C_3A cement; from 0.40 to 0.15 M/L for the 7.59% C_3A cement; and from 0.50 to 0.20 M/L for the 14% C_3A cement. The effect of temperature in reducing OH^- concentrations may be ascribable to the hydroxyl ions entering into reaction to balance the anions removed due to the additional liberation into the pore solution.

The effect of temperature on Cl^-/OH^- ratio of the pore solution depends on the similar changes in the Cl^- and OH^- concentrations. The concomitant elevation of free chlorides and the depression of OH^- concentration with increase in temperature, raises the Cl^-/OH^- ratio of the pore solution significantly. As an example, for the 14% C_3A cement treated with 0.3% chlorides, the Cl^-/OH^- ratio increases 19 fold due to an increase in temperature from 20 to 70° C. The Cl^-/OH^- ratios multiply manifold for all the three chloride levels when cements are cured at 70° C instead of 20° C. The increase in Cl^-/OH^- ratio with temperature is observed to be most drastic for the lowest chloride treatment level of 0.3%. Also the increase in the Cl^-/OH^- ratio is more marked for the 14% C_3A cement than for the other two lower C_3A cements. This further emphasizes the point that in terms of corrosion environment the high C_3A cements are more adversely affected by temperature increase than the low C_3A cements.

The pore solution chemistry of cement pastes cured at higher temperature shows that the corrosion behavior of steel in concrete exposed to high temperature would be different as compared to concrete exposed to normal temperatures. The increase in Cl^-/OH^- ratio at higher temperatures indicates that the corrosion initiation time of steel in concrete would be decreased and corrosion rates would be increased significantly.

5.3.4 Effect of Alkali Content of Cement

The alkali content of a cement has a strong influence on OH^- concentration as well as the unbound chlorides in the pore solution of hydrated cement. The data developed in this study on 14% C_3A cement with equivalent Na_2O content of 0.65 and 1.2%

show that the OH^- concentration in the pore solution of the high alkali cement is around 1.4 times that in the medium alkali cement for chloride levels of 0.3, 0.6 and 1.2%. However, for the chloride-free pastes, the OH^- concentration in cement 2 is twice that in cement 1. The pH values increase from an average value of 13.72 to 13.88 when the alkali content is increased from 0.65 to 1.2%. An increase in the equivalent Na_2O content from 0.65 to 1.2% doubles the unbound chlorides in the pore solution for all the three chloride levels.

An increase in alkali content of cement concomitantly increases the OH^- and Cl^- concentrations in the pore solution, the net effect being a slight increase in the Cl^-/OH^- ratio. The Cl^-/OH^- ratio for medium and high alkali cements for different levels of chloride indicate an average marginal increase of about 25% when the alkali content increases from 0.65 to 1.2%.

The marginal increase in the Cl^-/OH^- ratio introduced by an increase in the alkali content of cement is therefore not expected to change the corrosion behavior of steel reinforcement in concrete significantly.

5.3.5 Mode of Occurrence of Chlorides

It may be noted here that the pore solution tests carried out in this study relate to situations where chloride is present in the original concrete mix. This happens when chloride is added initially as a cement hydration accelerating admixture or is introduced through mix ingredients such as from unwashed chloride contaminated aggregates or brackish mix water. The latter is a common construction practice in the Middle East where desalinated or potable water is scarce. On the other hand, conditions of the accelerated corrosion tests (23) simulate chloride corrosion situations where chlorides

permeate to the steel-concrete interface through extraneous sources during the service life of concrete structures. Concrete structures exposed to marine environment or to deicer salts or to chloride-bearing soils and groundwater, as in the Middle East, represent typical situations of the second category. The chloride binding and corrosion initiation data from the pressure extrusion and accelerated corrosion monitoring tests show that the effect of C_3A in mitigating the effect of chlorides on corrosion is clearly present in situations of both categories.

Results of pore solution tests conducted on 2.43, 7.59 and 14% C_3A cements treated with internal and chlorides show that the cements exhibit more chloride-binding when treated with internal and external chlorides than when treated with external chlorides. The unbound chlorides in the pore solutions of 2.43, 7.59 and 14% C_3A cements treated with internal chlorides were 86, 63 and 59%. However, when the cements are treated with equal amounts of total external chlorides, introduced into hydrated cement pastes after 28-day curing, the unbound chlorides increased to 88.5, 82.9 and 79.3% for 2.43, 7.59 and 14% C_3A cements respectively.

The removal of chlorides due to increasing C_3A content is less effective for external chlorides compared to internal chlorides. Whereas, for cements treated with internal chlorides, the unbound chlorides increased by 2.9 times when the C_3A content of cement is increased from 2.43 to 14%, it was increased by 1.2 times only for the corresponding increase in the C_3A content for cements treated with external chlorides.

The significant differential in the chloride-binding for the internal and external chloride contamination can possibly be attributed to the fact that the the external chlorides were inducted into the cements after 28 days of curing when most of cement hydration was already completed. It seems plausible to assume that with chlorides

permeating into cement paste in which hydration is nearing completion, the possibility of chemical complexing of chlorides with hydrates is significantly reduced.

The above discussion indicates that in situations characterized by the permeation of chlorides from external sources, the threshold value in terms of total chlorides, acceptable as tolerable to reinforcement in concrete, will be lower compared to where the chlorides are initially added to the original concrete mix.

It is also of some interest to note that for the externally permeating chlorides, whereas the X-ray diffractograms of typical concrete removed from the corrosion monitoring specimens made with 9, 11 and 14% C_3A cement showed the presence of significant amount of calcium chloroaluminate, those for the concrete removed from the 2% C_3A did not show the presence of any detectable calcium chloroaluminate (23). On the contrary, pore solution tests on specimens with initially added internal chlorides show that even for the 2% C_3A cement pastes, a significant amount of chloride binding takes place. If chlorides are not bound by other cement hydrates such as C-S-H gel, then the chloride-binding in low C_3A cements indicates that the assumption that in low C_3A cements the entire available C_3A will preferentially combine with the sulfates of 4-5% gypsum ($CaSO_4.2H_2O$) added to regulate the time of set without removing any chlorides is not entirely correct. This may be true in situations where chlorides from external sources permeate after most of the hydration, including the reaction between C_3A and gypsum, is complete. However, in the case of chlorides which are added to the original mix and are present during hydration, it is very likely that C_3A reacts conjointly with chlorides and sulfates present in the mix.

5.4 MECHANISM OF CORROSION RESISTANCE PERFORMANCE OF BLENDED CEMENTS

Corrosion of reinforcement in concrete is an electrochemical process. It is now well recognized that depassivation of steel is a function of the Cl^-/OH^- ratio in the pore solution, rather than chloride concentrations alone, and this parameter can be regarded as a rough measure of relative corrosion risk in the alkaline chloride-bearing pore solutions of concrete. This focuses on the importance of the pore solution chemistry of concrete pore electrolyte, in determining the degree of risk posed to embedded steel in chloride-bearing concrete. Pozzolanic materials, such as microsilica, blast furnace slag and fly ash are known to consume alkaline $Ca(OH)_2$ precipitated in the aqueous phase within concrete, thereby reducing OH^- ion concentration and the alkalinity of the pore solution. Changes activated by these blending materials in the chemistry of the pore electrolyte are also known to significantly affect the levels of chlorides, likely to remain uncombined with cement hydrates. These compositional changes, related to the concentrations of OH^- and Cl^- ions in the pore solution, have a direct bearing on the electrochemistry of steel in concrete with reference to the degree of corrosion risk. The pore solutions have, therefore, been analyzed with special focus on the effect of these blending materials on alkalinity, and OH^- and Cl^- ion concentrations. Predictions of corrosion behavior, from the standpoint of pore solution chemistry, have also been evaluated using the results of time to corrosion initiation and corrosion rate measurements, carried out on reinforced concrete specimens made of plain and blended cement concretes exposed to an external chloride environment.

5.4.1 Chemical Environment and Corrosion Resistance of Blended Cement

Data developed on pore solution composition of microsilica blended cements show that partial cement replacement by microsilica causes concomitant increase in free chlorides and decrease in OH^- concentration in the pore solution, thereby increasing the Cl^-/OH^- ratios by several folds.

In the high C_3A parent plain cement, 10% microsilica blending causes the OH^- concentration to decrease by 4.3, 2.8 and 2.4 times for 0.3, 0.6 and 1.2% chloride additions compared to plain cement. However, 20% microsilica blending causes much steeper reductions in the OH^-, concentrations by 10, 28 and 21 times for 0.3, 0.6 and 1.2% chloride additions compared to the plain cement. In the chloride-free 10 and 20% microsilica blended cements, the reductions in the OH^- concentrations are 1.6 and 5.0 times compared to the plain cement. Similar reductions in the OH^- concentrations were observed when the 2.43% C_3A parent plain cement was blended with 10 and 20% microsilica. It is interesting to note that the pH of 20% microsilica blended cements for both the parent plain cements fall below the pH of saturated calcium hydroxide solution.

The decrease in the pore solution alkalinity due to microsilica blending is attributable to the combination of silica, which constitutes about 95% of the microsilica, with alkali hydroxides and calcium hydroxide. Diamond (81) and Page and Vennesland (37) measured alkali hydroxide concentrations in the pore solutions of plain and microsilica blended cements. It was observed that the concentrations of Na^+ and K^+ reduced with increasing levels of microsilica. However, the drop in the hydroxyl ion concentration was far steeper compared to the drops in the Na^+ and K^+ concentrations.

In the case of 14% C_3A parent cement, the substitution of cement by 10% microsilica increases the unbound chlorides by 3 times for 0.3% chloride addition and almost 2 times for 0.6% and 1.2% chloride additions. Increasing the microsilica blending to 20% further increases the unbound chlorides in the pore solution by 71% and 65% for 0.3 and 0.6% chloride addition, but only by 20% for 1.2% chloride addition over the respective chloride concentration values for the 10% microsilica blending. However, in the case of 2.43% C_3A parent cement, the increase in the unbound chlorides due to microsilica blending is significantly lower than it is achieved in the case of 14% C_3A parent cement. 10% microsilica blending to 2.43% C_3A parent cement, causes a decrease of 14% in the unbound chlorides for 0.3% chloride addition. 10% microsilica blending causes almost negligible change for 0.6% chloride addition, and 13% increase for 1.2% chloride addition, in the unbound chlorides. 20% microsilica blending to 2.43% C_3A cement causes the unbound chlorides to increase by 40, 16 and 32% for 0.3, 0.6 and 1.2% chloride additions. The decrease in the chloride-binding due to microsilica blending is confirmed by the DTA patterns obtained for the 1.2% chloride-bearing plain and microsilica blended cements made with the 14% C_3A parent plain cement. Whereas, there is a fairly well defined endothermic peak at about 320° C due to the formation of Friedel's salt in the plain cement, the response systematically weakens with increasing blending of the parent plain cement with microsilica, showing the progressive decomposition of Friedel's salt.

It is also noticed from the data developed on pore solution composition of microsilica blended cements made with low and high C_3A parent cements, that the increase in the unbound chlorides in the pore solution due to microsilica blending is more pronounced in the high 14% C_3A cement than in the low 2.43% C_3A cement. Whereas the 20% microsilica brings about 5.4, 3.1 and 2.1 times increase in the unbound

chlorides in 14% C_3A cement for 0.3, 0.6 and 1.2% chloride additions respectively, the corresponding increases observed in 2.43% C_3A cement are 1.4, 1.2 and 1.3. This clearly indicates that the increase in the unbound chlorides and hence the inhibition of the formation of Friedel's salt due to microsilica blending is proportional to the C_3A content of cement. Therefore, it is likely that the microsilica addition to a chloride bearing cement paste may combine with C_3A phase of the cement, thereby inhibiting the availability of C_3A for the formation of Friedel's salt.

The decomposition of Friedel's salt in microsilica blended cements is attributed to the lowering in the pore solution alkalinity by Page and Vennesland(37). However, results of pore solution tests conducted on plain and microsilica blended cements with alkali contents of 0.65 and 1.2% show an increase in the unbound chlorides with an increase in the alkali content of the cement. For example, for 0.6% chloride level, increase in the alkali content from 0.65 to 1.2%, increase the unbound chlorides by about two fold in the plain and 10 and 20% microsilica blended cements; and for 1.2% chloride level, the increase in the unbound chlorides, are 1.8 fold for the plain and about 1.5 fold for both microsilica blended cements. Increase in alkali content from 0.65 to 1.2% results in an average increase in the OH^- concentrations by 225, 115 and 1.5 mM/L in plain and 10 and 20% microsilica blended cements for both chloride levels. Although the OH^- concentration of the pore solution remains unchanged, the unbound chlorides in the pore solution of the 20% microsilica blended cement pastes increase significantly due to an increase in the alkali content of the cement. This shows that in microsilica blended cements which have greater affinity for hydroxyl ions, it is the alkali content of the cement or the OH^- concentration prior to pozzolanic reaction which controls the chloride-binding of the cement. The more the alkali content of cement or the pore solution alkalinity before the pozzolanic reaction, the more will be

unbound chlorides in the pore solution.

The results of this study thus, contradict the theory proposed by Page and Vennesland (37) which states that decrease in the chloride binding in the microsilica blended cements is attributable to the increase in the solubility of Friedel's salt (calcium chloroaluminate) due to decrease in the pore solution alkalinity.

The data developed in this study also show that the Cl^-/OH^- ratios in the pore solutions of the 10 and 20% microsilica blended cements steeply increase due to the cumulative interactive effect of an increase in the free chlorides and a decrease in the OH^- concentrations in the pore solution of the microsilica blended cements. In 14% C_3A cement, 10 and 20% microsilica blending causes 4 and 39 fold increase in Cl^-/OH^- ratio for 1.2% chloride level. However, in 2.43% C_3A parent cement, the reductions in the Cl^-/OH^- due to 10 and 20% microsilica blending are to a lesser extent, 4.2 and 19 times compared to the plain cement.

Thus, the chemical environment of microsilica blended cements indicate greatly increased aggressivity against the corrosion behavior of steel in microsilica blended cement concrete.

Incorporation of blast furnace slag and fly ash in concrete also cause adverse effects in terms of increased corrosion risks due to increase in the Cl^-/OH^- ratio in the pore solution. But, the Cl^-/OH^- ratios in the pore solution of blast furnace slag and fly ash blended cements are significantly lower compared to microsilica blended cements.

70% blast furnace slag blending causes the OH^- concentration in the pore solution to drop by 1.9 and 2.9 times for the parent plain cements of 2.43% (Na_2O:0.58 %)

and 14% (Na_2O:0.65 %) C_3A cements. When these cements are replaced by 30% fly ash the OH^- concentrations in the pore solution are decreased by 21 and 40% respectively. The decrease in the OH^- concentrations are attributable to the decrease in the calcium hydroxide content of cement as shown by the DTA and TGA results. Whereas, 70% blast furnace slag almost completely eliminates calcium hydroxide in the 1.2% chloride treated cement paste made with 14% C_3A parent plain cement, 30% fly ash reduces calcium hydroxide content from 30.6 to 13.1%. Although the DTA results show no crystalline $Ca(OH)_2$ in hardened cement paste, the observed alkalinity of the pore solution is probably due to the dissolved $Ca(OH)_2$ and the alkali hydroxides present in the the parent cement and the slag.

Partial cement replacement by blast furnace slag and fly ash decreases the unbound chlorides in the pore solution for the whole range of chloride levels from 0.3 to 1.2% used in this study. The decrease in the unbound chlorides is observed in both the parent cements of 2.43 and 14% C_3A. 70% cement replacement by slag reduces the unbound chlorides by an average value of 20% for 1.2% chloride level in both the parent cements. The reduction in unbound chlorides resulting from 30% fly ash blending is about 30% for both the parent cements treated with chloride levels ranging from 0.3 to 1.2%.

The effect of slag and fly ash blending on Cl^-/OH^- ratio in the pore solution is relatively small compared to other mineral admixtures such as microsilica. The reduction in the OH^- concentration outweighs the decrease in the free chlorides of the pore solution due to slag blending. The net effect, therefore, is an increase in the Cl^-/OH^- ratio of the pore solution in slag cements. In the 2.43% C_3A Type V cement, the Cl^-/OH^- ratio increases by 20 to 40% for different levels of chloride. However, in the

14% C_3A Type I cement, the slag blending causes much bigger increases of 67 to 105% in the Cl^-/OH^- ratios for different chloride levels. For the 2.43% C_3A Type V cement the Cl^-/OH^- ratios of the fly ash blended cements are less than those of the plain cement. However, for the 14% C_3A Type I parent cement, the Cl^-/OH^- ratios in the pore solution of the fly ash blended cement are more than for the plain cements; the maximum increase is about 41% in Type I 14% C_3A cement and the maximum reduction being 32% in the 2.43% C_3A cement.

5.4.2 Physical Characteristics and Corrosion Resistance Performance of Blended Cements

Although the increased aggressivity of pore solution of blended cement creates a highly adverse chemical environment, and very significantly increases the corrosion susceptibility of reinforcing steel in the blended cement concrete, the actual corrosion resistance performance of steel in these blended cement concrete show a significantly improved performance compared to that in the plain cement concrete. Whereas, 10 and 20% microsilica blending increases the corrosion initiation time of steel by 3 times, 70% slag and 30% fly ash blendings increase the corrosion initiation time by 2.11 and 1.75 times.

It must be noted that the corrosion initiation time testing conditions simulate chloride corrosion situations where chlorides permeate to the steel-concrete interface from extraneous sources during the service life of concrete structures. In these situations, the denser structure of the cement matrix plays a dominant and decisive role in significantly retarding the mobility of chlorides from the surface to the steel level. Microsilica, slag and fly ash blending, in addition to the unfavorable changes in the chemical

composition of the pore electrolyte, also bring about other significant favourable changes in the physical structure of the hardened cementitious matrix. These changes in the physical structure, are brought about by the important pozzolanic reactions. In microsilica blended cement concrete, the reactive ultrafine silica particles of silica fume fill the interstices of the fresh cement paste structure, and then react with the $Ca(OH)_2$ as well as alkali hydroxides of the hydrating cement. An insoluble C-S-H of C/S ratio of about 1 is formed within 24 hours at room temperature after mixing with water. It is generally recognized that in bituminous fly ashes, the most important pozzolanic reactions occur between reactive silica of fly ash and the calcium hydroxide of hydrated cement. Several studies on the cement-fly ash system indicate that the product of their reaction is a relatively poor quality calcium silicate hydrate, akin to the morphology of C-S-H I, with C/S ranging from 0.8 to 2.5. The formation of this hydrate results in the densification of the matrix and the segmentation of the pore structure by a space filling process during the hydration of cement. Also, slag blending brings about pore segmentation and blocking process, with reactive particles, which is superior to that brought by bituminous fly ash blending as hypothesized by Bakker (17).

Manmohan and Mehta (29) and Nyame and Illston (70) have shown that in concrete durability situations where permeability is a factor, it is the pore size distribution, rather than total porosity, which governs concrete performance. Permeability and chloride diffusion characteristics of hardened cement have a direct effect on corrosion initiation time of steel in concrete. Pore size distribution of this study show that 10 and 20% microsilica blended cement show a more refined pore structure than the plain cement even after a curing of only three days. However, slag and fly ash blended cements show a pore structure finer than that of plain cement only after a hydration period of about 28 days. The average pore radii of 6 month old mature pastes of 20

and 10% microsilica, slag and fly ash blended cements are 136, 167, 153 and 146 A° compared to 213 A° for the plain cement. Direct measurements of permeability and chloride diffusion show that the blended cements have significantly reduced permeability and chloride diffusion. For 20 and 10% microsilica blended cements, the concrete permeability is reduced by 16 and 12 times whereas the chloride diffusion of cement pastes is reduced by 300 and 150 times respectively compared to the plain cements. However, the reductions in permeability and chloride diffusion of slag and fly ash blended cements are lower than those in the microsilica blended cements. The permeability is reduced by 10 and 5 times, whereas the chloride diffusion is reduced by 39 and 6 times for slag and fly ash blended cements compared to the plain cement.

Another consequence of the pore blocking and segmentation which has a direct bearing on corrosion propagation in the post corrosion initiation period is its effect on electrical resistivity and oxygen diffusion. An enhanced electrical resistivity of concrete has been shown to have a strong influence on reducing corrosion action. Results of this study show that the electrical resistivity of 20 and 10% microsilica, slag and fly ash blended cement concrete is reduced by 5.7, 3.2, 2.6 and 2.2 times compared to the plain cement concrete. Microsilica blending marginally reduces oxygen diffusion, whereas slag blending reduces it by 5 time. Fly ash blending showed drastic decrease of 100 times in the oxygen diffusion compared to the plain cement concrete. The enhanced electrical resistivity and reduced oxygen diffusion significantly increase the corrosion resistance performance of blended cements in the post initiation period.

In the post corrosion initiation period, the corrosion rates of slag and fly ash blended cement concrete are reduced by about 60%. However, microsilica blended cement concrete show no significant reduction in the corrosion rate of steel. Goni and Andrade (80) have shown that corrosion rates of steel bear a linear relationship with

the Cl^-/OH^- in log-log representation. Thus, the significantly increased Cl^-/OH^- ratio in the pore solutions of 10 and 20% microsilica blended cements offset the beneficial effects of increased resistivity in the post initiation period, thereby resulting in about the same corrosion rates as for the plain cement concrete. However, the Cl^-/OH^- ratios in the pore solutions of slag and fly ash blended cements are marginally increased. Hence, the enhanced resistivity and decreased oxygen diffusion result in lower corrosion rates in slag and fly ash blended cement concrete than in plain cement concrete.

With regard to the corrosion behavior of steel in blended cement concretes a model similar to that proposed by Tutti(62) is shown in Fig. 5.3. Since the corrosion initiation time of steel in blended cement concrete is more compared to plain cement concrete as well as slag and fly ash blended cement concrete show reduced corrosion rates than plain cement concrete, the service life of structures made with blended cements is significantly increased compared to those made with plain cement as shown in Fig.5.1, even if the corrosion rates of steel in plain and blended cement concretes are assumed to be the same.

5.5 MECHANISM OF CONTROL OF ALKALI-SILICA REACTIONS IN PLAIN AND BLENDED CEMENTS

The mortar-bar expansion results show that for the plain parent cement, the expansions began immediately with no incubation period with the highest rate obtainable for the first 20 days, thereafter decreasing gradually to a low value. A highly unacceptable final value of 0.865%, 8.65 times the allowable 0.1% value, was measured at the end of the six-month period for the plain cement. Replacement by 10% and 20% microsilica decreased the six-month expansion values to 0.023% and 0.009% respec-

tively. For the 60% and 70% blast furnace slag cements , the corresponding values were 0.04% and 0.028%. Expansion with 30% fly ash blended cement is at the 6 months permissible limit (0.1%) and in view of the fact that the reactivity of the aggregate is unusually high and the alkali content is also high, this performance of fly ash should be acceptable.

The rapid accumulation of hydroxide ions in the pore solution as a cation charge balancing mechanism provides the driving force for ASR. The removal of these hydroxide ions from the pore solution is a key factor in the ASR prevention mechanism.

Microsilica, slag and fly ash inductions reduced hydroxide ion concentrations significantly. The reduction, however, was drastic with higher levels of microsilica. 20 and 25%. Also, in medium 0.9% alkali cements, 60% blast furnace slag appears to be an alkali remover comparable to 10% microsilica. However, in the case of high 1.5% alkali cements, 10% microsilica is appreciably more effective in removing hydroxide ions than 60% slag. It is seen that in the case of 1.5% alkali plain and blended cements, whereas 10% microsilica reduces OH^- concentration from 946 mM/L to 533 mM/L, 60% slag reduces it only to a level of 708 mM/L. 20 and 25% microsilica are manifold more effective as an alkali oxide remover for the whole range of alkali contents included in this program. This is specially so for the high 1.5% alkali cement where 25% microsilica is 37 times as effective as 70% slag.

The data developed in this study confirms the broad correlation reported earlier by others between the hydroxide ion concentration and the ASR generated expansions. However, within this broad correlation there are obvious deviations which are strongly indicative of other possible mechanisms also being concurrently operative in conjunc-

tion with alkali removal action.

Blast furnace slag, when inducted in large dosages of 60 to 70% would obviously act as an alkali diluent if its own alkali content is lower than that of the parent cement, as was the case in this study. For the same water to solids ratio, a higher evaporable water content would further facilitate this dilution mechanism. However, apart from these considerations, the data in this study show that the slag acts as an active remover of alkalies, and is specially effective in medium alkali cements, where the performance of 60% blast furnace slag cement as an alkali remover was found to be parallel to 10% microsilica cement. This is also indirectly shown by the data of Longuet et al (52) and explicitly by the data of Canham, Page and Nixon (74), although they state that slags were not found to be particularly efficient as alkali removers when compared with other cement extenders that are used to control ASR, such as fly ash and microsilica. However, our data also show that this effectiveness decreases as the alkali content of the cement increases. The effectiveness of 70% blast furnace slag is found to be 4.5, 2.1 and 1.5 for the 0.9, 1.2 and 1.5% alkali cements respectively.

The data also show that 30% fly ash blended cement removes alkalies more than 60 and 70% slag blended cement. For example, for 1.5% alkali content, the hydroxyl ion concentrations in fly ash, and 60 and 70% slag cements were found to be 440, 708 and 600 mM/L respectively. However, due to high alkali content of the fly ash, blending of 30% fly ash with a 1.2% alkali cement resulted in the blended cement with alkali content of 1.5%, which is the maximum alkali content in the blended cements used for mortar bar expansion tests. This high alkali content in the fly ash blended cement may be responsible for expansions greater than those in slag and microsilica blended cements.

In order to evaluate the effectiveness of slag as an ASR suppressor, a reference threshold value corresponding to a minimum hydroxide concentration of 250 mM/L (concentration defined pH = 13.4) to initiate and sustain alkali-silica reaction has been proposed by Diamond (75). It is seen that purely on the basis of pore solution chemistry, 70% slag would effectively control ASR for cement alkalies up to 1%. It is only in the case of 1.2% and 1.5% alkalies that the residual OH^- concentrations in 70% slag cements exceed the reference value of 250 mM/L. This discussion specifically pertains to the slag type used in this study. Obviously, slags of other reactiveness and compositions in terms of glass content and C/S ratio may react significantly differently.

Pore solution data show that incorporation of 25% microsilica virtually sweeps nearly all the hydroxide ions from the pore solution even in the high 1.5% alkali content cements. There are, however, questions about the wisdom of using this relatively high dosage. Apart from the two-fold drying shrinkage, the chemical environment for reinforcing steel corrosion is rendered significantly adverse. Therefore, it is desirable to keep microsilica dosage to a minimum, to achieve desired goals.

The pore solution data show that 10% addition is sufficient to bring down the OH^- concentration close to the threshold value of 250 mM/L in medium 0.9% alkali cements. However, for higher alkali contents of 1.2% and 1.5%, 10% microsilica does not bring the OH^- concentrations below the postulated threshold value of 250 mM/L. That these higher than 250 mM/L concentration do not cause expansions anywhere near the permissible value of of 0.1% is strongly indicated by our expansion data. The 10% microsilica cement (1.11% alkali content) having a hydroxide concentration of 368 mM/L shows 0.023% final expansion which is only one-quarter of the permissible 0.1% value. This indicates that for blended cements a threshold value of 250 mM/L is excessively conservative. This is possibly ascribable to the fact that in blended cements,

preventive mechanisms other than hydroxide ion removal may also be operative concomitantly. There is considerable evidence (76,77) to suggest that the beneficial role of microsilica in mitigating ASR expansion could also be partly explained by the fact that microsilica addition causes a reduction of global C/S ratio of the paste. A microsilica blended cement paste is relatively silica-rich compared to an identical paste without microsilica. It has been shown (77) that silica-rich C-S-H has a higher sorptive capacity for alkalies. CSH formed in microsilica blended cements would therefore entrap more alkalies leaving less concentrations in the pore fluid. This mechanism would also be operative in blast furnace slag cements if sufficient quantity of reactive slag is added to cement.

Apart from these significant chemical factors, the addition of reactive silica in the form of microsilica, fly ash or slag also brings about very significant changes in the physical structure of blended cements. Incorporation of such blend materials markedly refines pore structure and densifies binder matrix; this results in blocking and segmentation of the pores. Such physical changes effectively retard the transportation of alkalies to reaction sites, thereby mitigating ASR. Bakker (17) has explicitly modelled this mechanism for blast furnace slag cements. With its proven pore refining characteristics, there is no reason why a similar type of mechanism would not be operative for fly ash and microsilica blended cements.

With these preventive mechanisms acting concurrently with favourable chemical factors, the threshold for hydroxide ions should be significantly higher for blended cements than the postulated 250 mM/L. It appears that, at least for microsilica blended cements, it would certainly be in excess of 400 mM/L.

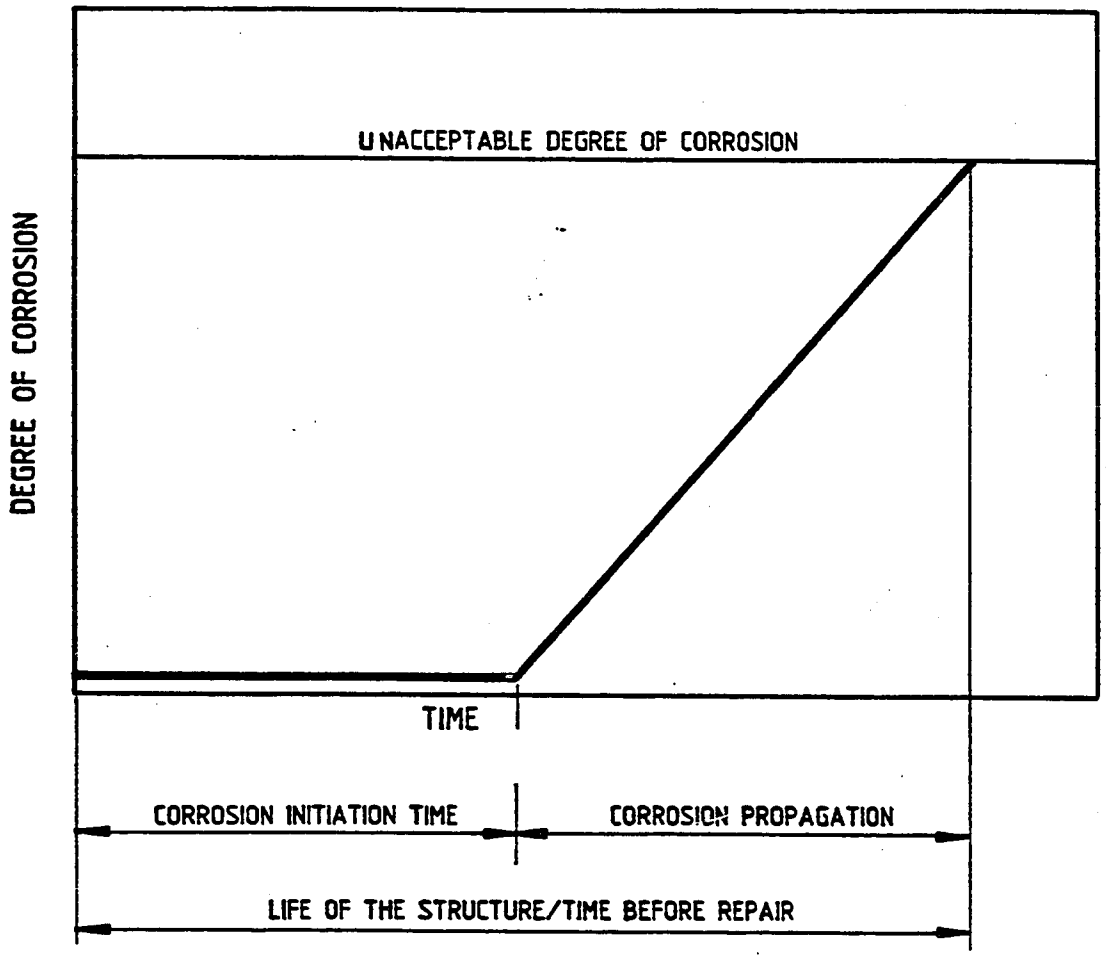

Fig. 5.1: Model for Corrosion Process of Steel in Concrete (ref. 62)

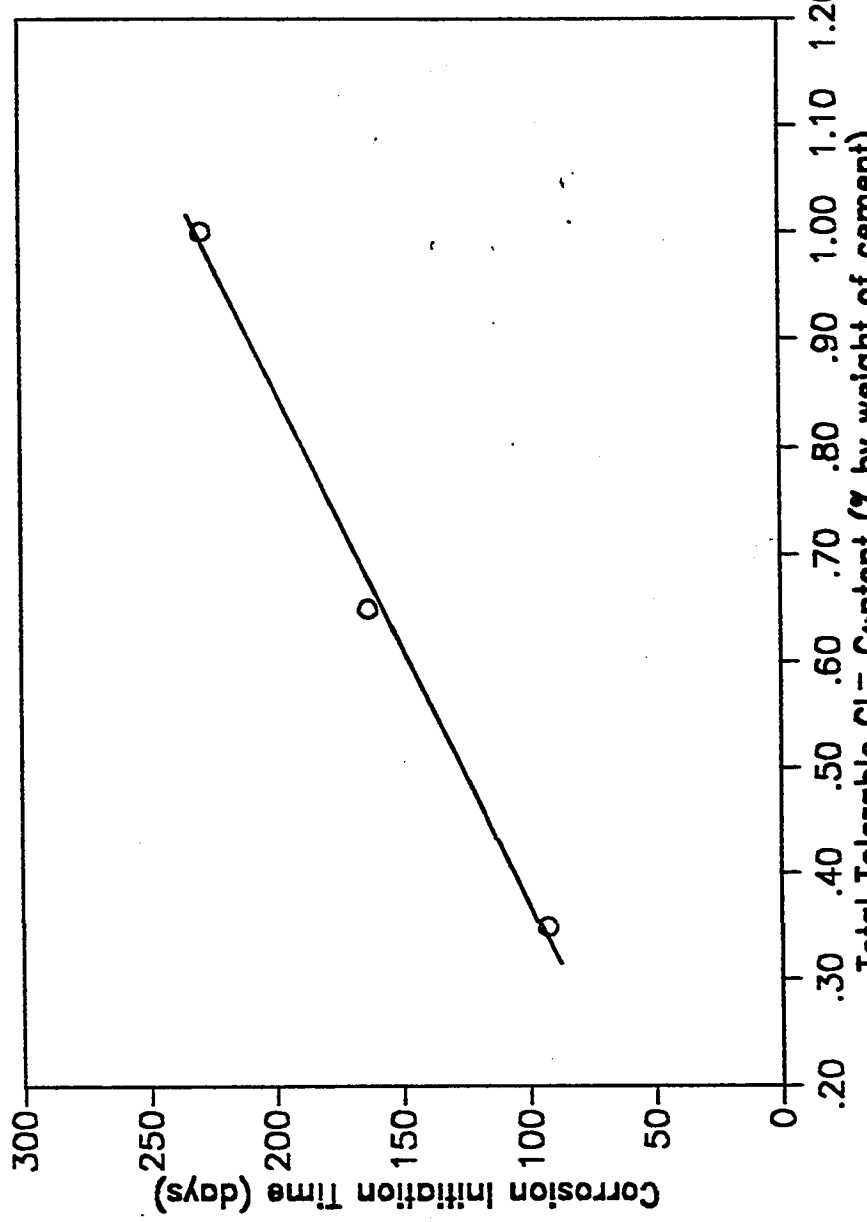

Fig. 5.2: Relationship Between Total Tolerable Chloride Content and Corrosion Initiation Time of Steel in Different C_3A Cement Concretes

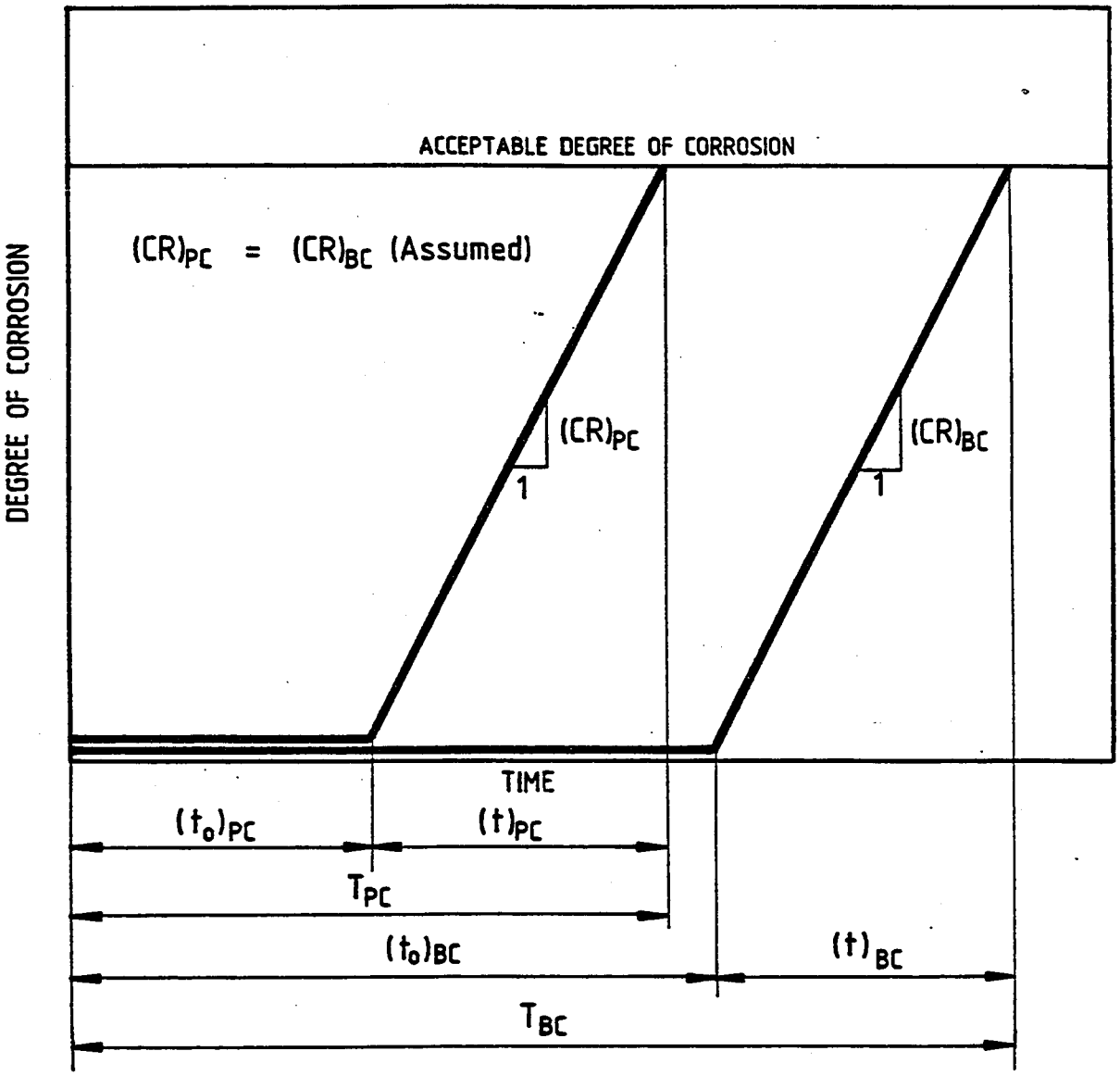

$(t_o)_{PC}$	CORROSION INITIATION TIME FOR PLAIN CEMENT CONCRETE
$(t)_{PC}$	CORROSION PROPAGATION TIME FOR PLAIN CEMENT CONCRETE
$(t_o)_{BC}$	CORROSION INITIATION TIME FOR BLENDED CEMENT CONCRETE
$(t)_{BC}$	CORROSION PROPAGATION TIME FOR BLENDED CEMENT CONCRETE
T_{PC}	LIFE OF STRUCTURE WITH PLAIN CEMENT CONCRETE
T_{BC}	LIFE OF STRUCTURE WITH BLENDED CEMENT CONCRETE
$(CR)_{PC}$	CORROSION RATE OF STEEL IN PLAIN CEMENT CONCRETE
$(CR)_{BC}$	CORROSION RATE OF STEEL IN BLENDED CEMENT CONCRETE

Fig. 5.3: Model for Corrosion Process of Steel in Plain and Blended Cement Concrete

Chapter 6

CONCLUSIONS

Cement Composition and Corrosion Resistance in Plain Cements

Effect of C_3A

1. The free chloride concentration in the pore solution of the hardened cement paste decreases with an increase in the C_3A content of the cement. Typically, for a 0.6% chloride addition, the unbound chlorides for the 2.43, 7.59, 8.52 and 14% C_3A cements are about 51, 25, 21 and 12% of the total chlorides. For chloride additions of 0.3, 0.6, 1.2 and 2.4% there is a 4.9, 4.4, 2.5 and 1.5 fold decrease in the free chloride content of the pore solution with an increase in the C_3A content from 2.43% to 14%. This indicates that high C_3A content of cement is specially beneficial for binding chlorides in the range of 0.3% to 0.6%.

2. For a threshold Cl^-/OH^- ratio of 0.30, the threshold chloride values for the 2.43, 7.59, 8.52 and 14% C_3A cements in terms of total acid-soluble chlorides are 0.40, 0.62, 0.68 and 1.0% by weight of cement. In terms of free water-soluble chlorides, the threshold values for these cements are 0.14, 0.16, 0.17 and 0.22% by weight of cement.

3. The effect of C_3A content in significantly influencing corrosion is confirmed by time to corrosion initiation data. In terms of corrosion initiation time the Type I 9, 11 and 14% C_3A cements performed 1.75, 1.93 and 2.45 times better than the Type V 2% C_3A cement.

4. With increasing level of chloride addition, although the absolute quantum of bound chloride increases, the ratio of bound to unbound chlorides decreases. For example, in the 14% C_3A cement the ratio of bound to unbound chloride is 14.4 times higher for the lower level of 0.3% chloride addition compared to 2.4% chloride addition.

5. As the chloride content increases, the chloride-binding performance ratio between higher and lower C_3A cements decreases significantly. For example, in terms of bound to unbound chloride ratio the 7 fold superiority of the 14% C_3A cement over the 2.43% C_3A cement at the 0.3% chloride addition level drops to 3.2 for the 2.4% chloride addition. This indicates that C_3A is effective in binding only a limited amount of chlorides.

6. The pore fluid analysis indicates some chloride binding even in the low 2.43% C_3A cement. Research needs to be carried out to clarify whether this binding is due to the C_3A phase or due to other cement compounds such as C_3S and its hydrates.

7. Corrosion rates of steel in post initiation period in plain cement concretes made with 2, 9, 11 and 14% C_3A cements are almost constant and do not show any definite relation with the C_3A content of the cement. This is attributable to very

high chloride contents ingressed into concrete at the time of corrosion measurement. Due to the limiting chloride binding capacity of C_3A at high chloride contents, the measured corrosion rates do not reflect the beneficial effect of high C_3A content.

Effect of Alkali Content

8. An increase in alkali content in 14% C_3A cement from 0.65 to 1.2% increases the OH^- concentration but significantly reduces the chloride binding capacity of cement. This is indicated by a 1.4 times increase in the OH^- concentration and a two-fold increase in the unbound chlorides in the pore solution for chloride levels ranging from 0.3 to 1.2%. The reduced chloride binding is attributable to a reduced formation in the Friedel's salt as observed by the DTA results. The interactive result of increase in OH^- and Cl^- concentrations is a marginal increase in the Cl^-/OH^- ratio of the pore solution.

   The conclusion of these data is to the effect that an increase in the alkali content of the cement does not reduce the corrosion risk.

Sulfate-Chloride Interaction

9. Alkalinity of pore solution is significantly increased by the addition of 4% sulfates in chloride-bearing hydrated cement pastes. Further increase in the sulfate addition to 8% registers only a marginal increase in the pore solution alkalinity. The increase in alkalinity with sulfate addition is due to the formation of sodium hydroxide as a result of reaction between sodium sulfate and calcium hydroxide liberated during cement hydration. The consumption of calcium hydroxide due to sulfate addition is confirmed by DTA and TGA test results.

10. Chloride ion concentration in pore solution is increased with the addition of sulfates for both chloride levels of 0.6 and 1.2% in all the three cements tested. DTA results show that sulfate addition significantly reduces the formation of Friedel's salt which possibly results in an increase in the chloride ion concentration. Chloride binding performance ratio of Type I (C_3A: 14%) to Type V (C_3A: 2.43%) decreases as sulfate levels are increased for a given chloride content.

11. The interactive combined effect of increase in alkalinity and chloride ion concentration with sulfate addition is not a consistent increase or decrease in the Cl^-/OH^- ratio of the pore solution. For a given chloride level, whether sulfate addition increases or decreases the Cl^-/OH^- ratio of the pore solution depends upon the interactive effect of equivalent alkali content and C_3A content of the cement.

Effect of Temperature

12. An increase in exposure temperature from 20 to 70° C results in a two fold decrease in the OH^- concentration and a 1.2 to 9.1 fold increase in the unbound chlorides in the pore solutions of 2.43, 7.59 and 14% C_3A cements treated with 0.3, 0.6 and 1.2% chlorides. This increase in the unbound chlorides is more pronounced in the high C_3A cement than in the low C_3A cements.

13. The concomitant elevation of free chlorides and the depression in OH^- concentration with increase in temperature from 20 to 70° C raises the Cl^-/OH^- ratio in the pore solution significantly and this increase depends on the C_3A content of the cement and the chloride treatment level. This increase in the Cl^-/OH^- is maximum for the lowest chloride level of 0.3% in the 14% C_3A cement.

Mode of Chloride Occurrence- Internal and External Chlorides

14. Plain cements show more chloride-binding when contaminated with internal chlorides, introduced through constituent materials in the original mix, compared to when contaminated with external chlorides, introduced from external environment after significant degree of hydration. The removal of chlorides with increasing C_3A content of cement is less effective for external chlorides compared to internal chlorides.

Threshold Cl^-/OH^- Ratio

15. Threshold Cl^-/OH^- in the pore solutions of hydrated cement mortars using ordinary portland cements of 2.43, 7.59 and 14% C_3A contents are found to be dependent on the pore solution alkalinity. For the range of pore solution alkalinity available in the mortars tested, it is indicated that for pore solution pH of 13.0 and 13.2, the threshold Cl^-/OH^- ratios may be taken as 1.8 and 1.3 respectively.

Blended Cements

Alkalinity in Chloride-Free Blended Cements

16. Microsilica, blast furnace slag and fly ash blending in chloride- free cement pastes reduce the OH^- concentration in the pore solution as well as calcium hydroxide content, which represents reserve alkalinity in hydrated cement pastes.

    The OH^- concentrations in the pore solution decrease progressively with increasing replacement levels of microsilica. For 25% microsilica blending, the alkalinity of the pore solution drops to a value below that of saturated calcium

hydroxide. These reductions in the OH^- concentrations are accompanied by reductions in calcium hydroxide content of the hydrated cements. For microsilica blending of 20% and more, calcium hydroxide is completely eliminated from the hydrated cement pastes.

60 and 70% slag blending causes reduction in OH^- concentrations of chloride-free pastes by 1.4 and 2.4 times. For 70% slag blending the calcium hydroxide content is reduced from 30.6 to 4.4% compared to the plain cement.

30% fly ash blending reduces OH^- concentration in the pore solution and calcium hydroxide content by 1.4 and 2.4 times respectively.

The reduction in pore solution alkalinity and calcium hydroxide contents due to the incorporation of these blending materials is attributable to pozzolanic reactions resulting in the formation of secondary C-S-H gel.

Chemical Environment of Chloride-Bearing Blended Cements

17. For microsilica blended cements, the OH^- concentration in the pore solutions of chloride-bearing hydrated pastes drop steeply with increasing cement replacement levels by microsilica. The depression in OH^- concentration, however, is in general significantly more pronounced for chloride-bearing microsilica cement pastes, compared to chloride-free pastes. For 20% microsilica blended cements made with 2.43 and 14% C_3A parent plain cements the pore solution pH drops below that of saturated calcium hydroxide solution.

18. Partial substitution of cement by microsilica increases unbound chlorides in the pore solution of microsilica blended cements made with parent plain cements of 2.43 and 14% C_3A. However, this increase is more pronounced in microsilica blended cements made with 14% C_3A cements compared to those made with

2.43% C_3A cement, for both 10 and 20% replacement levels. For example, 20% microsilica blending increases the unbound chlorides by 5.4 times in the 14% C_3A cement, whereas it increases unbound chlorides by only 1.4 times for the 2.43% C_3A cement.

19. Cl^-/OH^- ratio in the pore solution increases steeply with increasing cement replacement by microsilica due to the cumulative interactive effect of an increase in the free chlorides and a decrease in the OH^- concentration. In the 14% C_3A cement, 10 and 20% microsilica blending causes 4 and 39 fold increase respectively in the Cl^-/OH^- ratio for 1.2% chloride level. However, in the 2.43% C_3A cement, the increase in the Cl^-/OH^- ratio due to 10 and 20% microsilica blending is to a lesser extent.

20. 70% replacement of cement by blast furnace slag causes the OH^- concentration in the pore solutions of 2.43 and 14% C_3A cements to decrease by about 2 and 3 times respectively compared to the plain cement.

    DTA results of 70% slag blended cement treated with 1.2% chlorides show that calcium hydroxide content is completely eliminated due to the pozzolanic reaction.

21. For 2.43 and 14% C_3A parent plain cements, the unbound chlorides in the pore solution due to 70% slag blending are reduced by an average value of 20%.

22. 70% slag blending causes the Cl^-/OH^- ratios in the pore solution to increase only moderately. For 2.43% C_3A cement, the slag blending causes 20 to 40% increase in the Cl^-/OH^- ratios for different levels of chloride. However, for 14% C_3A cement, the increase in the Cl^-/OH^- ratios for different levels of chloride are

67 to 105%.

23. 30% fly ash blending to 2.43 and 14% C_3A cements causes 21 to 40% reductions in the OH^- concentrations. Calcium hydroxide content in the 1.2% chloride-bearing hardened cement paste is reduced to 13.1% as compared to 30.6% in the plain cement.

24. 30% fly ash blending causes the unbound chlorides to decrease by an average value of 30% in both 2.43 and 14% C_3A cements.

25. For 30% cement blending by fly ash, the decrease in the unbound chlorides outweighs the decrease in the OH^- concentration, thereby causing a marginal decrease of 20 to 40% in the Cl^-/OH^- ratio in the pore solution. However, in the 14% C_3A cement, the net effect of concomitant decrease in OH^- concentration and unbound chlorides is a marginal increase in the Cl^-/OH^- ratio in the pore solution, the maximum increase being 41%.

26. The above data on Cl^-/OH^- ratio which measures corrosion risk indicates that in terms of chemical environment the highest corrosion aggressivity is obtainable for microsilica blended cements (39 fold) followed by a much reduced aggressivity for blast furnace slag cement (2 fold). The fly ash blending has only marginal effect on chemical environment.

Alkali-Silica Reactions and OH^- Concentration in Pore Solution in Blended Cements

27. Incorporation of 10 to 20% microsilica and 60 to 70% slag reduced expansions

from nine times the permissible expansion to safe values ranging from one-tenth to one-half the allowable expansion. However, 30% fly ash blended cement showed expansions at six months equal to permissible limit (0.1%). In view of the fact that the reactivity of aggregate used was unusually high and the alkali content of the fly ash was also high, this performance should be acceptable.

28. The data developed in this study confirm a broad correlation between the hydroxide ion concentration and ASR generated expansions. However, there are obvious deviations which are strongly indicative of other concurrently operative mechanisms in addition to the alkali removal action.

29. Blast furnace slag is shown as an active remover of alkalies and is specially effective in medium alkali cements where, for equal alkali contents, the performance of 60% slag cement is comparable to that of 10% microsilica cement. However, the effectiveness of the slag decreases as alkali content of the cement increases.

30. Fly ash is found to be more effective in removing alkalies than 60 and 70% blast furnace slag and is comparable to 15% microsilica blended cement in removing alkalies, particularly for lower levels of alkali content.

31. 25% microsilica addition virtually sweeps nearly all the hydroxide ions from the pore solution. 10% microsilica significantly reduces OH^- concentration, although in 1.2% and 1.5% alkali cements the hydroxide ion concentrations remain above the postulated threshold of 250 mM/L. However, the expansion for 10% microsilica cement with OH^- concentrations of 368 mM/L is well below the allowable limit. This suggests that for blended cements the 250 mM/L value is excessively conservative and a value close to 400 mM/L would be more realistic.

32. The validity of a higher threshold value for OH^- concentration in pore solution is based on the favourable physical changes in addition to the chemical factor. Microsilica, slag or fly ash addition brings about a marked refinement and segmentation of the pore structure thereby effectively retarding the transportation of alkalies to reaction sites.

33. Both from the standpoint of expansion and 400 mM/L threshold value, it seems that for most cases of medium to high alkali cements, 10% cement replacement by microsilica is adequate for ASR control.

Physical Characteristics of Blended Cements

34. Although the increased aggressivity of pore solution of blended cements creates an adverse chemical environment and significantly increases corrosion vulnerability of reinforcing steel in the blended cement concrete, the actual corrosion resistance performance in terms of corrosion initiation time for external chlorides in the blended cement concrete show a significantly improved performance compared to the plain cement concrete.

    Corrosion initiation times of steel in microsilica, slag and fly ash blended cements were 3, 2.1 and 1.75 times compared to the plain cement concrete.

35. The significantly improved corrosion ressistance performance of steel in blended cements is attributed to highly favourable changes in the physical structure of the hardened cement matrix in terms of pore refinement brought about by the blending materials.

36. The blending materials used in this study significantly improved the pore size distribution of hardened cement.

10 and 20% microsilica blended cements show a more refined pore structure than that of plain cement even after a curing period of only three days. The average pore radii for 6-month old mature pastes of 10 and 20% microsilica blended cements are 167 and 136 A° compared to 213 A° for the plain cement.

Slag and fly ash blended cements show a more refined pore structure than the plain cement only after a hydration period of 28-days. The average pore radii of 70% slag and 30% fly ash blended mature cement pastes are found to be 153 and 146 A° compared to 213 A° for the plain cement.

37. Permeability is also significantly reduced due to incorporation of the blending materials in concrete. The decrease in permeability was maximum for 20% microsilica blended cement concrete followed by 10% microsilica, 70% slag and 30% fly ash blended cement concretes. For 20 and 10% microsilica, 70% slag and 30% fly ash blended cement concrete the coefficients of permeability are reduced by 16, 12, 10 and 5 times compared to the plain cement concrete.

38. Chloride diffusion of the hardened blended cement pastes is significantly reduced compared to that of the plain cement. The decrease in chloride diffusion is drastic for 20 and 10% microsilica blending being 300 and 150 folds less than that of the plain cement. Slag and fly ash blending also reduce the chloride diffusion by 39 and 6 folds respectively compared to the plain cement.

39. Electrical resistivity, which controls flow of corrosion current in the post-initiation period, is also found to be increased due to microsilica, slag and fly ash blending.

10 and 20% microsilica blending enhances the electrical resistivity by 5.7 and 3.2 times compared to the plain cement concrete. Slag and fly ash blending increases

the electrical resistivity of concrete by 2.6 and 2.2 times respectively.

40. Decrease in oxygen diffusion is moderate for microsilica blended cement concrete. However, for the slag and fly ash blending the decrease in oxygen is found to be 5 and 100 fold respectively compared to plain cement concrete.

REFERENCES

1. Rasheeduzzafar, Dakhil,F.H., and Gahtani,A,S., *The Deterioration of Concrete Structures in the Environment of the Middle East*, ACI Jouranal, Proceedings Vol.81, No.1, January-February 1984, pp. 13-20.

2. Rasheeduzzafar, Dakhil,F.H., and Gahtani,A,S., *The Deterioration of Concrete Structures in the Environment of Saudi Arabia*, The Arabian Journal of Science and Engineering, Vol. 7, No. 3, 1982, pp. 191-232. ACI SP-79, pp. 589-605.

3. Rasheeduzzafar, Dakhil,F.H, and Gahtani,A.S., *Field Studies on the Durability of Concrete Construction in a High Chloride Sulfate Environment*, International Journal of Housing Science, Vol. 4, No. 3, 1980, pp. 203-223.

4. Rasheeduzzafar, Dakhil,F.H., Al-Gahtani,A.S., Al-Saadoun,S.S., Badar,M.A., and Medallah,K.Y., *Proposal for a Code of Practice to Ensure Durability of Concrete Construction in the Arabian Gulf Environment*, Proceedings, Second International Conference on the Deterioration and Repair of Reinforced Concrete in Arabian Gulf, Bahrain, 11-13 October. 1987, pp. 595-631.

5. Sims,I., Poole,A.B., *Potentially Alkali-Reactive Aggregates from the Middle East*, Concrete, May 1980, pp. 27-30.

6. French,W.J., Poole,A.B., *Deleterious Reactions Between Dolomites from Bahrain and Cement Paste*, Cement and Concrete Research, Vol. 4, 1974, pp. 925-937.

7. Henriksen, J.F., *The Corrosion and Protection of Steel in Saturated Ca* $(OH)_2$ *Contaminated with NaCl*, Corrosion Science, Vol 20, 1980, pp. 1241-1249.

8. Verbeck,G.J., *Field and Laboratory Studies of the Sulfate Reistance of Concrete*, Portland Cement Association Research Department Bulletin 227.

9. *Sun and Salt-the scourge of Concrete in the Gulf*, Civil Engineer, 19 June, 1975, pp. 32.

10. *Concrete in Hot Countries*, FIP Publication.

11. Hausmann,D.A., *Steel Corrosion in Concrete: How Does It Occur*, Materials Protection, Vol. 6, No. 11, 1967, pp. 19-23.

12. P.K.Mehta,. *Pozzolanic and Cementitious By-Porducts in Concrete--Another Look*, ACI SP-114, 1989, pp. 1-41.

13. Dunstan,E.R, *A Possible Method of Identifiying Fly Ashes that will Improve the Sulfate Resistance of Concretes*, Cement, Concrete and Aggregates, Vol. 2, No, 1, Semmer 1980, pp. 20-30. .

14. Mehta,P.K., *Effects of Fly Ash Composition on Sulfate Resistance of Cement*, ACI Journal, Novermber-December 1986, pp. 994-1000.

15. Hogan,F.J and Meksel,J.W., *The Evaluation for Durability and Strength of Ground Granulated Blast Furnace Slag*, ASTM Cement, Concrete and Aggregates, Vol. 3, No. 1, pp. 40-52.

16. Lea,F.M., *The Chemistry of Cement and Concrete*, 3rd edition, Chemical Publication Co., New York, 1971.

17. Bakker,R.F.M., *Permeability of Blended Cement Concrete*, SP-79, American Concrete Institute, Detroit, pp. 589-605.

18. Mehta,P.K., *Durability of Concrete in Marine Environment*, SP-79, American Concrete Institute, Detroit, pp. 1-20.

19. Roy,D.M., and Idorn,G.M., *Hydration, Structure and Properties of Blast Furnace Slag Cements, Mortars and Concrete*, ACI Journal Proceedings, Vol. 79, No. 6 Nov.-Dec. 1982, pp. 445-457

20. Rasheeduzzafar, Dakhil,F.H, Al-Gahtani,A.S, Saadoun,S.S. and Badar,M. *Influence of Cement Composition on the Corrosion of Reinforcement and Sulfate Resistance of Concrete*, ACI Materials Journal, Vol. 87, March-April 1990, pp. 114-122.

21. Cohen,D. and Bentur,A., *Durability of Portland Cement-Silica Fume Pastes in Magnesium Sulfate and Sodium Sulfate Solutions*, ACI Materials Journal, Vol. 85, No. 3, May-June 1985, pp. 148-157.

22. Mehta,P.K., *Mechanism of Expansion Associated with Ettringite Formation*, Cement and Concrete Research, Vol. 3, No. 1, 1973, pp. 1-6

23. Rasheeduzzafar, Dakhil,F.H., Bader,M.A., Gahtani,A.S., and Al-Saadoun,S.S., *New Cement Specifications for Durable Concretes in Saudi Arabia*, Reports, Project No. AR-6-138, King Abdulazeez City of Science and Technology, Riyadh.

24. Al-Amoudi.O.S.B., Rasheeduzzafar and Maslehuddin.M, *Permeability and Corrosion Resisting Characteristics of Fly Ash Concrete in Arabian Gulf Countries*, SP 114, American Concrete Institute, Detroit, pp. 295-313.

25. Berry,E.E., and Malhotra,V.M, *Fly Ash in Concrete*, Chapter 2, Supplementary Cementing Materials for Concrete, CANMET, 1987, Edited by V.M.Malhotra.

26. Holden,W.R., Short,N.R. and Page, C.L., *The Influence of Sulfates and Chlorides on Durability*, Corrosion of Reinforcement in Concrete Construction, Ellis Horwood Publishers, London, 1983, pp. 143-150.

27. E.P.Douglas, Chapter 6, Supplementary Cementing Materials for Concrete, CANMET, 1987, Edited by V.M.Malhotra.

28. Sellevold,E.J. and Nilsen,T., *Condensed Silica Fume in Concrete: A World review*, Chapter 3, Supplementary Cementing Materials for Concrete,

CANMET, 1987, Edited by V.M.Malhotra.

29. D.Manmohan and P.K.Mehta., *Influence Pozzolanic, Slag, and Chemical Admixtures of Pore Size Distribution and Permeability of Hardened Cement Pastes*, Cement, Concrete, and Aggregates, Vol. 3. No.1, Summer 1981, pp.. 63-67.

30. B.K Marsh, R.L.Day and D.G.Bonner, *Pore Structure Characteristics Affecting the Permeability of Cement Paste Containing Fly Ash*, Cement and Concrete Research, Vol. 15, No. 6, Nov. 1985, pp. 1027-1038.

31. Vennesland,O. and Gjorv,O.E, *Silica Concrete Protection against Corrosion of Embedded Steel*, SP 79, American Concrete Institute, Detroit, pp. 719-729.

32. Rasheeduzzafar, Al-Saadoun,S.S, Al-Gahtani,A.S, and Dakhil,F.H., *Effect of Tricalcium Aluminate Content of Cement on Corrosion of Steel in Concrete*, Cement and Concrete Research, Vol. 20, No. 5, Sep. 1990, pp.723-738.

33. Roberts, M.H., *Effect of Calcium Chloride on the Durability of Pre-Tensioned Wire in Prestressed Concrete*, Magazine of Concrete Research, Vol. 14, No. 42, Nov. 1962, pp. 143-154.

34. Monfore,G.M., and Verbeck, G.J., *Corrosion of Prestressed Wire in Concrete*, ACI Journal, Proceedings, Vol. 57, No. 5, Nov. 1960, pp.491-516. Structural Engineering. Vol. 3, No. 3, Oct. 1975, pp.. 113-125.

35. Verbeck,G.J., *Field and Laboratory Studoes of the Sulfate Resistance of Concrete*, Performance of Concrete, University of Toronto Press, Toronto, 1968, pp. 113-12

36. Baumel,A., *Effect of Calcium Chloride on Corrosion Behavior of Steel in Concrete*, Beton Herstellung-Verwendung (dusseldorf), Vol. 10, p 256 (1960), (in German).

37. C.L.Page and O.Vennesland, *Pore Solution Composition and Chloride-Binding*

Capacity of Silica-Fume Cement Pastes, Materials and Structrures, Vol. 16, No. 91, 1983, pp. 19-25. First Crack Strength of Ferrocement in Flexure,

38. Diamond,S., *Chloride Concentrations in Concrete Pore Solutions Resulting from Calcium and Sodium Chloride Admixtures*, Cement, Concrete, and Aggregates, Vol. 8, No. 2, Winter 1986, pp. 97-102.

39. Mehta,P.K., *Effect of Cement Composition on Corrosion of Reinforcing Steel in Concrete*, Chloride Corrosion of Steel in Concrete, STP-629, American Society of Testing and Materials, Philadelphia, 1977, pp. 12-19.

40. Schwiete,H.E., Ludwig,U., and Albeck,J., *Combination of Calcium Chloride and Calcium Sulfate in Hydration of Aluminate-Ferrite Clinker Constitiuents*, Zement-Kalk-Gipss, No. 5, 1969, pp. 225-234.,

41. Lerch, Ashton,F.W., and Bogue,R.H., *National Bureau of Standards*, Journal of Research, Vol. 2, RP 54, 1929, pp. 715-731.

42. Andrade,C. and Page, C.L., *Pore Solution Chemistry and Corrosion in Hydrated Cement Systems Containing Chloride Salts: A Study of Cation Specific Effects*, Bristish Corrosion Journal, Vol. 21, No. 1, 1986, p 49-53.

43. Kawamura,M., Kayyali,O.A., and Haque,M.N., *Effects of a Fly Ash on Pore Solution Composition in Calcium and Sodium Chloride-Bearing Mortars*, Cement and Concrete Research, Vol 18, No. 5, Sep. 1988, pp. 763-773.

44. Rasheeduzzafar, Dakhil,F.H, Al-Gahtani,A.S, Saadoun,S.S., *Exposure Site Studies on the Effect of Cement Composition of Corrosion of Reinforcing Steel in Concrete*, Arabian Journal for Science and Engineering, Vol. 4, No. 2, Theme issue: Corrosion, pp. 235-248.

45. Smolezyk,H.G., *Liquid in Concrete Pores-Composition and Diffusion in the Liquid of Hardened Cement Paste*, CEMIJ, Netherlands.

46. Gjorv,O.E., *Reinforced Concrete Wharves in Norwegian Harbours*, The

Norwegian Committee on Concrete in Sea Water. Ingenieur-forlaget A/S, Osio 1968.

47. Verbeck,G.J., *Mechanisms of Corrosion of Steel in Concrete*, Corrosion of Metals in Concrete, SP-49, American Concrete Institute, Detroit, 1978, pp. 21-38.

48. Ramachandran,V.S., *Possible States of Chloride in Hydration of Tricalcium Silicate in the Presence of Calcium Chloride*, Materials and Structures, Vol. 4, 1971, No. 19, pp. 3-12. pp.. 155-164.

49. Ramachandran,V.S., *Calcium Chloride in Concrete: Science and Technology*, Applied Science Publishers,Ltd., London, 1976.

50. Ramachandran,V.S.,, Seeley,R.C. and Polomark,G.M., *Free and Combined Chloride in Hydrating Cement and* Cement Components, Materials and Structures, Vol. 17, No. 100, 1984, pp. 284-289.

51. Diamond,S. and Lopez-Flores,F., *Fate of Calcium Chloride Dissolved in Concrete Mix Water*, Journal of American Ceramic Society, Vol. 64, No. 11, 1981, pp. C162-164.

52. Longuet,P., Burglen,L. and Zelwer,A., *The Liquid Phase of Hydrated Cement*, Rev Mater. Constr., No. 676, 1973, pp. 35-42.

53. Lambert,P., Page, C.L., and Short, N.R., *Pore Solution Chemistry of the Hydrated System Tricalcium Silicate/Sodium Chloride/Water*, Cement and Concrete Research, Vol. 15, No. 4, 1985, pp. 657-680.

54. Gouda,V.K., *Corrosion and Corrosion Inhibition of Reinforcing Steel, I. Immersed in Concrete Solution*, British Corrosion Journal, Vol. 5, 1970, pp. 198 - 203.

55. Diamond,S., *Effects of Microsilica (Silica Fume) on Pore Solution Chemistry of Cement Pastes*, Communication of Journal of the American Ceramic

Society, Vol. 66, May 1983, pp. C-82 - 84.

56. Bakker,R.F.M., *About the Cause of the Resistance of Blast Furnace Cement Concrete to the Alkali-Silica Reaction*, CEMIJ, Netherlands.

57. Monfore,G.E., *The Electrical Resistivity of Concrete*, Journal, PCA Research and Development Laboratories, Vol. 10, No, 2, May 1968, pp. 35-48.

58. Maguire,D., and Olen,M., *Report on an Investigation into the Electrical Prperties of Concrete*, Transaction, S. African Institute of Electrical Engineers, Vol. 31, No. 11, Nov. 1940, pp. 301-303.

59. Barneyback Jr.,R.S. and Diamond,S., *Expression and Analysis of Pore Fluids from Hardened Cement Pastes and Mortars*, Cement and Concrete Research, Vol. 11, No. 2, 1981, pp. 279-285.

60. Clear,K.C. and Harrigan,E.T., *Sampling and Testing for Chloride Ion in Concrete*, Report No. FHWA-RD-77-85, Federal Highway Administration, Washington, D.C., 1977.

61. Page,C.L., Short.N.R. and El-Terras,A., *Diffusion of Chloride Ions in Hardened cement Pastes*, Cement and Concrete Research, Vol. 11, No. 3, 1981, pp. 359-406.

62. Tuutti,K., *Service Life of Structures with Regard to Corrosion of Embedded Steel*, Performance of Concrete in Marine Environment, SP-65, American Concrete Institute, Detroit, 1980, pp. 223-236.

63. Browne,R.D., *Design for Durability*, Proceedings, 7th European Ready Mixed Concrete Congress, Institute of Concrete Technology, London, 1983.

64. Tritthart,J., *Chloride Binding in Cement, II. The Influence of the Hydroxide Concentration in the Pore Solution of Hardened Cement Paste on Chloride Binding*, Cement and Concrete Research, Vol.19, No.5, 1989, pp.683-691.

65. Rasheeduzzafar, Hussain,S.E. and Al-Saadoun, S.S., *Effect of Cement*

Composition on Chloride Binding and Corrosion of Reinforcing Steel in Concrete, Cement and Concrete Research, Vol. 21, No. 5, 1991, pp.777-794.

66. Arya,C., Buenfeld,N.R., and Newman,J.B., *Factors Influencing Chloride-Binding in Concrete*, Cement and Concrete Research, Vol.20, No.2, 1990, pp.291-300.

67. Yonezewa,T., Ashworth,V. and Procter,R.P.M., Proceedings, 8th International Conference on Alkali-Aggregate Reaction, Kyoto, 1989, pp. 153-160.

68. Mehta,P.K. and Manmohan,D., *Pore Size Distribution and Permeability of Hardened Cement Pastes*, Proceedings of 7th International Congress on Chemistry of Cement, Paris, 1988, Vol. III, pp. VII-1 to VII-5.

69. Hughes,D.C., *Pore Structure and Permeability of Hardened Cement Paste*, Magazine of Concrete Research, Vol. 37, No.133, Dec. 1985, pp. 227-233.

70. Nyame,B.K. and Illston, J.M., *Capillary Pore Structure and Permeability of Hardened Cement Pastes*, Proceedings of the 7th International Congress on Chemistry of Cements, Paris, Vol.3, 1980, pp. VI-182 to 185.

71. Preece,C.M., Gronvold,F.O. and Frolund.T., *The Influence of Cement Type on the Electrochemical Behaviour of Steel in Concrete*, Corrosion of Reinforcement in Concrete Construction, Ellis Horwood Publishers, London, 1983, pp. 393-405.

72. Byfors,K., *Influence of Silica Fume and Fly Ash on Chloride Diffusion and pH Values in Cement Pastes*, Cement and Concrete Research, Vol.17, No.1, 1987, pp. 115-130.

73. Gewertz,M.W., Tremper,B., Beaton,J.L. and Stratfull,R.F., *Causes and Repair of Deterioration to a California Bridge due to Corrosion of Reinforcing Steel in Marine Environment*, Highway Research Board Bulletin, 182, 1958,

pp. 18-41.

74. Canham,I., Page,C.L. and Nixon,P.J., *Aspects of the Pore Solution Chemistry of Blended Cements Related to the Control of Alkali Silica Reaction*, Cement and Concrete Reasearch, Vol.17, No.5, 1987, pp. 839-844.

75. Diamond,S., *Alkali Reactions in Concrete - Pore Solution Effects*, Proceedings of 6th International Conference on Alkalies in Concrete, Copenhagen, 1983, pp. 155-166.

76. Bhatty,M.S.Y., *Mechanism of Pozzolanic Reactions and Control of Alkali-Aggregate Expansion*, Cement, Concrete and Aggregates, Vol.7, No.2, 1985, pp. 69-77.

77. Glasser,F.P., and Marr,J., *The Effect of Mineral Additives on the Composition of Cement Pore Fluids*, Proceedings British Ceramic Society, Vol. 35, 1984. pp.419-429.

78. Roberts,M.H., *Carbonation of Concrete made with Dense Natural Aggregates*, BRE Information Paper IP 6/81, April 1981.

79. Shalon, R., *Cement Content as a Factor in the Corrosion of Reinforcement*, Architectural Review, July 1959, pp. 77-81.

80. Goni,S. and Andrade,C., *Synthetic Concrete Pore Solution Chemistry and Rebar Corrosion Rate in the Presence of Chlorides*, Cement and Concrete Research, Vol.20, No.4, 1990, pp. 525-539.